

Faculty 8 - Natural Sciences and Technology  
Saarland University, Homburg/Saar, Germany

# **Effect of coumarin and diallyl polysulfides on HCT116 colon cancer cells**

*Dissertation for Awarding a Doctoral Degree in Natural  
Sciences (Dr. rer. nat.)*

University of the Saarland

2013

Submitted by

**BSc. MSc. Nathaniel Edward Bennett Saidu**

Born: 23 March 1984 in Bo, Sierra Leone

**Tag des Kolloquium:** 25/04/2013

**Dekan:** Prof. Dr. Helms

**Berichterstatter:** Prof. Dr. M. Montenarh und Prof. Dr. C. Jacob.

**Vorsitz:** Prof. Dr. U. Müller.

**Akad. Mitarbeiter:** Dr. M. Engel.

## Summary

Polysulfanes from garlic are regarded as potential chemopreventive compounds as they have proven to be effective inhibitors of cancer cells. Yet, certain aspects of the triggered inhibitory effects remain unclear.

The aim of this study was, hence, to determine the anti-carcinogenic properties of novel coumarin and diallyl polysulfides against HCT116 colorectal cancer cells. These polysulfides inhibited the viability and proliferation of cultured HCT116 cells in a time- and dose-dependent manner. The mechanism of cell inhibition included cell cycle arrest and induction of apoptosis.

While polysulfanes are known to cause oxidative stress, little is known about the underlying signalling cascades leading to antioxidant defence or apoptosis. It was, thus, hypothesised in this study that polysulfanes may induce ROS generation and/or regulate cellular thiol, which in turn may regulate signalling pathways leading to cell survival or apoptosis. The effect of polysulfanes on cellular thiol, ROS and ER stress signalling pathways was hence analysed. An immediate rise in the level of  $O_2^{\cdot-}$ ,  $H_2O_2$  and an overall thiol depletion was found. There was also an increase in PERK and eIF2 $\alpha$  phosphorylation along with Nrf2, HO-1, and NQO1 protein levels in a time- and concentration-dependent manner. Pre-treatment of cells with antioxidants drastically reduced the high expression levels of these proteins. A direct role of Nrf2 was shown by its interaction with the stress response element of the HO-1 promoter.

Interestingly, however, not only did DATTS fail to induce cell cycle arrest in the G<sub>2</sub>/M phase of the cell cycle in normal epithelial ARPE-19 cells, but also apoptosis and ER stress.

This study, shows for the first time, a parallel but not equal activation of signaling pathways by DATTS in particular, with a competitive ultimate cellular outcome. Results also suggest that the inhibitory and apoptotic effects are more prominent in HCT116 cancer cells than in ARPE-19 noncancer cells.

## Zusammenfassung

Polysulfane sind Inhaltsstoffe des Knoblauchs, die als potentielle pharmakologisch wirksame Verbindungen betrachtet werden, da sie sich als Hemmstoffe des Krebszellwachstums herauskristallisiert haben. Zahlreiche Aspekte dieser Hemmung sind noch unklar.

Das Ziel dieser Studie war es daher, die antikarzinogenen Eigenschaften von neuartigen Cumarin- und Diallylpolysulfanen in der Darmkrebszelllinie HCT116 zu bestimmen. Diese Polysulfane hemmen Wachstum und Vitalität der kultivierten HCT116 Zellen in einer zeit- und dosisabhängigen Weise. Der Mechanismus der Hemmung umfasst einen Zellzyklusarrest und die Induktion von Apoptose.

Während Polysulfane dafür bekannt sind, oxidativen Stress zu verursachen, ist nur wenig über die Signalwege bekannt, die zur Verteidigung mittels Antioxidantien oder Apoptose führen. Dieser Arbeit liegt die Hypothese zugrunde, dass Polysulfane zu ROS-Entstehung führen und/oder zelluläres Thiol regulieren könnten, was wiederum Signalwege regulieren könnte, die über Apoptose oder Überleben entscheiden. Tatsächlich konnte ein unmittelbarer Anstieg von  $O_2^{\cdot-}$ -Radikalen und  $H_2O_2$ , sowie eine Abnahme der Thiolkonzentration gezeigt werden. Es war auch ein zeit- und dosisabhängiger Anstieg der Expression von ER-Stress Markerproteinen zu beobachten. Die Vorbehandlung der Zellen mit Antioxidantien reduzierte die Expression dieser Proteine drastisch. Eine direkte Rolle von Nrf2 auf HO-1 wurde durch die Interaktion mit dem StRE-Promotorelement des HO-1 Gens gezeigt.

Interessanterweise konnte Diallyltetrasulfan (DATTS) in der normalen Epithelzelllinie ARPE-19 weder einen  $G_2/M$  Zellzyklusarrest, noch ER-Stress oder Apoptose induzieren.

Diese Studie zeigte erstmals eine parallele, aber nicht identische Aktivierung von

Signalwegen durch DATTS mit kompetitivem Ausgang für die Zelle. Die Ergebnisse legen außerdem nahe, dass die hemmenden und apoptotischen Effekte von DATTS in HCT116 Krebszellen deutlich stärker sind als in ARPE-19 Nicht-Krebszellen.

### **Acknowledgement**

I would like to express my greatest gratitude to my supervisor Prof. Dr. Mathias Montenarh for not only giving me the opportunity to be trained as a young researcher in his lab, but also for all his help, valuable advice, and abundant patience and guidance through all of the successes and failures during the course of this project. It has been a great pleasure and wonderful learning experience to work under his supervision. His support and encouragement during this testing time were tremendous.

I am thankful to Prof. Dr. Claudia Götz and Prof. Dr. Karen Rother for their help, patience and encouragement, and for listening to me whenever I needed someone to talk to. Their valuable advice had helped me throughout this project.

Many thanks to Prof. Dr. Claus Jacob and his group from the University of the Saarland for providing the diallyl polysulfides for this project. Thanks to Prof. Gilbert Kirsch and colleagues and especially Dr. Sergio Valente from Université de Lorraine in Metz, France for synthesising and providing me with the coumarin polysulfides.

I would also like to thank Prof. Imad Abu Asali of the University of Damascus, Syria for helping with some of the reactive oxygen species assays. Special thanks to Dr. Reinhard Kappl and his team for giving me the opportunity to do some of the ROS experiments in their Biophysics lab.

My warmest thanks to all my lab colleagues in the Department of Medical Biochemistry and Molecular Biology especially Dr Carolin Schneider, Dr Emmanuel Ampofo, Mr Jürgen Günther, Sabrina Welker, Lisa Schwind and Catalina Gumhold. They cheered me up when things got a bit difficult. Their help and support throughout this work were tremendous. I am particularly thankful to Mrs. Sabine Kartarius for not only introducing me to some of the lab techniques, but also for being always by my side when needed. Special thanks to our secretary Mrs. Marianne Buchholz for all her help over the years and most especially, for finding me a home to live in during the course of this project.

## Acknowledgement

---

I am deeply thankful to Nishad Panchal, Amar Patel, Nirav Patel, Angela Werny, Tamba Nepor and Maike Kuschel for all the love and support, camaraderie, entertainment, and caring they provided throughout the years.

Many thanks to the Marie Curie European Funding Organisation for the financial support towards this research project. Thanks also to all the lovely members of the RedCat Initial Training Network for their valuable suggestions and the joys and laughter we all shared throughout the project.

I would also like to thank my family for being there when I needed them and for supporting me to achieve the best I can. Their love and financial support have seen me through many difficulties.

Last but not least I would like to thank God almighty, without the inner strength he has given me I would not have been able to succeed.

## List of Figures

- Figure 1. Sources of polysulfides.
- Figure 2. Chemical structures of diallyl and coumarin polysulfides.
- Figure 3. Reaction scheme for the synthesis of diallyl tetrasulfide and coumarin polysulfides.
- Figure 4. Structure of coumarin and atom numbering.
- Figure 5. Chemical properties and reactivity of polysulfides which may explain aspects of their biological activity.
- Figure 6. Proposed mechanism for polysulfide-induced ROS generation.
- Figure 7. The cell cycle with its regulatory proteins.
- Figure 8. Components of garlic.
- Figure 9. Representative grid square of the hemacytometer slide.
- Figure 10. Antioxidants.
- Figure 11. Reduction of yellow MTT to a purple colour formazan.
- Figure 12. Schematic representation of the production and detection of  $O_2^{\cdot-}$  by DHE.
- Figure 13. Schematic representation of the production and indirect detection of  $H_2O_2$ .
- Figure 14. Reduction of Ellman's Reagent to a mixed disulfide and 2-nitro-5-thiobenzoic acid (TNB).
- Figure 15. Caspase 3/7 cleavage of the luminogenic substrate containing the DEVD sequence.
- Figure 16. Bioluminescent reaction catalyzed by firefly luciferase.



- Figure 17. The ability of diallyl polysulfides to reduce cell viability and induce apoptosis depends on the length of the sulfur chain.
- Figure 18. DATTS affect the viability of HCT116 cells in both dosage and time dependent manners.
- Figure 19. DATTS treatment affects HCT116 cell morphology which can be reversed upon withdrawing treatment.
- Figure 20. The influence of DATTS on cell cycle distribution.
- Figure 21. DATTS inhibits CDK1 and phospho-cdc25C (Thr48) protein expressions in HCT116 cells.
- Figure 22. DATTS modulates p53, bcl-2 and bax protein expression, induces cytochrome c release from the mitochondria and activates caspase 3 in HCT116 cells.
- Figure 23. Antioxidant pretreatment reduce DATTS-mediated cytotoxicity and apoptosis induction.
- Figure 24. DATTS transiently induces  $O_2^{\cdot-}$  and  $H_2O_2$  in a time and dose-dependent manner.
- Figure 25. DATTS mediates thiol oxidation and depletion.
- Figure 26. DATTS activates the phosphorylation of PERK, which in turn induces eIF2 $\alpha$  phosphorylation at serine 51 in HCT116 cells.
- Figure 27. DATTS induces nuclear translocation of Nrf2.
- Figure 28. DATTS induces HO-1 and NQO1 protein expressions and increases StRE-luciferase activity in HCT116 cells.
- Figure 29. DATTS induces ATF3 in HCT116 cells.
- Figure 30. Stimulation of HCT116 colorectal cells with DATTS induces a signalling cascade involving calcium ions, activation of phospho-p38, phospho-c-

jun, and up-regulation of ATF3 expression.

- Figure 31. DATTS affect the viability of HCT116 cells in both time and dosage dependent manners. It also induce apoptosis by modulating bax and bcl-2 expressions, induce cytochrome *c* release and activate both caspase 3/7 and PARP cleavages in HCT116 cells.
- Figure 32. DATTS treatment affects the organisation of HCT116 cellular microtubule network.
- Figure 33. Influence of DATTS on CK2 protein expression and kinase activity.
- Figure 34. DATTS affects the viability of both HCT116 and ARPE-19 cells.
- Figure 35. DATTS treatment affects HCT116 cell morphology a lot more than it does to ARPE-19 cells.
- Figure 36. The influence of DATTS on HCT116 and ARPE-19 cell cycle distributions.
- Figure 37. DATTS induces cytochrome *c* release and activates caspase 3 in HCT116 cells but not in ARPE-19 cells. It also modulates  $\gamma$ H2AX protein expression and PARP cleavage in HCT116 cells but not in ARPE-19 cells.
- Figure 38. DATTS induces oxidative/ER stress protein expressions in HCT116 cells but not in ARPE-19 cells.
- Figure 39. Coumarin polysulfides affect the viability of HCT116 cells in both time and dosage dependent manners.
- Figure 40. The influence of SV29 on cell cycle distribution.
- Figure 41. Coumarin polysulfides induce PARP cleavage.
- Figure 42. SV29 modulates bcl-2 and bax expression, induces cytochrome *c* release and activates caspase 3/7 in HCT116 cells.

- Figure 43. Coumarin polysulfides compared with diallyl polysulfides.
- Figure 44. Coumarin polysulfides induce p53 expression in HCT116 cells.
- Figure 45. Coumarin polysulfides down-regulate cdc25C expression in HCT116 cells and inhibit the phosphatase activity of recombinant cdc25C phosphatase.
- Figure 46. Scheme of a generalised DATTS-induced signalling cascade leading to apoptosis.
- Figure 47. Proposed mechanism of the apoptotic signal transduction pathway activated by DATTS, involving inhibition of microtubule dynamics.
- Figure 48. Proposed mechanism of the endoplasmic reticulum signal transduction pathway activated by DATTS.
- Figure 49. Proposed mechanism for DATTS-induced ROS generation, eIF2 $\alpha$  phosphorylation, Nrf2 and HO-1 inductons.
- Figure 50. Scheme of the MAP kinase signalling pathway activated by DATTS.
- Figure 51. Influence of polysulfides on cancer cell and normal cells.
- Figure 52. Proposed mechanism of the cell growth inhibition and apoptotic signal transduction pathway activated by coumarin polysulfides in HCT116 colon cancer cell.

**List of Tables.**

- Table 1. Selected biological effects of coumarin and coumarin derivatives reported in literature.
- Table 2. Reactive oxygen and sulphur species.
- Table 3. Instruments.
- Table 4. Experimental materials.
- Table 5. Experimental kits and systems.
- Table 6. Chemicals.
- Table 7. Stock solutions of test compounds.
- Table 8. Antibiotics.
- Table 9. LB medium and Agar plates.
- Table 10. TYM-medium and buffers.
- Table 11. Buffer for DNA isolation.
- Table 12. Buffers for SDS PAGE electrophoresis.
- Table 13. Buffers for  $\beta$ -galactosidase assay.
- Table 14. PBS and protein binding buffers.
- Table 15. Buffers for Western blotting.
- Table 16. Stock solutions and buffers for immunofluorescence assays.
- Table 17. CK2 kinase buffer and reaction mixture.
- Table 18. Kerbs-Ringer buffer.
- Table 19. Cell lines.
- Table 20. Type(s) of *E. coli* strain

## List of Tables

---

Table 21. Separating gel solution.

Table 22. Stacking gel solution.

Table 23. Antibodies used.

## Abbreviations

aa	Amino acid
APS	Ammonium persulfate
AMP	Adenosine monophosphate
ARE	Antioxidant response element
ASC	Ascorbic acid
ATCC	American Type Culture Collection
ATF3	Activating transcription factor 3
ATF4	Activating transcription factor 4
ATF6	Activating transcription factor 6
ATP	Adenosine triphosphate
$\beta$ -Met	$\beta$ -Mercaptoethanol
Bp	Base pair
BSA	Bovine serum albumin
<i>ca.</i>	<i>circa</i>
cAMP	Cyclic adenosine monophosphate
cDNA	Complementary deoxyribonucleic acid
CHOP (GADD153)	CCAAT/enhancer-binding protein homologous protein
CHX	Cycloheximide
CK2	Protein kinase CK2 formerly known as Casein Kinase 2
CMH1	1-Hydroxy-3-methoxycarbonyl-2,2,5,5-tetramethylpyrrolidine

## Abbreviations

---

CMH	Cysteine hydrochloride monohydrate
cpm	Counts per minute
CT/C-terminus	Carboxy-terminus
Da	Dalton
DADS	Diallyl disulfide
DAPI	4', 6'-Diamidino-2-phenylindole
DAS	Diallyl sulfide
DATS	Diallyl trisulfide
DATTS	Diallyl tetrasulfide
DCFH-DA	2,7-Dichlorodihydrofluorescein diacetate
DEPC	Diethyl pyrocarbonate
DHE	Dihydroethidium
diH <sub>2</sub> O	Deionized water
DISC	Death inducing signaling complex
DMAT	2-dimethylamino-4, 5, 6, 7-tetrabromobenzimidazole
DMEM	Dulbecco's modified eagle medium
DMSO	Dimethylsulfoxide
DNA	Deoxyribonucleic acid
DNA-PK	DNA dependent protein kinase
dNTP	Deoxyribonucleotide triphosphate
dsDNA	Double-strand deoxyribonucleic acid
DTNB	5,5'-Dithio-bis-(2-nitrobenzoic acid)

## Abbreviations

---

DTT	Dithiothreitol
EB	Ethidiumbromide
ECL	Enhanced chemiluminescence
<i>E. coli</i>	<i>Escherichia coli</i>
EDTA	Ethylene diamine tetraacetic acid
EGCG	Epigallocatechin-3-gallate
EGFR	epidermal growth factor receptor
EGTA	Ethyleneglycol bis(2-aminoethyl ether)-N,N,N',N' tetraacetic acid
eIF2 $\alpha$	eukaryotic initiation factor 2 alpha
ER	Endoplasmic reticulum
ERK	Extracellular signal-regulated kinase
EPR	Electron paramagnetic resonance
ESR	Electron spin resonance
<i>etc.</i>	<i>et cetera</i>
Et <sub>3</sub> N	Triethylamine
Et <sub>2</sub> O	Diethyl ether
EtOH	Ethanol
FACS	Fluorescence activated cell sorting
FCS	Fetal calf serum
FADD	Fas-associated via death domain
FL	Full length



## Abbreviations

---

g	Gram
<i>g</i>	<i>Gravity</i>
G <sub>0</sub> -phase	Resting phase of the cell cycle
G <sub>1</sub> -phase	First Gap-phase of the cell cycle
G <sub>2</sub> -phase	Second Gap-phase of the cell cycle
Gal	Galactose
GAPDH	Glycerol aldehydephosphate-dehydrogenase
GF	Growth factor
GSH	Glutathione
GSSG	Reduced glutathione
GST	Glutathione S-transferase
GTP	Guanosin triphosphate
h	Hour
Hb	Hemoglobin
HD	Homeodomain
HEPES	4-(2-Hydroxyethyl)-1-piperazineethanesulfonic acid
HIPK2	Homeodomain-interacting protein kinase 2
His	Histidine
HO-1	Heme oxygenase-1
HRP	Horseradish peroxidase
ICAD	Inhibitor of caspase-activated DNase
i.e.	id est/that is

## Abbreviations

---

IF	Immunofluorescence
IgG	Immunoglobulin G
IP	Immunoprecipitation
IPTG	Isopropyl $\beta$ -D-1-thiogalactopyranoside
IRE-1	Inositol requiring enzyme 1
IUPAC	International Union of Pure and Applied Chemistry
JNKs	c-Jun N-terminal kinases
kb	Kilo base pairs
kDa	Kilodalton
Keap1	Kelch-like Ecd associated protein 1
LB	Luria-Broth
$\mu$	micro
M	Molar
MAPK	Mitogen-activated protein kinase
MeOH	Methanol
min	Minute
MnO <sub>2</sub>	Manganese dioxide
MOPS	3-(N-morpholino)-propanesulfonic acid
MPF	M-phase promoting factor
M-phase	Mitosis (cell division) phase of the cell cycle
MTT	3-(4,5-Dimethylthiazol-2-yl)-2,5-diphenyltetrazolium bromide
MW	Molecular Weight

## Abbreviations

---

NAC	<i>N</i> -Acetyl cysteine
NaCl	Sodium chloride
NaOH	Sodium hydroxide
N	Nitrogen
NQO1	NAD(P)H:quinone oxidoreductase 1
Nrf2	Nuclear factor-E2-related factor 2
O.D.	Optical density
ONPG	Ortho-nitrophenyl- $\beta$ -galactoside
PARP	Poly-ADP-Ribose-Polymerase
PBS	Phosphate buffer with salt
PCR	Polymerase chain reaction
PDGF	Platelet derived growth factor
Pdx-1	Pancreatic duodenal homeobox-1
PEBP	Phosphatidylethanolamine-binding protein
PEG	Polyethylene glycol
PERK	Pancreatic ER kinase
P <sub>i</sub>	Phosphate
PMSF	Phenylmethylsulfonyl fluoride
PVDF	Polyvinylidene fluoride
RNA	Ribonucleic acid
RNase	Ribonuclease
ROS	Reactive oxygen species

## Abbreviations

---

RPE	Retina pigment epithelial
rpm	Revolution(s) per minute
RSS	Reactive sulfur species
Ser	Serine
SAP	Shrimp alkaline phosphatase
SDS PAGE	Sodium dodecyl sulfate polyacrylamide gel electrophoresis
S-Phase	Synthesis phase of the cell cycle
sec	Second
SOD	Superoxide dismutase
SST	Somatostatin
StRE	Stress response element
SV25	Coumarin disulfide
SV29	Coumarin trisulfide
SV28	Coumarin tetrasulfide
SV40	Simian Virus 40
THF	Tetrahydrofuran
Thr	Threonine
<i>Taq</i>	<i>Thermophilus aquaticus</i>
TBB	4,5,6,7-Tetrabromobenzotriazole
TBS	Trisbuffer with salt
TCA	Trichloroacetic acid
TEMED	Tetramethylethylenediamine

## Abbreviations

---

TG	Thapsigargin
TGF	Tumour growth factor
TNB	2-Nitro-5-thiobenzoic acid
TNF- $\alpha$	Tumour necrosis factor $\alpha$
TPA	12-O-Tetradecanoylphorbol-13-acetat
Tris	Tris-(hydroxymethyl)-aminomethane
UPR	Unfolded protein response
UV	Ultraviolet
V	Volt
VEGF	Vascular endothelial growth factors
WB	Western blotting
WT	Wild-type
X-gal	5-Bromo-4-chloro-3-indolyl- $\beta$ -D-galactopyranoside
% (v/v)	Volume/volume percentage solution
% (w/v)	Weight/volume percentage solution

## **Table of Contents**

<b>Summary</b> .....	i
<b>Zusammenfassung</b> .....	iv
Acknowledgement.....	vi
List of Figures .....	viii
List of Tables.....	xii
Abbreviations .....	xiv
<b>1 Introduction</b> .....	1
<b>1.1 Polysulfides</b> .....	1
1.1.2 Sources of polysulfides.....	1
<b>1.2 Coumarins</b> .....	4
1.2.1 Biological activities associated with coumarin and coumarin derivatives.....	4
1.2.2 Coumarins induce cell cycle arrest and apoptosis in cancer cells. ....	5
<b>1.3 History of the “stinking rose”</b> .....	6
1.3.1 Garlic and its components .....	7
1.3.2 The chemistry of garlic .....	8
1.3.3 Generation of Reactive Oxygen Species (ROS) .....	9
1.3.4 Biological activities associated with polysulfides from garlic. ....	11
<b>1.4 Rationale of the project</b> .....	14
1.4.1 <i>The aims of the present study</i> .....	15
<b>2 Materials</b> .....	16
<b>2.1 Instruments</b> .....	16
2.1.1 Experimental materials .....	18
2.1.2 Experimental Kits and systems .....	19
<b>2.2 Chemicals</b> .....	19
<b>2.3 Buffers and solutions</b> .....	21

## Table of Contents

---

2.3.1	Stock solutions of test compounds .....	21
2.3.2	Antibiotics .....	22
2.3.3	Bacterial buffer.....	22
2.3.4	TYM-media.....	23
2.3.5	Buffer for plasmid isolation.....	23
2.3.6	Buffers for SDS- PAGE Electrophoresis.....	24
2.3.7	Buffers for $\beta$ -galactosidase assay.....	24
2.3.8	PBS and protein extraction buffers.....	25
2.3.9	Buffers for Western blotting .....	25
2.3.10	Stock solutions and buffers for immunofluorescence assays.....	26
2.3.11	CK2 kinase buffer and reaction mixture.....	26
2.3.12	Kerbs-Ringer buffer.....	26
<b>2.4</b>	<b>Cell lines</b> .....	<b>27</b>
<b>2.5</b>	<b>Test compounds</b> .....	<b>28</b>
<b>3</b>	<b>Methods</b> .....	<b>29</b>
<b>3.1</b>	<b>Cell culture</b> .....	<b>29</b>
3.1.1	Cell splitting .....	29
3.1.2	Freezing of cells.....	29
3.1.3	Thawing of cells.....	30
3.1.4	Counting of cells.....	30
3.1.5	Treatment of cells.....	31
3.1.6	Cell viability studies.....	32
3.1.7	Evaluation of cell morphology .....	33
3.1.8	Immunofluorescence analysis .....	33
3.1.9	Cell cycle analysis .....	34
<b>3.2</b>	<b>Measurement of Reactive Oxygen Species (ROS)</b> .....	<b>35</b>
3.2.1	Measurement of ROS using electron paramagnetic resonance (EPR) .....	35

## Table of Contents

---

3.2.2	Determination of O <sub>2</sub> <sup>•-</sup> in cell culture .....	36
3.2.3	Determination of H <sub>2</sub> O <sub>2</sub> in cell culture .....	37
3.2.4	Determination of total thiol content .....	37
<b>3.3</b>	<b>DNA techniques</b> .....	<b>38</b>
3.3.1	Plasmid amplification .....	38
3.3.2	DNA midipreparation.....	39
3.3.3	DNA quantification.....	40
3.3.4	Preparation of competent <i>E. coli</i> cells.....	41
3.3.5	Reporter constructs.....	41
3.3.6	Transient transfection and co-transfection of cells.....	42
<b>3.4</b>	<b>Protein methods</b> .....	<b>42</b>
3.4.1	Preparation of whole cell extracts.....	42
3.4.2	Nuclear and cytosolic fractionation.....	43
3.4.3	Cytosolic fractionation for cytochrome c release.....	43
3.4.4	Caspase 3/7 assay.....	44
3.4.5	Protein quantification .....	45
3.4.6	Sodium dodecyl sulfate polyacrylamide gel electrophoresis .....	46
3.4.7	Western blot analysis.....	48
3.4.8	Protein kinase assay.....	53
3.4.9	<i>In vitro</i> phosphatase assay for cdc25.....	53
3.4.10	Luciferase reporter assay.....	54
<b>4</b>	<b>Statistical analysis</b> .....	<b>56</b>
<b>5</b>	<b>Results</b> .....	<b>57</b>
5.1	Reduction of cell viability by diallyl polysulfides is dependent on the length of the sulphur chain.....	57
5.1.1	DATTS treatment leads to changes in HCT116 cell morphology .....	60



## Table of Contents

---

5.1.2	Treatment of HCT116 colon cancer cells with DATTS induces cell cycle arrest and apoptosis.....	62
5.1.3	DATTS inhibits CDK1 expression and cdc25C phosphorylation on threonine 48 .....	64
5.1.4	DATTS induces the mitochondrial apoptotic pathway in HCT116 colon cancer cells .....	65
5.1.5	DATTS-induced apoptosis is reduced by antioxidants.....	67
5.2	DATTS treatment induces formation of superoxide anion radicals and hydrogen peroxide in a time- and dosage-dependent manner.....	70
5.2.1	DATTS treatment leads to thiol depletion in HCT116 cells .....	73
5.3	DATTS induces both PERK and eIF2 $\alpha$ phosphorylation in HCT116 cells .....	73
5.3.1	DATTS induces Nrf2 nuclear translocation in HCT116 cells.....	77
5.3.2	DATTS induces HO-1 expression in HCT116 cells .....	80
5.3.3	DATTS induces expression of ATF3 in HCT116 cells involving calcium ions and some MAP kinases.....	87
5.4	DATTS-induced antioxidant response is not able to prevent apoptosis in HCT116 cells.....	93
5.5	DATTS causes a dosage-dependent disruption of HCT116 cellular microtubule network .....	97
5.6	Influence of DATTS on CK2 expression and kinase activity .....	98
5.7	Effect of DATTS on HCT116 cells compared to ARPE-19 Cells .....	100
5.7.1	Evaluation of cell viability .....	101
5.8	Coumarin polysulfides .....	109
5.8.1	Evaluation of cell viability .....	109
5.8.2	Treatment of HCT116 cells with coumarin trisulfide induces cell cycle arrest and apoptosis.....	111
<b>6</b>	<b>Discussion</b> .....	<b>122</b>
<b>7</b>	<b>References</b> .....	<b>145</b>
	<b>Publications</b> .....	<b>169</b>
	<b>Curriculum Vitae</b> .....	<b>170</b>

## 1 Introduction

### 1.1 Polysulfides

According to the International Union of Pure and Applied Chemistry (IUPAC) GOLD BOOK, polysulfides are defined as, "Compounds  $R-[S]_n-R$ , with a chain of sulfur atoms ( $n \geq 2$ ) and  $R \neq H$ ". They are generally divided into two groups, namely, anions and organic. Polysulfides belonging to the anion group have the formula  $S_n^{2-}$ , in which  $n$  is a number from 3 to 10 or more and are generally prepared by dissolving sulfur in solutions containing the sulfide ion,  $S^{2-}$ . Organic polysulfides on the other hand have the general formula  $RS_nR$ , where  $R = \text{alkyl or aryl}$ . These sulfur compounds have often been used as additives in the chemical industry for the manufacture of rubbers, adhesives and sealants [1, 2]. Organic polysulfides in particular have been found as biologically active ingredients in a number of *Allium* plant species including garlic and leeks [3, 4, 5]. The chemistry underlying the biological activity of these polysulfides is currently emerging. This polysulfide chemistry however, seems to include a combination of several distinct transformations, such as oxidation reactions, superoxide radical and peroxide generation, decomposition with release of highly electrophilic sulfur species, inhibition of metalloenzymes, perturbations of metal homeostasis and membrane integrity and interference with different cellular signalling pathways. Emerging evidence is pointing towards major beneficial effects of some of these polysulfides in agriculture and medicine, including antifungal, antibacterial, coronary heart diseases, cancer chemoprotection and cancer chemotherapy [5].

#### 1.1.2 Sources of polysulfides

A growing body of research is showing that dietary agents such as certain plants, spices, fruits and vegetables, which are critical to good health, may be sources for polysulfides {for review, see [6]}. These agents contain essential vitamins, minerals, fibre and phytochemicals that protect from chronic diseases. Polysulfides in particular have been found in many plants and lower organisms in addition to *Allium* species. Diallyl polysulfides for example, have been found in garlic (*Allium*

*sativum*), leek (*Allium ampeloprasum*) and in onion (*Allium cepa*), whilst coumarins (from which coumarin polysulfides are made) have been found in tonka beans (*Dipteryx odorata*), vanilla grass (*Anthoxanthum odoratum*) and in cassia cinnamon (*Cinnamomum aromaticum*) [7], to name but few (Fig. 1). These coumarins are joined together by sulfur bridges to make coumarin polysulfides [8, 9]. Other edible species also contain cyclic polysulfides with significant therapeutic potentials, such as Shiitake mushrooms (lenthionine and 1,2,3,4,5,6-thiepane, 1,2,4,6-tetrathiepane, 1,2,4-trithiolane) [10, 11], asparagus (1,2,3-trithiane-5-carboxylic acid, a plant growth inhibitor also suspected to act as contact allergen in dermatitis) [12] and the Mimosaceae *Parkia speciosa*. (lenthionine and a range of di- and polysulfides) [13]. Linear polysulfides, such as diallyl trisulfide (Fig. 2) and diallyl tetrasulfide (Fig. 2) and chemically related methyl-, ethyl- and propyl-based tri- and tetrasulfides also occur in trees, such as in barks of *Scorodophleus zenkeri* Harms from which a range of different di- and trisulfides with anticancer, antibacterial and antifungal activity have been isolated [14, 15, 16, 17].

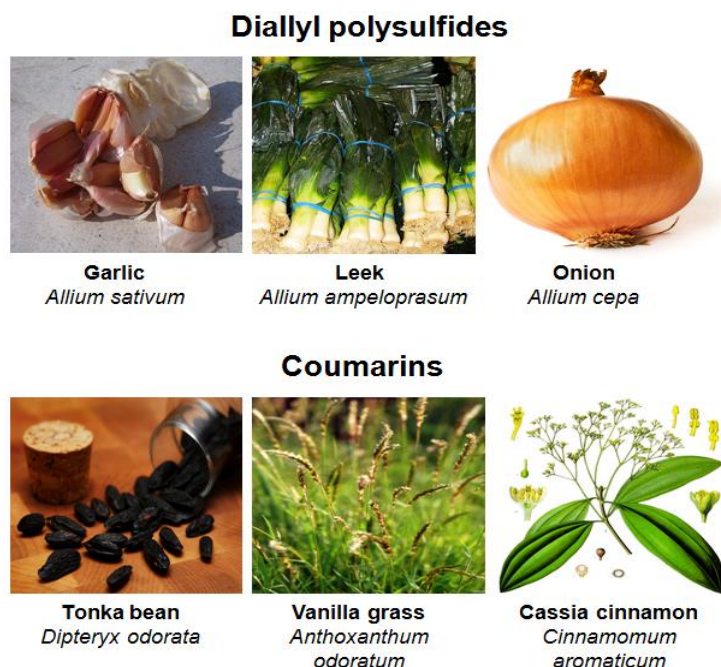


**Figure 1.** Sources of polysulfides. Adapted from Prasad *et al.*, 2012 [6].

The chemical structures of some of the polysulfides found in *Allium* plants and those of coumarin polysulfides are given in Figure 2. The reaction scheme for the synthesis of some of these polysulfides is also given in Figure 3. The synthesis of diallyl tetrasulfide for example was described by Derbesy and Harpp [18], whilst that of the coumarin polysulfides was described by Valente and colleagues [8, 9].

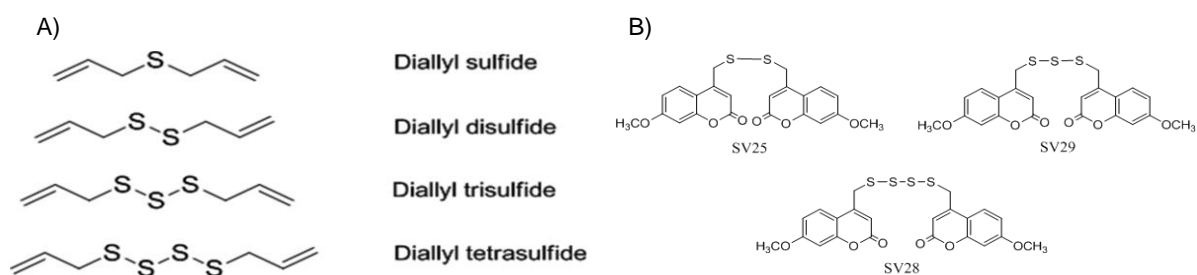


**Figure 2.** Chemical structures of A) diallyl polysulfides and B) coumarin polysulfides - SV25 - coumarin disulfide, SV29 - coumarin trisulfide and SV28 - coumarin tetrasulfide

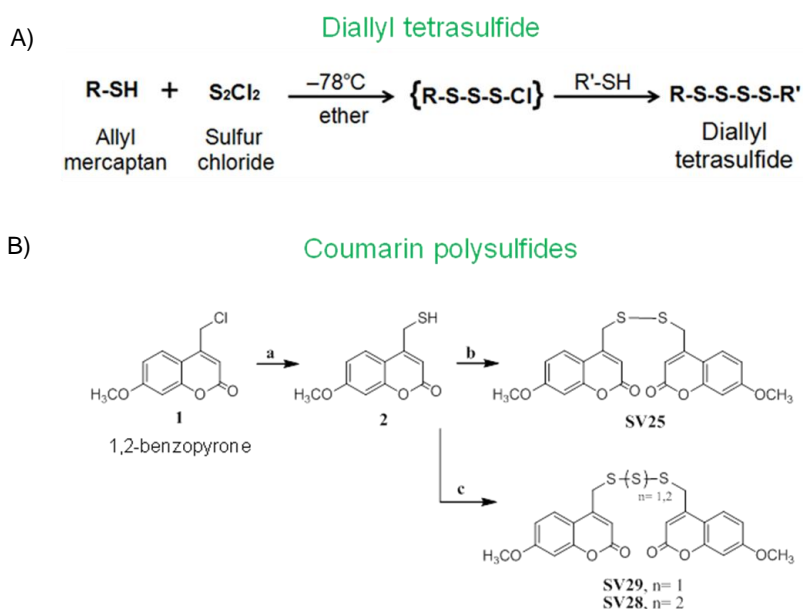


**Figure 3.** Reaction scheme for the synthesis of A) diallyl tetrasulfide and B) coumarin polysulfides. **a:** 1) thiourea, EtOH/Et<sub>2</sub>O, reflux, overnight ; 2) 2 N NaOH; **b:** MnO<sub>2</sub>, dry THF, 70°C, 1 h; **c:** Et<sub>3</sub>N, sulfur dichloride or disulfur dichloride, 0°C, 1 h.

## 1.2 Coumarins

Coumarin (2H-1-benzopyran-2-one) (Fig. 4), which owes its class of name to 'Coumarou', an amazonian dialect name for the tonka bean (*Dipteryx odorata*) tree, is an oxygen heterocyclic crystalline white compound with a sweet aromatic creamy odour. It has a widespread occurrence in the plant kingdom and plays an essential role in the realm of natural products (Fig. 1) [7]. The coumarin compound was first isolated from the tonka bean (*Dipteryx odorata*) in 1820 by a German scientist known as A. Vogel [19], and until the late 1890s it was obtained commercially only from this natural source. Since then, scientist have found substantial amounts of coumarins in vanilla grass, woodruff, lavender, licorice, strawberries, apricots, cherries, cinnamon, sweet clover and bison grass [20]. Coumarins may also be found in nature in combination with sugars as glycosides [21]. These coumarins are of great interest because they exhibit a broad range of applications: as perfumery; optical brightening agents; and dyes in laser technology [20]. Coumarin and its derivatives also display a broad range of biological properties such as coronary vasodilation, anticoagulant , anti-cancer, anti-bacterial, anti-HIV [22, 23, 24, 31, 32] and antifungal activities [25]. Some of these biological activities will be briefly discussed in the next section as part of this PhD thesis.

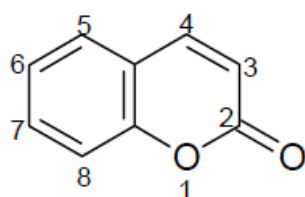


**Figure 4.** Structure of coumarin and atom numbering.

### 1.2.1 Biological activities associated with coumarin and coumarin derivatives

Over the years, coumarins and coumarin derivatives have generated a huge interest amongst scientists trying to unravel new natural products for the cure of diseases

such as cancer. They have proved for many years to have significant therapeutic potentials [26, 27, 28, 29, 30]. Studies have shown that some coumarins and their derivatives have multiple biological activities including disease prevention, growth modulation and antioxidant properties [23]. These compounds are known to exert anti-tumour effects [33, 34] and can cause considerable changes in the regulation of immune responses, cell growth and differentiation [35, 36, 37, 38, 39, 40]. In 1998 for example, Weber and colleagues showed that coumarin and its metabolite 7-hydroxycoumarin can exert antitumour activities against several human tumour cell lines [41]. Selected reports of the biological effects of coumarins and/or their derivatives are presented in Table 1, and some of the effects specific to cancer are discussed below in more detail.

### **1.2.2 Coumarins induce cell cycle arrest and apoptosis in cancer cells.**

Studies have shown that most coumarins and their derivatives induce cell cycle arrest and apoptosis in some cancer cells [42]. In 2007, Chuang and colleagues found out that not only was coumarin able to reduce cell viability, but also caused reactive oxygen species (ROS) production, cell cycle arrest in the G<sub>0</sub>/G<sub>1</sub> phase and subsequently apoptosis. They reported that coumarin treatment caused decreased expression of G<sub>0</sub>/G<sub>1</sub>-associated proteins, which may have led to the G<sub>0</sub>/G<sub>1</sub> arrest. They observed a decrease in the expression levels of anti-apoptotic proteins bcl-2 and bcl-xL, and an increase in the expression of the pro-apoptotic protein bax [42].

Reports also suggest that coumarins are potent against various kinds of cancer, including gastric [43, 44], malignant melanoma [43, 45], prostate and renal cell carcinoma [45, 46]. These coumarins come from a wide variety of natural sources and their vital roles in plant and animal biology have not been fully exploited. Furthermore, as new coumarin derivatives are being discovered or synthesised, new biological activities will certainly continue to be discovered, and this will subsequently help in identifying potential drug candidates from these compounds, which will eventually help in fighting diseases such as cancer.

<b>Biological activity</b>	<b>Reference</b>
Anticancer	Manojkumar <i>et al.</i> , 2009 [48]; Kotali <i>et al.</i> , 2008 [52]; Chuang <i>et al.</i> , 2007 [42]; Kostova <i>et al.</i> , 2006 [23]; Lopez-Gonzalez <i>et al.</i> , 2004 [55]; Finn <i>et al.</i> , 2001 & 2002 [53, 54]; Seliger and Pettersson 1994 [56].
Antifungal	Bisignano <i>et al.</i> , 2000 [19].
Anti inflammatory	Sandeep <i>et al.</i> , 2009 [49]; Asad <i>et al.</i> , 2009 [47].
Anticoagulant	Kostova <i>et al.</i> , 2006 [23].
Antimicrobial	Mohareb <i>et al.</i> , 2009 [50]; Kolancilar <i>et al.</i> , 2008 [51]; Bisignano <i>et al.</i> , 2000 [19].

**Table 1** Selected biological effects of coumarin and coumarin derivatives reported in literature.

### **1.3 History of the “stinking rose”**

Allium plants such garlic, onions and related plants have had important dietary and medicinal roles for centuries. There are numerous sketchy evidences of beneficiary effects of these plants to date but controlled studies have not shown consistent, long-term effects. That however, does not mean that the Allium plants don't work; only that scientific standards have not yet been met. Garlic - whose botanical name is *Allium sativum*, and belongs to the Allium genus of the Alliaceae family - is an Asiatic crop which has spread to other continents and is now broadly cultivated. Garlic is often referred to as the “stinking rose” because of its pungent odour. It is one natural product that has long been used at the beginning of recorded history as

a medicinal and cooking ingredient in most parts of the world. Its name is derived from the old English term *garleac*, which means "spear leek", and its history involves a lot of ancient cultures. It has been cherished by many for its healing powers and yet reviled by others for its pungent smell. Garlic was found to not only add flavour to food but also to boost strength, performance and prevent diseases in workers at most Egyptian pyramids and ancient Greek temples. The ancient Greek physician Hippocrates, who was revered and regarded by many as being the father of modern medicine, prescribed garlic for a variety of conditions; one of which was to treat cancerous tumours. It was also used in Greece as a "performance enhancing" agent in most Olympic athletes {for review, see [57]}. In China, it has long been recommended for fever, headache, cholera and dysentery [5]. In Korea, women have used garlic to bless themselves with supernatural powers and immortality, whilst in India it was used to warm the body, improve blood circulation, and cure digestive problems.

### **1.3.1 Garlic and its components**

We humans are becoming increasingly reliant on natural products for medical purposes simply because they are the most productive source of leads for the development of drugs. The cells of living organisms - plants, fungi, insects, and higher animals - are the sites of intricate and complex synthetic activities that result in the formation of a remarkable range of organic compounds, several of them of great practical importance to mankind. Knowing the health benefits of garlic and the fact that it has been around for such a long time makes one wonder why it is only now taking centre stage in combating various physiological threats such as cancer, immune dysfunction and cardiovascular diseases. It wasn't until the middle of the 19th century that a French chemist first reported the isolation of garlic oil from garlic plants. Also, in 1892, the German chemist F. W. Semmler reported that garlic oil, when fractionally distilled at low pressure, contained diallyl disulfide, diallyl trisulfide and diallyl tetrasulfide [58]. As modern medicine unearths the wonders of garlic, it is increasingly becoming evident that the chemical composition of this *Allium* plant includes not only the reactive sulphur species such as allicin (Fig. 6) but a host of



other chemicals such as antioxidants, enzymes and minerals including calcium, copper, iron, manganese, phosphorus, potassium and selenium [58, 59, 60].

### 1.3.2 The chemistry of garlic

Of increasing interest to a growing body of research is the investigation of the chemistry of polysulfides as biologically active ingredients of garlic. Garlic plant - particularly garlic bulb, is well known to contain a large number of biologically active sulfur compounds [59, 60]. These reactive sulfur species are enzymatically generated as part of binary plant defence system and each exhibits its own chemical properties and biochemical activity. A typical example is seen in allicin, the compound commonly associated with the biological activity of garlic. In garlic, allicin is synthesised and temporarily stored in the vacuoles 'on demand', i.e. when the clove is physically injured (e.g. chopping, crushing) or attacked by microbes [58, 59, 61]. Alliin, a chemically unreactive sulfoxide and precursor for allicin is, however, produced and stored in the cytosol when the cysteine derivative  $\gamma$ -glutamyl-S-alk(en)yl-L-cysteine is hydrolysed and oxidised [60]. Once the garlic clove is physically injured, alliin gets enzymatically converted to the highly reactive thiosulfinate allicin by the C-S-lyase enzyme alliinase. Allicin, which has been associated with cytotoxic effects against several cancer cells [61, 62, 63], is highly unstable and can be easily decomposed if left at room temperature for a long period of time or if exposed to higher temperatures (like during cooking for example). Decomposition and degradation of allicin results in a range of 'second generation' products including: diallyl sulfide (DAS), DADS, DATS and DATTS. Other decomposition products of allicin includes: dithiins 3-vinyl-3,4-dihydro-1,2-dithiin, 2-vinyl-2,4-dihydro-1,3 dithiin and ajoene. Of course, other follow-on reactions of allicin and polysulfides may occur, especially with intracellular thiols, resulting in additional sulfur species, such as thiolated cysteine and cysteine residues in peptides and proteins. The polysulfides can also be reduced, by glutathione for example, to form allylmercaptan, allyl perthiol and possibly allyl hydrotrisulfide (for a review, see [58, 63]).

Another striking area of the chemistry of garlic is to do with formulations of a network of chemical and biochemical reactions that are geared towards understanding aspects of the biological activity of polysulfides. This area of garlic is currently emerging and most of it is only speculative at the moment. The chemistry seems to involve several distinct chemical reactions that interfere with diverse cellular signalling pathways (Fig. 7). Some of these chemical reactions include protein thiolations [62, 63, 65], hydrophobic interactions [65] and generation of reactive oxygen species [66, 67]. Even more fascinatingly, some of these chemical reactions seems to trigger others in eliciting response leading to several cellular signalling pathways. As part of this PhD thesis, therefore, aspects of this polysulfide chemistry will be explored.

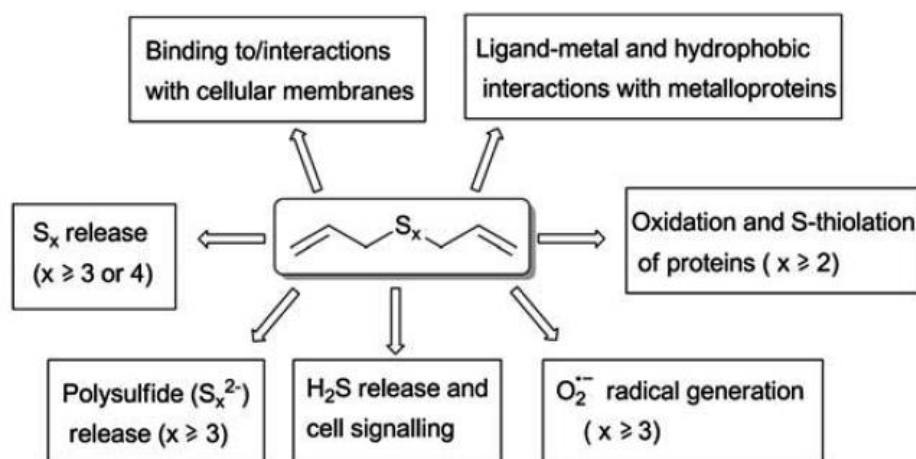


**Fig. 5** Chemical properties and reactivity of polysulfides which may explain aspects of their biological activity. Please note that some parts of this scheme are only speculative. Taken from Schneider *et al.*, 2011 [68].

### 1.3.3 Generation of Reactive Oxygen Species (ROS)

Reactive Oxygen Species (ROS) are small, highly reactive molecules that play a vital role in cell signalling. They can be organic or inorganic and their reactivity is mostly due to the unpaired electrons they carry. They are normally natural byproducts of oxygen metabolism, however they can also be formed by exogenous sources such as ionising radiation. The mechanism through which diallyl polysulfides generate

ROS is not quite understood at the moment. The general consensus, though, is that these polysulfides react with glutathione (GSH) in the presence of enzymes such as glutathione transferase and are reduced to perthiols. The perthiols are easily oxidized to perthiyl radicals, which can further react with GSH to form polysulfide radical anions (Fig. 6). These then can reduce molecular oxygen to generate ROS (for review, see [62, 63, 67, 73]). A schematic representation of how diallyl polysulfides induce ROS generation is given in Figure 8, and some of the radicals generated are shown in Table 2.

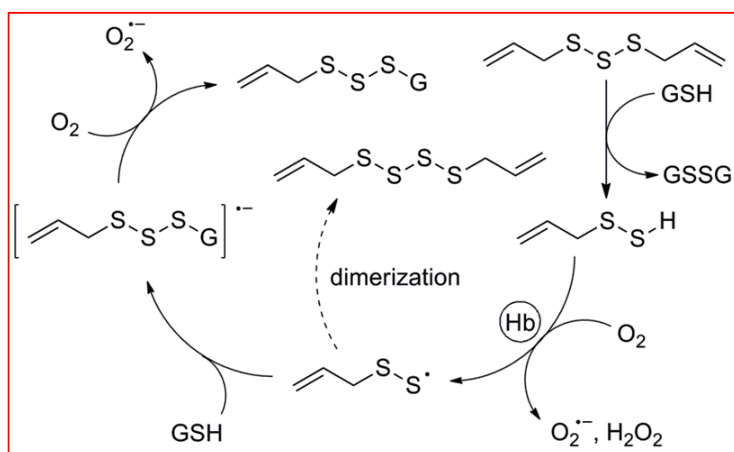


**Figure 6.** Proposed mechanism for polysulfide-induced ROS generation. For example, in the presence of an enzyme such as glutathione transferase, diallyl trisulfide will react with intracellular components such as GSH and  $O_2$  to generate ROS.

ROS can cause oxidative damages to DNA. The nature of damages includes mainly base modifications, deoxyribose oxidation, strand breakage and DNA-protein cross-links. All of these of course may lead to tumour progression, mutation and metastasis [63, 64, 69]. ROS production may also interfere with normal cell signalling, resulting thereby in alteration of the gene expression, and development of cancer by redox regulation of transcription factors/activators and/or by oxidatively modulating the protein kinase cascade [70, 71, 72].

Furthermore, ROS can cause tissue damage by reacting with sulfhydryl groups in proteins. They can disrupt key cytoskeleton components (such as microfilaments

and microtubules) of the cell through modifications of specific cysteine residues of both actin and tubulin [74, 75].

Type	Reactive species	Chemical formula
<b>ROS</b>		
<i>Non-Radical</i>	Peroxide	ROOR
	Singet oxygen	O <sub>2</sub>
<i>Radical</i>	Hydroxyl-radical	HO <sup>•</sup>
	Superoxide anion	O <sub>2</sub> <sup>•-</sup>
<b>RSS</b>		
<i>Non-Radical</i>	Thiol	RSH
	Disulfide	RSSR
	Sulfenic acid	RSOH
	Thiosulfinate (disulfide-S-monoxide)	RS(O)SR
	Thiosulfonate (disulfide-S-dioxide)	RS(O) <sub>2</sub> SR
<i>Radical</i>	Thiyl-Radical	RS <sup>•</sup>

**Table 2** Reactive oxygen and sulphur species (adapted from Giles and Jacob., 2002 [77]).

#### 1.3.4 Biological activities associated with polysulfides from garlic.

Before delving into this part of the thesis, it should be noted beforehand that the emerging details of the biological activities of some of these compounds are often quite sketchy and we have little or no knowledge about, the mechanism through which the response is elicited. In some cases this knowledge is only speculative.

Therefore, as part of this thesis, aspects of the biological activities associated with polysulfides will be studied.

Like the coumarins and their derivatives, recently published results of animal and *in vitro* studies have shown that active ingredients in garlic have multiple biological activities including disease prevention, growth modulation and antioxidant properties [5, 63, 80]. Components of garlic are involved in cholesterol lowering and may also reduce the risks of atherosclerosis and allied cardiovascular complexities [77]. A review by Fleischauer and Arab (2001) [81] of the epidemiologic literature in garlic consumption addressing cancers of the stomach, colon, head and neck, lung, breast and prostate in a Chinese population, suggests a preventive effect of garlic particularly in stomach and colorectal cancers. A major breakthrough was made when polysulfides from garlic were used to treat various types of diseases (for review, see [4, 5, 63]). Polysulfides can inhibit cell proliferation and they may do so by targeting members of the cell cycle signalling cascades, leading to growth arrest [79]. Figure 5 shows some of the cell cycle regulatory proteins that may be targeted by components of garlic such as polysulfides.

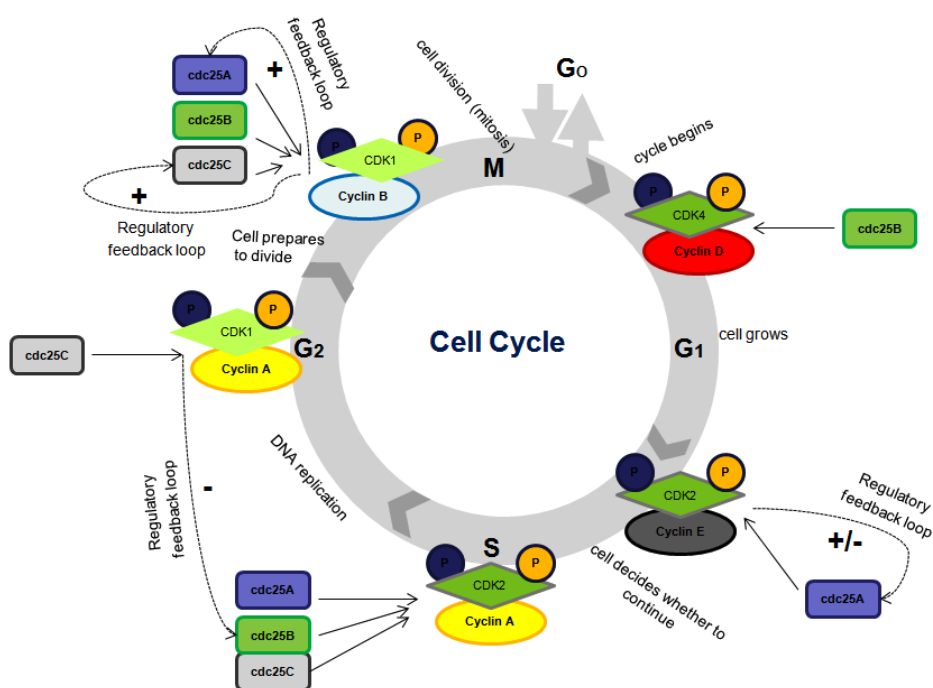


**Figure 7.** The cell cycle with its regulatory proteins.

Furthermore, garlic components such as DADS have been attributed to not only inhibit cell proliferation, but also to induce oxidative stress and apoptosis in most cancer cells [69, 70, 76, 78].

From these data, it seems to be clear that garlic - or some of its components - definitely has an impact on the cell cycle and the cell cycle proteins. It is still unclear though, whether and how polysulfides from garlic target these cell cycle molecules directly or whether they act via reactive oxygen species (ROS) and DNA damage which then induces the downstream pathway with ATR, chk1 and cdc25C for example. It may also be that longer-chain polysulfides such as DATS and diallyl tetrasulfide (DATTS) may react differently in inducing cell cycle arrest and/or apoptosis. It also remains an open question which is the key molecule for the switch from cell cycle arrest to apoptosis. Some of these areas will also be explored as part of this PhD thesis.

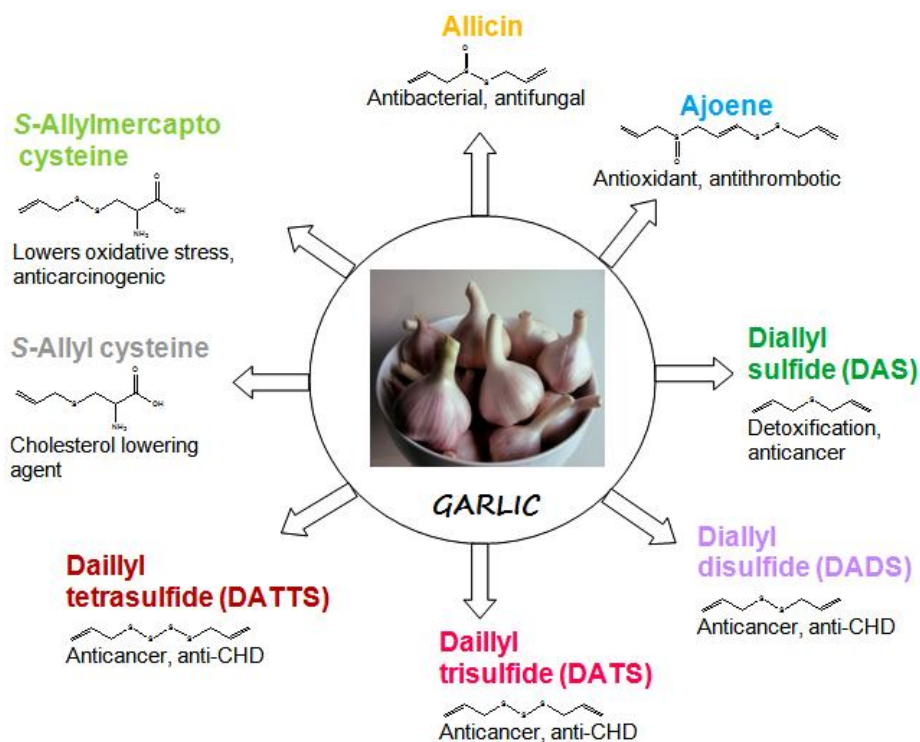


**Figure 8.** Components of garlic and their biological activities.

## **1.4 Rationale of the project**

A host of natural compounds are today being used in cancer therapy and prevention, whilst a lot more are still being investigated for their anticancer capabilities. There have long been indications that coumarins and garlic protect from cancer. Garlic in particular has a variety of different compounds which increase immune competence; suppress cell division and cell proliferation or which induce apoptosis [5, 63, 70, 80]. Most importantly, reports suggest that the biological activity of the garlic compounds in particular increase with the length of the sulfur chain [62]. The purity of some of these compounds, however, have been questionable. Prof. Claus Jacob from the Institute of Bioorganic Chemistry, University of the Saarland, synthesised and highly purified diallyl mono-, di-, tri- and tetrasulfides. He also synthesised control compounds where sulfur atoms were replaced by carbon and where C=C double-bonds were replaced by C-C single bonds. Using cancer cell lines, results from preliminary work in our group suggested that diallyl tri- and diallyl tetrasulfides may inhibit cell growth and cause them to go into apoptosis [82]. Control experiments revealed that the sulfur chain of the polysulfides are essential for this activity, whereas the C=C double bonds are not necessary. Previous studies have already shown that diallyl mono-, di- and tri-sulfides can cause oxidative stress in a variety of cancer cells through the generation of ROS [67, 69, 82]. They have also been shown to cause alterations in intracellular thiol levels which affect cellular functions, including signalling pathways which may in turn cause cell cycle arrest and induction of apoptosis [73, 75]. Although diallyl polysulfides cause oxidative stress, little is known about the underlying signalling cascades leading to antioxidant defence or apoptosis, and unlike diallyl mono-, di- and tri-sulfides, which have all been well characterised, the corresponding diallyl tetrasulfide has hardly been used.

Interestingly, in order to find new drugs with anticancer activities similar to or better than diallyl polysulfides, Dr. Sergio Valente from Université de Lorraine in Metz, France, made use of both coumarins and polysulfides and synthesised novel hybrid-type bis-coumarin polysulfides as disulfur, trisulfur and tetrasulfur coumarins.

### **1.4.1 The aims of the present study**

Cancer research these days is generally focused on the discovery of novel drugs that are able to prevent cancer cell growth and induce apoptosis. Therefore, not only is there a new appeal for the highly purified and newly synthesised compounds, but also investigating for their effects on cancer cells, which may unravel new pathways or new components within old pathways. This allowed major questions to be asked in this work, such as, (i) are the newly synthesised coumarin derivatives and the more pure diallyl polysulfides, anticancer agents? If yes, then what is the mechanism involved? (ii) do the polysulfides have the same effect on normal cells as in cancer cells? Hence, the aims of the present study were a) to investigate the anticancer activities of coumarin and diallyl polysulfides on HCT116 colon cancer cells, b) to identify the most potent (in terms of antigrowth and apoptosis) of these compounds, c) to unravel the mechanism of action of the potent compounds, d) to focus on the molecular aspects of interactions with their recognised cellular targets, such as microtubules and e) to compare the effects of these sulfur compounds on cancer cells to that on normal cells.



## 2 Materials

### 2.1 Table 3. Instruments

Instrument	Source
96-well microplate luminometer. Gamma radiation survey monitor LB122.	Berthold Technologies, Bad Wildbad, Germany
Autoclave Varioklav <sup>®</sup> 400	H+P Labortechnik, Oberschleissheim, Germany
Bench-top centrifuge Sigma 4K10	Sigma Laborzentrifugen GmbH, Osterode, Germany
Fixed-angle rotor for Avanti J series centrifuge JLA 8.1000, JA 10, JA 25.50. Fixed-angle rotor for Optima series ultracentrifuge 701Ti. J2-HS Refrigerated high-speed centrifuge.	Beckman Coulter, Fullerton, USA
Certomat <sup>®</sup> shaking incubator R & H	Sartorius, Goettingen, Germany
Laboratory balance ALS120-4, EW420	Kern and Sohn, Balingen, Germany
Laboratory pH meter InoLab pH 537	WTW, Weilheim, Germany
Magnetic stirrer JKA RCT	JKA Werke GmbH & Co. Staufen, Germany
Microcentrifuge 5415C, 5415R (Cool). Thermomixer 5436 & Comfort.	Eppendorf, Hamburg, Germany
Mighty Small <sup>™</sup> SE250 Mini-Vertical gel	Hofer Scientific Instruments,

Materials

---

electrophoresis units.  Mighty Small™ multiple gel casters SE200.	Heidelberg, Germany
Milli-Q Plus water filtration purification system	Millipore, Schwalbach/Ts, Germany
Nanodrop ND-1000 spectrophotometer	Peqlab, Karlsruhe, Germany
Pipette PIPETMAN P10, P20, P200, P1000	Gilson, Villiers le Bel, France
Pipetus® pipette controller	Hirschmann, Eberstadt, Germany
Platform rocking shaker 3013	GFL, Burgwedel, Germany
Power supply for electrophoresis system Consort E455	Keutz, Reiskirchen, Germany
Sonifier® cell disruptor B15	Branson, Danbury, CT, USA
TECAN infinite M200PRO	Tecan Group AG, Männedorf, Switzerland
Thermo scientific Heraeus® B6030 microbiological incubator.  Thermo scientific Heraeus® BBD6220 CO <sub>2</sub> incubator.  Thermo scientific Heraeus® biological safety cabinet.	Heraeus, Hanau, Germany
Transonic T460	Elma GmbH, Singen, Germany
UV table	Bachofer, Reutlingen, Germany
UV/visible spectrophotometer Ultrospec 2100pro	Amersham Biosciences, Freiburg, Germany
Vortex Genie 2	Bender and Hobein AG, Zurich,

## Materials

	Switzerland
Vacuum gel dryer	Labortechnik Froebel, Lindau, Germany
Water bath GFL	Julabo, Seelbach, Germany
Zeiss Axiovert 100 inverted microscope. Zeiss LSM 510 meta spectral confocal microscope	Carl Zeiss, Goettingen, Germany

### 2.1.1 Table 4. Experimental materials

Experimental material	Source
1.7 ml micro test tube. DynaGrad <sup>®</sup> syringe tip filters 0.22 µm.	Carl Roth, Karlsruhe, Germany
15 and 50 ml Falcon tubes. 60 and 100 mm cell culture dishes. 6- and 24-well cell culture plates. 96 Microwell plates (Cell culture). Petri dishes 94 mm for bacteria culture	Greiner Bio-One GmbH, Frickenhausen, Germany
Blotting paper	Macherey-Nagel, Dueren, Germany
Cover slips 10x10 mm	Marienfeld, Lauda-Koenigshofen, Germany
Fluoro Nunc <sup>TM</sup> 96 Microwell plates	Nunc, Wiesbaden, Germany
Microscope slides 76x26 mm	Gerhard Menzel, Braunschweig, Germany

P81 Ion-exchange filterpaper. 3 MM Filterpaper	Whatman, Kent, UK
Parafilm M all-purpose laboratory film	Pechiney Plastic Packaging, Chicago, USA
Pipette tips, 10, 20, 200, and 1000 $\mu$ l.	ABIMED, Langenfeld, Germany
PVDF Western blotting membrane 0.45 $\mu$ m	Roche, Diagnostics, Mannheim, Germany
Semi-micro disposable plastic cuvette	Sarstedt, Nuembrecht, Germany
UV quartz cuvette 10 mm	Hellma, Muehlheim, Germany

### 2.1.2 Table 5. Experimental Kits and systems

Kit	Source
Caspase-Glo <sup>®</sup> 3/7 Assay kit Luciferase assay kit	Promega GmbH, Mannheim, Germany
Effectene <sup>TM</sup> transfection kit	Qiagen, Hilden, Germany
Nucleobond <sup>®</sup> AX-plasmid-purification kit	Macherey-Nagel, Dueren, Germany

### 2.2 Table 6. Chemicals

Chemical	Source
Penicillin/Streptomycin	Biochrom K.G, Berlin, Germany
Bio-Rad protein assay	Bio-Rad, Munich, Germany

## Materials

Ethidiumbromide (EB)	Boehringer, Ingelheim, Germany
CK2 inhibitor (TBB), Thapsigargin (TG)	Calbiochem, Darmstadt, Germany
Acrylamide/Bisacrylamide Rotiphorese <sup>®</sup> Gel30, Agarose, Ampicillin, ECL Lumi-Light Western blot detection reagents – Luminol (3-Aminophthalhydrazide) and PCA (p-Coumaric-Acid), 37% Formaldehyde, LB-Medium, Lysozyme, Agar-Agar, Tetramethylethylenediamine (TEMED)	Carl Roth GmbH, Karlsruhe, Germany
TritonX-100, Tween20	Fluka, Neu-Ulm, Germany
DMEM and RPMI-1640 cell culture medium	Gibco, Munich, Germany
Skimmed milk powder	J.M. Gabler Saliter, Oberguenzburg, Germany
Radiochemical [ <sup>32</sup> P]γATP (10 μCi/μl)	Hartmann Analytic, Braunschweig, Germany
Generuler <sup>™</sup> DNA 1kb/100bp plus ladder, Prestained/Unstained SDS-Molecular weight standard	Fermentas, GmbH, St. Leon, Germany
Dimethylsulfoxide (DMSO)	Merck, Darmstadt, Germany
Amplex <sup>®</sup> Red Hydrogen Peroxide assay kit and epigallocatechin-3-gallate (EGCG)	Molecular Probes, Darmstadt, Germany
Foetal Calf Serum (FCS), Bovine Serum Albumin (BSA)	PAA Laboratories, GmbH, Pasching, Austria
McCoy's 5A cell culture medium	PromoCell, Heidelberg, Germany

4,6-Diamidino-2-phenylindol (DAPI), Complete™, Protease inhibitor cocktail.	Roche, Mannheim, Germany
Ammonium persulfate (APS), Trypanblue	Serva, Heidelberg, Germany
3-(4,5-Dimethylthiazol-2-yl)-2,5-diphenyltetrazolium bromide (MTT), Ascorbic acid (ASC), Dihydroethidium (DHE), Dithiothreitol (DTT), Ethylenediaminetetraacetic acid (EDTA), Ethyleneglycol bis(2-aminoethyl ether)-N,N,N',N' tetraacetic acid (EGTA), Glutathione (GSH), HEPES, N-Acetyl cysteine (NAC), Nonidate P-40 (NP-40), <i>ortho</i> -Nitrophenyl-β-galactoside (ONPG)	Sigma-Aldrich, Munich, Germany
Ellman's reagent (5,5' –Dithiobis(nitrobenzoic acid) ), and Cysteine hydrochloride monohydrate (CMH)	Thermo Scientific, Schwerte, Germany

## 2.3 Buffers and solutions

### 2.3.1 Table 7. Stock solutions of test compounds

Compound	Stock solution and storage
DAS	80 mM DAS. Dissolved in DMSO. Aliquot and stored at -20°C. Used within 2 days.
DADS	80 mM DADS. Dissolved in DMSO. Aliquot and stored at -20°C. Used within 2 days.
DATS	80 mM DATS. Dissolved in DMSO. Aliquot and stored at -20°C. Used

## Materials

	within 2 days.
DATTS	80 mM DATTS. Dissolved in DMSO. Aliquot and stored at -20°C. Used within 2 days.
SV25	80 mM SV25. Dissolved in DMSO. Freshly prepared.
SV29	80 mM SV29. Dissolved in DMSO. Freshly prepared.
SV28	80 mM SV28. Dissolved in DMSO. Freshly prepared.
NAC	80 mM NAC. Dissolved in diH <sub>2</sub> O. Aliquot and stored at -20°C. Used within a month.
ASC	20 mM ASC. Dissolved in diH <sub>2</sub> O. Freshly prepared.
GSH	20 mM GSH. Dissolved in diH <sub>2</sub> O. Freshly prepared.
EGCG	20 mg/ml. Dissolved in DMSO. Freshly prepared.

### 2.3.2 Table 8. Antibiotics

Antibiotics	Component
<b>Ampicillin</b> 50 mg/ml (1000x)	50 mg Ampicillin. Dissolved in 1 ml diH <sub>2</sub> O, filtered and stored at -20°C.
<b>Kanamycin</b> 25 mg/ml (1000x)	25 mg Kanamycin. Dissolved in 1 ml diH <sub>2</sub> O, filterer and stored at -20°C.
<b>Tetracycline</b> 6.5 mg/ml (500x)	6.5 mg Tetracycline. Dissolved in 1 ml ethanol, filtered and stored at -20°C.

### 2.3.3 Table 9. Bacterial buffer

Bacteria medium	Component

<b>LB-Broth medium</b> (pH 7.3)	1% Bacto-Tryptone, 0.5% Bacto-Yeast extract and 1% NaCl. Dissolved in diH <sub>2</sub> O, autoclaved and stored at room temperature
<b>LB-Broth-Agar plates</b> (pH 7.3)	1% Bacto-Tryptone, 0.5% Bacto-Yeast extract, 1% NaCl and 2% Bacto-Agar. Dissolved in diH <sub>2</sub> O, autoclaved and agar allowed to cool down to about 50°C in a sterilised bacteria cabinet. Added antibiotics (50 µg/ml ampicillin, 12.5 µg/ml tetracycline or 25 µg/ml kanamycin; were applicable). Poured component into petri dishes, allowed to solidify and stored at 4°C.

### 2.3.4 Table 10. TYM-media

TYM-medium	Component
<b>LB-Broth medium</b> (pH 7.3)	20 g Bacto-Tryptone, 5 g Bacto-Yeast extract, 5 g NaCl and 2 g MgSO <sub>4</sub> . Dissolved in 1 l diH <sub>2</sub> O and autoclaved.
<b>TfBI</b>	30 mM K-Acetate, 50 mM MnCl <sub>2</sub> , 100 mM KCl, 10 mM CaCl <sub>2</sub> , and 15% Glycerol. Dissolved in diH <sub>2</sub> O and autoclaved.
<b>TfBII</b> pH 7.0	10 mM Na-Mops, 10 mM KCl, 75 mM CaCl <sub>2</sub> , and 15% glycerol. Dissolved in diH <sub>2</sub> O and autoclaved.

### 2.3.5 Table 11. Buffer for plasmid isolation

Buffer	Component
<b>Solution 1</b> (pH 8.0)	50 mM Tris-HCl, 10 mM EDTA and 100 µg/ml DNase free RNase A. Dissolve in diH <sub>2</sub> O and store at 4°C.
<b>Solution 2</b>	200 mM NaOH and 1% SDS. Dissolve in diH <sub>2</sub> O and store at room temperature



<b>Solution 3</b> (pH 5.5)	3 M K-Acetate. Dissolve in diH <sub>2</sub> O and store at 4°C.
----------------------------	---

### 2.3.6 Table 12. Buffers for SDS- PAGE Electrophoresis

Buffer	Component
<b>Gel solution A</b> (for both separating and stacking gels) Ready-to-use	Acrylamide 30% and Bisacrylamide 0.8% Stored at 4°C
<b>Gel solution B</b> (for both separating and stacking gels)	4 g SDS and 181.5 g Tris-HCl, pH 8.8. Dissolved in 1000 ml diH <sub>2</sub> O and stored at 4°C
<b>Gel solution C</b> (for stacking gel)	4 g SDS and 60 g Tris-HCl, pH 6.8. Dissolved in 1000 ml diH <sub>2</sub> O and store at 4°C
<b>APS</b>	Ammonium persulfate. Dissolved 1 g in 10 ml diH <sub>2</sub> O and store at 4°C
<b>3 x SDS sample buffer</b>	195 mM Tris-HCl, 6% SDS, 15% β-mercaptoethanol, 30% glycerol and 0.03% bromophenol blue. Dissolved in diH <sub>2</sub> O and stored at room temperature
<b>Electrophoresis buffer</b> (pH 8.8)	25 mM Tris-HCl, pH 8.8, 192 mM glycerol and 3.5 mM SDS. Dissolved in diH <sub>2</sub> O and stored at room temperature

### 2.3.7 Table 13. Buffers for β-galactosidase assay

Solution	Component
----------	-----------

## Materials

<b>0.1 M Sodium phosphate solution</b> pH 7.5	0.2 M Na <sub>2</sub> HPO <sub>4</sub> (41 ml), 0.2 M NaH <sub>2</sub> PO <sub>4</sub> (9 ml). Dissolved in 50 ml diH <sub>2</sub> O and stored at 4°C.
<b>100×Mg solution</b>	0.1 M MgCl <sub>2</sub> , 4.5 M β-mercaptoethanol. Dissolved in diH <sub>2</sub> O and stored at 4°C.
<b>4 mg/ml ONPG</b> pH 7.4	4 mg/ml ONPG. Dissolved in 0.1 M sodium phosphate solution and stored at 4°C.

### 2.3.8 Table 14. PBS and protein extraction buffers

Buffer	Component
<b>PBS (pH 7.4)</b>	137 mM NaCl, 2.7 mM KCl, 8 mM Na <sub>2</sub> HPO <sub>4</sub> and 1.5 mM KH <sub>2</sub> PO <sub>4</sub> . Dissolved in diH <sub>2</sub> O and stored at 4°C
<b>Protein binding buffer (pH 7.6)</b>	20 mM Tris-HCl, 100 mM NaCl, 0.5 mM EDTA, 1 mM DTT, 10% glycerol, 0.1% Tween 20 and 2% skimmed milk powder. Dissolved in diH <sub>2</sub> O. Freshly prepared
<b>Cellular protein extraction buffer</b> RIPA lysis buffer pH 8.0	50 mM Tris-HCl, 150 mM NaCl, 0.5% Na-deoxycholate, 1% Triton X-100 and 0.1% SDS. Dissolved in diH <sub>2</sub> O and stored at 4°C

### 2.3.9 Table 15. Buffers for Western blotting

Buffer	Component
<b>Transfer buffer (pH 8.3)</b>	20 mM Tris-HCl and 150 M glycerol. Dissolved in diH <sub>2</sub> O and stored at 4°C
<b>Blocking buffer (pH</b>	0.1% Tween 20 and 5% skimmed milk powder. Dissolved in

7.5)	PBS and stored at 4°C
<b>Washing buffer 1</b> (pH 7.5)	0.1% Tween 20 and 1% skimmed milk powder. Dissolved in PBS and stored at 4°C
<b>Washing buffer 2</b> (pH 7.5)	0.1% Tween 20 in PBS and stored at 4°C

### 2.3.10 Table 16. Stock solutions and buffers for immunofluorescence assays

Stock solution	Component
<b>DAPI</b> 5 µg/ml (50x)	50 µg DAPI. Dissolved in 10 ml methanol. Working concentration 0.1 µg/ml. Store at -20°C.
<b>Mounting medium</b>	5% Polyvinylalcohol 25/140 and 10% glycerol. Dissolve in PBS and autoclave. Store at -20°C.

### 2.3.11 Table 17. CK2 kinase buffer and reaction mixture

Buffer	Component
<b>CK2 kinase buffer</b> (pH 7.5)	50 mM Tris-HCl, 100 mM NaCl, 10 mM MgCl <sub>2</sub> and 1 mM DTT. Dissolved in diH <sub>2</sub> O and stored at -20°C
<b>CK2 reaction mixture</b> (pH 8.5)	41.6 mM Tris-HCl, 250 mM NaCl, 8.4 mM MgCl <sub>2</sub> , 2 mM DTT, 84 µM ATP and 0.32 mM synthetic peptide for CK2. Dissolved in diH <sub>2</sub> O and stored at -20°C

### 2.3.12 Table 18. Kerbs-Ringer buffer

Buffer	Component
<b>Kerbs-Ringer</b>	142 mM NaCl, 5.5 mM KCl, 1.4 mM MgSO <sub>4</sub> , 1.4 mM KH <sub>2</sub> PO <sub>4</sub> ,

<b>buffer</b> (KRB) - pH 7.4	3.1 mM CaCl <sub>2</sub> . Dissolved in diH <sub>2</sub> O, gased with carbogen, adjusted to pH 7.4 and stored at 4°C.
---------------------------------	--

## 2.4 Table 19. Cell lines

Cell type	Description	ATCC Number	Growing medium	Source
p53- positive HCT116	Human epithelial colorectal cancer cells. Have a mutation in codon 13 of the ras protooncogene.	CCL-247™	maintained at 37°C and 5% CO <sub>2</sub> in McCoy's 5A medium (PromoCell, Heidelberg, Germany) with 10% fetal calf serum (FCS).	Lab collection
ARPE-19	Human Retinal pigment epithelial noncancer cells	CRL-2302™	maintained at 37°C and 5% CO <sub>2</sub> in a Dulbecco's modified Eagles medium (DMEM) supplemented with 2 mM L-glutamine, 1 mM gentamicin and 10% FCS.	Prof. Dr. Berthold Seitz, Homburg, Germany
HeLa	Human epithelial cervical cancer cells.	CCL-2™	maintained at 37°C and 5% CO <sub>2</sub> in a Dulbecco's modified Eagles medium (DMEM) supplemented with 2 mM L-glutamine, 1 mM gentamicin and	Lab collection

			10% FCS.	
C3H10T1/2	Murine pluripotent stem cells.	CCL-226™	maintained at 37°C and 5% CO <sub>2</sub> in a Dulbecco's modified Eagles medium (DMEM) supplemented with 2 mM L-glutamine, 1 mM gentamicin and 10% FCS.	Lab collection
LNCaP	Androgen-sensitive human prostate cancer cells	CRL-1740™	maintained at 37°C in RPMI 1640 medium supplemented with 10% FCS in an atmosphere enriched with 5% CO <sub>2</sub> .	Lab collection

## 2.5 Test compounds

The diallyl polysulfides were kindly provided by Prof. Dr. Claus Jacob, whilst the coumarin polysulfides were from Dr Sergio Valente. To make stock solutions, each compound was dissolved in the appropriate medium and stored accordingly (see Table 8). In the treatment of cells, the appropriate compound stock solution was diluted in the cell culture medium to the desired concentration and applied to the cells before incubation.

## **3 Methods**

### **3.1 Cell culture**

All of the cells used in this study were grown in the appropriate media that was supplemented with 10% FCS in an incubator at 37°C and with 5% CO<sub>2</sub> in a moist atmosphere. The cell were grown in/on one of the following: 100 or 60 mm culture dish (Greiner), 6, 24 or 96 well plate (Greiner).

#### **3.1.1 Cell splitting**

Before splitting the cells, the cell culture medium and PBS were first pre-warmed in a water bath at 37°C . Using the microscope, the cells were screened for density, dead cells or contamination. The medium of the cells was removed from the dish using a pastuer pipette under vacuum. The cells were washed with pre-warmed PBS and the PBS carefully removed using a pastuer pipette under vacuum. 1 ml trypsin/EDTA [0.25% (w/v) Trypsin, 0.1% (w/v) EDTA] was added and then carefully removed as in above. The culture dish was incubated for 1 min at 37°C for detachment of cells, new dishes were prepared with 5 ml medium and the cells were added before been transferred to the incubator again.

#### **3.1.2 Freezing of cells**

To preserve cells for longer time periods, cells were trypsinised and fresh medium added. The suspension was filled into a 15 ml Falcon tube, centrifuged for 7 min at 4°C and 250 *g*. The supernatant was discarded whilst the sediment was resuspended in a 0.5 ml culture medium with 40% FCS, and then 0.5 ml medium with 20% DMSO were added dropwise. Cell suspension was incubated in a cryogenic atmosphere for 2 h and then transferred to a cryogenic storage dewar of liquid nitrogen where it was stored until required.

### 3.1.3 Thawing of cells

To thaw a frozen cell suspension, the vial containing the suspension was placed for about 1 min in a water bath at 37°C with gentle agitation by hand every 5 – 10 sec. The suspension was then immediately transferred to a new 50 ml sterile Falcon tube. To wash the storage solution off the thawed cells, 10 ml of culture medium was added dropwise whilst shaking gently. Cells were centrifuged for 5 min at 4°C and 250 g. The supernatant was discarded whilst the sediment was resuspended in a culture medium with 10% FCS and transferred to a new labelled cell culture dish for incubation.

### 3.1.4 Counting of cells

To count the cells, they were first trypsinised and harvested with PBS. An aliquot from the suspension was mixed with the same volume of trypan blue and subjected to microscopy analysis. Only dead cells are stained with trypan blue so we could count the living cells which are not coloured by using a Neubauer-counting chamber (Fig. 9). A volume of 0.1 mm<sup>3</sup> is represented by each grid square of the Neubauer-counting chamber (Fig. 9). In order to avoid counting the same cells more than once, cells touching only the upper and left lines and within the grid square were counted and cell number calculated as shown below.

**Cells = count x df x (1 x 10<sup>4</sup>) x vol**, where,

Cells = total number of cells in original suspension;

count = average cell count per Neubauer-counting chamber square;

df = 2 = dilution factor from cell suspension + dye;

(1 x 10<sup>4</sup>) = Neubauer-counting chamber square/volume = 1 square/10<sup>-4</sup> ml;

vol = total volume of original suspension in ml

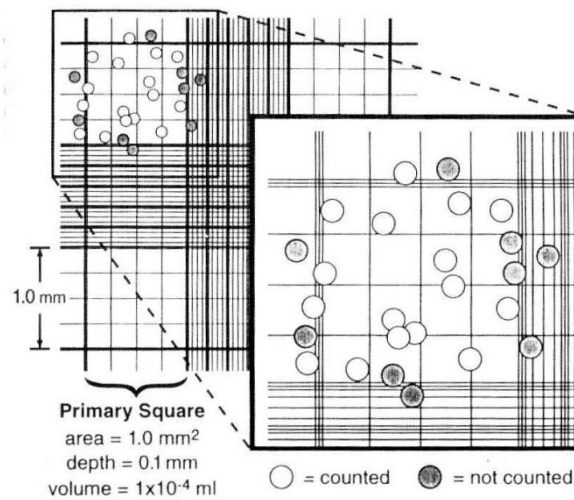


**Figure 9.** Depicts the way cells were counted in a representative grid square of the hemacytometer slide. Adapted from Tsimbouri *et al.*, 2001 [83].

### 3.1.5 Treatment of cells

The compounds to be tested were each dissolved in the appropriate solvent. Cells were generally treated 24 h after seeding them with various concentrations (ranging from 0 to 250  $\mu\text{M}$ ) of the test compound. For evaluation of antioxidants on the test compounds, cells were pretreated 0.5 h or 1 h with the appropriate antioxidant (Fig. 10) before incubation with the test compound. Cells were then incubated for various time periods (ranging from 0 - 96 h) at 37°C and with 5% CO<sub>2</sub>.



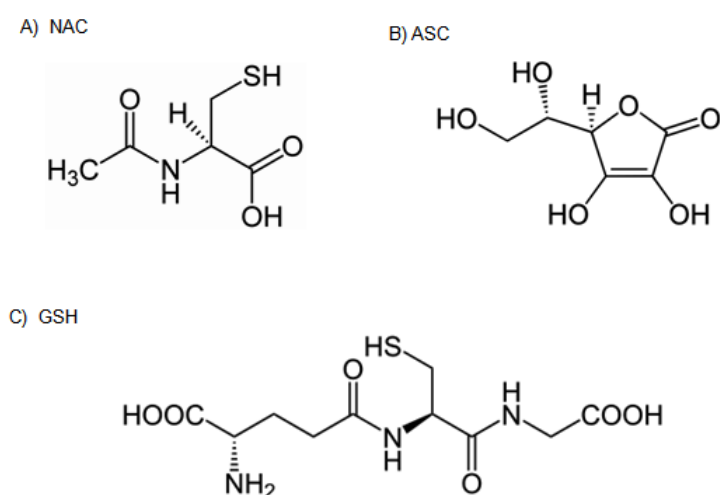


**Figure 10.** Antioxidants: A) *N*-acetyl cysteine (NAC), B) ascorbic acid (ASC) and C) glutathione (GSH).

### 3.1.6 Cell viability studies

The MTT assay was used to determine the effect of various compounds on either HCT116 colorectal cells or the ARPE-19 retinal pigment epithelial cells. The MTT [3-(4,5-Dimethylthiazol-2-yl)-2,5-diphenyltetrazolium bromide, Sigma] assay is a colorimetric assay which is able to detect cell proliferation, viability and cytotoxicity. This assay is based on the cleavage of the yellow tetrazolium salt MTT to purple formazan crystals in the presence of NADH and NADPH by metabolic activity of viable cells (Fig. 11) [84]. Viable, metabolic active cells produce in the respiratory chain the pyridine nucleotide cofactors (NADH and NADPH) which are then responsible for cellular reductions and therefore responsible for the cleavage of MTT. For this assay, cells were seeded at  $1 \times 10^4$  cells per well to a final volume of  $500 \mu\text{l}$  in a 24-well plate, and incubated overnight. Cells were then incubated with the appropriate compound concentration or with 0.05% DMSO solvent control for the specified time period. Viability of the cells was determined by MTT assay according to the manufacturer's instructions. One hour before the end of treatment,  $50 \mu\text{l}$  MTT (5 mg/ml PBS) were added. The enzymatic reaction took place at  $37^\circ\text{C}$  in a humidified atmosphere. Following 1 h MTT treatment, media was disposed off and cells solubilised by adding  $500 \mu\text{l}$  solubilising solution (0.05% (w/v) SDS in DMSO and 0.01% acetic acid) to each well and allowing the crystals to completely dissolve.

The spectrophotometrical absorbance of the purple-blue formazan dye was determined in an ELISA reader at 595 nm.

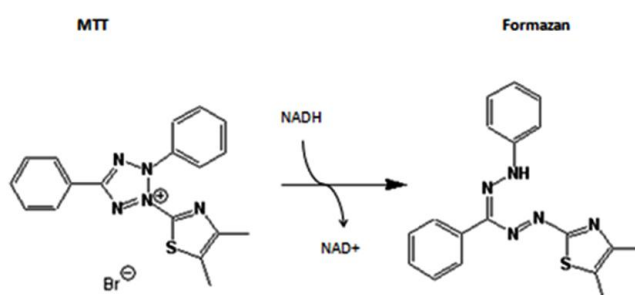


**Figure 11.** Reduction of yellow MTT to a purple colour formazan in the presence of NADH and NADPH by metabolic viable cells. Adapted from Roche molecular biochemicals: Apoptosis and cell proliferation, 2<sup>nd</sup> edition [84].

### 3.1.7 Evaluation of cell morphology

HCT116 or ARPE-19 cells were seeded into a 6 well plate ( $2 \times 10^5$  cells/well) and allowed to attach overnight before incubation with various concentrations of DATTS, DATTS + antioxidant, DMSO solvent control or left untreated for the required time periods. Cells were washed with PBS, fixed with either methanol or 3.7% formaldehyde in PBS for 10 min at 37°C and washed again 3 x 5 min. The cells were then subjected to 0.5  $\mu\text{M}/\text{ml}$  4',6-diamidino-2-phenylindole (DAPI) treatment (for 10 min at 37°C) for nuclear staining before being washed 3 x 5 min for the final time and analysed using an Axiovert fluorescence microscope (Carl Zeiss, Germany)

### 3.1.8 Immunofluorescence analysis

HCT116 cells were grown on coverslips until they were 50-70% confluent. Media was changed, and cells washed with pre-warmed PBS, pH 7.4 before being treated with different concentrations of DATTS or with DMSO. After incubations for the specified time periods (as indicated in the figures), the cells were washed once with PBS, pH 7.4 and then fixed with 2% (v/v) formaldehyde in PBS, pH 7.4 for 15 min at

room temperature. Cells were then washed with PBS, pH 7.4, 3 x 10 min. They were permeabilised on ice for 5 min with 0.2% (v/v) Triton X-100. Cells were washed again 3 x 10 min with PBS, pH 7.4 and then blocked with PBS, pH 7.4, containing 2% (w/v) bovine serum albumin (BSA) 3 x 10 min at room temperature, on a shaker. They were then incubated with a primary antibody against either cytochrome c or tubulin for 30 min at 37°C in a humidified chamber. Cells were washed under the same conditions as above and then incubated with the secondary antibody (ALEXA-Fluor™ 488 or ALEXA-Fluor™ 594) at 37°C for 30 min in a dark humidified chamber. Cells were then treated with 0.5 µM/ml 4',6-diamidino-2-phenylindole (DAPI) for 15 min at 37°C and washed again with PBS, pH 7.4, 3 x 10 min on a shaker. The coverslips were finally fixed with a drop of mounting medium and cells analysed using a Zeiss Axioskop fluorescence microscope.

### **3.1.9 Cell cycle analysis**

Cell cycle analysis was done by flow cytometry using propidium iodide (PI) staining. The determination was based on the measurement of DNA content of nuclei labelled with PI [85 86]. The idea is that PI fluorescent probe binds nuclei in proportion to the amount of DNA present in the cell. Cells in the various stages of the cell cycle can then be quantified based on the amount of fluorescent dye taken, which is proportional to the amount of DNA in that particular phase of the cell cycle.

HCT116 or ARPE-19 cells ( $5 \times 10^4$ ) were allowed to grow on a 10 cm petri dish overnight. The medium was changed and cells were treated accordingly before being incubated for the various time periods. Cells were collected and washed two times with cold PBS before being resuspended in PBS and fixed with 70% ethanol. The cells were further incubated with RNase and propidium iodide to label DNA as previously described at 37°C for 30 min. The incubation step was to ensure that the RNase has digested all the RNA, which otherwise would interfere with the DNA signal. Cells were then analysed in a cytofluorimeter (Guava easyCyte HT system, Millipore) according to the manufacturer's instructions.

## **3.2 Measurement of Reactive Oxygen Species (ROS)**

### **3.2.1 Measurement of ROS using electron paramagnetic resonance (EPR)**

The electron paramagnetic resonance (EPR), also known as electron spin resonance (ESR) is a technique based on resonance frequencies of unpaired electrons in the sample. The EPR uses spin probes such as CMH1 (1-hydroxy-3-methoxycarbonyl-2,2,5,5-tetramethylpyrrolidine). The presence of radical species in the sample are measured based on signal areas that are produced which are proportional to the number of excited electron spins. In effect, the EPR intensity of resonance frequencies increases with an increase in the amount of radicals detected.

HCT116 cells were seeded in 10 cm cell culture dishes ( $5 \times 10^4$  cells/ml dish) and grown overnight. Medium was then changed and cells were treated with either 0.05% DMSO or 40, 120, 200, 280, 350 and 440  $\mu\text{M}$  of DATTS for 60 min. After removal for cell culture medium, cells were washed with Ringer buffer (KRB), pH 7.4 collected and resuspended in 2 ml KRB, and spun at  $7,000 \times g$  and  $4^\circ\text{C}$  for 10 seconds. Supernatant was removed and cell pellet resuspended in 50  $\mu\text{l}$  of pre-warmed KRB, pH 7.4 and 3  $\mu\text{l}$  CMH1. This sample was then put into the glass EPR capillary tube (Noxygen Science Transfer & Diagnostics, Germany). The tube was then placed inside the cavity of the e-scan spectrometer (Bruker, Germany) for data acquisition. EPR acquisition parameters were: microwave frequency = 9.652 GHz; modulation frequency: 86 kHz; modulation amplitude: 1 G; center field: 3583 G; sweep width: 60 G; microwave power: 21.90 mW; number of scans: 20; and temperature  $37^\circ\text{C}$ . In another set of experiments, HCT116 cells were pretreated for 0.5 h with either ASC or with superoxide dismutase (SOD) before being exposed to 500  $\mu\text{M}$  DATTS for another 1 h. Samples were then prepared and subjected to EPR measurement same way as described above.

### 3.2.2 Determination of $O_2^{\cdot-}$ in cell culture

Production of superoxide radical was assessed by oxidation of dihydroethidium (DHE) to 2-hydroxyethidium (Fig. 12). DHE is a fluorescence dye that is specific for  $O_2^{\cdot-}$ . It exhibits blue-fluorescence in the cytosol. When it is oxidised, however, it intercalates within the cell's DNA, staining its nucleus with a bright fluorescent red, which can be measured using a fluorescence reader.

Cells were seeded in 96 well plates and grown overnight. Cells were then treated with 40  $\mu\text{M}$  of DATTS or DMSO (0.5% final concentration) as solvent control for 0, 5, 10, 20, 25 and 30 min. After removal of the cell culture medium, cells were washed with PBS, and 190  $\mu\text{l}$  of 25  $\mu\text{M}$  DHE dissolved in PBS was added to each well immediately before the measurement was started. The transient increase in fluorescence (DHE ex/em: 563/587 nm) was measured using a CytoFluor series 4000 (applied Biosystems) multi-well plate reader. In another experiment, cells were seeded in 96 well plates and grown overnight. After removal of the cell culture medium, cells were washed with PBS, and 190  $\mu\text{l}$  of 25  $\mu\text{M}$  DHE dissolved in PBS was added to each well. Immediately before the measurement was started, increasing concentrations of DATTS or DMSO (0.5% final concentration) as solvent control was added. The dosage-dependent increase in fluorescence (DHE ex/em: 563/587 nm) was measured in the same way as above.

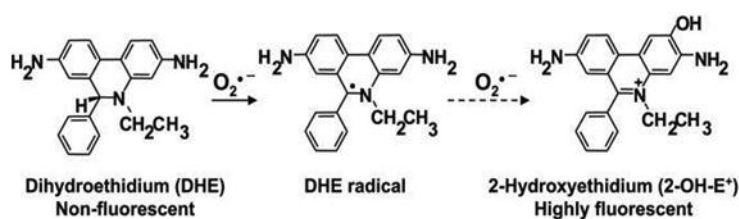


**Figure 12.** Schematic representation of the production and detection of  $O_2^{\cdot-}$  by DHE. When  $O_2^{\cdot-}$  is produced in DATTS treated cells, it reacts with DHE to produce 2-hydroxyethidium. Adapted from Dikalov *et al.*, 2007 [87].

### 3.2.3 Determination of H<sub>2</sub>O<sub>2</sub> in cell culture

The level of H<sub>2</sub>O<sub>2</sub> produced in HCT116 cells following treatment with DATTS was determined using an Amplex<sup>®</sup> Red hydrogen peroxide/peroxidase assay kit (Invitrogen, Darmstadt, Germany), according to the manufacturer's instructions. In the presence of peroxidase, the Amplex<sup>®</sup> Red reagent reacts with H<sub>2</sub>O<sub>2</sub> in a 1:1 stoichiometry to produce the red-fluorescent oxidation product, resorufin [87] (Fig 13). Resorufin has excitation and emission maxima of approximately 571 nm and 585 nm, respectively, and because the extinction coefficient is high ( $58,000 \pm 5,000 \text{ cm}^{-1}\text{M}^{-1}$ ), the assay can be performed either fluorometrically or spectrophotometrically. The reaction can be used to detect as little as 10 picomoles of H<sub>2</sub>O<sub>2</sub> in a 100  $\mu\text{l}$  volume or  $1 \times 10^{-5}$  U/ml of horseradish peroxidase (HRP). The electrochemical mediator Amplex<sup>®</sup> Red reagent and the enzyme HRP were added to cultured HCT116 cells treated with either DATTS or epigallocatechin-3-gallate (an inducer of H<sub>2</sub>O<sub>2</sub>) as positive control. The release of H<sub>2</sub>O<sub>2</sub> was measured accordingly. H<sub>2</sub>O<sub>2</sub> levels were quantified in comparison with a H<sub>2</sub>O<sub>2</sub> standard curve.

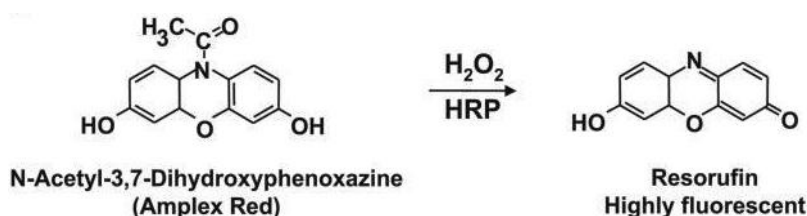


**Figure 13.** Schematic representation of the production and indirect detection of H<sub>2</sub>O<sub>2</sub>. Horseradish peroxidase (HRP) and Amplex Red are used as enzyme and electrochemical mediator, respectively. Peroxy radicals formed by the activity of HRP on the peroxide irreversibly oxidize Amplex Red to resorufin which is subsequently quantified electrochemically by its reduction to dihydroresorufin. Adapted from Dikalov *et al.*, 2007 [87].

### 3.2.4 Determination of total thiol content

Total intracellular thiol levels were measured using a colorimetric Ellman's reagent-based assay as previously described [88]. Ellman's reagent {5,5' -dithio-bis-(2-nitrobenzoic acid)}, often referred to as DTNB, is a water soluble compound that

reacts with free thiols to yield a mixed disulfide and 2-nitro-5-thiobenzoic acid (TNB) as shown in Figure 14. The product formed is yellow coloured and can be easily measured and quantified using a spectrophotometer set at 412 nm.

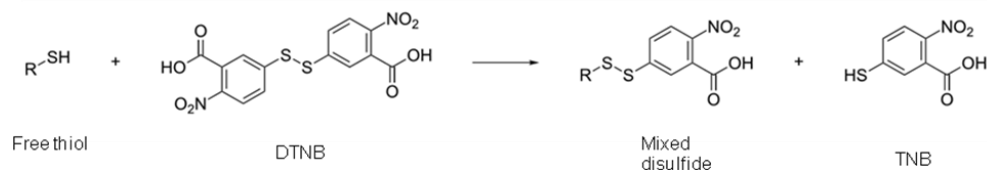


**Figure 14.** Reduction of Ellman's Reagent to a mixed disulfide and 2-nitro-5-thiobenzoic acid (TNB)

HCT116 cells were seeded in 10 cm cell culture dishes ( $5 \times 10^4$  cells/ml dish) and grown overnight. Medium was then changed and cells were treated with 40  $\mu$ M of DATTS for 0, 5, 10, 20, 30, 60, 120 or 240 min. After removal for cell culture medium, cells were washed with PBS, collected in 250  $\mu$ l PBS, and snap-frozen in liquid nitrogen. Following thawing and removal of cellular fragments by centrifugation at 12,000  $\times$  g for 10 min at 4°C, the total thiol content of cell lysates was determined using 5,5'-dithio-bis-(2-nitrobenzoic acid) (Ellman's reagent) and cysteine hydrochloride monohydrate as a standard. In another experiment, HCT116 cells were seeded in the same way as above. Medium was changed and cells were treated with increasing DATTS concentrations or with DMSO solvent control (final concentration 0.5%). After incubation for 2 h, cells were lysed and the total thiol content of cell lysates was determined in the same way as in the previous step.

### 3.3 DNA techniques

#### 3.3.1 Plasmid amplification

Mammalian cell transfections and co-transfections required plasmid DNA constructs. These therefore had to be amplified to ensure there was sufficient amount for the planned experiments. The amplification of these plasmid DNAs was by transformation of competent *E. coli* XL1-blue cells (see section 3.3.4 on how to

prepare competent *E. coli* cells) followed by DNA midipreparation using the Nucleobond®AX-plasmid-purification kit (Macherey-Nagel, Dueren, Germany). Transformation was achieved by adding about 100 ng of the plasmid to 100 µl prethawed (on ice) competent cells, followed by heat shock at 37°C for 45 seconds. The heat-shocked cells were cooled on ice for 2 min before being recovered by adding 800 µl of LB medium and then incubated at 37°C with shaking for 60 min. To plate the transformed cells, cells are gently harvested by centrifugation at 1,050 x g for 1 min. 800 µl of the supernatants was removed and the cells were resuspended in the remaining 100 µl medium. Resuspended cells were plated on LB plates with the corresponding antibiotics and incubated at 37°C overnight.

### 3.3.2 DNA midipreparation

To isolate plasmid DNA from the previous step, a DNA midipreparation which employs the use of a Nucleobond®AX-plasmid-purification kit (Macherey-Nagel) was done. Following transformation, a single colony was picked and cultivated by incubating in 100 - 200 ml LB medium containing antibiotics for about 16 h or until the O.D.<sub>600 nm</sub> = 0.5-1, on a shaking rotor with 250 rpm. The bacteria cells were then harvested by centrifugation (Beckman J2-HS centrifuge, rotor JA10) at 4°C and 6,000 x g for 15 min. The cell pellet was resuspended in a 4 ml pre-cooled RNase A buffer. 4 ml of cell lysis buffer (Solution 2) was added and the mixture mixed briefly by gentle hand-shaking. The mixture was incubated at room temperature for 3 min before adding 4 ml pre-cooled neutralising solution (Solution 3). The mixture was briefly mixed by inverting the test-tube several times until an off-white flocculate was formed, before incubating on ice for a further 5 min. The lysate was passed through a pre-wet Nucleobond® Folded Filter with AX 100 columns in a small funnel. An AX-100 binding column was equilibrated by applying 2.5 ml buffer N2 (100 mM Tris-HCl, 15% ethanol, 900 mM KCl, 0.15% Triton X-100; pH 6.3) to the column and allowed to empty by gravity flow. The cleared cell lysates from the Folded Filter were then loaded onto this column and allowed to empty by gravity flow. The column was washed with 10 ml buffer N3 (100 mM Tris-HCl, 15% ethanol, 1.15 M KCl, pH 6.3) and the flow-through discarded. The plasmid DNA was eluted and collected by 5 ml



buffer N5 (100 mM Tris-HCl; pH 8.5, 15% ethanol, 1 M KCl). 3.5 ml isopropanol was then added to precipitate the eluted plasmid DNA. The DNA was pelleted by centrifugation at 16,000 x g for 30 min at 4°C. The supernatant was discarded and the DNA pellet washed with 500 µl of 70% (v/v) ethanol. After vortexing briefly, the mixture was centrifuged at 16,000 x g for 10 min at room temperature. Ethanol was removed and the DNA pellet was dried at room temperature for at least 10 min and then redissolved in sterile deionised water. The DNA concentration was measured and diluted to a final concentration of 1 µg/µl. The DNA was used straight away or kept at either 4°C for short-term or at -20°C for long-term storage.

Cell strain	Genotype
XL1-blue	<i>recA1 endA1 gyrA96 thi-1 hsdR17 supE44 relA1 lac</i> [F' <i>proAB lac<sup>f</sup>ZΔM15 Tn10 (Tet<sup>r</sup>)</i> ]

**Table 21.** Type(s) of *E. coli* strain

### 3.3.3 DNA quantification

UV spectrometry was used to quantify the purified plasmid DNA. Since nucleotides absorb UV light with an absorption peak at 260 nm, the spectrometric measurements were done at this wavelength and plasmid DNA quantified based on the Lambert-Beer equation given below:

Absorbance is defined by the Lambert-Beer equation as  $A = \epsilon \times b \times c$

where,  $\epsilon$  = extinction coefficient,  $b$  = pathlength and  $c$  = concentration

When the molar coefficient and pathlength are constant, absorbance is proportional to the concentration. Also, for a standard cuvette reader, the pathlength is usually defined as 1 centimeter and because dsDNA has an average extinction coefficient of  $0.02 (\mu\text{g/ml})^{-1}\text{cm}^{-1}$ , it thus mean that an  $A_{[260]}$  of 1 corresponds to a concentration of 50 µg/ml dsDNA. Most samples however contain contaminates such as proteins and

single stranded DNA/RNA that absorb maximally at 280 nm. Therefore, to make up for this interference, the equation below was used.

$$A_{[260]}/A_{[280]} = \text{pure dsDNA}$$

where,  $A_{[260]}$  = the absorbance at 260 nm and  $A_{[280]}$  = the absorbance at 280 nm

A plasmid DNA with  $A_{[260]} / A_{[280]}$  ratio between the ranges of 1.65 and 2 was considered pure.

### 3.3.4 Preparation of competent *E. coli* cells

For plasmid DNA amplification, *E. coli* cells that have the ability to be transformed (otherwise known as competent *E. coli* cells) were required. The protocol for preparation of these type of cells was modified as described in [89]. The desired strain was streaked out on an LB plate containing the appropriate antibiotics and incubated over night at 37°C. A single colony was picked from the plate and grown over night in 3 ml LB medium. The following day, 100 µl of the culture was inoculated into a 20 ml pre-warmed TYM medium. The cells were grown at 37°C until O.D.<sub>600 nm</sub> = 0.2 - 0.8. Afterwards the culture was diluted into 500 ml fresh TYM medium and incubated at 37°C until O.D.<sub>600 nm</sub> = 0.6-1.0. The 500 ml culture was then quickly placed into an ice-water bath and swirled gently to ensure fast cooling. Cells were harvested by centrifugation at 4°C and 4,000 x g for 10 min. The cell pellet was resuspended in a 100 ml cold TfBI buffer with gentle shaking on ice before being centrifuged again. The supernatant was poured out and the cells resuspended again in a 20 ml TfBI buffer by gentle shaking on ice. The cell suspension was then aliquoted into pre-chilled microfuge test tubes and snap frozen in liquid nitrogen before being stored at -80°C.

### 3.3.5 Reporter constructs

p3xATF3-luc, p3xStRE-luc and pCMV-Flag-NLS-Nrf2-DN which have been used elsewhere [90, 91, 92], were all kindly provided by Prof. Dr. G. Thiel, Medical

Biochemistry and Molecular Biology, Homburg. The LacZ reporter was readily available in the our lab. pCDNA3-Myc3-Nfr2 and p3xFLAG-ATF6 were purchased from Addgene (Cambridge, USA).

### **3.3.6 Transient transfection and co-transfection of cells**

HCT116 colon cancer cells were seeded into a 6 well plate ( $2 \times 10^5$  cells/well) and allowed to attach overnight. Cells were then transfected using Effectene<sup>®</sup> Transfection Reagent (Qiagen, Hilden, Germany) according to the manufacturer's instructions. In brief, 16 to 24 h after seeding cells, 0.2  $\mu$ g of *LacZ* and 0.2  $\mu$ g DNA from p3xStRE-luc, p3xATF3-luc, p3xFLAG-ATF6 or the empty vector (pGL3-Basic) were each separately added to a 3.2  $\mu$ l "Enhancer", mixed and incubated 2-5 minutes at room temperature to condensate DNA by interaction with the "Enhancer". In order to produce condensed Effectene-DNA complexes, 10  $\mu$ l of Effectene Transfection Reagent was added to the mixture and incubated for a further 10 min at room temperature. Cells were washed with PBS and 1.6 ml fresh medium was added. The Effectene-DNA complex was mixed with 0.6 ml culture medium and then directly added to cells and incubated for 24 h at 37°C with 5% CO<sub>2</sub>. In another set of experiments, cells were grown overnight as above and then transfected with 0.4  $\mu$ g pGL3-Basic or 0.4  $\mu$ g p3xStRE-luc or co-transfected with 0.2  $\mu$ g each of p3xStRE-luc and pCDNA3-Myc3-Nrf2 or p3xStRE-luc and pCMV-Flag-NLS-Nrf2-DN using the Effectene<sup>®</sup> Transfection Reagent as described above.

## **3.4 Protein methods**

### **3.4.1 Preparation of whole cell extracts**

Following incubation of HCT116 cells with DATTS, cells were collected in cold phosphate buffered saline (PBS, pH 7.4) and centrifuged together with the cell culture medium at 4°C and 250 x *g* for 7 min. After one washing step with cold PBS, cells were lysed with 50 – 150  $\mu$ l RIPA buffer (50 mM Tris-HCl, pH 8.0, 150 mM

NaCl, 0.5% sodium desoxycholate, 1% Triton X – 100, 0.1% sodium dodecylsulfate (SDS) supplemented with the protease inhibitor cocktail Complete™ according to the manufacturer's instructions (Roche Diagnostics, Mannheim, Germany). The cell lysate was left on ice for 15 min, subjected to sonification (3 x 1 min) at 4°C and then cell debris was removed by centrifugation at 16,250 x *g* at 4°C for 30 min. The protein content of the supernatant was determined according to the Bradford method using the Bio-Rad protein assay reagent (Bio-Rad, Munich, Germany).

### **3.4.2 Nuclear and cytosolic fractionation**

Cytosolic and nuclear fractionation was performed after harvesting the cells for protein expression analysis. After one washing step with cold PBS as described earlier, cells were thoroughly resuspended in 50 – 150  $\mu$ l cytosolic lysis buffer (10 mM Hepes-KOH, pH 7.9, 1.5 mM MgCl<sub>2</sub>, 10 mM KCl and freshly prepared 0.5 mM DTT and 0.5% NP40) supplemented with freshly prepared protease inhibitor cocktail Complete™ according to the manufacturer's instructions (Roche Diagnostics, Mannheim, Germany). The cell lysate was left on ice for 20 min before being subjected to centrifugation at 16,250 x *g* at 4°C for 4 min. After centrifugation, the supernatant was removed (cytosolic extract) and the pellet was lysed again with 50 – 100  $\mu$ l nuclear lysis buffer (10 mM Hepes-KOH, pH 7.9, 25% glycerol, 420 mM NaCl, 1.5 mM MgCl<sub>2</sub>, 0.2 mM EDTA and freshly prepared 0.5 mM DTT and 0.5% Triton X-100) supplemented with freshly prepared protease inhibitor cocktail Complete™. Cytosolic and nuclear extracts were further analyzed by Western Blot.

### **3.4.3 Cytosolic fractionation for cytochrome c release**

Cytosolic extracts for cytochrome c release were generated by resolving treated cells in cold phosphate buffered saline (PBS, pH 7.4) and centrifuged together with the cell culture medium at 4°C and 250 x *g* for 7 min. The pellets were further resuspended in cold PBS and snap frozen in liquid nitrogen. Cellular fragments were removed by centrifugation at 12,500 x *g* at 4°C for 10 min. Extracts were immediately

used for Western blot analysis or stored at -20°C (for the short term) or -80°C (for the long term).

#### **3.4.4 Caspase 3/7 assay**

Caspase activity was determined with Caspase-Glo<sup>®</sup> 3/7 Assay [93]. During apoptosis, members of a family of cysteine proteases with aspartate specificity - the caspases, undergo proteolytic processing and activation, and then orchestrate the central apoptotic events [94]. This assay is a two in one method that involves a fluorometric quantification and immunoblot detection of caspase activation and cleavage. It is a simple robust luminescent assay that has more sensitivity and selectivity for caspase 3/7. It measures caspase 3/7 activity based on the release of a fluorophore from a substrate that contains the tetrapeptide sequence DEVD. When a cleaved and active caspase 3/7 is present in a cell lysate containing the caspase activity reagent, it cleaves the substrate (z-DEVD-NH) thereby releasing a luminescent signal (which is proportional to the amount of caspase activity present), produced by luciferase (Fig. 15). The assay was modified as described in Ref. [96]: Cells were harvested and extracted for 5 min on ice in lysis buffer (10 mM Tris-HCl, pH 7.4, 10 mM MgCl<sub>2</sub>, 150 mM NaCl, 0.5% NP-40, 10 mM DTT) supplemented with the protease inhibitor cocktail complete<sup>™</sup>. Lysates were centrifuged for 10 min at 12,500 x *g* at 4°C and the supernatants were removed and assayed for protein content. The protein concentration was set to 1 µg/µl. The lysate was further diluted 1 to 10 in a protein buffer (50 mM Tris/HCl pH 7.4, 10 mM KCl and 5% glycerol). 20 µl of diluted protein extract was incubated with the same volume of Caspase-Glo<sup>®</sup> reagent for 1 h at room temperature and measured in a luminometer.

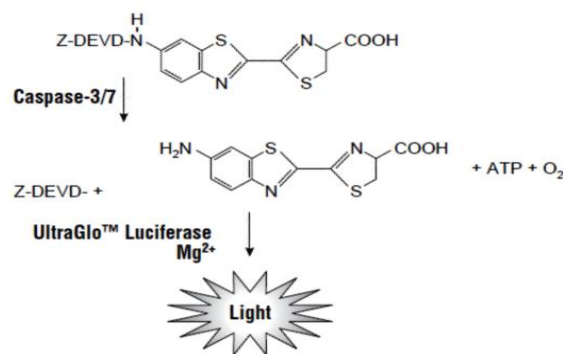


**Figure 15.** Showing caspase 3/7 cleavage of the luminogenic substrate containing the DEVD sequence. Diagram taken from Promega Technical Bulletin (Caspase-Glo<sup>®</sup> 3/7 Assay - Part# TB323) [93].

### 3.4.5 Protein quantification

It is important to determine protein concentration as not only does it help in calculating yield, but also ensures that equal amount of protein samples are used in studies like protein expression, protein thiolation, phosphatase and kinase activity assays. The method that was employed to do this was a colorimetric reaction called "Bradford assay" in which unknown samples were compared to a calibration of known concentrations of bovine immunoglobulin (IgG). The Bradford assay is a rapid method for microgram protein quantification utilising protein-dye binding [96]. It involves the use of Coomassie brilliant blue G 250, which, when bound to a protein, changes from a cationic to an anionic state and the absorption alters from 465 nm (dark red) to 595 nm (dark blue). This absorption change is proportional to the amount of protein present in the sample.

The Bradford assay in this study was performed by mixing 1  $\mu$ l of protein extract with 799  $\mu$ l of diH<sub>2</sub>O and 200  $\mu$ l of Bio-rad Bradford reagent (Bio-rad). The reaction was incubated at room temperature for 5 min and then measured against a blank (1  $\mu$ l extraction buffer + 799  $\mu$ l diH<sub>2</sub>O + 200  $\mu$ l Bio-rad Bradford reagent) at a wavelength of 595 nm by spectrophotometry. Using the read out absorbance for each unknown sample, protein concentrations were calculated according to the pre-prepared bovine IgG-standard curve in  $\mu$ g/ $\mu$ l. The bovine IgG-standard curve was prepared by measuring absorbance at 595 nm of 0, 1, 5, 10 and 20  $\mu$ g IgG samples by the

Bradford method. A standard curve was then drawn with bovine IgG concentrations as X-axis and absorbance at 595 nm as Y-axis.

### **3.4.6 Sodium dodecyl sulfate polyacrylamide gel electrophoresis**

An SDS PAGE (sodium dodecyl sulfate polyacrylamide gel electrophoresis) Bio-Rad method developed by Laemmli [97] and Weber [98] was employed in this study to separate proteins according to their sizes and mobility differences in an electric field. SDS works by disrupting non-covalent bonds in the proteins, denaturing them, and causing the molecules to lose their original conformation. This effectively imparts a negative charge on the protein that is relative to the mass of that protein. Once the samples, along with a molecular weight marker (protein ladder), are loaded into the wells on the gel, a current is passed through the gel. This current allows the proteins to move through the gel with the smaller ones moving faster whilst the larger ones lag behind. Upon completion of the sample run, the current is stopped and the protein is transferred to a PVDF membrane and analysed by immunoblotting.

To prepare SDS PAGE gels, the Mighty Small™ SE250 Mini-Vertical gel system (Hoefer Scientific Instruments) was employed. In this system, a single gel is composed of a lower part known as the "resolving or separating gel" (see Table 21) and an upper part known as the "stacking gel" (see Table 22). The percentage of the stacking gel is 4.3%, and that of the resolving or separating gel varies from 7.5% to 20%. Whilst low percentage gels are used for separating large proteins, small proteins are separated in high percentage gels.

The gel rack, including white and transparent glass plates of sizes 73 mm x 100 mm and 80 mm x 100 mm respectively, and other apparatus {Mighty Small™ multiple gel casters SE200 (Hoefer Scientific Instruments)}, all designed for preparing 4-5 gels simultaneously, were cleaned and assembled according to the manufacturer's instructions. These plates were placed together with a space of 1 mm thickness between them. The resolving or separating gel constituents (Table 21) were gently mixed and a layer of approximately 3/4 of the volume of the spaces in the gel rack was poured in between the plates using a Pasteur pipette. To avoid gel shrinkage

and air bubbles, which may affect the way the proteins run on the gel, a thin layer of isopropanol was put on top of the gel in each space and the gel was left to polymerise. Once the separating gel had polymerised, the isopropanol was removed with the aid of Whatman filter paper. The stacking gel (Table 22) was then made up and a layer of this was added on top of the separating gel. A sample well comb was then inserted into the solution between the plates and the gel left to polymerise at room temperature. Upon polymerisation, the gel was gently removed from the gel rack and wrapped in a wet paper towel before being stored at 4°C until required for use.

Protein samples were then prepared with SDS sample buffer and whilst they were being incubated at 95°C for 5 min, the gel and the electrodes were assembled in the SDS PAGE chamber. The chamber was filled with SDS PAGE running buffer. Using a 50 µl Hamilton syringe, each of the samples were loaded into a sample well on the gel. A prestained molecular weight marker (Fermentas) was loaded into a separate well before replacing the lead to the tank. A current of constant voltage (25 V for one gel or 50 V for two gels) was applied to the tank for about 1 to 2 h or until the tracking dye reached the bottom of the gel. After which, proteins were transferred to a PVDF membrane (Roche) and detected by immunoblotting.

Separating gel	7.5%	10%	12.5%	15%	20%
Gel solution A (ml)	9	12	15	18	24
Gel solution B (ml)	9	9	9	9	9
diH <sub>2</sub> O (ml)	18	15	12	9	3
APS (µl)	200	200	200	200	200
TEMED (µl)	20	20	20	20	20

**Table 21.** Separating gel solution.



<b>Stacking Gel</b>	<b>4.3%</b>
<b>Gel solution A (ml)</b>	2.2
<b>Gel solution C (ml)</b>	3.8
<b>diH<sub>2</sub>O (ml)</b>	9
<b>APS (<math>\mu</math>l)</b>	100
<b>TEMED (<math>\mu</math>l)</b>	40

**Table 22.** Stacking gel solution.

### 3.4.7 Western blot analysis

For tank blotting, polyvinylidene fluoride (PVDF) membrane with a pore size of 0.45  $\mu$ m was used for the protein transfer. The PVDF membrane was first activated by placing it in methanol at room temperature for about 1 min, followed by rinsing with transfer buffer. A transfer stack was made by raising in transfer buffer and putting together the following, from bottom to top (in the direction of the current, i.e., negative to positive): a thin layer of sponge; three layers of filter paper; the gel containing the proteins; the PVDF membrane; another three layers of filter papers; and a sponge. Air bubbles between the SDS polyacrylamide gel and the PVDF membrane were expelled before stacking. Proteins were transferred to the PVDF membrane by running the tank blot system filled with transfer buffer at 120 mA overnight at room temperature. The PVDF membrane was then removed from the pack and immunoblotting was performed by blocking non-specific binding regions of the membrane with 5% skimmed milk in PBS with 0.1% Tween-20 for 1 h at room temperature. Specific mono or polyclonal antibodies were each separately used in dilutions given Table 23. The membrane was then incubated in the appropriate antibody solution (see Table 23) either for 1 h at room temperature or overnight with gentle shaking at 4°C (or as indicated on the antibody data sheet). After washing the membrane with PBS-Tween-20 containing 1% skimmed milk (3 x 10 min), it was then incubated with the appropriate peroxidase-coupled secondary antibody in the

## Methods

---

appropriate dilution at room temperature for 1 h. The membrane was further washed (3 x 10 min) in PBS-Tween-20. Signals were developed and visualised by the Lumilight system of Roche Diagnostic (Mannheim, Germany). To ensure equal loading of samples, the membrane was also incubated with antibodies against either GAPDH, nucleolin,  $\beta$ -actin or  $\alpha$ -tubulin followed by the appropriate secondary antibody and signals developed as described above.

Antibody	Dilution	MW	Species	Type	Source
$\alpha$ -tubulin	1:1000	55 kDa	mouse	monoclonal antibody	Sigma-Aldrich, Munich, Germany
ATF3	1:1000	21 kDa	rabbit	polyclonal antibody	Santa Cruz Biotechnology, Heidelberg, Germany
ATF4	1:1000	50 kDa	rabbit	polyclonal antibody	Santa Cruz Biotechnology, Heidelberg, Germany
ATF6	1:1000	50 (cleaved), 90 (full-length) kDa	rabbit	polyclonal antibody	Abcam, Cambridge, UK
Bax	1:1000	28 kDa	mouse	monoclonal antibody	Santa Cruz Biotechnology, Heidelberg, Germany

## Methods

bcl-2	1:1000	28 kDa	rabbit	polyclonal antibody	Cell Signaling Frankfurt, Germany
$\beta$ -actin	1:1000	43 kDa	goat	polyclonal antibody	Santa Cruz Biotechnology, Heidelberg, Germany
Caspase 3/7	1:1000	17, 19 (cleaved products), 35 (full- length) kDa	rabbit	monoclonal antibody	Cell Signaling Frankfurt, Germany
cdc25C (H6)	1:1000	55 kDa	mouse	monoclonal antibody	Santa Cruz Biotechnology, Heidelberg, Germany
cdc25C (Thr48)	1:1000	80 kDa	rabbit	polyclonal antibody	Cell Signaling Frankfurt, Germany
CDK1	1:3000	34 kDa	rabbit	polyclonal antibody	Epitomics, Berlin, Germany
CHOP/GADD153	1:1000	30 kDa	mouse	monoclonal antibody	Santa Cruz Biotechnology, Heidelberg, Germany
c-jun	1:1000	43 kDa	rabbit	polyclonal antibody	Santa Cruz Biotechnology, Heidelberg, Germany

## Methods

CK2 $\alpha$	1:1000	46 kDa	rabbit	antiserum	Serum # 26, Lab collection
CK2 $\alpha'$	1:1000	42 kDa	rabbit	antiserum	Serum # 30, Lab collection
CK2 $\beta$	1:1000	28 kDa	rabbit	antiserum	Serum # 32, Lab collection
Cytochrome c	1:1000	15 kDa	mouse	monoclonal antibody	Santa Cruz Biotechnology, Heidelberg, Germany
elf2 $\alpha$	1:1000	38 kDa	rabbit	polyclonal antibody	Cell Signaling Frankfurt, Germany
Flag	1:3000	-	mouse	monoclonal antibody	Sigma-Aldrich, Munich, Germany
GAPDH	1:1000	37 kDa	rabbit	polyclonal antibody	Santa Cruz Biotechnology, Heidelberg, Germany
HO-1	1:1000	28 kDa	rabbit	polyclonal antibody	Cell Signaling Technology, USA
HSP90	1:1000	90 kDa	rabbit	polyclonal antibody	Santa Cruz Biotechnology, Heidelberg, Germany
Nrf2	1:1000	100 kDa	goat	polyclonal antibody	Santa Cruz Biotechnology, Heidelberg,

## Methods

					Germany
NQO1	1:1000	29 kDa	mouse	monoclonal antibody	Cell Signaling Frankfurt, Germany
Nucleolin	1:3000	90 kDa	rabbit	antiserum	Serum # 36, Lab collection
p21	1:1000	21 kDa	mouse	monoclonal antibody	Calbiochem/MERK, Darmstadt, Germany
p38	1:1000	38 kDa	mouse	monoclonal antibody	Santa Cruz Biotechnology, Heidelberg, Germany
phospho-p38 (p-p38)	1:1000	38 kDa	rabbit	monoclonal antibody	Epitomics, Berlin, Germany
p53 (DO1)	1:1000	53 kDa	mouse	monoclonal antibody	Santa Cruz Biotechnology, Heidelberg, Germany
PARP	1:10000	89 (cleaved), 116 (full- length) kDa	rabbit	polyclonal antibody	Cell Signaling Frankfurt, Germany
Phospho-c-jun (p-c-jun)	1:1000	43 kDa	mouse	monoclonal antibody	Santa Cruz Biotechnology, Heidelberg, Germany

Phospho- elf2 $\alpha$ (p- elf2 $\alpha$ )	1:1000	36 kDa	rabbit	polyclonal antibody	Cell Signaling Frankfurt, Germany
Phospho-PERK (p-PERK)	1:500	170 kDa	rabbit	polyclonal antibody	BioLegend, London, UK

**Table 23.** Antibodies used.

### 3.4.8 Protein kinase assay

To study *in vitro* CK2 kinase activity, 30  $\mu\text{g}$  of total protein was mixed with kinase buffer {50 mM Tris-HCl, pH 7.5, 100 mM NaCl, 10 mM MgCl<sub>2</sub>, 1 mM dithiothreitol (DTT)} to a final volume of 20  $\mu\text{l}$ . 30  $\mu\text{l}$  of CK2 mix (25 mM Tris-HCl, pH 8.5, 150 mM NaCl, 5 mM MgCl<sub>2</sub>, 1 mM DTT, 50  $\mu\text{M}$  ATP, 0.19 mM (final concentration), CK2 specific substrate peptide with the sequence RRRDDDSDDD and 10  $\mu\text{Ci}/500 \mu\text{l}$  [<sup>32</sup>P]  $\gamma$ ATP) was added and the reaction mix incubated at 37°C for 5 min. The reaction was stopped on ice and the sample pipetted onto Whatman-P81 cation-exchange paper and washed 3 x 5 min with 85 mM phosphoric acid and 1 x 5 min with ethanol. The filter paper was dried and counted for Čerenkov radiation in a scintillation counter (Liquid Scintillation Analyser 190S AB/LA; Canberra-Packard GmbH, Dreieich, Germany).

### 3.4.9 *In vitro* phosphatase assay for cdc25

The enzymatic activity of the GST-Cdc25 recombinant enzyme was performed in 96-well plates in a specific reaction buffer (50 mM Tris-HCl, 50 mM NaCl, 1 mM EDTA and 0.1% SDS, pH 8.1) containing 3-O-methylfluorescein phosphate (500  $\mu\text{M}$ ) as substrate. The GST-cdc25 proteins, diluted in assay buffer, were used at a final concentration of 1  $\mu\text{g}/\text{well}$ . After 2 h at 30°C, 3-O- methylfluorescein fluorescent emission was measured with a CytoFluor system Perseptive Applied Biosystems; excitation filter: 475 nm and emission filter: 510 nm.

### 3.4.10 Luciferase reporter assay

Luciferase reporter assays are designed to monitor transcription factor binding activities. These sort of assays involve the construction of a luciferase reporter vector, containing a specific transcription factor-binding element upstream of the luciferase gene. In the Promega Firefly luciferase for example, light is produced by converting the chemical energy of luciferin oxidation through an electron transition, forming the product molecule oxyluciferin and the reaction is catalysed by Firefly luciferase, a monomeric 61 kDa protein, which uses  $\text{ATP}\cdot\text{Mg}^{2+}$  as a co-substrate (Fig 16).

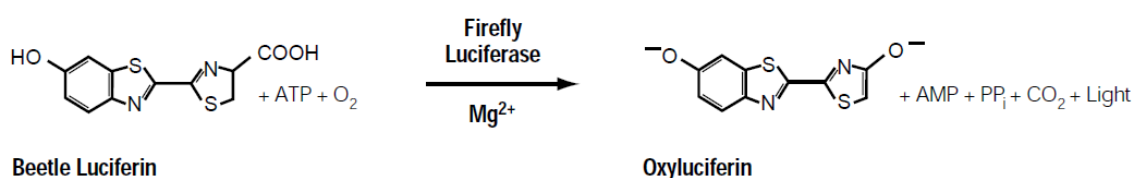


**Figure 16.** Bioluminescent reaction catalysed by firefly luciferase.

Luciferase assays were carried out by cotransfection of a *LacZ* reporter gene and the appropriate luciferase-reporter plasmid. The *LacZ* reporter gene was incorporated into this assay in order to determine transfection efficiency. Twenty four hours after transfection, cells were treated with DATTs, thapsigargin, or left untreated for various time periods. The induction of luciferase activity was then measured using the Promega Luciferase Assay System, according to the manufacturer's instructions. Briefly, 4 volumes of diH<sub>2</sub>O was added to 1 volume of 5 x lysis to make a 1 x lysis buffer, which was equilibrated to room temperature before use. Cells were harvested and lysed by adding sufficient 1 x lysis buffer to cover the cells (e.g., 400  $\mu\text{l}$ /60mm culture dish or 200  $\mu\text{l}$  per well of a 6-well plate). Cells were incubated in the 1 x lysis buffer for 15 min at room temperature. The resulting cell suspension was transferred to a microfuge tube and was centrifuged at 12,000 x *g* for 15 seconds at room temperature. The cell lysate was then either stored at  $-80^{\circ}\text{C}$

or for later use or straightaway subjected to a luciferase assay. One hundred micro litres of the Luciferase Assay Reagent was pipetted into each well of a 96 well plate and 20  $\mu$ l of cell lysate were then added to each well containing the Luciferase Assay Reagent followed by vortexing briefly. To enhance reliability, each sample was made in triplicates and luciferase activity was then measured using a Tecan Luminometer.

A  $\beta$ -galactosidase assay to determine transfection efficiency was performed in parallel to the luciferase assay using the same prepared cell lysates. Thirty micro liters of lysate were incubated with *o*-nitrophenyl-  $\beta$ -D-galactopyranoside (ONPG) (Sigma) at 37°C with shaking for 5 min - 4 h until the transparent solution mixture turned to a bright yellow colour. The absorbance values of the yellow mixture were then measured at 405 nm.

Reaction mixture for  $\beta$ -galactosidase assay:

Cell lysates	30 $\mu$ l
0.1 M sodium phosphate solution	201 $\mu$ l
100 x Mg solution	3.0 $\mu$ l
4 mg/ml ONPG	66 $\mu$ l



#### **4 Statistical analysis**

Results are represented as means  $\pm$  SD. For statistical evaluation, Student's t test was applied using Origin6.1 with  $p < 0.05$  considered as significant, marked with one asterisk or  $p < 0.01$  considered as very significant, marked with two asterisks.

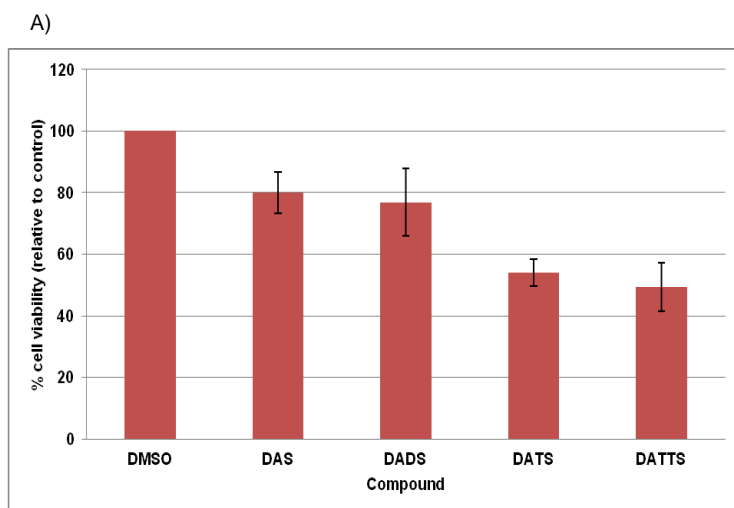
## 5 Results

### ***5.1 Reduction of cell viability by diallyl polysulfides is dependent on the length of the sulphur chain.***

Previous works in our lab have shown that polysulfanes have the capability to inhibit cell growth and reduce its viability. Using 1,6-heptadiene and 1,9-decadiene, which are synthetic carbon-analogues of DADS and DATTS, it was shown that neither 1,6-heptadiene nor 1,9-decadiene had any significant influence on cell viability as opposed to DADS and DATTS, which both reduced cell viability in a dosage- and time-dependent manner. This excludes the question of whether other factors such as the reactivity of allyl-groups may be responsible for the reduction in cell viability. Furthermore, since most of these polysulfides harbour two reactive C=C double bonds, one may argue that they might be responsible for the reduction in cell viability.

To address this, control experiments were also done in our lab and it was shown that these C=C double bonds have very little or no influence on cell viability [82]. My first set of experiments was therefore aimed at identifying the most active diallyl polysulfide against cancer cells. For this reason, the effect of diallyl mono- (DAS), diallyl di- (DADS), diallyl tri- (DATS) and diallyl tetrasulfide (DATTS) on cell viability and DNA damage was analysed using the HCT116 colorectal cancer cell line as a suitable model system. This cell line was chosen because it has been the gold standard for performing gene knockout [99]. It has been extensively used in cancer research because it contains several mutations that inactivate tumour-suppressor genes or activate oncogenes, which results in disruption of key signalling pathways and cellular functions [100, 101, 102]. HCT116 cells were treated for 24 h with either DMSO solvent alone to serve as a negative control or with 50  $\mu\text{M}$  of DAS, DADS, DATS or DATTS and cell viability was measured with an MTT assay. As shown in Figure 17 (A), 50  $\mu\text{M}$  of DAS, DADS, DATS or DATTS led to a reduction in cell viability by about 20%, 25%, 43% and 50% respectively, 24 h after treatment. The result clearly showed that DATTS is more potent against HCT116 colon cancer cells than DATS, which in turn is more potent than DADS and DAS. The activity of these

compounds was explored further at protein expression levels in a second experiment. Poly-ADP-ribose polymerase (PARP) is a protein known to be involved in not only DNA damage and repair, but also programmed cell death [82, 103, 105]. Proteolytic cleavage of PARP by caspases is a hallmark of apoptosis in most cell lines [9, 82, 88, 104, 105, 106] and diallyl polysulfides are known to induce its cleavage [82, 104]. In order to analyse the effect of various polysulfides on PARP cleavage, HCT116 cells were treated for 24 h with either DMSO or with 50  $\mu$ M of DAS, DADS, DATS or DATTS. Cells were then lysed and the whole cell extract transferred onto a 7.5% SDS-polycacrylamide gel. After transfer to a PVDF membrane, the filter was incubated with antibodies directed against PARP. PARP cleavage was observed in all polysulfide treated cells and even more so in DATTS treated cells, whilst there was little or no cleavage in DMSO control treated cells (Fig. 17B). This result was in agreement with the decreasing cell viability in the first experiment (Fig. 17A) and it was therefore concluded that DATTS is more active in killing HCT116 cells than DATS, DADS and DAS. Hence, the focus was on DATTS in all subsequent experiments in exploring the effects of diallyl polysulfides on HCT116 colorectal cancer cells.



## Results

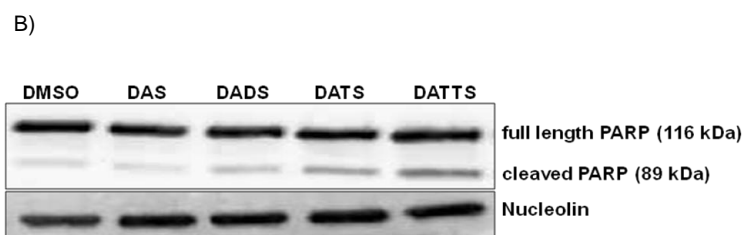


**Figure 17.** The ability of diallyl polysulfides to reduce cell viability and induce apoptosis depends on the length of the sulfur chain. (A) HCT116 cells were seeded in 24-well plates and treated with 50  $\mu$ M DAS, DADS, DATS, DATTS or 0.05% DMSO for 24 h. Afterwards, MTT assay was used to determine cell viability. Data are depicted as means  $\pm$  SD, ( $n = 3$ ). (B) HCT116 cells were treated for 24 h with 0.05% DMSO as a control or 50  $\mu$ M DAS, DADS, DATS or DATTS and cell extracts were analysed for PARP cleavage using SDS polyacrylamide gel electrophoresis and Western blotting. Total protein extract (75  $\mu$ g) was separated on a 7.5% SDS–polyacrylamide gel, blotted on a PVDF membrane and PARP protein expression was detected using the corresponding antibody. Nucleolin was used as a loading control.

The next obvious questions that came to mind were 1) does DATTS reduce HCT116 cell viability in a time- and dosage-dependent manner? and 2), since diallyl tetrasulfide is synthesized from allyl mercaptan and sulfur chloride ( $S_2Cl_2$ ) as described by Derbesy and Harpp [18], does reactivity of the allyl-group of allyl mercaptan play a role in cell viability? To answer these two questions, two separate set of experiments were carried out. In the first set of experiments, HCT116 cells were treated with 0.05% DMSO, 50  $\mu$ M allyl mercaptan (AISH) or 50  $\mu$ M DATTS for 8, 24, 48 and 72 h. In the second set of experiments, HCT116 cells were either left untreated (0 h) or treated with 25, 50, or 100  $\mu$ M DATTS for 24 h. Cells in both sets of experiments were then analysed for cell viability by the MTT assay as previously described. As shown in Figure 18 (B), 50  $\mu$ M of DATTS was able to reduce HCT116 cell viability by about 20%, 50%, 62% and 75% for 8, 24, 48 and 72 h, respectively, whilst AISH had minimal effect relative to DMSO control. In Figure 18 (A), it can be seen that cell viability was reduced by about 21%, 49% and 46% with 25, 50, or 100  $\mu$ M treatment, respectively. Based on results from the two sets of experiments, it can be safely concluded that DATTS reduce HCT116 cell viability in both a time- and dosage-dependent manner and that AISH has very little effect on cell viability.

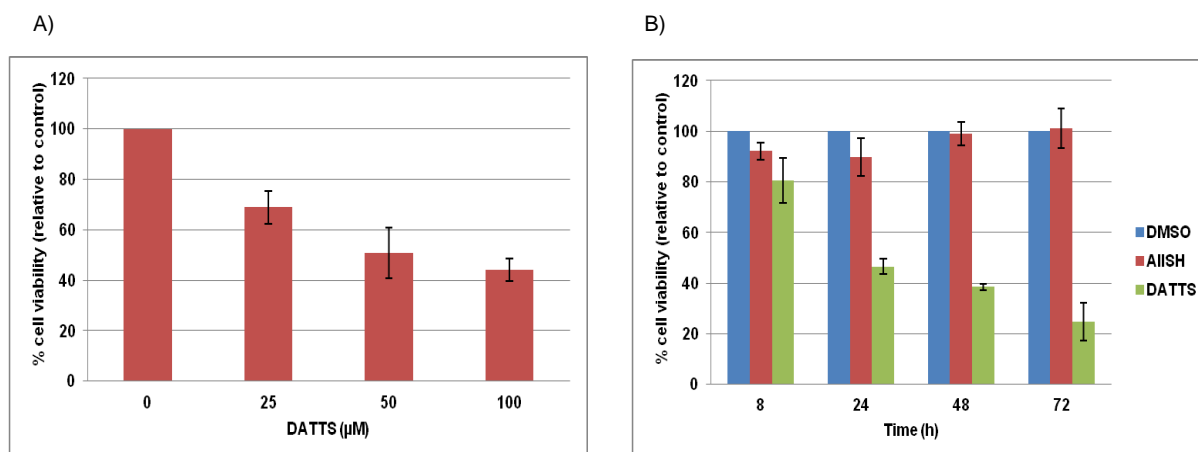
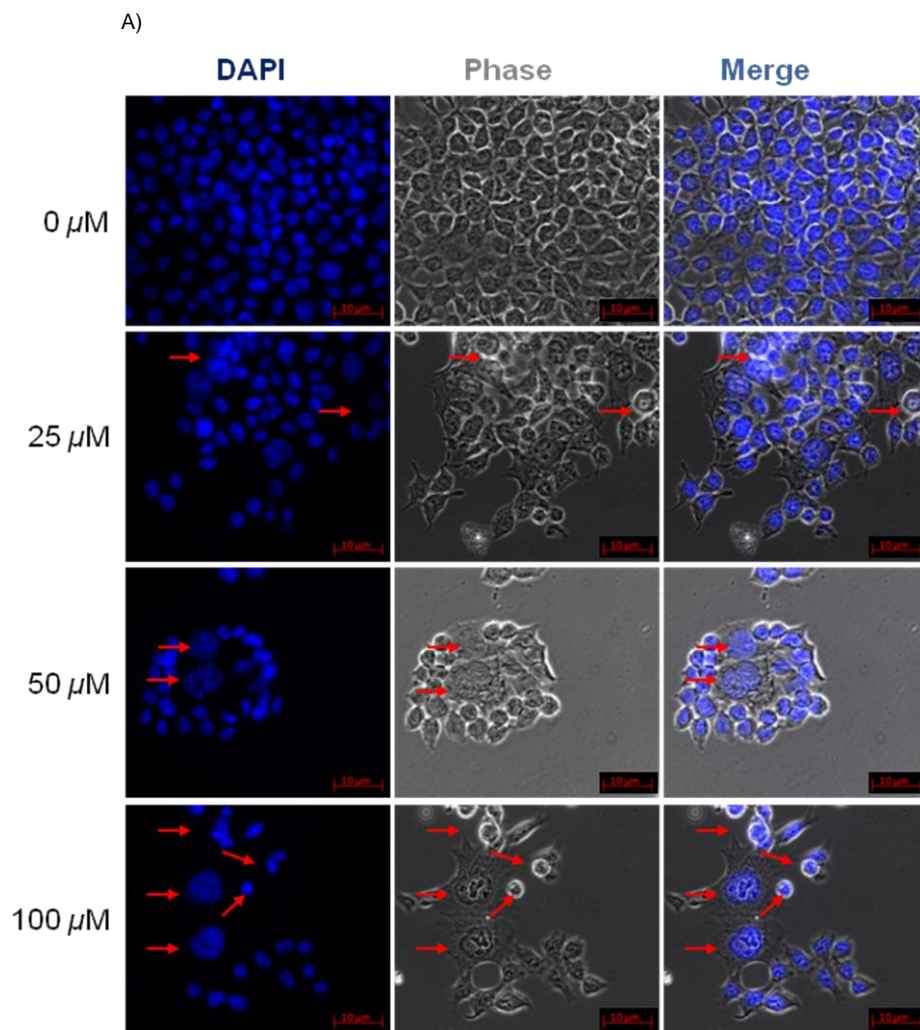


**Figure 18.** DATTS affect the viability of HCT116 cells in both dosage and time dependent manners. (A) cells were seeded in 24-well plates and treated with either DMSO (0  $\mu\text{M}$ ) or with 25, 50 or 100  $\mu\text{M}$  DATTS for 24 h. Afterwards, MTT assay was used to determine cell viability. (B) cells were seeded in 24-well plates and treated with 50  $\mu\text{M}$  DATTS, 50  $\mu\text{M}$  ally mercaptan (AIIISH) or DMSO for 8, 24 and 48 h. Afterwards, MTT assay was used to determine cell viability. Untreated (as in A) or DMSO control cells (as in B) showed the most viable cells and were set to 100%. The results represent the mean  $\pm$  SD of three separate experiments.

### 5.1.1 DATTS treatment leads to changes in HCT116 cell morphology

To fully understand whether the inhibitory effect of DATTS on HCT116 cell growth was due to apoptosis, the appearance of typical apoptotic nuclear morphology in HCT116 cells was explored. Cells were incubated with 0, 25, 50 or 100  $\mu\text{M}$  DATTS for 24 h. The nuclei of the cells were then stained with 4',6-Diamidino-2-phenylindole (DAPI) solution and analysed with fluorescence microscopy. As shown in Figure 19 (A), DATTS does indeed affect HCT116 cell morphology. It causes cell death, which increases with increase in DATTS concentration. The nuclei of all treated cells showed classical features of proceeding apoptotic events characterised by significant chromatin condensation, shrinkage, loss of nuclear construction and formation of apoptotic bodies. As DATTS concentration increases, more and more cells die and they tend to float in the media suspension with very little of them attached to the cell culture plate. The cell nucleus swells and disintegrates and

formation of apoptotic bodies begin to appear as indicated by the red arrows. These features, however, are not observed in control cells, where cells remain attached to the bottom of the cell culture plate and continue to grow at their normal rate. The question was then asked, whether cells will return to their normal selves once DATTS treatment was withdrawn and fresh media applied to the cells. For this, cells were photographed under fluorescence microscopy before been subjected to 50  $\mu\text{M}$  DATTS and further photographed after 24, 48 and 72 h. Media was changed, a fresh one applied, and cells were allowed to grow for a further 48 h. As shown in Figure 19 (B), DATTS treatment greatly affected cell morphology and proliferation, which was also time-dependent. This condition, however, was reversed once treatment was withdrawn and cells were able to fully recover.



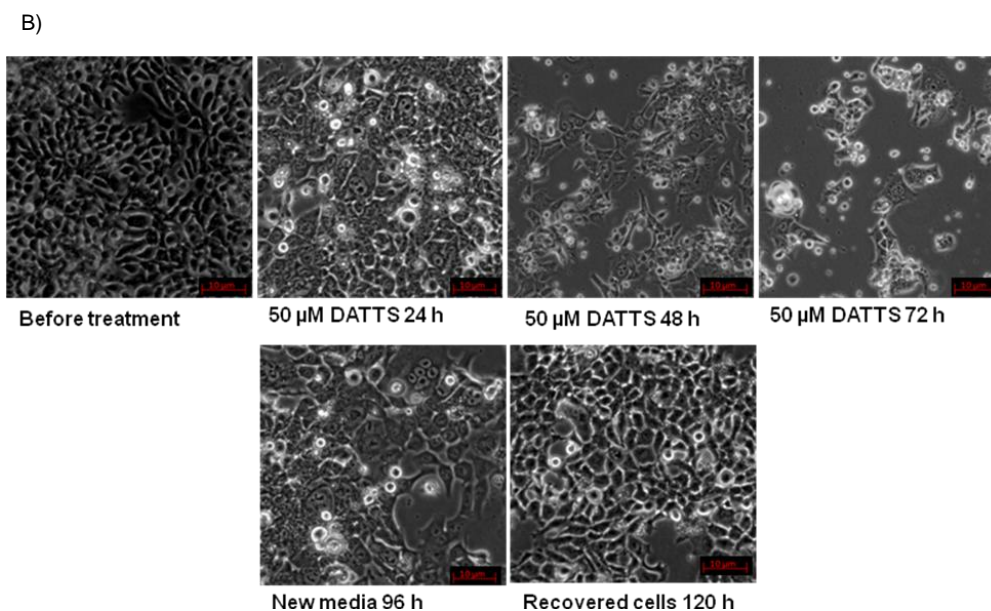


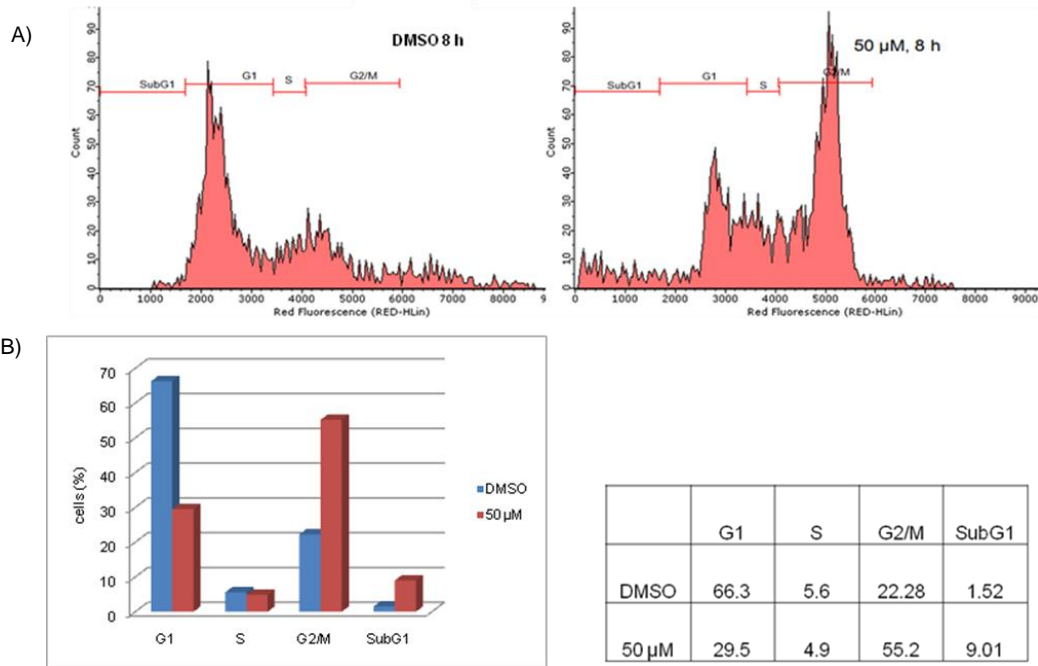
**Figure 19.** DATTS treatment affects HCT116 cell morphology which can be reversed upon withdrawing treatment. HCT116 cells were cultured in 6 well plates overnight before incubation with 0, 25, 50 or 100  $\mu$ M DATTS for 24 h (A) or incubated with 50  $\mu$ M DATTS for 24, 48 and 72 h before withdrawing treatment, applying fresh media and incubating for another 48 h. The nucleus was stained with DAPI (blue). Afterwards, cell morphology and viability was assessed by microscopy at a scale bar of 50  $\mu$ m.

### 5.1.2 Treatment of HCT116 colon cancer cells with DATTS induces cell cycle arrest and apoptosis

Since reduced cell viability may also be due to a range of biochemical processes such as cell cycle arrest and/or apoptosis, the question of whether DATTS treated cells arrest in subG<sub>1</sub>, G<sub>1</sub>- or G<sub>2</sub>-phase of the cell cycle and the degree of apoptosis was addressed. HCT116 cells were therefore either treated with DMSO or 50  $\mu$ M DATTS for 8 and 24 h as described in the methods section and cell cycle analysis was performed by flow cytometry. As indicated in Figures 20 (A), (B), (C) and (D), the incubation of HCT116 cells in the presence of DATTS resulted in an increased accumulation of cells in the subG<sub>1</sub> phase in a manner similar to that observed with the MTT assays and increased cell arrest in the subG<sub>1</sub> phase is widely considered a confirmation of apoptosis induction. After 8 h, about 55% of DATTS-treated cells arrested in the G<sub>2</sub>/M phase and about 9% in subG<sub>1</sub>. 24 h on, 37% of DATTS-treated

## Results

cells arrested in the G<sub>2</sub>/M phase of the cell cycle, whilst about 26% were in the subG<sub>1</sub> phase. These findings suggest that HCT116 cells may also undergo cell cycle arrest at the G<sub>2</sub>/M phase along with induction of apoptosis after exposure to DATTS.





## Results

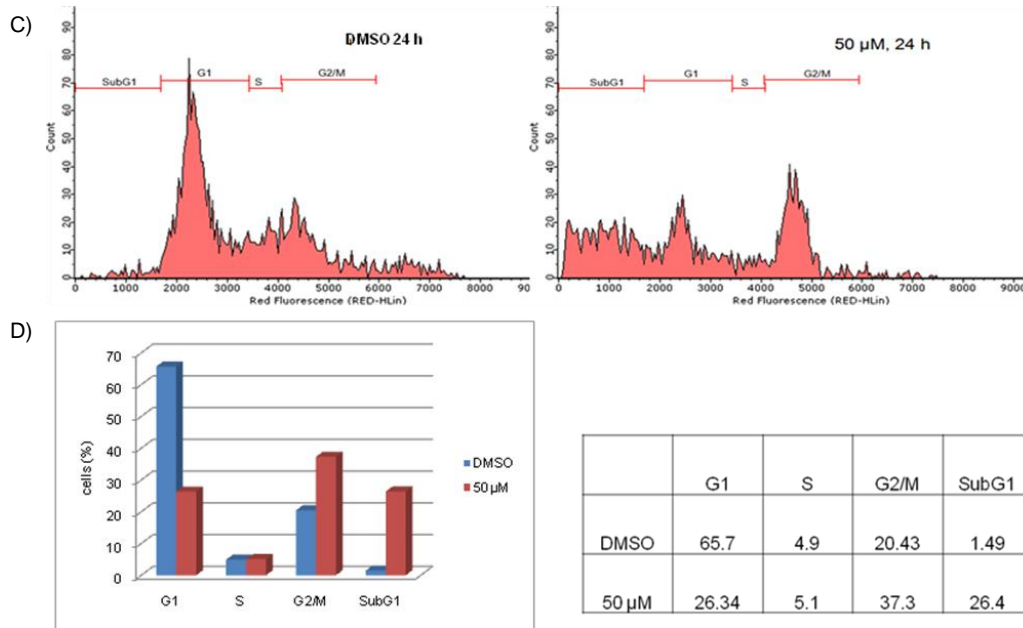


**Figure 20.** The influence of DATTS on cell cycle distribution. HCT116 cells were treated for 8 (A and B) and 24 h (C and D) with either DMSO or with 50  $\mu$ M DATTS and then analysed by FACS. (A and C) FACS analysis of the treated cells. (B and D) Percentage distribution. One representative of at least three similar independent experiments is shown here.

### 5.1.3 DATTS inhibits CDK1 expression and cdc25C phosphorylation on threonine 48

cdc25C is a protein phosphatase responsible for dephosphorylating and activating CDK1, which is a vital step in regulating the entry of cells into mitosis [107, 108, 109, 110]. Inactivation of cdc25C and/or CDK1 induces G<sub>2</sub>/M cell cycle arrest [110, 111, 112, 113]. In response to DNA damage, the checkpoint kinases Chk1 and Chk2 phosphorylate cdc25C at the serine 216 (Ser216) residue, thereby creating a binding site for the 14-3-3 protein. The binding of cdc25C to the 14-3-3 protein sequesters cdc25C into the cytoplasm thereby preventing untimely mitosis [114, 115]. Other CDK1-catalyzed phosphorylation sites have also been identified, which includes threonine 48 (Thr48) and threonine 76 (Thr67). They are required for maximal biological activity of cdc25C [111, 115]. It was therefore crucial in this study to analyse the effect of DATTS on both CDK1 and cdc25C phosphorylation. HCT116 cells were seeded and treated as described in the methods section. After harvesting

cells at the various time periods, 75  $\mu\text{g}$  of total protein from cell extracts was loaded on to a 12.5% SDS-polycacrylamide gel and analysed by Western blot for CDK1 and phospho-cdc25C (Thr48) expression. From Figure 21 (A) and (B), it can be clearly seen that DATTS inhibited both CDK1 and phospho-cdc25C protein expressions over the course of 72 h. This inhibition is even more prominent in phospho-cdc25C after 3 h of treatment indicating deactivation of this protein by DATTS.

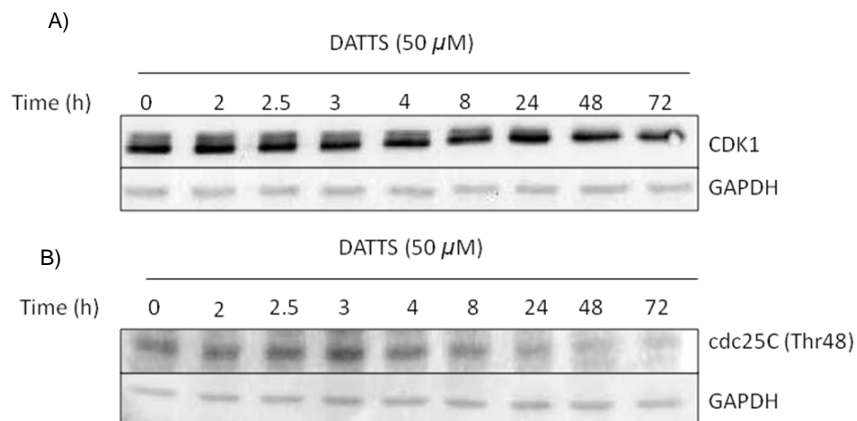


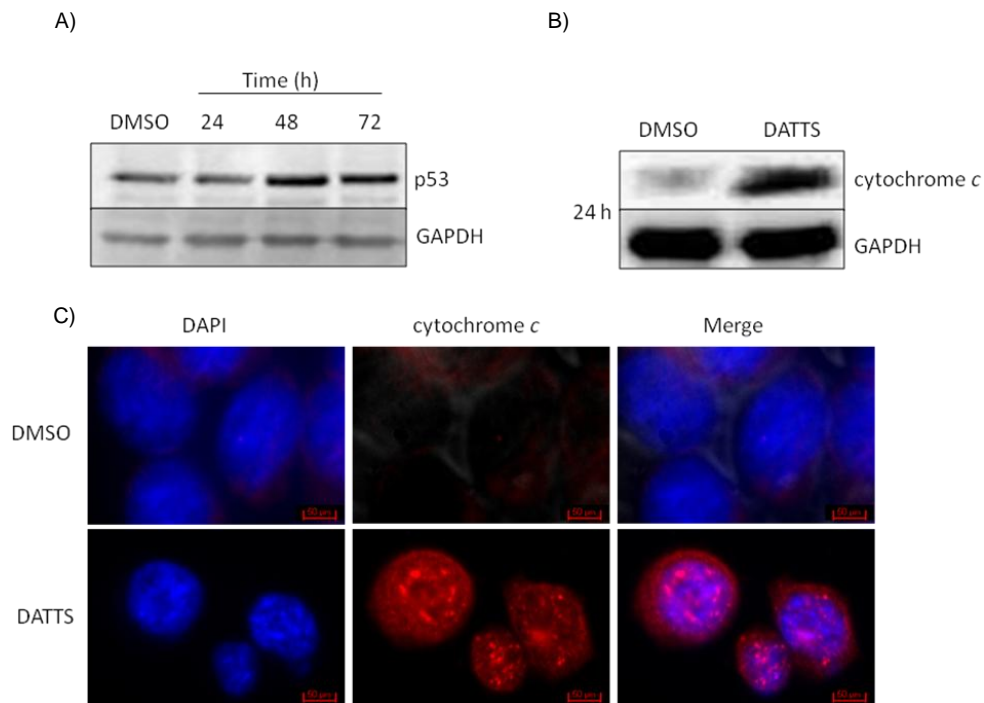
**Figure 21.** DATTS inhibits CDK1 and phospho-cdc25C (Thr48) protein expressions in HCT116 cells. HCT116 cells were untreated (0 h) or treated with 50  $\mu\text{M}$  DATTS for 2, 2.5, 3, 4, 8, 24, 48, and 72 h and protein expression was studied by Western blotting. The proteins (50  $\mu\text{g}$  whole cell extract) were separated on a 12.5% SDS-polyacrylamide gel, blotted on a PVDF membrane. CDK1 (A) and cdc25C (Thr48) (B) expressions were visualised with the appropriate antibody on an ECL system.

#### 5.1.4 DATTS induces the mitochondrial apoptotic pathway in HCT116 colon cancer cells

Apoptosis plays a crucial role as a protective device against tumour. In this study, so far, cell viability, PARP cleavage, DAPI staining, and cell cycle analysis have indicated DATTS induced apoptosis. It was therefore imperative to investigate which apoptotic pathway is triggered by DATTS. The mitochondrial apoptotic pathway is characterised mostly by caspase activation that is subsequent to cytochrome *c* release into the cytosol, which in turn is regulated by pro- and anti-apoptotic *bcl-2* family proteins. The expression level of these proteins along with that of *p53* (as it is

## Results

implicated in both cell cycle arrest and apoptosis) was therefore examined (as described in the methods section) following DATTS treatment. As shown in Figure 22 (B) and (C), both Western blot and immunofluorescence indicate an increase in cytochrome *c* release into the cytosol. In Figure 22 (A), (D) and (E), there were increases in p53 and bax protein expressions, and a decrease for that of bcl-2, whilst in Figure 22 (F), caspase 3 cleavage was observed. All of which suggests that DATTS does indeed induce the mitochondrial apoptotic pathway.



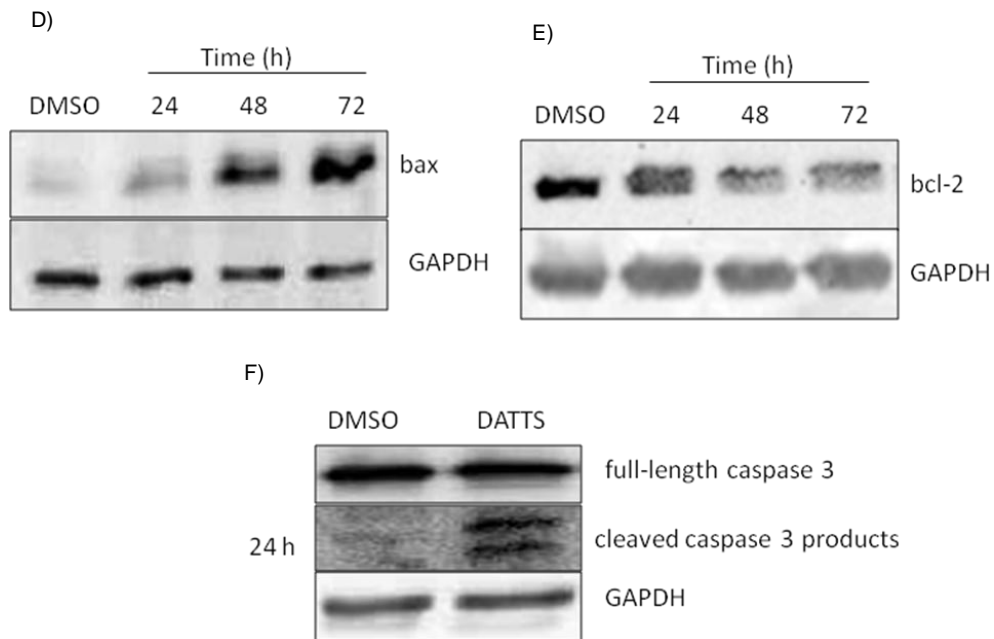


**Figure 22.** DATTS modulates p53, bcl-2 and bax protein expression, induces cytochrome *c* release from the mitochondria and activates caspase 3 in HCT116 cells. HCT116 cells were treated with either 50  $\mu\text{M}$  DATTS or with DMSO. Protein expression was studied by Western Blotting. The proteins (whole cell extracts) were separated on a 12.5% SDS-polyacrylamide gel, blotted on a PVDF membrane and p53 (A), cytochrome *c* (B), bax (D) or bcl-2 (E) was visualised with the appropriate antibody. For the immunofluorescence assay in (C), HCT116 cells were treated with either DMSO (control) or with 50  $\mu\text{M}$  DATTS for 24 h. After this time, cells were fixed and incubated with the appropriate primary and secondary antibody before staining the nucleus (blue) with DAPI. Cytochrome *c* release into the cytosol (red) was analysed using a Zeiss Axioskop fluorescence microscope at a scale bar of 50  $\mu\text{m}$ . For (F), HCT116 colorectal cancer cells were treated with DMSO or 50  $\mu\text{M}$  DATTS for 24 h. Caspase activation was analysed by Western Blot. Cell lysates were separated by electrophoresis as in (A). Full-length caspase 3 and its cleavage products were detected with a caspase 3-specific antibody. GAPDH was used as a loading control. One representative of at least 3 Western blots is shown here.

### 5.1.5 DATTS-induced apoptosis is reduced by antioxidants

Recently, quite a few studies have indicated that reactive oxygen species (ROS) are involved in diallyl disulfide (DADS)-induced cell cycle arrest and apoptosis [69, 70, 116]. If that is also the case for DATTS-induced apoptosis, then using potent

antioxidants such *N*-acetyl cysteine (NAC) should be able to prevent DATTS-induced apoptosis. To test this hypothesis and evaluate the contribution of ROS to the DATTS-induced DNA damage and apoptosis, HCT116 cells were treated with DATTS in the absence or presence of NAC, ascorbic acid (ASC) or glutathione (GSH) for microscopy analysis (Fig. 23A) or in the absence or presence of NAC and ASC for Western blot analysis of PARP cleavage (Fig. 23B) and  $\gamma$ H2AX protein expression (Fig. 23C). Evident from Figure 23 (A), it can be clearly seen that in the presence of GSH and more in particular in the presence of NAC, DATTS did very little to the morphology of HCT116 cells. Also, as shown in Figure 23 (B), DATTS induced PARP cleavage after 24 and 48 h in the absence of NAC and ASC. In the presence of NAC however, there was only marginal cleavage of PARP, indicating that this particular antioxidant prevented apoptosis, whereas ASC was not sufficient to inhibit PARP cleavage indicating that DATTS triggers different pathways that may be parallel and independent of each other. NAC also reduced  $\gamma$ H2AX protein expression (Fig. 23C). Taken together, it can be assumed with some degree of certainty that thiols and possibly oxidative stress involving ROS production might be contributing factors to the DATTS influence on cell viability, cell cycle arrest and the subsequent apoptotic cell death.

## Results

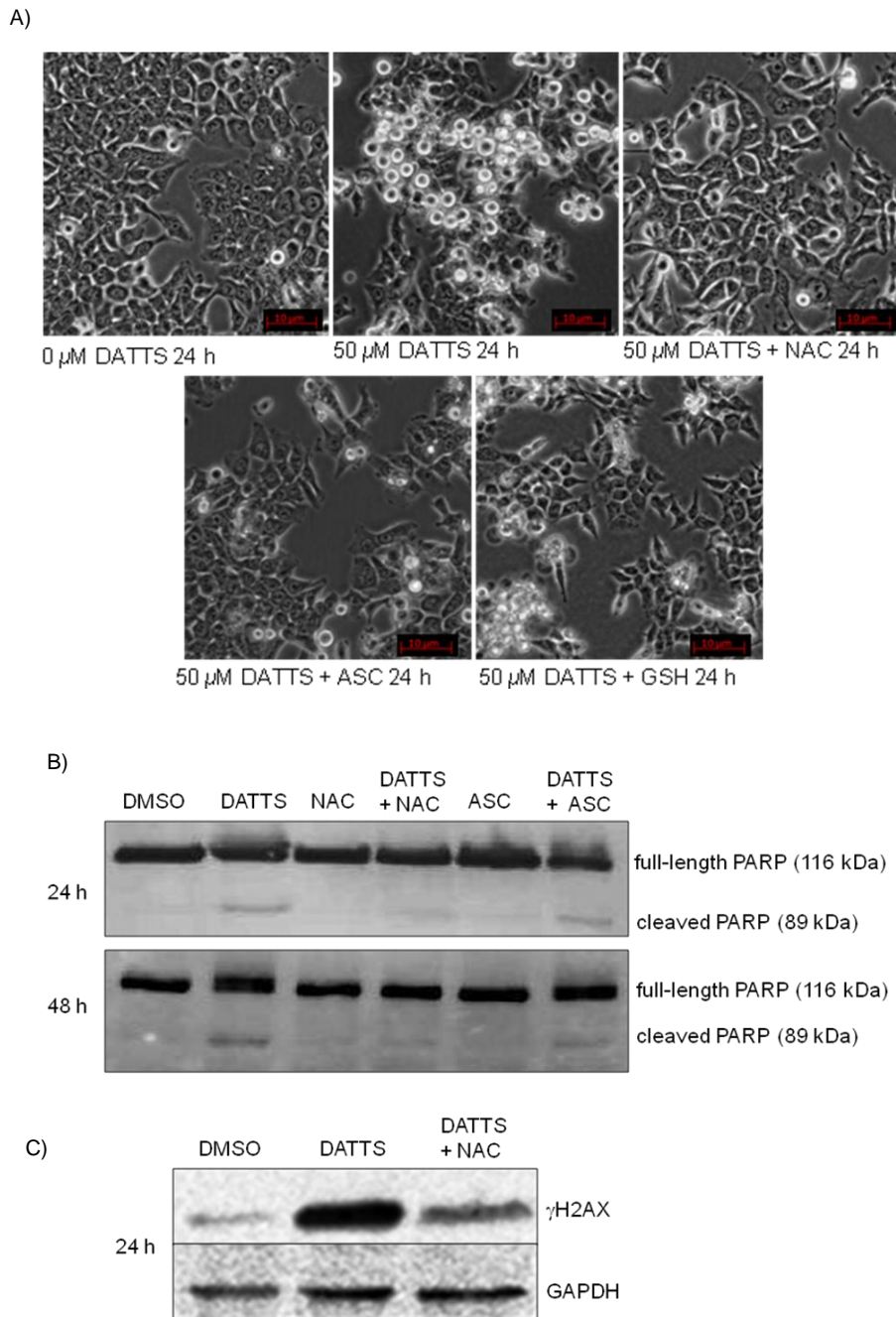


**Figure 23.** Antioxidant pretreatment reduce DATTS-mediated cytotoxicity and apoptosis induction. Pretreatment of HCT116 cells with the antioxidants *N*-acetyl cysteine (NAC), ascorbic acid (ASC) or glutathione (GSH) 0.5 h before incubation with DATTS prevents DATTS induced cell damage (A), DNA damage and apoptosis (A), (B) and (C). DATTS-induced cell damage (A) was analysed using a Zeiss Axioskop fluorescence microscope at a scale bar of 10  $\mu$ m. One representative of at least 2 independent experiments is shown here.

## ***5.2 DATTS treatment induces formation of superoxide anion radicals and hydrogen peroxide in a time- and dosage-dependent manner***

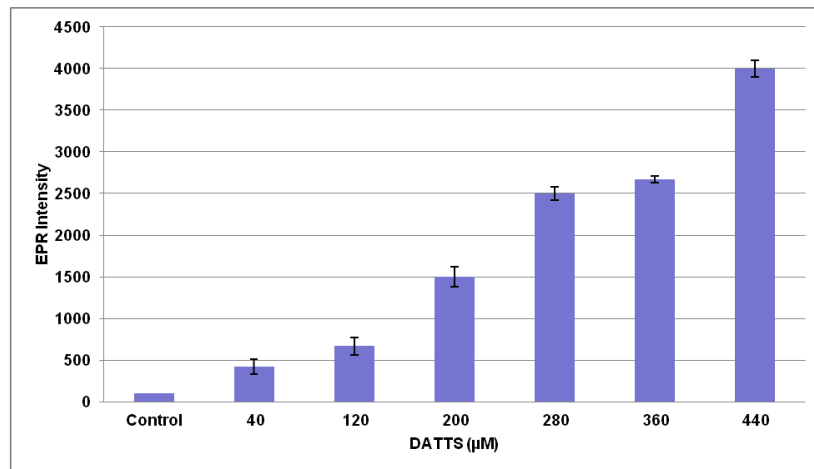
Since it was shown in this study that DATTS-induced apoptosis can be reduced by antioxidants, which indicates that ROS may be involved in the observed apoptotic cell death, it became paramount to investigate not only the DATTS-induced ROS production but also the specific radicals that may be involved and the impact of these on intracellular thiol levels. A sound knowledge of this will shed more light on DATTS-induced redox signalling and how these redox balances may affect many cellular functions in HCT116 cancer cells, including signalling pathways, which in turn may cause cell cycle arrest and induction of apoptotic cell death. The first task was to actually show that DATTS does induce ROS production. For this, HCT116 cells were treated either with DMSO or with increasing concentrations of DATTS (Fig. 24A) for 1 h. In another experiment, the cells were pretreated for 0.5 h with either ASC or with superoxide dismutase (SOD) before being exposed to 500  $\mu\text{M}$  DATTS for another 1 h. This high concentration was determined by titration experiments for the spin probe - electron paramagnetic resonance (EPR), hence the 500  $\mu\text{M}$  DATTS. As shown in Figure 24 (A), there is a linear correlation between increasing DATTS concentrations and EPR intensity. As the DATTS concentration increases, so does the EPR intensity. Pretreatment of HCT116 cells with ASC or SOD, however, lowers the EPR intensity (Fig. 24B), which is more pronounced in cells that were pretreated with ASC than those pretreated with SOD. This probably is due to the fact that SOD does not enter the cells [117], as opposed to ASC which does [118].

The second task was to investigate if DATTS induces superoxide anion radicals and hydrogen peroxide as these two ROS are implicated in most oxidative stresses leading to apoptotic cell death [69, 70, 116]. For this,  $\text{O}_2^{\cdot-}$  generation in HCT116 cells treated with DATTS was investigated using the dihydroethidium (DHE) assay according to the manufacturer's instructions. As shown in Figures 24 (C) and (D), DATTS caused an immediate increase in DHE oxidation to fluorescent 2-hydroxyethidium in a time and dosage-dependent manner. Next,  $\text{H}_2\text{O}_2$  generation in the same cell line was investigated using the Amplex Red assay. From Figures 24

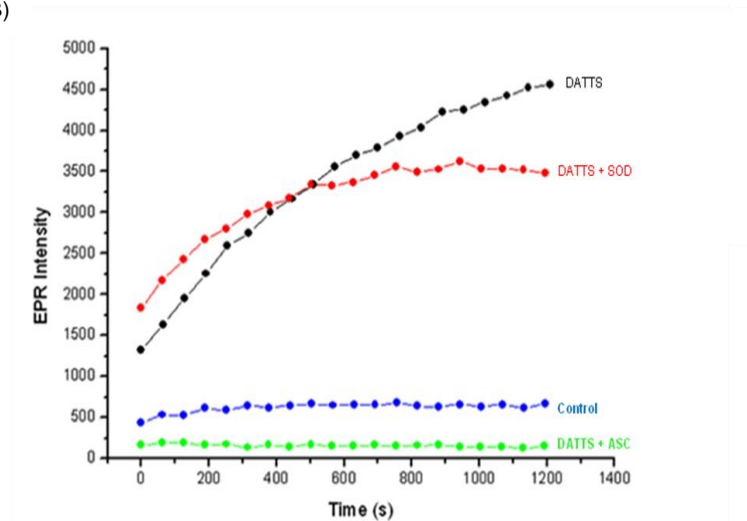
## Results

(E) and (F), it can be seen that DATTS also caused a slight increase in  $\text{H}_2\text{O}_2$  levels in both a time- and dosage-dependent manner. Changes in  $\text{H}_2\text{O}_2$  level observed in DATTS treated cells, however, is rather small compared to the changes observed for the  $\text{O}_2^{\cdot-}$  level in the same cells, indicating that  $\text{O}_2^{\cdot-}$  plays a more important role than  $\text{H}_2\text{O}_2$ .

A)



B)





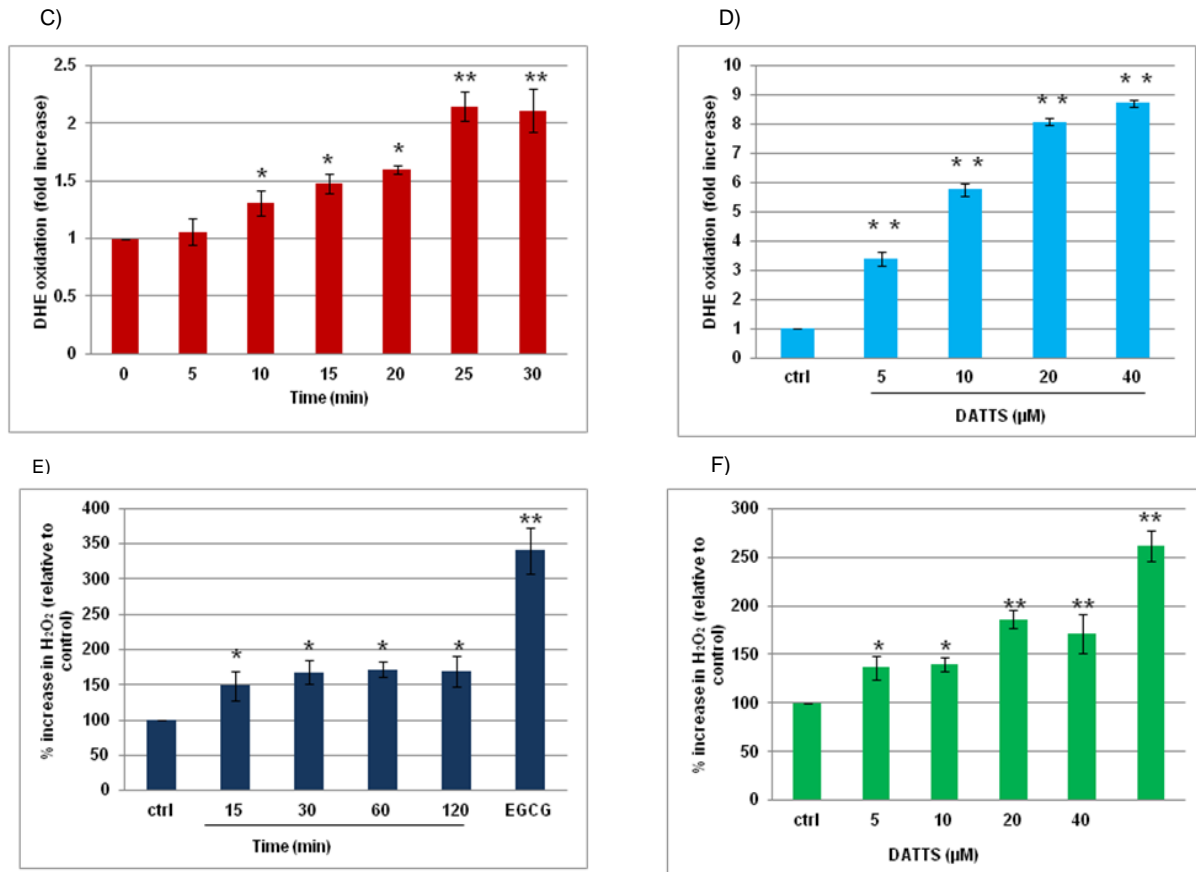


**Figure 24.** DATTS transiently induces  $O_2^{\cdot-}$  and  $H_2O_2$  in a time and dose-dependent manner. (A) increase in EPR intensity correlates with increase in DATTS concentration. (B) pretreatment of HCT116 cells with antioxidants reduces the DATTS induced-radical EPR intensity. (C) increase in DHE oxidation in HCT116 cells, indicative of  $O_2^{\cdot-}$  formation following treatment with 40  $\mu M$  DATTS for 0, 5, 10, 15, 20, 25 and 30 min. (D) dose-dependent increase in  $O_2^{\cdot-}$  formation after 20 min of treatment with DATTS. Data are expressed as a fold increase in DHE oxidation rate in relation to solvent control. (E)  $H_2O_2$  produced in HCT116 cells following treatment with 25  $\mu M$  epigallocatechin-3-gallate or 40  $\mu M$  DATTS for 15, 30, 60 and 120 min. (F) dose-dependent increase in  $H_2O_2$  production after 30 min of treatment with DATTS. Data are expressed as a percentage increase in  $H_2O_2$  produced in relation to solvent control. The mean of three independent experiments is shown. \*\* $p < 0.01$  or \* $p < 0.05$ .

### 5.2.1 DATTS treatment leads to thiol depletion in HCT116 cells

In the present study, experiments with NAC and GSH have indicated that thiols may be targets for DATTS. Furthermore, it has been reported that alterations in intracellular thiol levels may affect cellular functions, including signaling pathways which may in turn cause cell cycle arrest and induction of apoptosis [119, 120]. Therefore, using cysteine hydrochloride monohydrate as a standard, total thiol levels were measured 2 h after treatment of HCT116 cells with increasing concentrations of DATTS, or at various time intervals after treatment within 40  $\mu$ M DATTS. As shown in Figures 25 (A) and (B), DATTS caused a significant time and dose-dependent depletion of total thiols. In Figure 25 (B), DATTS caused total thiol depletion of about 52% after 2 h treatment.

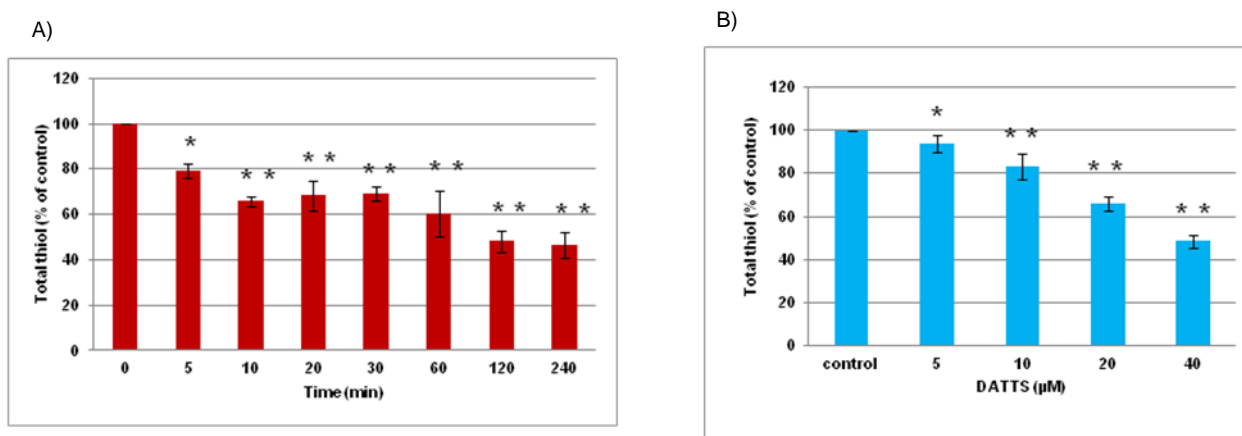


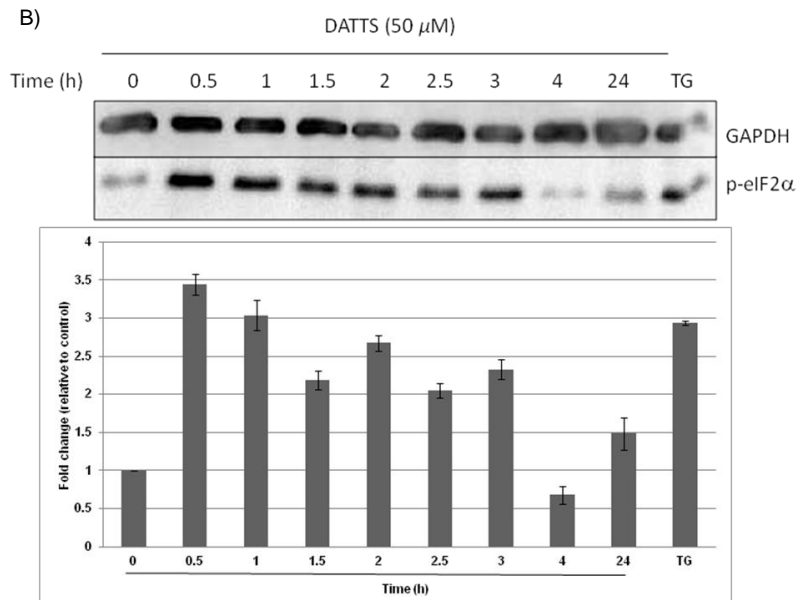
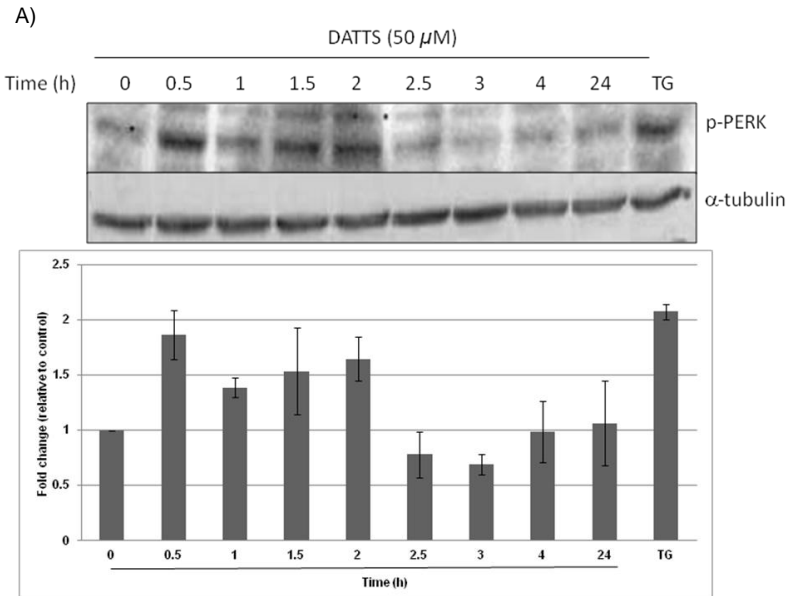
**Figure 25.** DATTS mediates thiol oxidation and depletion. (A), time-dependent oxidation of total thiol levels measured in HCT116 cells after treatment with DATTS and (B), dose-dependent oxidation of total thiol levels measured in HCT116 cells 2 h after treatment with DATTS. Data are expressed as a percentage decrease in thiol depletion relative to solvent control. The mean of three independent experiments is shown. \*\* $p < 0.01$  or \* $p < 0.05$ .

### 5.3 DATTS induces both PERK and eIF2 $\alpha$ phosphorylation in HCT116 cells

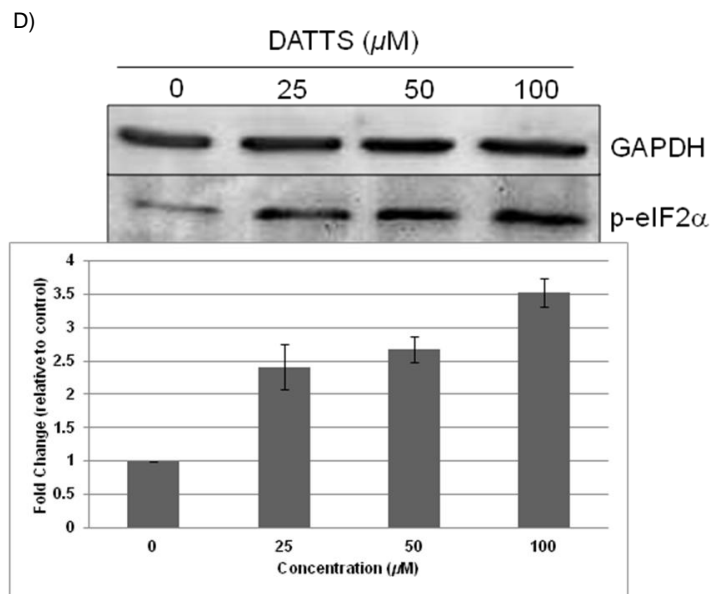
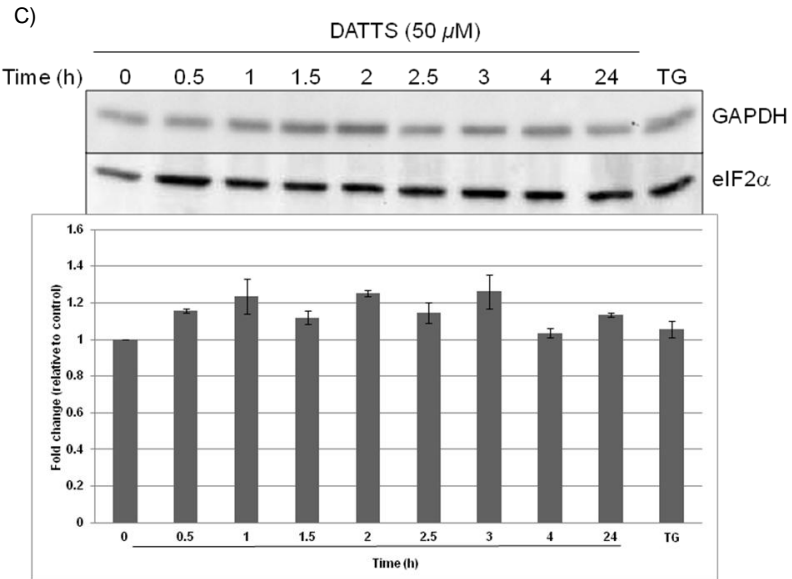
Diallyl disulfide has been shown to induce apoptosis in human colon cancer cells (COLO 205) through the induction of reactive oxygen species (ROS) and ER stress

[70]. In response to cellular stress and in particular to ER stress, PERK kinase is activated by phosphorylation. In order to study whether PERK becomes phosphorylated after DATTS treatment of HCT116, cells were extracted and the proteins analysed by Western blotting using an antibody directed against phospho-PERK. As shown in Figure 26 (A), a rapid but transient increase in the amount of phospho-PERK was observed, indicating activation of the PERK kinase. One of the down-stream substrates of the PERK kinase is the eukaryotic initiation factor 2 $\alpha$  (eIF2 $\alpha$ ), which is inactivated by phosphorylation. This inactivation leads to a down-regulation of the general translation machinery [122]. Thus, it was an interesting question whether DATTS treatment of HCT116 cells and ROS generation might induce phosphorylation of eIF2 $\alpha$ . For this, we either treated the cells with 10 nM thapsigargin (a compound known to induce ER stress) [122], to serve as a positive control, or with DATTS for different time periods. Western blot analysis with antibodies directed against phosphorylated eIF2 $\alpha$  revealed an immediate increase in phosphorylated eIF2 $\alpha$  (Fig. 26B) within 30 min of treatment with DATTS. This increase persisted until 3 h post treatment. However, as shown in a further Western blot analysis (Fig. 26C), total eIF2 $\alpha$  protein level does not seem to be greatly affected by DATTS in HCT116 treated cells. Furthermore, the DATTS-induced phosphorylation of eIF2 $\alpha$  seems to be concentration dependent. Presented in Figure 26 (D), the increase in DATTS concentration led to an increase in the level of p-eIF2 $\alpha$  protein. In order to evaluate the contribution of ROS to the DATTS-induced eIF2 $\alpha$  phosphorylation, HCT116 cells were treated with DATTS in the absence or presence of glutathione (GSH), *N*-acetyl cysteine (NAC) or ascorbic acid (ASC). As shown in Figure 26E, DATTS induced eIF2 $\alpha$  phosphorylation 2 h after treatment. The induction of eIF2 $\alpha$  phosphorylation was slightly reduced in the presence of GSH, even more so in the presence of NAC and strongly in the presence of ASC. Reductions in eIF2 $\alpha$  phosphorylation relative to DMSO control were about 25, 68 and 94% for treatments in the presence of GSH, NAC and ASC respectively. These data support the idea that ROS was indeed responsible for the phosphorylation of eIF2 $\alpha$ . The weak reduction in the phosphorylation of eIF2 $\alpha$  by GSH and NAC indicated that DATTS may not be directly implicated in the phosphorylation of eIF2 $\alpha$ .

# Results



# Results



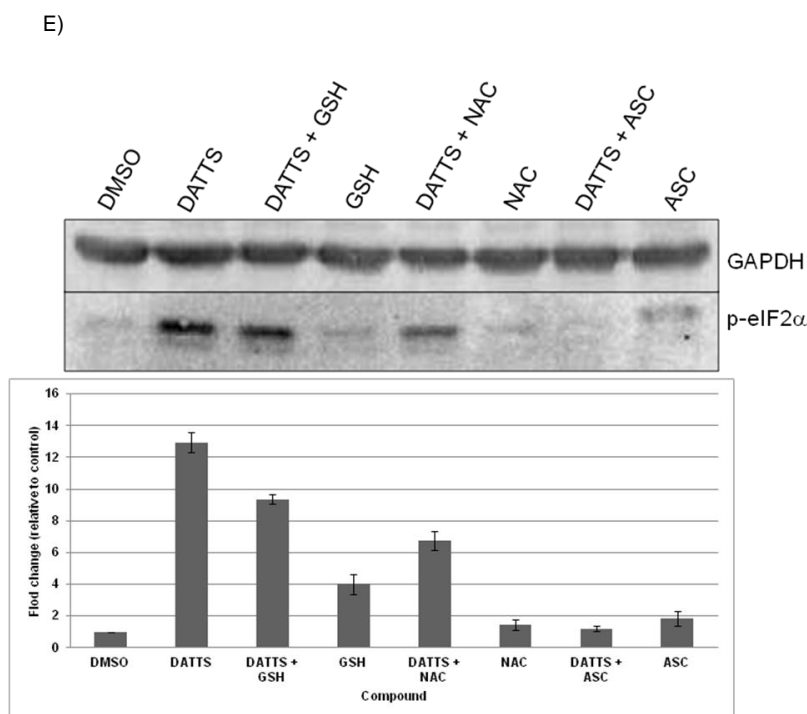
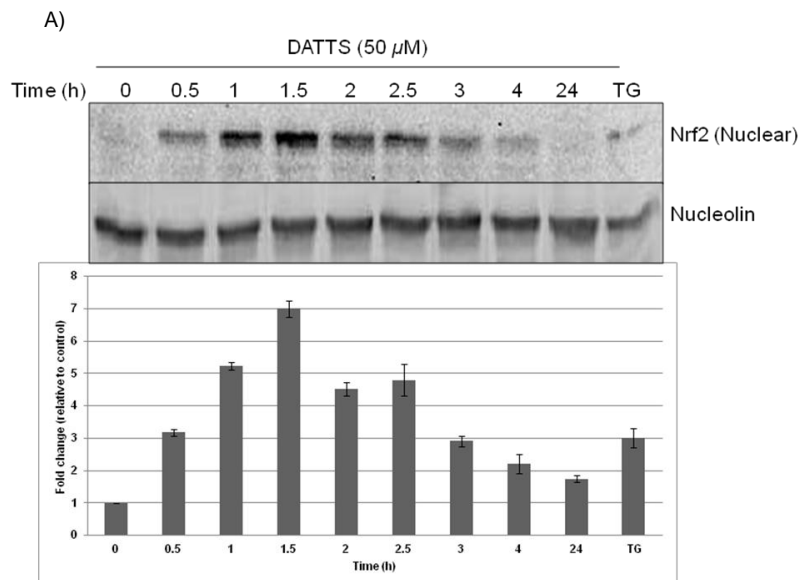


**Figure 26.** DATTS activates the phosphorylation of PERK, which in turn induces eIF2 $\alpha$  phosphorylation at serine 51 in HCT116 cells. HCT116 cells were untreated (0 h) or treated with 50  $\mu$ M DATTS for 0.5, 1, 1.5, 2, 2.5, 3, 4, and 24 h. For a positive control, cells were treated with 10 nM thapsigargin (TG) for 4 h and protein expression was studied by Western blotting. The proteins (100  $\mu$ g) were separated on a 12.5% SDS-polyacrylamide gel, blotted on a PVDF membrane. p-PERK (A) p-eIF2 $\alpha$  (B) and eIF2 $\alpha$  (C) expressions were visualised with the appropriate antibodies. (D) cells were seeded in 6-well plates and treated with 0, 25, 50 or 100  $\mu$ M DATTS for 2 h. (E) cells were seeded in 6-well plates and treated with DATTS in the absence or presence of glutathione (GSH), N-acetyl cysteine (NAC) or ascorbic acid (ASC). Cells were lysed and then the cell extract analyzed by SDS polyacrylamide gel electrophoresis followed by Western Blot with a p-eIF2 $\alpha$  specific antibody. The bar diagrams (A – E) show the mean  $\pm$  SEM of the density of the bands, expressed as a fold change relative to GAPDH (loading control). One representative of at least 3 independent experiments is shown here.

### 5.3.1 DATTS induces Nrf2 nuclear translocation in HCT116 cells

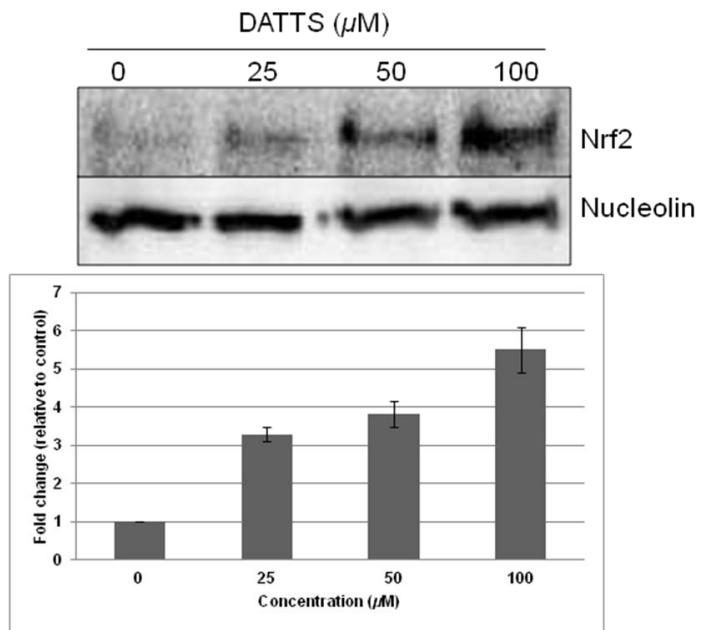
Another cellular factor which might react after ROS stress is Nrf2 [92, 123, 124, 125]. Nrf2 predominantly resides in the cytoplasm where it is complexed to its inhibitor, Keap-1. Oxidative stress, however, has been proposed to increase nuclear translocation, DNA-binding and transcriptional activity of Nrf2, among other effects, leading to up-regulation of HO-1 expression, which provides an adaptive survival

response against ROS-derived oxidative cytotoxicity. DATTS-induced nuclear translocation of Nrf2 was therefore evaluated. For this, HCT116 cells were either treated with 10 nM thapsigargin (control) or 50  $\mu$ M DATTS for different time periods. The nuclear fraction from the cell extract was analysed by Western blot with antibodies directed against Nrf2 (as described in the methods section). Presented in Figure 27 (A), an immediate increase in nuclear Nrf2 was observed between 0.5 and 1.5 h post treatment. From 2 – 4 h post treatment, a diminishing increase in Nrf2 protein level was observed. Twenty four hours post treatment, Nrf2 protein was completely abolished. This result indicates that DATTS causes a rapid but transient Nrf2 translocation from the cytoplasm into the nucleus. Figure 27 (B) also shows that the DATTS induced nuclear translocation of Nrf2 is concentration dependent. In the next step, the question was asked whether the increase in nuclear Nrf2 might be induced by ROS or by DATTS directly. Hence, the experiment described above was repeated, this time in the presence of GSH, NAC or ASC, as shown in Figure 27 (C), DATTS induced the nuclear translocation of Nrf2 which was completely abolished in the presence of all three antioxidants. These results indicated that DATTS, possibly directly and also via ROS, was responsible for the nuclear translocation of Nrf2.



## Results

B)





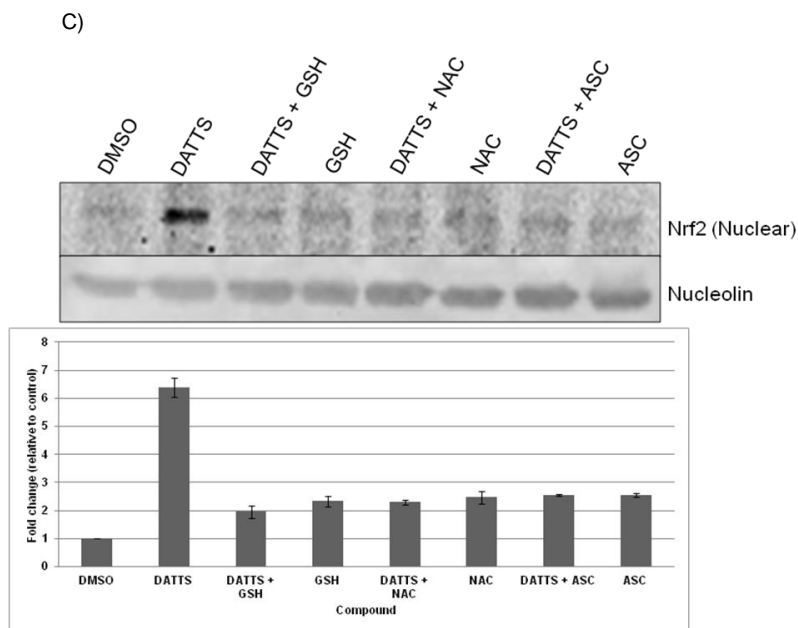


**Figure 27.** DATTS induces nuclear translocation of Nrf2. (A) HCT116 cells were untreated (0 h) or treated with 50  $\mu\text{M}$  DATTS for 0.5, 1, 1.5, 2, 2.5, 3, 4, and 24 h. For a positive control, cells were treated with 10 nM thapsigargin (TG) for 4 h and protein expression was studied by Western blotting. Nuclear proteins were separated on a 10% SDS-polyacrylamide gel, blotted on a PVDF membrane. Nrf2 expressions were visualised with the appropriate antibody. (B) cells were seeded in 6-well plates and treated with 0, 25, 50 or 100  $\mu\text{M}$  DATTS for 2 h. (C) cells were seeded in 6-well plates and treated with DATTS in the absence or presence of glutathione (GSH), *N*-acetyl cysteine (NAC) or ascorbic acid (ASC). Cells were lysed and then the nuclear cell extract analyzed by SDS polyacrylamide gel electrophoresis followed by Western Blot with an Nrf2 specific antibody. The bar diagrams (A – C) show the mean  $\pm$  SEM of the density of the bands, expressed as a fold change relative to nucleolin (loading control).

### 5.3.2 DATTS induces HO-1 expression in HCT116 cells

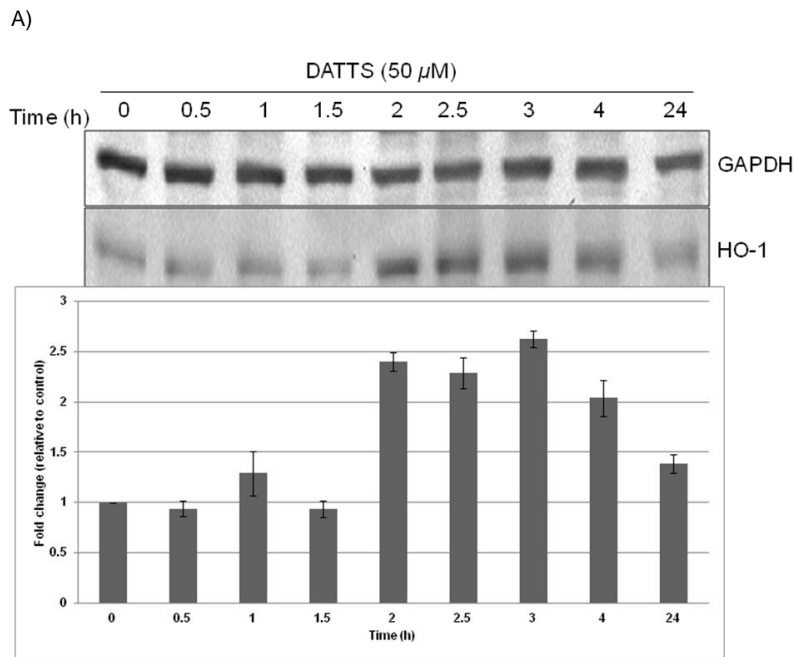
It has been shown that Nrf2 activation by stress signals leads to the transcription of the *HO-1* gene and subsequently the up-regulation of HO-1 protein expression [92]. The influence of DATTS on HO-1 protein expression was therefore evaluated. HCT116 cells were treated with DATTS for different time periods and analysed by Western blot using antibodies directed against HO-1 and GAPDH. As shown in Figure 28 (A), an increase in HO-1 protein expression was observed 2 h after treatment with DATTS and this persisted at least until 4 h post treatment. 24 h post treatment, HO-1 up-regulation was still visible even though at a much lower level,

which suggests that DATTS has a transient effect on HO-1 induction in HCT116 cells. Next, the question was asked whether the expression of HO-1 might be dependent on the concentration of DATTS. As shown in Figure 28 (B), the amount of HO-1, as detected by Western blot, increased with the concentration of DATTS. Also analysed was whether the expression of HO-1 might be dependent on the redox state of the cell. Therefore, HCT116 cells were treated with DATTS in the absence or presence of either GSH, NAC or ASC. As shown in Figure 28 (C), all three agents reduced the level of HO-1 compared to cells treated with DATTS alone.

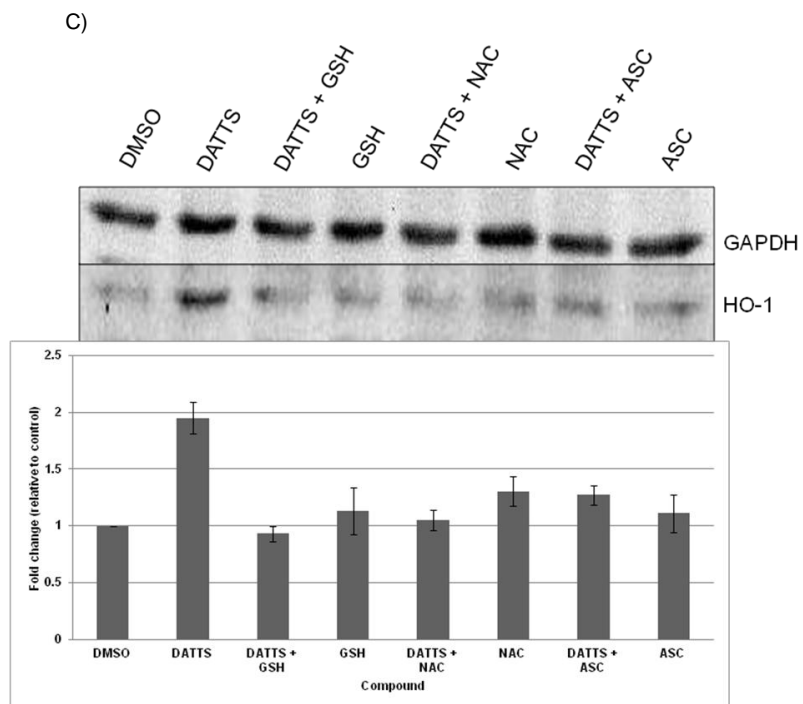
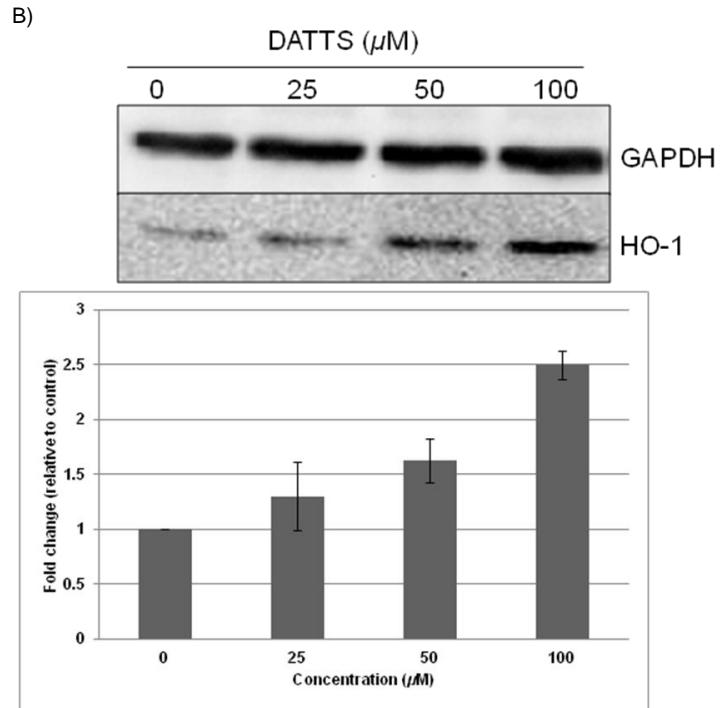
Nrf2 contains a potent transcription activation domain [125], and it recognises and binds to consensus ARE/StRE sequences found in the promoter regions of several Phase 2 enzymes including HO-1 [125, 127, 128]. In order to explore directly the role of Nrf2 in up-regulating the HO-1 expression, the activation of the Nrf2 pathway in HCT116 cells using an StRE driven luciferase reporter assay was analysed. Treatment of cells with DATTS strongly induced reporter activity (Fig. 28D). This increase in reporter activity coincided with an increase in HO-1 protein expression (Fig. 28E), thus indicating activation of not only the Nrf2 pathway, but also demonstrating that DATTS enhances transcription of the *HO-1* gene which might be responsible for the higher protein levels of HO-1 observed. A similar increase in the transcription from the StRE promoter was observed when HCT116 cells were treated with thapsigargin. We also observed an increase in the level of HO-1 protein in cells treated with thapsigargin. In principle, one will normally expect HCT116 cells harbouring the dominant-negative form of mutant Nrf2 to be less sensitive to the DATTS treatment compared to cells without. A reporter construct with the StRE-luc was therefore used and transfected with either wild-type or a dominant-negative mutant form of the Nrf2 or an empty vector as a control into HCT116 cells. The HCT116 cells transfected with the StRE-luc construct along with the dominant-negative Nrf2 (Nrf2-DN) failed to induce HO-1 expression (Fig. 28G) and to increase the StRE-luc activity (Fig. 28F) in response to DATTS treatment, compared to cells co-transfected with StRE-luc construct and the Nrf2 expression plasmid. Treatment of HCT116 cells co-transfected with StRE-luc construct and the Nrf2 expression plasmid showed a much higher activity and protein expression (Figs. 28F and G) compared to cells transfected with the StRE-luc alone or the empty vector. Taken

together, these findings support the notion that the up-regulation of HO-1 is mediated via Nrf2 activation.

NAD(P)H: quinone oxidoreductase (NQO1) is a cytosolic flavoprotein that catalyzes the detoxification of quinine. NQO1 is implicated in the protection against oxidative stress [129, 130]. The NQO1 promoter contains several antioxidant response elements including binding sites for Nrf2. Thus, the question was asked whether Nrf2 might also induce the expression of NQO1. However, as shown in Figure 28 (H), there was only a minor induction of NQO1 protein expression after 50  $\mu$ M DATTS treatment of HCT116 cells. The experiment was therefore repeated with increasing concentrations of DATTS. As shown in Figure 28 (I), there was a clear dose dependent increase in the protein level of NQO1 after DATTS treatment. Thus, not only HO-1 but also NQO1 is induced as an antioxidant defense.

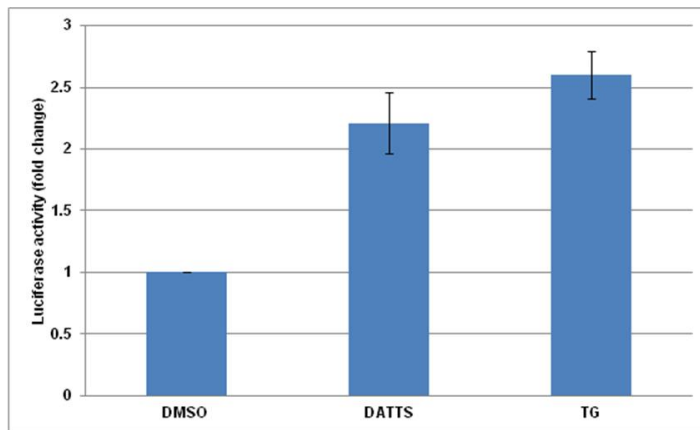


## Results

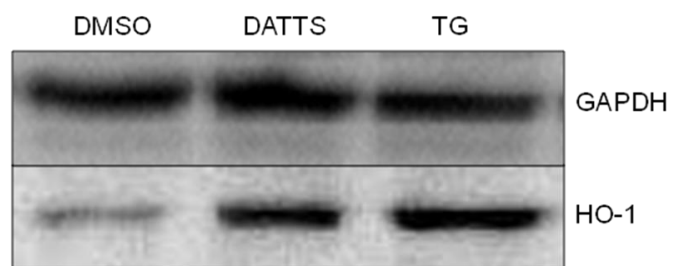


## Results

D)

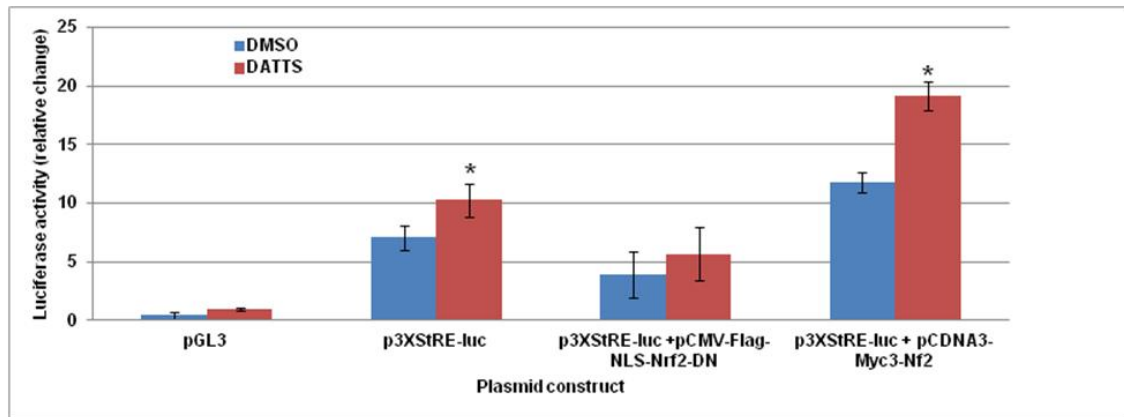


E)

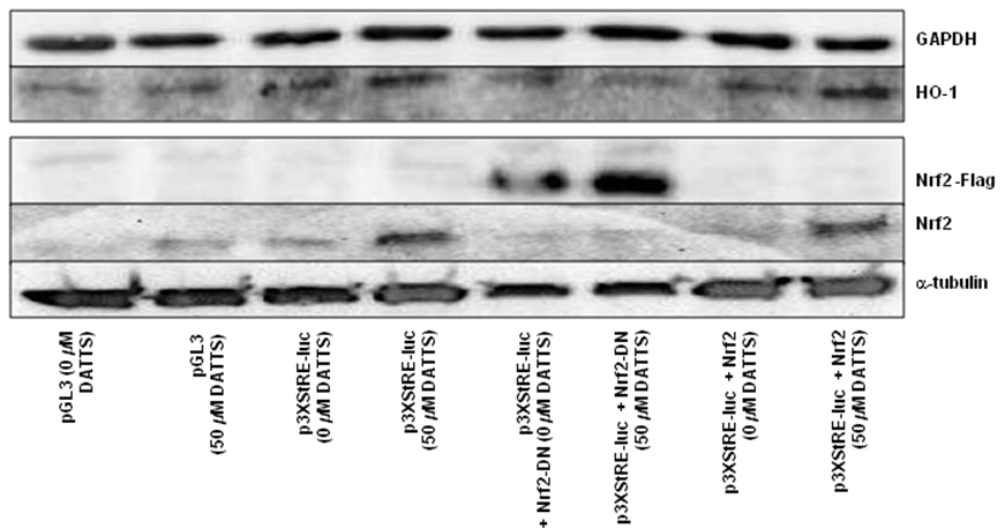


# Results

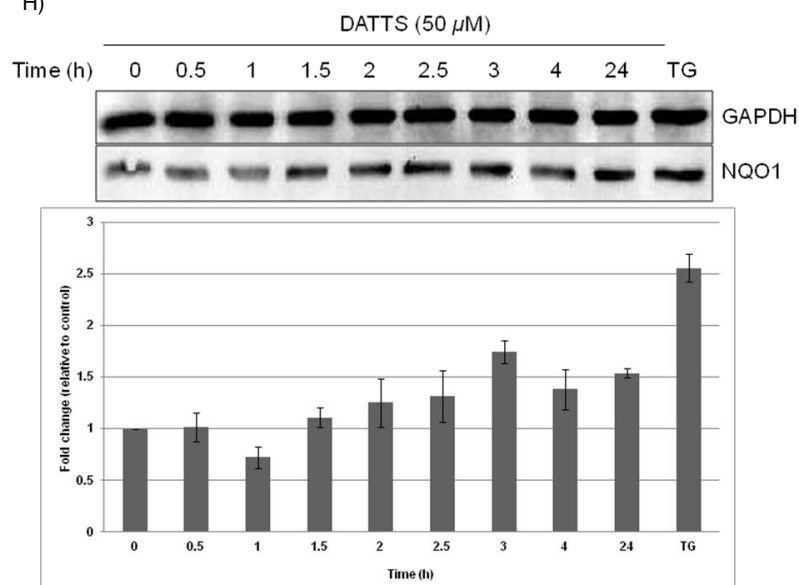
F)



G)



H)



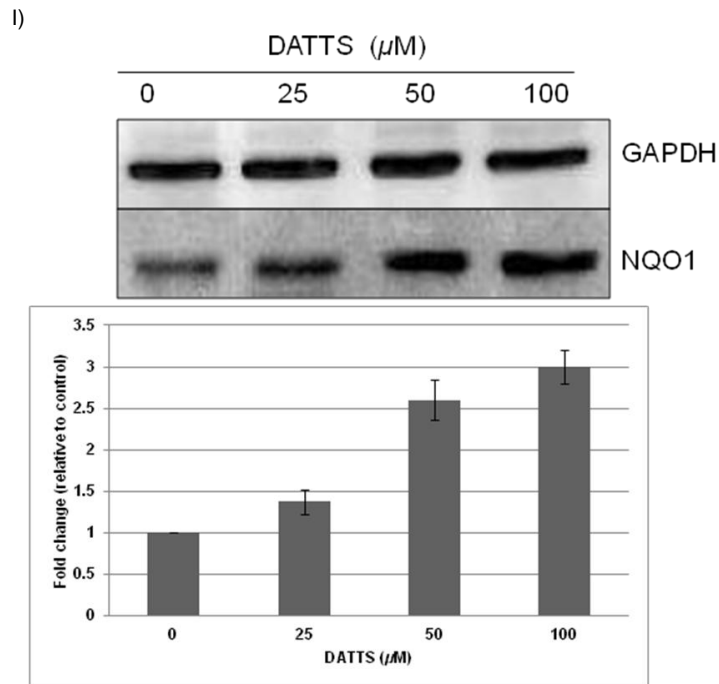


**Figure 28.** DATTS induces HO-1 and NQO1 protein expressions and increases StRE-luciferase activity in HCT116 cells. HCT116 cells were untreated (0 h) or treated with 50  $\mu\text{M}$  DATTS for 0.5, 1, 1.5, 2, 2.5, 3, 4, and 24 h and protein expression was studied by Western blotting. The proteins (100  $\mu\text{g}$ ) were separated on a 12.5% SDS-polyacrylamide gel, blotted on a PVDF membrane. HO-1 (A) and NQO1 (H) expressions were visualised with the appropriate antibody. (B and I) cells were seeded in 6-well plates and treated with 0, 25, 50 or 100  $\mu\text{M}$  DATTS for 2 h. (C) cells were seeded in 6-well plates and treated with DATTS in the absence or presence of glutathione (GSH), *N*-acetyl cysteine (NAC) or ascorbic acid (ASC). Cells were lysed and then the cell extract analyzed by SDS polyacrylamide gel electrophoresis followed by Western Blot with either a HO-1 or NQO1 specific antibody. The bar diagrams (A – C, H and I) show the mean  $\pm$  SEM of the density of the bands, expressed as a fold change relative to GAPDH (loading control). (D) cells were seeded into a 6 well plate and transfected with p3xStRE-luc as described in the materials and methods. Cell extracts of unstimulated or stimulated cells with either DATTS or thapsigargin (TG) were prepared using the reporter lysis buffer (Promega, Mannheim, Germany). These were then analysed for luciferase activities. Luciferase activity was normalized to the protein concentration. (E) 50  $\mu\text{g}$  of proteins from (D) were separated on a 12.5% SDS-polyacrylamide gel, blotted on a PVDF membrane. HO-1 expressions were visualised with the appropriate antibody. (F) cells were seeded, transfected or cotransfected and then treated as described in the materials and methods. Cell extracts were prepared using the reporter lysis buffer (Promega, Mannheim, Germany). These were then analysed for luciferase activities. Luciferase activity was normalized to the protein concentration. (G) 50  $\mu\text{g}$  of proteins from (F) were separated on a 12.5% SDS-polyacrylamide gel, blotted on a PVDF membrane. HO-1 and Nrf2 protein expressions were visualised with the appropriate antibody.

### 5.3.3 DATTS induces expression of ATF3 in HCT116 cells involving calcium ions and some MAP kinases

Activating transcription factor 4 (ATF4) is a downstream target for phosphorylated eIF2 $\alpha$  and when activated, ATF4 acts on downstream target genes of its own, which includes the transcription factors ATF3 [131], CCAAT-enhancer binding protein  $\beta$  (C/EBP $\beta$ ) [132], and C/EBP homology protein (CHOP) [133]. As shown in Figure 29 (A) and (B), DATTS treatment causes a rapid but transient increase in the amount of ATF3 proteins and a marginal one in that of the ATF4 proteins. ATF3 functions as a transcriptional repressor when bound as a homodimer to DNA and it has been shown to regulate cell cycle progression, cell growth, apoptosis, and stress response, dependent on the cell type [134]. Also, expression of ATF3 has been shown to be controlled, at least in part, by various components of mitogen-activated protein kinase (MAPK) family in different models [135]. Among them are the p38 protein kinase, the extracellular-signal-regulated kinases (ERKs) and the c-Jun N-terminal kinases (JNKs). The activation of these MAPK kinases tend to promote cell survival. Furthermore, it has been reported that both p38 protein kinase and JNK can serve as mediators between elevated calcium ions (Ca<sup>2+</sup>) and enhanced ATF3 gene transcription [135]. The questions were therefore asked whether (1) DATTS-induced ATF3 expression is cell specific, (2) some of these MAPK kinase are required for DATTS-induced ATF3 expression in HCT116 cancer cells and (3) if so, does it involve Ca<sup>2+</sup> ions? To address these questions, pharmacological approaches were used to assess the activations of some of these kinases and their roles on the DATTS-induced signalling cascade leading to ATF3 expression.

Firstly, various cell types (HCT116, ARPE-19, C3H10T1/2 and LNCaP) were each incubated with either 0.05% DMSO or with 50  $\mu$ M DATTS for 2 h and cell extracts were analysed by Western blotting. Figure 29 (C) shows that DATTS induced ATF3 expression in both the human epithelial colorectal cancer cell (HCT116) line and the androgen-sensitive human prostate cancer cell (LNCaP) line. DATTS also induced ATF3 expression in the human epithelial ARPE-19 noncancer cell but to a much lower extent and an even marginal one in the murine C3H10T1/2 pluripotent stem cells, which indicates that DATTS-induced ATF3 expression may not be cell line specific.



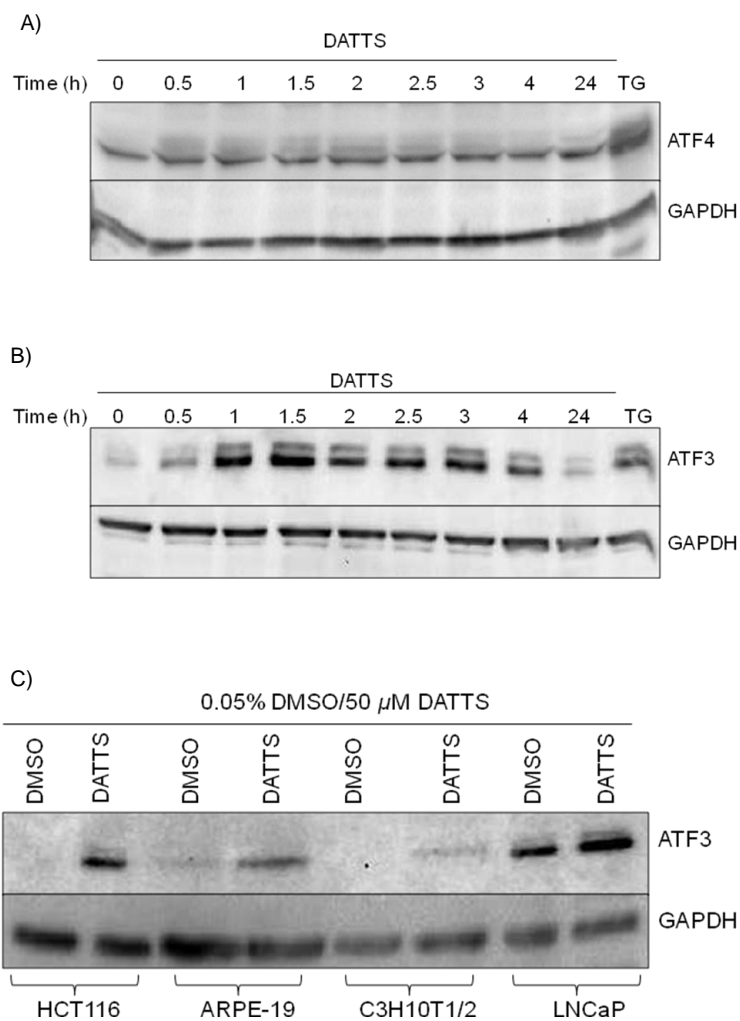
Secondly, in order to explore the role of DATTS in up-regulating ATF3 protein expression, HCT116 cells were transfected with an ATF3 driven luciferase reporter for 24 h and then treated with DMSO, DATTS or thapsigargin as described in the materials and methods section. Treatment of cells with DATTS slightly induced reporter activity by about 1.4 folds (Fig. 29D). This increase in reporter activity coincided with an increase in ATF3 protein expression in both DATTS and thapsigargin (a calcium ionophore well known to induce ATF3 protein expression) treated cells (Fig. 29E), thus, indicating that DATTS enhances transcription of the *ATF3* gene, which might be responsible for the higher protein levels of ATF3 observed.

Thirdly, HCT116 cells were either treated with DMSO or with 50  $\mu$ M DATTS for 2, 4 and 6 h. Cell extracts were prepared and Western blot analysis carried out for phosphorylated p38 and c-jun protein expressions. As shown in Figures 30 (A) and (B), DATTS treatment upregulated the protein expression of both phosphorylated p38 and c-jun in HCT116 cell.

Finally, cells were preincubated with SB203580 (p38-specific inhibitor), PD98059 (ERK-specific inhibitor), BAPTA-AM (intracellular calcium chelator), Nifedipine (calcium channel blocker) or with A23187 (divalent cation ionophore) before being incubated with DATTS. Cell extracts were prepared and analysed by Western blotting. As shown in Figure 30 (C), preincubation of HCT116 cells with the calcium ionophore A23187 did not block DATTS-induced ATF3 expression but rather enhances it. Preincubation with acetoxymethyl ester of the cytosolic  $\text{Ca}^{2+}$  chelator BAPTA-AM, on the other hand, completely blocked DATTS-triggered up-regulation of not only ATF3 (Fig. 30C), but also phospho-p38 and c-jun (Fig. 30E and F), suggesting a possible role of  $\text{Ca}^{2+}$  ions in DATTS-induced ATF3 protein expression. These  $\text{Ca}^{2+}$  ions seem to be influxes from internal stores because the DATTS-induced up-regulation of ATF3 expression was not blocked in HCT116 cells treated with the calcium channel blocker nifedipine. Therefore,  $\text{Ca}^{2+}$  influx from outside (involving L-type voltage gated  $\text{Ca}^{2+}$  channels) is possibly not involved in this signalling cascade. Preincubation with the p38-specific inhibitor compound SB203580 blocked DATTS-triggered up-regulation of ATF3, indicating that p38 protein kinase may be essential to induce the biosynthesis of ATF3 in DATTS-

## Results

stimulated HCT116 cells. Preincubation with the ERK-specific inhibitor compound PD98059, however, did not block the biosynthesis of ATF3 in DATTs-stimulated HCT116 cells, indicating that activation of ERK may not be required for the induction of ATF3 gene transcription. This data suggests that stimulation of HCT116 colorectal cells with diallyl tetrasulfide induces a signalling cascade involving calcium ions, activation of p38 protein kinase, activation of c-jun, and up-regulation of ATF3 expression.



## Results

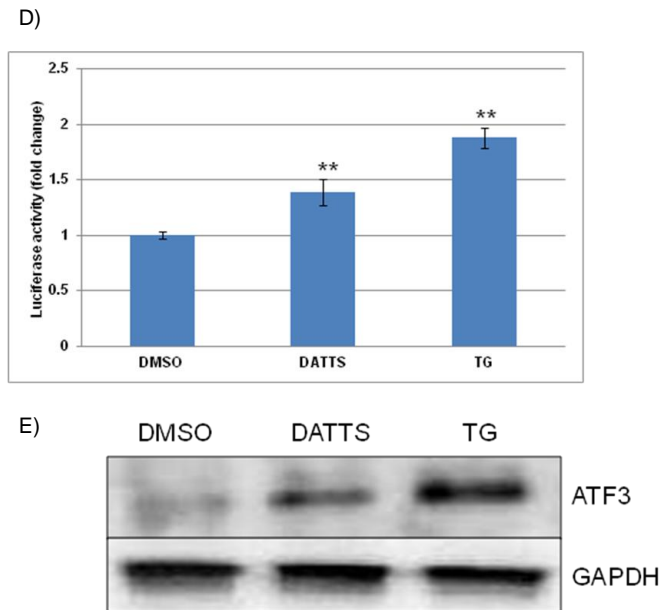
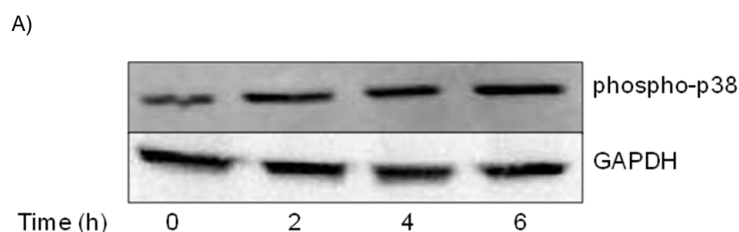
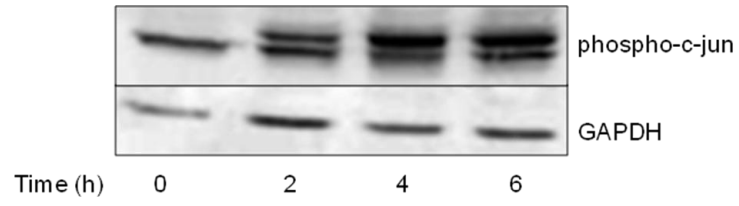


**Figure 29.** DATTS induces ATF3 in HCT116 cells. (A) and (B) HCT116 cells were untreated (0 h) or treated with 50  $\mu$ M DATTS for 0.5, 1, 1.5, 2, 2.5, 3, 4, and 24 h. For a positive control, cells were treated with 10 nM thapsigargin (TG) for 4 h and protein expression was studied by Western blotting. ATF4 (A) and ATF3 (B) as well as GAPDH expressions were visualised with the appropriate antibody. (C) HCT116, ARPE-19, C3H10T1/2 and LNCaP cells were each incubated with either DMSO or with 50  $\mu$ M DATTS for 2 h and protein expression in each cell line was studied by Western blotting. ATF3 and GAPDH (loading control) expressions were visualised with the appropriate antibody. (D) cells were seeded in a 6 well plate and transfected with p3xATF3-luc as described in the materials and methods. Cell extracts of unstimulated or stimulated cells with either DATTS or thapsigargin were prepared using the reporter lysis buffer (Promega, Mannheim, Germany). These were then analysed for luciferase activities. Luciferase activity was normalized to total protein concentration. (E) 50  $\mu$ g of proteins from (D) were separated on a 12.5% SDS-polyacrylamide gel, blotted on a PVDF membrane. ATF3 and GAPDH (loading control) expressions were visualised with the appropriate antibody.

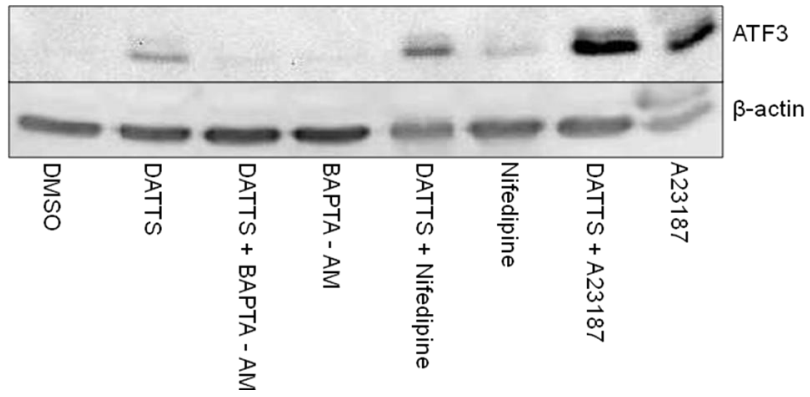


## Results

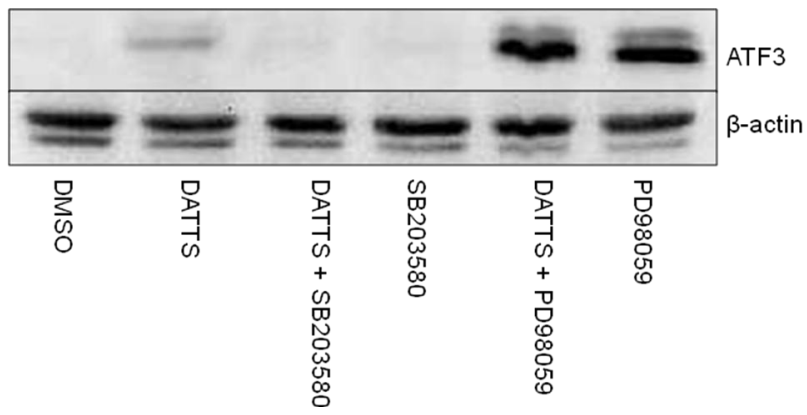
B)



C)



D)



## Results

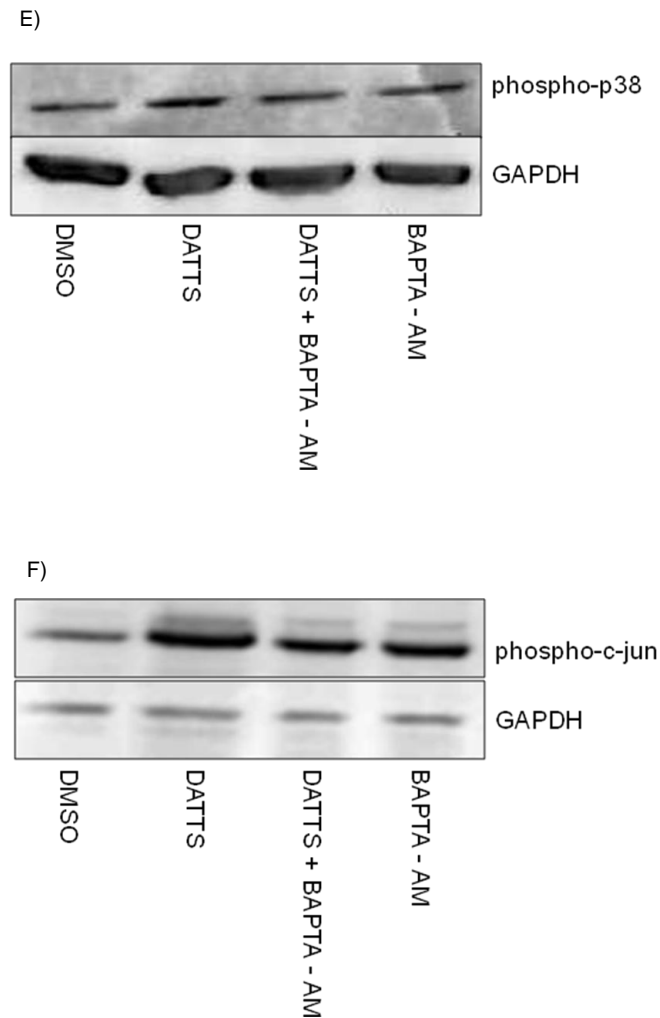


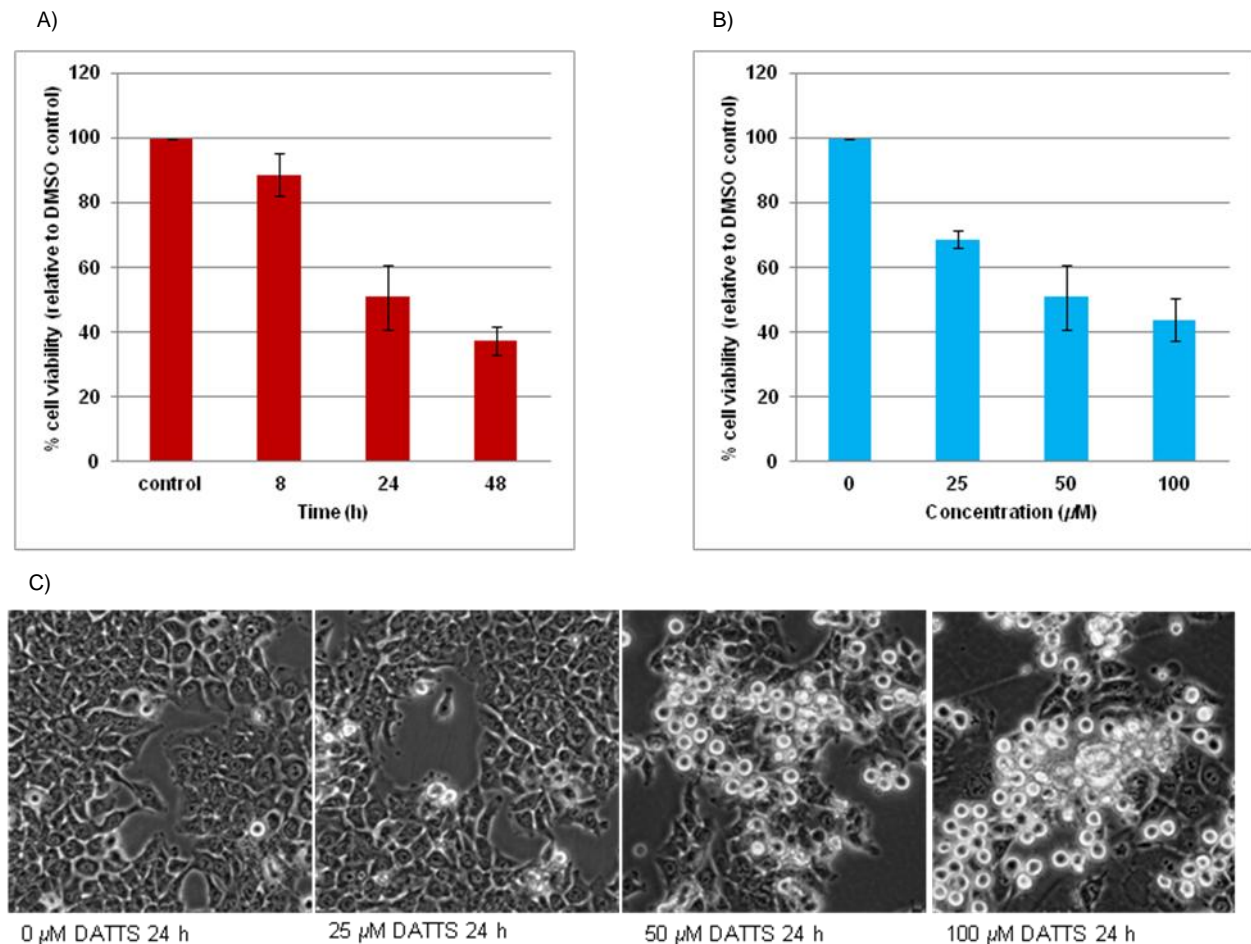
**Figure 30.** Stimulation of HCT116 colorectal cells with DATTS induces a signalling cascade involving calcium ions, activation of phospho-p38, phospho-c-jun, and up-regulation of ATF3 expression. (A) and (B) HCT116 cells were untreated (0 h) or treated with 50  $\mu$ M DATTS for 2, 4, and 6 h and protein expression was studied by Western blotting. Proteins were separated on a 12.5% SDS-polyacrylamide gel, blotted on a PVDF membrane. phospho-p38 (A) and phospho-c-jun (B) expressions were visualised with the appropriate antibody. (C) HCT116, cells were incubated for 2 h with DMSO, DATTS, DATTS + BAPTA-AM, BAPTA-AM, DATTS + Nifedipine, Nifedipine, DATTS + A23187 or with A23187 alone. (D) HCT116, cells were incubated for 2 h with DMSO, DATTS, DATTS + SB203580, SB203580, DATTS + PD98059 or with PD98059 alone. Protein expression was studied by Western blotting. Proteins were separated on a 12.5% SDS-polyacrylamide gel, blotted on a PVDF membrane. ATF3 expressions were visualised with the appropriate antibody. For (E) and (F) cell lysates from (C) that contains DMSO, DATTS, DATTS + BAPTA-AM or BAPTA-AM alone, were separated on a 12.5% SDS-polyacrylamide gel, blotted on a PVDF membrane. phospho-p38 (E) and phospho-c-jun (F) expressions were each visualised with the appropriate antibody. GAPDH or  $\beta$ -actin was used as a loading control.

#### **5.4 DATTS-induced antioxidant response is not able to prevent apoptosis in HCT116 cells**

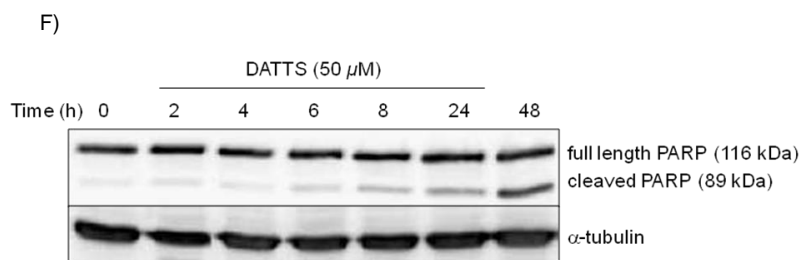
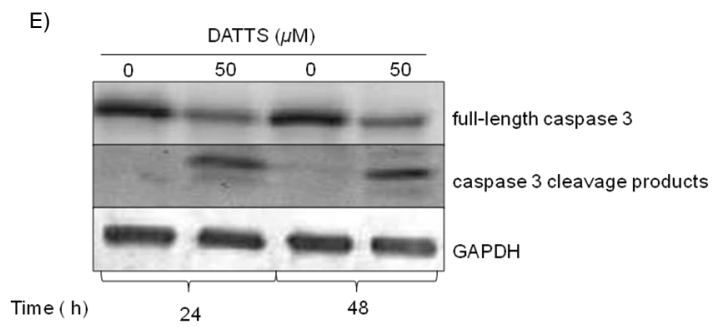
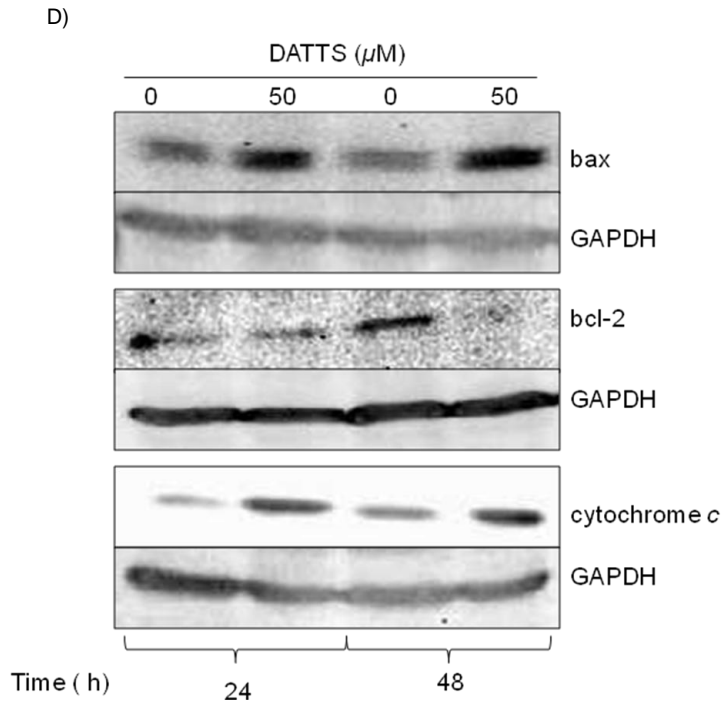
Having shown that DATTS induced an immediate but transient antioxidant response, the question was then asked whether this immediate but transient antioxidant response would be able to protect cell viability and eventually apoptosis over a longer period of time. Cells were treated with DATTS for various time intervals and then analyzed for viability by an MTT-assay. As shown in Figure 31, after 8 h treatment, only a very little loss in cell viability is observed, whereas after 24 h, and even more after 48 h, a considerable loss in viability down to about 40% of the control is observed (Fig. 31A). Next, it was tested whether this loss of viability is dose dependent. Therefore, the experiment was repeated with 25, 50 and 100  $\mu\text{M}$  DATTS for 24 h and then viability was tested by an MTT-assay. As shown in Figure 31 (B), there is a dose dependent decrease in cell viability. Morphological analysis of HCT116 cells after treatment with 0, 25, 50 and 100  $\mu\text{M}$  DATTS also revealed clear apoptotic bodies with increasing DATTS concentration (Fig. 31C). In order to support the observation that cells might go into apoptosis, the expressions of the pro-apoptotic bax, the anti-apoptotic bcl-2 as well as cytochrome *c* release into the cytoplasm were analysed as further indications for apoptosis. As shown in Figure 31 (D), after treatment of HCT116 cells with DATTS, an increase in the expression of bax, a decrease in bcl-2 and an increase in the amount of cytochrome *c* in the cytoplasm were observed. As a further indication of apoptosis, cleavage of caspase 3 was detected 24 and 48 h after treatment of the cells with DATTS (Fig. 31E). Poly-ADP-ribose polymerase (PARP) is a well known substrate of caspase 3/7 and its cleavage is a signature for DNA damage and in most cases also points towards final execution of apoptosis. It has been shown that most polysulfides, including diallyl polysulfides and polysulfides containing coumarin derivatives, induce apoptosis in cancer cells [20]. The ability of DATTS to induce PARP cleavage was therefore tested. As shown in Figure 31 (F), the amount of the PARP cleavage product (89 kDa) increased with time. Considerable amounts of the cleavage product occur 48 h after treatment, confirming the previous results that apoptosis is a late event after DATTS treatment. In order to study the contribution of ROS to the DATTS induced apoptosis, HCT116 cells were treated with DATTS in the presence and absence of

## Results

GSH, NAC or ASC. Cells were lysed and then the cell extract analysed by SDS polyacrylamide gel electrophoresis followed by Western blot with a PARP specific antibody. As shown in Figure 31 (G), DATTS induced PARP cleavage after 24 h in the absence of GSH, NAC and ASC. In the presence of GSH and NAC however, there was no cleavage of PARP, indicating that these antioxidants prevented apoptosis, whereas ascorbic acid was not sufficient to inhibit PARP cleavage. This means that DATTS triggers different pathways in parallel and independently of each other, and that the antioxidant is triggered by ROS while the apoptotic one via disulfide formation.



## Results





## Results

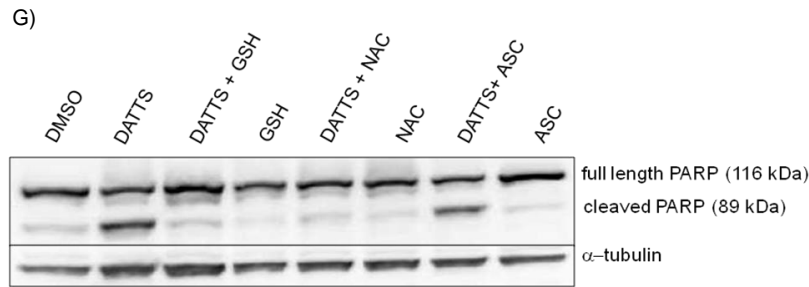


**Figure 31.** DATTS affect the viability of HCT116 cells in both time and dosage dependent manners. It also induces apoptosis by modulating bax and bcl-2 expressions, induce cytochrome c release and activate both caspase 3/7 and PARP cleavages in HCT116 cells. (A) cells were seeded in 24-well plates and treated with 50  $\mu$ M DATTS or 0.05% DMSO for 8, 24 and 48 h. Afterwards, MTT assay was used to determine cell viability. (B) cells were seeded in 24-well plates and left untreated (0  $\mu$ M) or treated with 25, 50 or 100  $\mu$ M DATTS for 24 h. Afterwards, MTT assay was used to determine viable cells as in (A). (C) HCT116 cells were cultured in 6 well plates overnight before incubation with 0, 25, 50 or 100  $\mu$ M DATTS for 24 h. Afterwards, cell morphology was assessed by microscopy. (D - E) HCT116 cells were treated with 0 or 50  $\mu$ M DATTS for 24 and 48 h, protein expressions and caspase activation were then studied by Western Blotting. The proteins were separated on a 12.5% SDS-polyacrylamide gel, blotted on a PVDF membrane. bax, bcl-2 or cytochrome c (D) was visualised with the appropriate antibody, whilst full-length caspase 3/7 and its cleavage products (E) were detected with a caspase 3-specific antibody (8G10). GAPDH was used as a loading control. (F) HCT116 cells were left untreated (0 h) or treated with DATTS for 2, 4, 6, 8, 24 and 48 h, and protein expression was studied by Western Blotting. Cell extracts were separated by electrophoresis on a 7.5% SDS-polyacrylamide gel and then blotted on a PVDF membrane. PARP cleavage was visualised with the appropriate antibody.  $\alpha$ -tubulin was used as a loading control. In another set of experiments (G), HCT116 cells were treated for 24 h with 50  $\mu$ M DATTS either in the absence or presence of 20  $\mu$ M GSH, 5 mM NAC or 100  $\mu$ M ASC. Cells were also treated for 24 h with 0.05% DMSO to serve as a control. Cell extracts were then treated for PARP cleavage using SDS-polyacrylamide gel electrophoresis and Western blotting. Total protein extract (75  $\mu$ g) was separated on a 7.5% SDS-polyacrylamide gel, blotted on a PVDF membrane and PARP was detected using the corresponding antibody.  $\alpha$ -tubulin was used as a loading control. One representative of at least 3 Western blots is shown here.

### ***5.5 DATTS causes a dosage-dependent disruption of HCT116 cellular microtubule network***

Certain antimicrotubule agents such as nocodazole are known to target the cellular microtubule network, resulting in aberrant formation of the mitotic spindle, subsequent blockage of the cell cycle in G<sub>2</sub>/M phase, and apoptotic cell death [138]. Also, since tubulin contains thiol residues, it could well be that DATTS targets these thiol residues thereby altering the tubulin thiol redox status, which may contribute to not only the observed cell cycle arrest in the G<sub>2</sub>/M phase in the previous experiment, but also apoptotic cell death. It therefore became ideal to test whether DATTS could directly affect the organisation of the microtubule network of cells. HCT116 cells were therefore treated with either a DMSO control or a range of concentrations of DATTS (25  $\mu$ M, 50  $\mu$ M and 100  $\mu$ M). After 24 h of incubation, the microtubule network was visualized by immunofluorescence. The microtubule network in DMSO control cells exhibited normal arrangement with microtubules seen to traverse intricately throughout the cell, these cells displaying a normal compact rounded nucleus (Fig. 32). In contrast, DATTS caused a dose-dependent loss of microtubule network, with only a diffuse stain visible throughout the cytoplasm (Fig. 32).

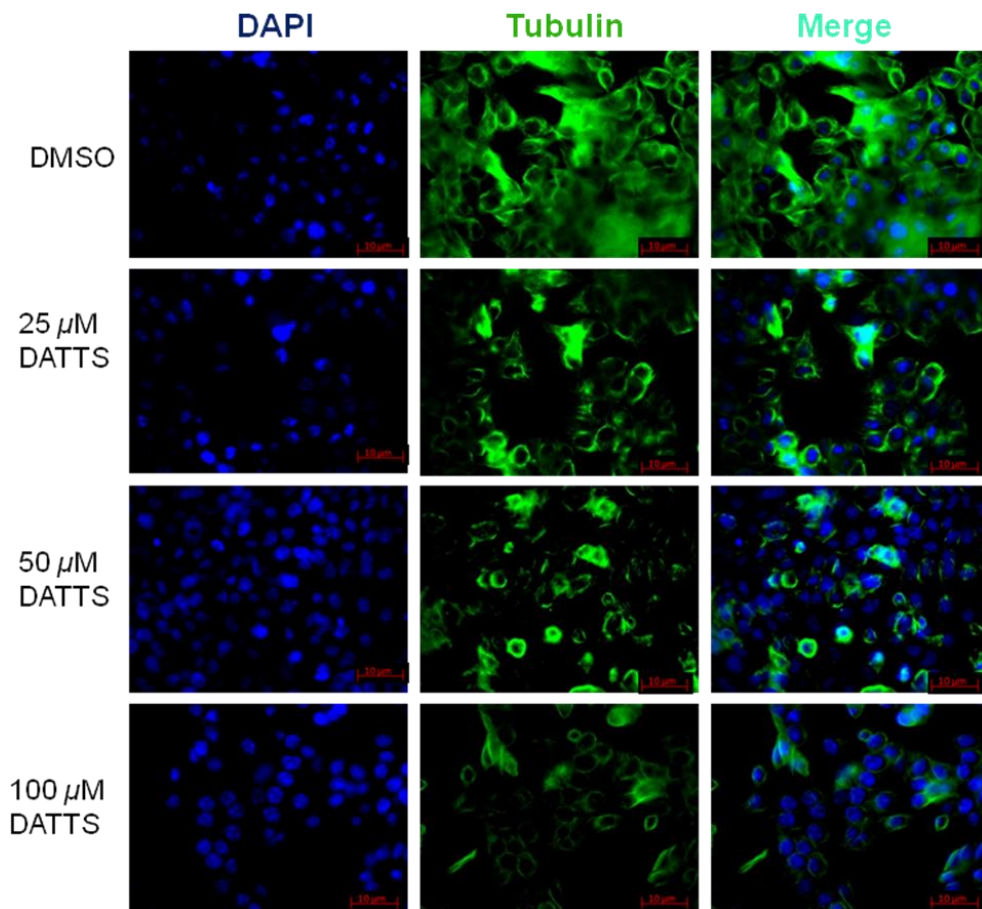


**Figure 32.** DATTS treatment affects the organisation of HCT116 cellular microtubule network. HCT116 cells were cultured in 6 well plates overnight before incubation with 0, 25, 50 or 100  $\mu\text{M}$  DATTS for 24 h. Cells were fixed with formaldehyde before being incubated with monoclonal anti- $\alpha$ -tubulin for 30 min at 37°C followed by 30 min incubation at 37°C with the ALEXA-Fluor™ 488 secondary antibody. After three washing steps, the cells were briefly stained with DAPI. The organisation of the microtubule network (green) and nucleus (blue) was visualised with a Zeiss Axioskop fluorescence microscope at a magnification of 40 x.

### 5.6 Influence of DATTS on CK2 expression and kinase activity

Protein kinase CK2 is a pleiotropic enzyme which is ubiquitously expressed in eukaryotic cells. It is composed of two catalytic  $\alpha$  - or  $\alpha'$ -subunits and two non-catalytic  $\beta$ -subunits [137]. Several studies have shown that life without CK2 $\alpha$  and/or CK2 $\beta$  is impossible. The important role of this enzyme in the viability of eukaryotic cells is further supported by the great number of substrates whose activities are

regulated by CK2 phosphorylation [137]. Not only is CK2 implicated in the regulation of the cell cycle, but also has anti-apoptotic properties [138, 139], associates with ER membrane proteins (such as Sec63) and transcription factors (such as ATF4 and Nrf2) [140, 141]. It was also recently shown in our lab that the G<sub>2</sub>/M regulatory phosphatase cdc25C is a substrate of protein kinase CK2. In spite of these numerous functions of this important enzyme, it was asked whether diallyl tetrasulfide will stimulate the kinase activity of CK2 in HCT116 colorectal cancer cells. To test this possibility, HCT116 cells were either left untreated (0 h) or treated with 50  $\mu$ M DATTS. Lysates were prepared and either analysed for CK2 protein expression or for CK2 kinase activity. The kinase activity in cell extracts was measured using a synthetic peptide substrate, RRRDDDSDDD, in the presence of [<sup>32</sup>P] $\gamma$ ATP. As shown in Figure 33 (A), DATTS-induced CK2 kinase activity increases with increase in time. There was, however, no further increase observed in the kinase activity beyond 1.5 h of cell incubation with DATTS. The DATTS-induced CK2 kinase activity seems to correspond with DATTS-induced CK2 protein expression. As evident in Figure 33 (B), DATTS treatment of HCT116 cells resulted in a moderate increase in the protein levels of CK2 $\alpha'$  and CK2 $\beta$  in particular, signifying that DATTS indeed does have an influence on both CK2 kinase activity and protein expressions. This DATTS effect on CK2, however, is an early event similar to that of DATTS-induced PERK and eIF2 $\alpha$  phosphorylations.

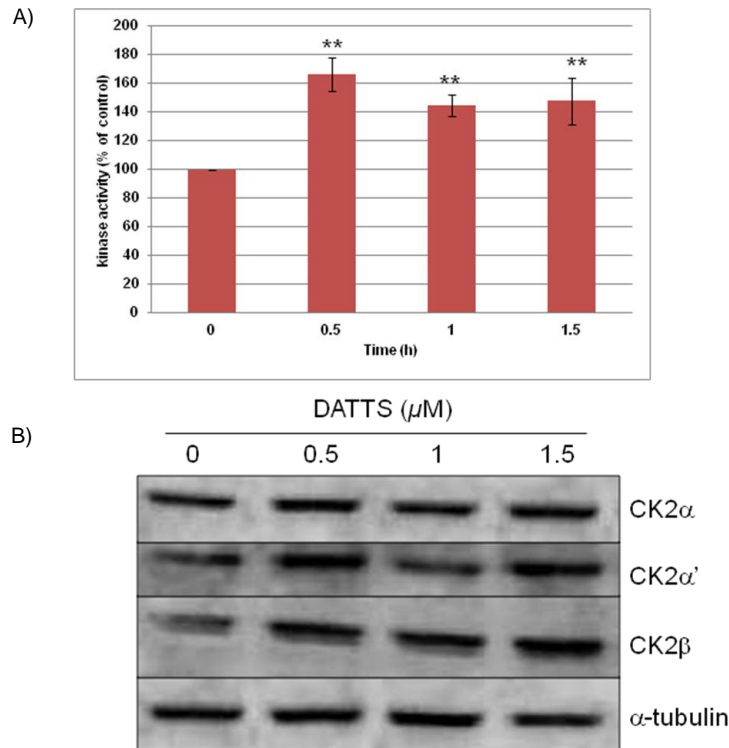


**Figure 33.** Influence of DATTS on CK2 protein expression and kinase activity. HCT116 cells were left untreated (0 h) or treated with 50  $\mu$ M DATTS for different time periods (0 - 1.5 h). (A) cells were lysed and the kinase activity of CK2 in the cell extract were measured with a synthetic peptide substrate, RRRDDDSDDD, in the presence of [ $^{32}$ P] $\gamma$ ATP. (B) cell extracts in (A) were analysed on a 12.5% SDS-polyacrylamide gel, blotted on a PVDF membrane. CK2 $\alpha$ ,  $\alpha'$ ,  $\beta$  and  $\alpha$ -tubulin were visualised using the appropriate antibody. Result is the means  $\pm$  SD of three individual experiments. \*\*, significantly different from cells incubated with 0  $\mu$ M DATTS,  $p \leq 0.01$ .

### 5.7 Effect of DATTS on HCT116 cells compared to ARPE-19 Cells

Diallyl polysulfide-induced cell cycle arrest and apoptosis in cancer cells have been extensively addressed both in this study and elsewhere. In contrast, the effect of these polysulfides on normal cells is poorly understood. To address this issue, the effect of DATTS on human epithelial cells of normal and cancerous origins were evaluated. For this purpose, the study was focussed on cell viability, apoptosis and the unfolded protein response/endoplasmic reticulum stress pathways.

### 5.7.1 Evaluation of cell viability

A similar question as in previous studies was asked; whether DATTS reduce ARPE-19 cell viability and if so, how does it compare with that observed in HCT116 cells. To answer this question, two separate sets of experiments were carried out: one, an MTT assay and the other, a trypan blue cell count. In the first set of experiments, HCT116 and ARPE-19 cells were treated with either 0.05% DMSO or 50  $\mu$ M DATTS for 8, 24, 48 and 72 h. Cells were then analysed for cell viability by the MTT assay as previously described. In the second set of experiments, HCT116 and ARPE-19 were seeded ( $1 \times 10^4$  cells/well) and left to attached overnight in the incubator. The next day, a sample of cells in separate wells were counted using the trypan blue cell count method. The rest of the cells were then left either untreated or treated with 0.05% DMSO or 50  $\mu$ M DATTS for 8, 24, 48 and 72 h. The cells were further counted using the same trypan blue method after each of the time periods of treatment stated above. As shown in Figure 34 (A), (B), (C) and (D), 8, 24, 48 and 72 h after DATTS treatment, HCT116 cell viability was reduced by about 20%, 52%, 62% and 76%, respectively, whilst that of ARPE-19 was about 2%, 16%, 30% and 18%, respectively. It can be concluded that DATTS has an effect on the viability of both HCT116 and ARPE-19 cells. This effect, however, is a lot more pronounced in HCT116 cells than in ARPE-19 cells. Also, ARPE-19 cells seem to adapt to the DATTS effect after some time, which is evident from the 30% decrease in cell viability after 48 h but only 18% after 72 h shown in Figure 34 (C) and (D). A similar pattern was observed with the trypan blue cell count results shown in Figure 34 (E) and (F), where DATTS inhibited ARPE-19 cell growth for 24 and 48 h but then, going into 72 h, cells began to grow at their normal rate.

## Results

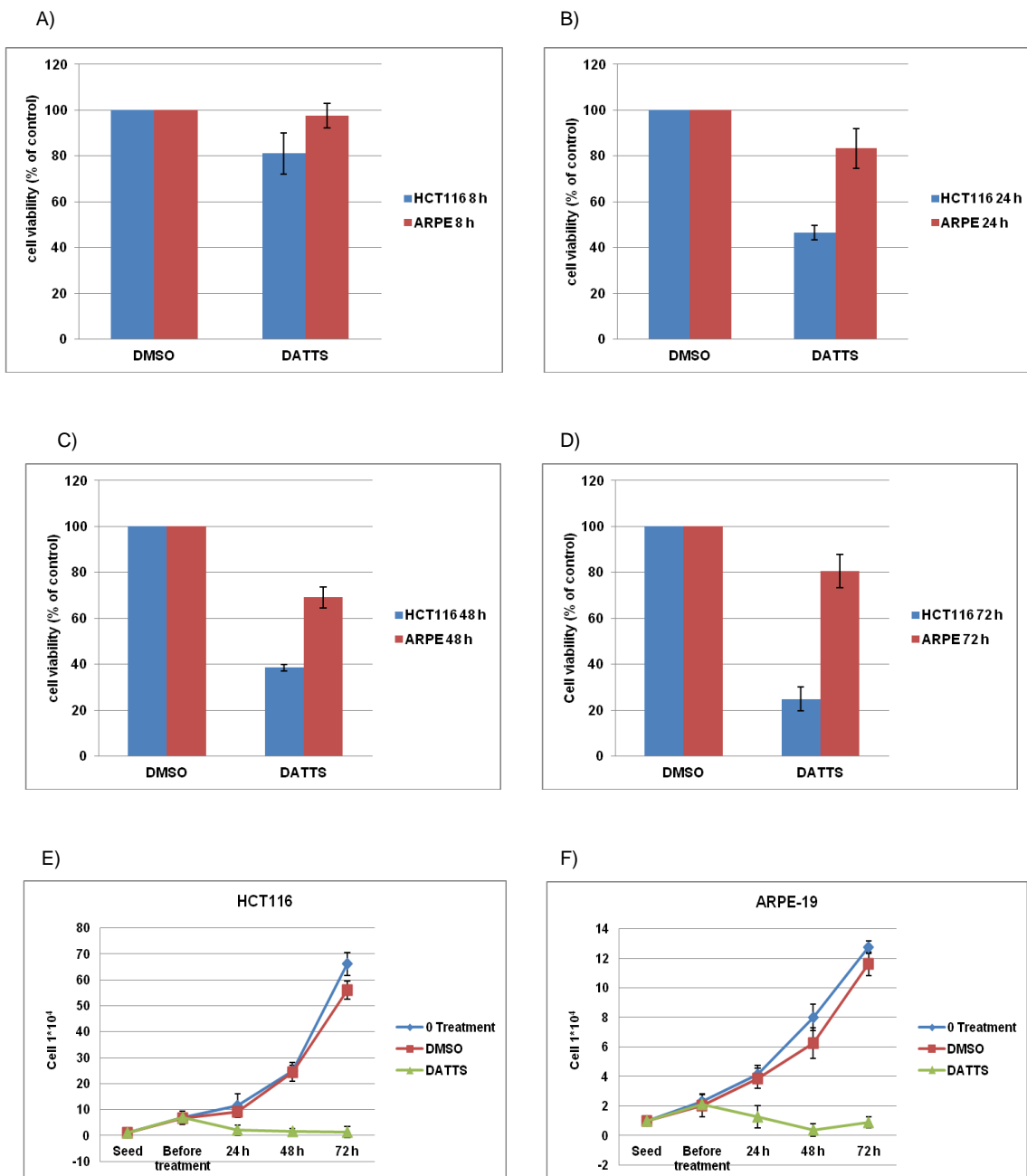


**Figure 34.** DATTs affects the viability of both HCT116 and ARPE-19 cells. HCT116 and ARPE-19 cells were treated with either 0.05% DMSO or 50  $\mu$ M DATTs for 8 (A) 24 (B) 48 (C) and 72 (D) h. Cells were then analysed for cell viability by the MTT assay as previously described. HCT116 (E) and ARPE-19 (F) cells were seeded ( $1 \times 10^4$  cells/well) and left to attached overnight in the incubator. The next day, a sample of cells from each cell line in separate wells was counted using the trypan blue cell count method. The rest of the cells were then either left untreated or treated with 0.05% DMSO or 50  $\mu$ M DATTs for 24, 48 and 72 h. The cells were further counted using the same trypan blue method after each of the time periods of treatment stated in the materials and methods section. Data was analysed using Microsoft excel 2007. The results represent the mean  $\pm$  SD of three separate experiments.

As in previous experiments, the morphology of ARPE-19 cells was assessed following DATTS treatment at different concentrations for 24 h. These were then compared to HCT116 cells that were exposed to the same conditions for the same amount of time. As shown in Figure 35 (A) and (B), DATTS does affect the morphology of both HCT116 cancer cells and ARPE-19 noncancer cells. A significant loss of nuclear construction and formation of apoptotic bodies were, however, observed in HCT116 cells at higher DATTS concentrations (Fig. 35A) than in ARPE-19 cells (Fig. 35B), which is in agreement with both the trypan blue and MTT cell viability assays.

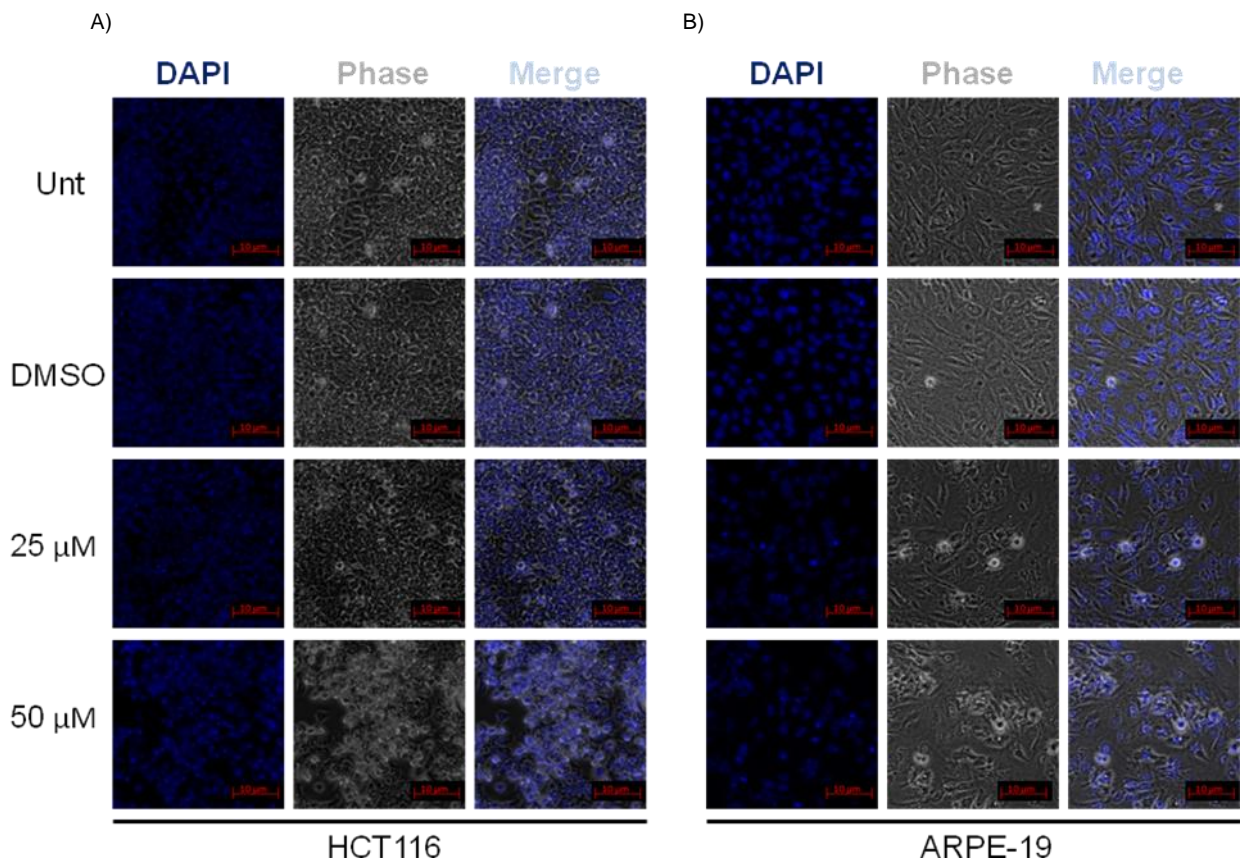
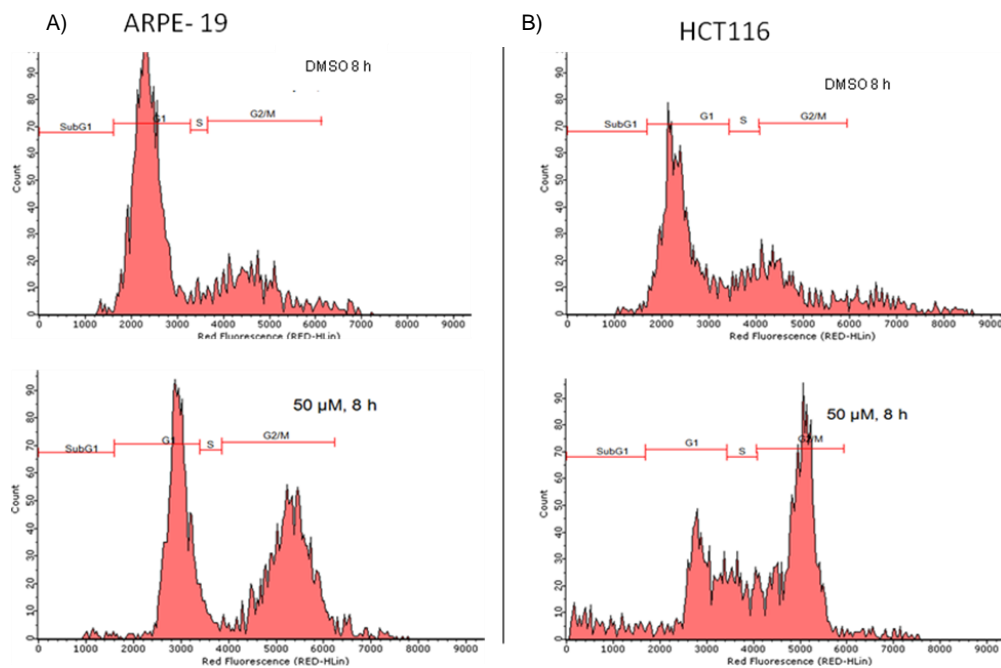


**Figure 35.** DATTS treatment affects HCT116 cell morphology (A) a lot more than it does to ARPE-19 cells (B) HCT116 and ARPE-19 cells were each cultured in 6 well plates overnight before incubation with 0.05% DMSO, 25 or 50  $\mu\text{M}$  DATTS or in another case, left untreated (Unt) for 24 h (A) The nucleus was stained with DAPI (blue). Afterwards, cell morphology and viability was assessed by microscopy at a scale bar of 10  $\mu\text{m}$ .



## Results

Loss of nuclear construction and reduced cell viability is still not enough to confirm apoptosis in DATTS-treated ARPE-19 cells. In some cases, the observed effect could be interpreted as cell necrosis. In order to clarify this point, ARPE-19 cells were therefore either treated with 0.05% DMSO or 50  $\mu$ M DATTS for 8 and 24 h as described earlier, and cell cycle analysis was performed by flow cytometry. As shown in Figure 36 (A - D), DATTS treatment after 8 and 24 h caused a G<sub>2</sub>/M cell cycle arrest in both cell lines. Interestingly, however, DATTS failed to influence apoptosis in ARPE-19 cells, where very little or no subG<sub>1</sub> peak was observed, compared to those observed in HCT116 cells.



## Results

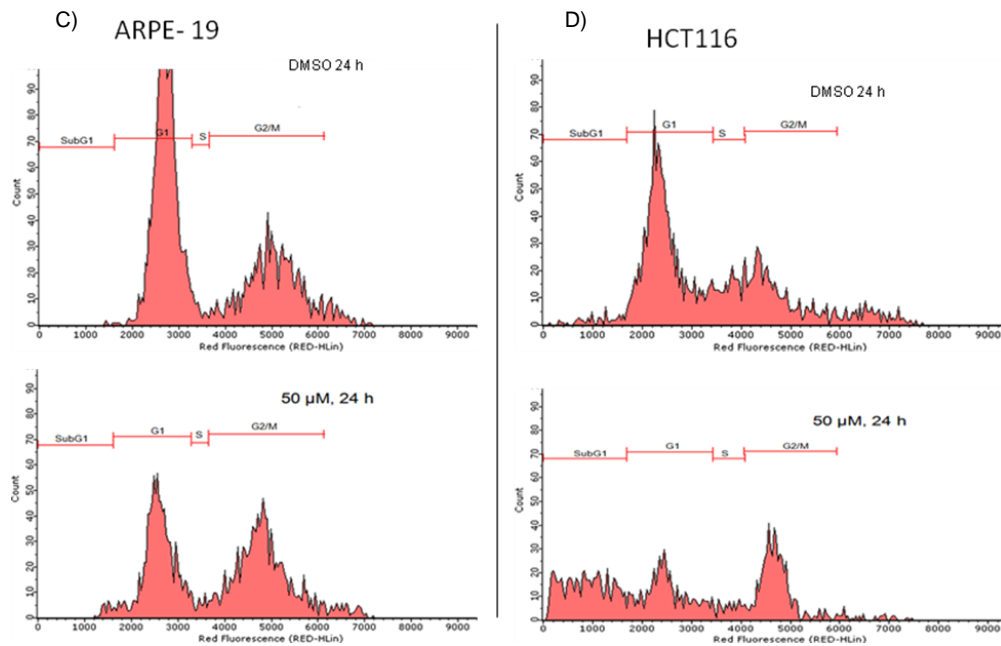


**Figure 36.** The influence of DATTS on HCT116 and ARPE-19 cell cycle distributions. HCT116 and ARPE-19 cells were each treated for 8 (A and B) and 24 h (C and D) with either 0.05% DMSO or 50  $\mu$ M DATTS and then analysed by FACS. FACS analysis of the treated cells are shown in (A) and (B), 8 h after treatment and (C) and (D) 24 h after treatment. One representative of at least three similar independent experiments is shown here.

Normal epithelial cells, under normal physiological conditions, do undergo basal apoptosis as a part of the normal process of cellular turnover. This however happens on such a low scale that it is quite often not detected on the expression levels of both pro-apoptotic and anti-apoptotic proteins [142]. To test this possibility, the apoptotic response of both the human epithelial HCT116 cancer cells and the ARPE-19 noncancer cells were assessed by Western blot. Cells were treated with 0.05% DMSO or with 50  $\mu$ M DATTS for 0, 8, 24, 48 and 72 h and expression of cytochrome *c*, PARP, caspase 3 or  $\gamma$ H2AX were analysed (Fig. 37A, C and D). As shown in Figure 37 (A - D), DATTS treatment caused an increase in cytochrome *c* release into the cytosol of HCT116 cells, but not in ARPE-19 cells. It also caused caspase 3 cleavage and activation along with that of PARP, and an increase in  $\gamma$ H2AX protein expression in HCT116 cancer cells but not in ARPE-19 noncancer cells, which is in agreement with the cell cycle analysis results. The results indicate that DATTS does cause apoptosis in HCT116 cancer cells, but not in ARPE-19 noncancer cells, and that the signs of apoptosis observed in ARPE-19 cells are

## Results

probably not due to DATTS but rather an apoptotic machinery that is a part of the normal process of cellular turnover in this normal epithelial cell type.

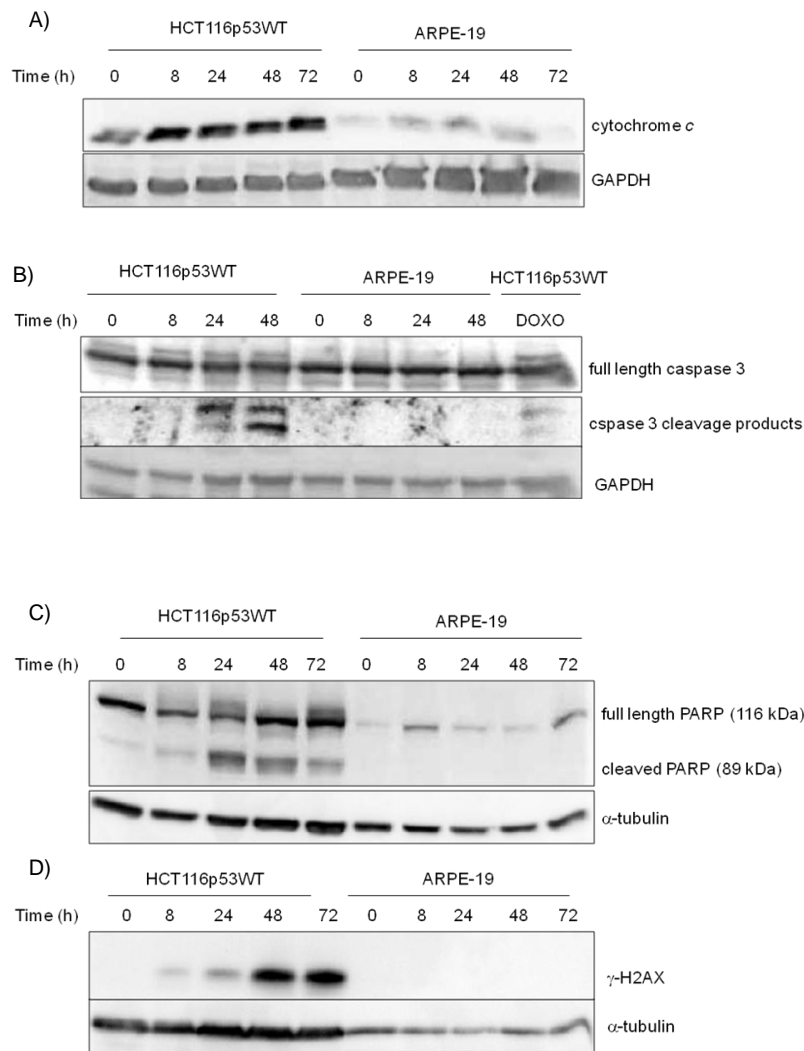
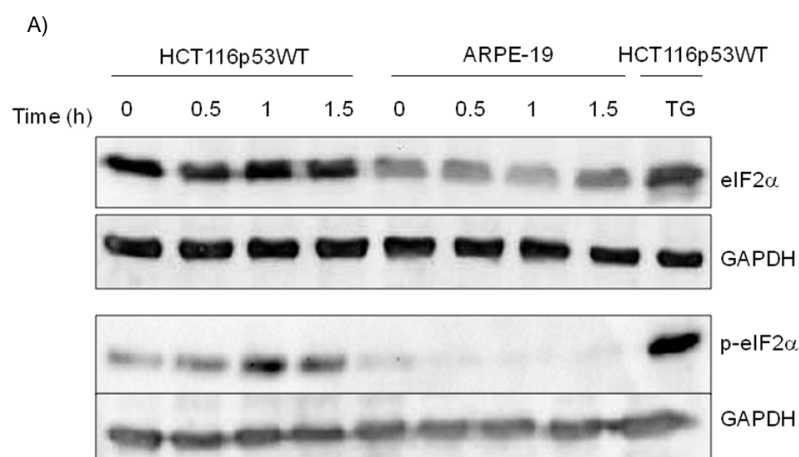
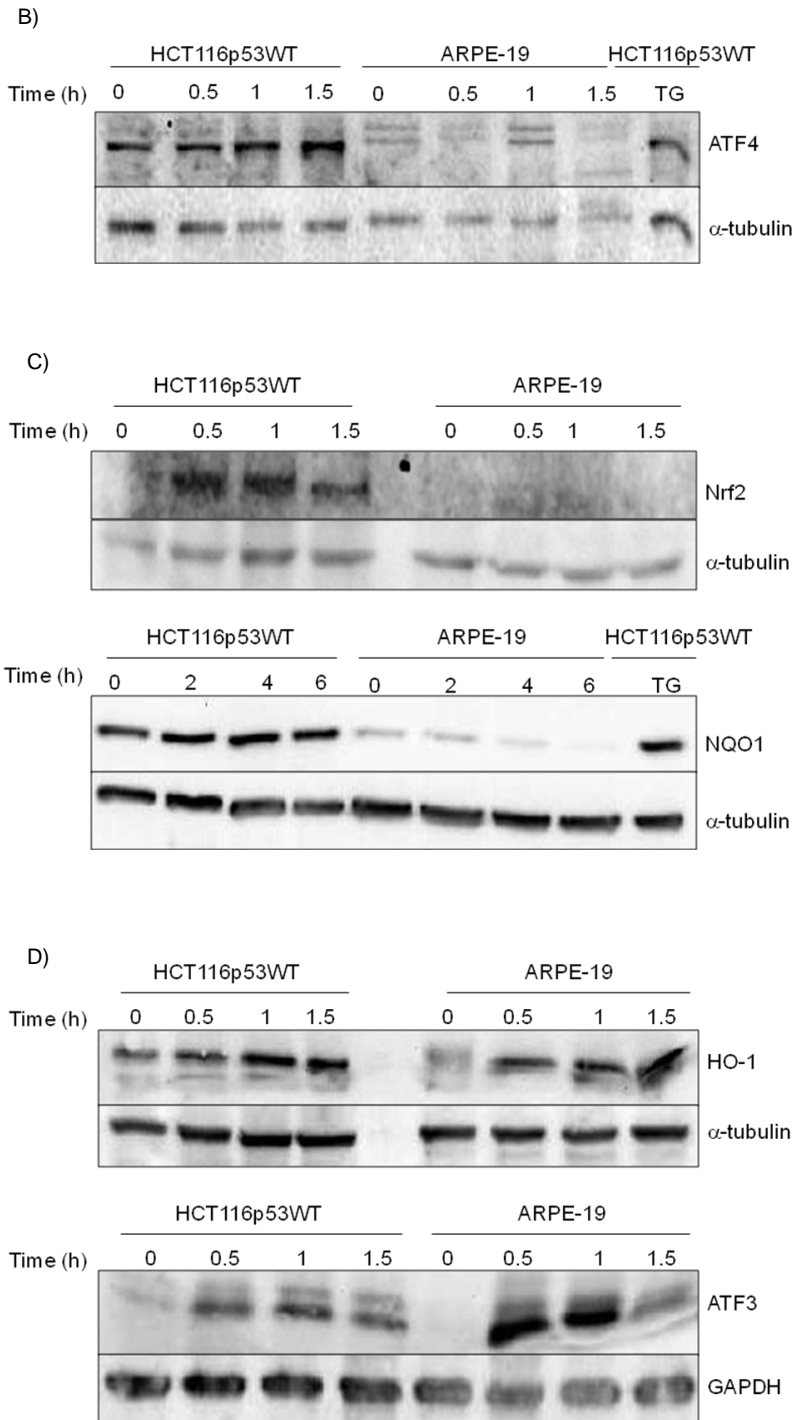


**Figure 37.** DATTS induces cytochrome *c* release and activates caspase 3 in HCT116 cells but not in ARPE-19 cells. It also modulates  $\gamma$ H2AX protein expression and PARP cleavage in HCT116 cells but not in ARPE-19 cells. HCT116 and ARPE-19 cells were untreated (0 h) or treated with DATTS for 8, 24, 48 and 72 h, and protein expression was studied by Western blotting (A - D). For (B), HCT116 and ARPE-19 cells were each left either untreated (0 h) or treated with 50  $\mu$ M DATTS for 8, 24 and 48 h. As a positive control, HCT116 cells were treated with 20  $\mu$ g/ml doxorubicin for 24 h or left untreated. Caspase 3 cleavage was analysed by Western blot. GAPDH (A and B) or  $\alpha$ -tubulin (C and D) was used as a loading control. One representative of at least 3 Western blots is shown here.

Since we showed that DATTS induces not only the phosphorylation of eIF2 $\alpha$  and Nrf2 in HCT116 cancer cells but also some of their downstream targets, we began to ask the question of, whether DATTS can, in fact, induce these same oxidative/ER stress signal proteins in ARPE-19 noncancer cells in a similar manner. To test this possibility, HCT116 and ARPE-19 cells were cultured overnight and treated the following day with 50  $\mu$ M DATTS, or left untreated (0 h) for 0.5, 1 and 1.5 h. Nuclear extracts were prepared separately for Nrf2 expression studies. In some cases, cells were treated with 10 nM thapsigargin (a well-know ER stress inducer) to serve as a positive control. Flag ATF6 was also used as a positive control for ATF6 expression studies. Expression levels of eIF2 $\alpha$ , p-eIF2 $\alpha$ , ATF4, Nrf2, HO-1, NQO1, ATF3 and ATF6 were analysed by Western blotting (Fig. 38A - E). Either GAPDH or  $\alpha$ -tubulin was used as a loading control. As shown in Figure 38 (A - E), DATTS induced the protein expression of p-eIF2 $\alpha$ , ATF4, Nrf2, HO-1, NQO1, ATF3 and ATF6 in a time dependent manner in HCT116 cells. However, unlike in HCT116 cells, DATTS was unable to induce the expression of most of these proteins, with the exception of ATF3 and HO-1 (which are involved in oxidative stress response) in ARPE-19 cells. These results indicate that, unlike in HCT116 cells, the antioxidant response machinery in ARPE-19 cells is efficient in adapting the cells to the DATTS-induced oxidative/ER stress and probably preventing them from going into apoptosis.



## Results



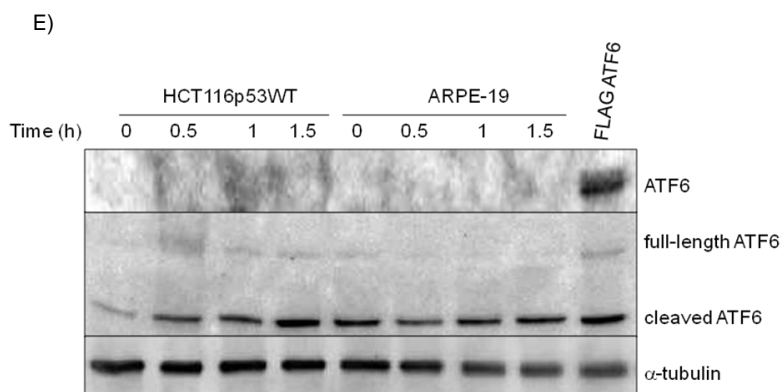


**Figure 38.** DATTS induces oxidative/ER stress protein expressions in HCT116 cells but not in ARPE-19 cells. HCT116 and ARPE-19 cells were untreated (0 h) or treated with 50  $\mu$ M DATTS for 0.5, 1 and 1.5 h. For a positive control, HCT116 cells were treated with 10 nM thapsigargin (TG) for 4 h, or in some cases transfected with FLAG-ATF6 and protein expression was studied by Western blotting. The proteins (100  $\mu$ g) were separated on a 12.5% SDS-polyacrylamide gel, blotted on a PVDF membrane. Nuclear (C) and cytosolic proteins were also prepared and separated on a 10% SDS-polyacrylamide gel, blotted on a PVDF membrane. eIF2 $\alpha$  and p-eIF2 $\alpha$  (A), ATF4 (B), Nrf2 and NQO1 (C), HO-1 and ATF3 (D) and ATF6 (E) expressions were visualised with the appropriate antibody. GAPDH or  $\alpha$ -tubulin was used as a loading control.

## 5.8 Coumarin polysulfides

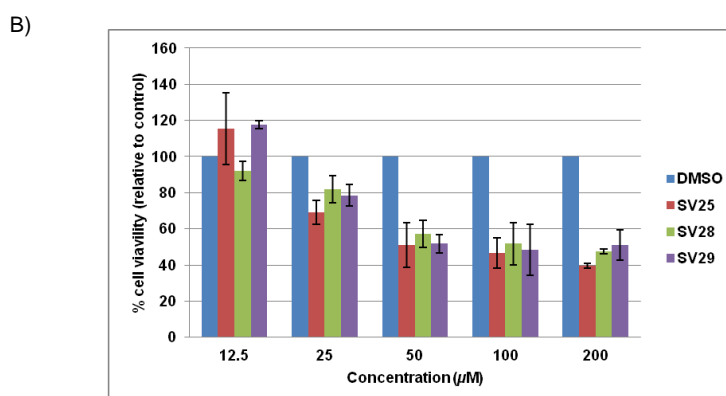
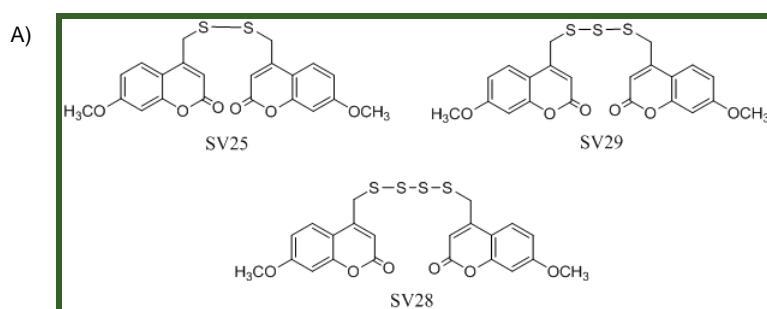
Coumarins and coumarin derivatives as well as diallyl polysulfides are well known as anticancer drugs [37, 40, 142]. In order to find new and possibly better drugs with anticancer activities, coumarins were combined with polysulfides by Dr. Sergio Valente (from Université de Lorraine in Metz, France) in the form of di-coumarin polysulfides. These novel compounds were then tested in the HCT116 colorectal cancer cell line in a similar way to that of diallyl tetrasulfide.

### 5.8.1 Evaluation of cell viability

Previous studies on diallyl polysulfides have shown that treatment of tumour cells with diallyl polysulfides reduced their viability considerably depending on the length of the sulfur chain (Fig. 39). The newly synthesised coumarin polysulfides (SV25, SV28 and SV29) (Fig. 39A) were therefore tested for their effect on HCT116 cells in

## Results

different concentrations (12.5, 25, 50, 100 and 200  $\mu\text{M}$ ). As a control, cells were treated with the solvent DMSO alone. Cell viability was measured with an MTT assay. As shown in Figure 42 (B), using 25  $\mu\text{M}$  SV25, SV28 or SV29 led to reduction in cell viability by 30%, 18% or 22%, respectively. At a concentration of 50  $\mu\text{M}$ , cell viability was reduced to around 50%. At higher concentrations, there was slightly further reduction in cell viability. Using 50  $\mu\text{M}$  of the coumarin polysulfides, time dependency of the treatment was also analysed. Cells were incubated with 50  $\mu\text{M}$  SV25, SV28 or SV29 for 8, 24 and 48 h and then cell viability was measured by an MTT assay. The values shown in Figure 39 (B) and (C) are the averages of three independent experiments, and the bars indicate standard deviation. The graphs shown in Figure 39 (C) demonstrate that cell viability was already reduced to around 50% after 24 h treatment and further reduced to around 20% viability after 48 h. Thus, these experiments showed a dosage and a time dependent effect of all three coumarin polysulfides.



C)

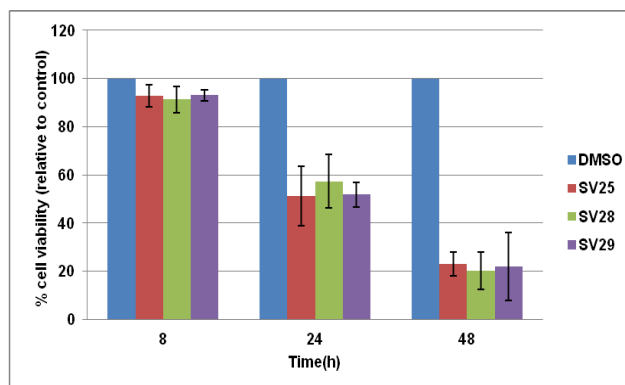


**Figure 39.** Coumarin polysulfides affect the viability of HCT116 cells in both time and dosage dependent manners. (A) structures of three of the compounds synthesised - 4,4'-disulfanediybis(methylene)bis(2H-chromen-2-one) (SV25), 4,4'-trisulfanediybis(methylene)bis(2H-chromen-2-one) (SV29) and 4,4'-tetrasulfanediybis(methylene)bis(2H-chromen-2-one) (SV28). (B) Cells were seeded in 24-well plates and treated with 0.05% DMSO, 12.5, 25, 50, 100 or 200  $\mu$ M SV29 for 24 h. Afterwards, MTT assay was done to determine the amount of viable cells. (C) Cells were seeded in 24-well plates and treated with 50  $\mu$ M SV25, SV28, SV29 or 0.05% DMSO for 8, 24 and 48 h. Afterwards, MTT assay was used to determine the number of viable cells as in (B). Data are depicted as means  $\pm$  SD, (n = 3).

### 5.8.2 Treatment of HCT116 cells with coumarin trisulfide induces cell cycle arrest and apoptosis.

Reduced cell viability might be due to cell cycle arrest or apoptosis. Therefore, the question of whether coumarin polysulfide-treated cells might arrest in G<sub>1</sub>- or G<sub>2</sub>-phase of the cell cycle was addressed. For this, HCT116 cells were treated with 0, 25 or 50  $\mu$ M SV29 for 24 h. Cells were harvested and incubated with propidium iodide to label DNA. Cells were then analysed in a cytofluorimeter. As shown in Figure 40, SV29 treated cells clearly accumulated in the G<sub>2</sub>-phase arrest. A subG<sub>1</sub> peak confirmed that cells go into apoptosis. Untreated HCT116 cells showed a normal cell cycle profile with about 63% of the cells in G<sub>1</sub>-phase, around 5% in S-phase and about 24% of cells in G<sub>2</sub>-phase.



## Results

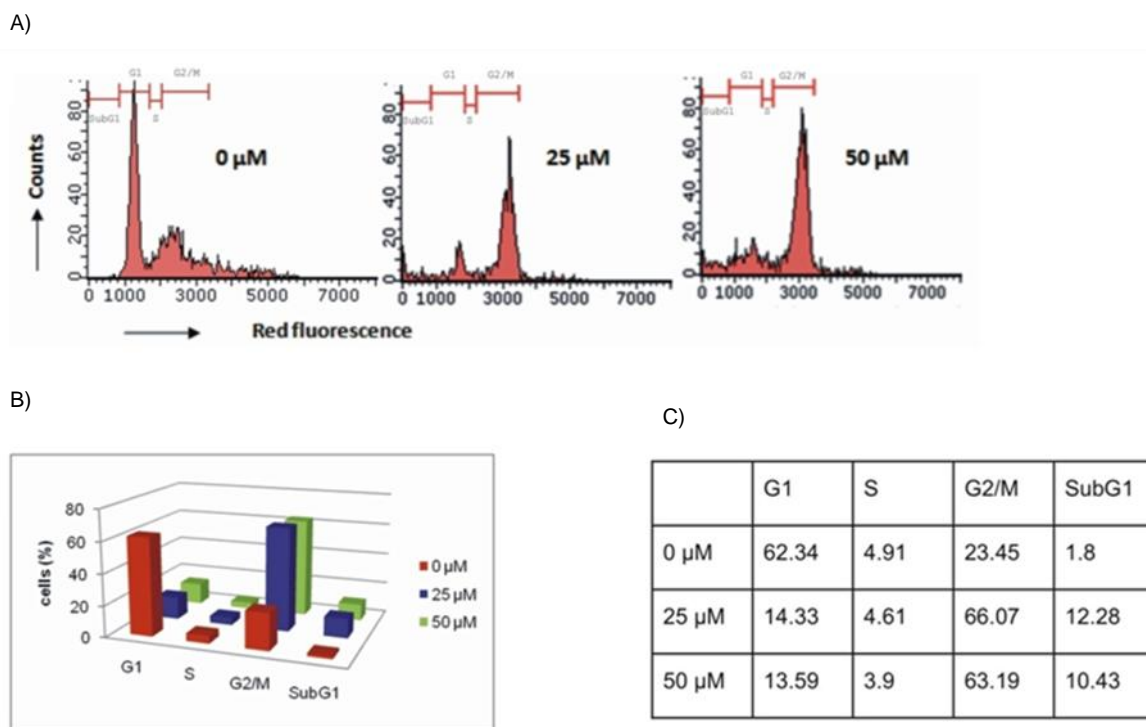


**Figure 40.** The influence of SV29 on cell cycle distribution. HCT116 cells were treated for 24 h with 0, 25 or 50  $\mu\text{M}$  SV29 and then analysed by FACS. (A) FACS analysis of the treated cells. (B) Percentage distribution. (C) Data for (B). One representative of at least three similar independent experiments is shown here.

Reduced cell viability can also be an indication of apoptosis. In order to analyse whether coumarin polysulfides might indeed induce apoptosis, HCT116 cells were treated with the two coumarins (SV25 and SV29) for different times. Cells were lysed and the cell extract analysed on a 7.5% SDS polyacrylamide gel. After transfer to a PVDF membrane, the filter was incubated with antibodies directed against PARP. Starting at 24 h after treatment of the cells with the coumarin polysulfides, PARP cleavage was observed; from a molecular weight of 116 KDa into the 89 KDa cleavage product (Fig. 41). In agreement with these data, increase in the level of  $\gamma\text{H}_2\text{AX}$ , which detects DNA double strand breaks and is a further indication of apoptosis (data not shown) was also observed. In order to support the conclusion about apoptosis induction, the experiment described above was repeated. However, since no significant difference between the cells treated with SV25 and SV29 was found, further experiments were performed with only SV29.

## Results

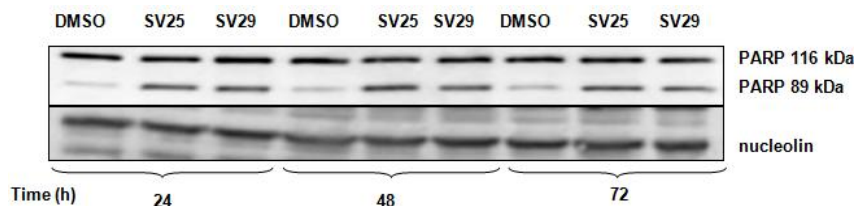
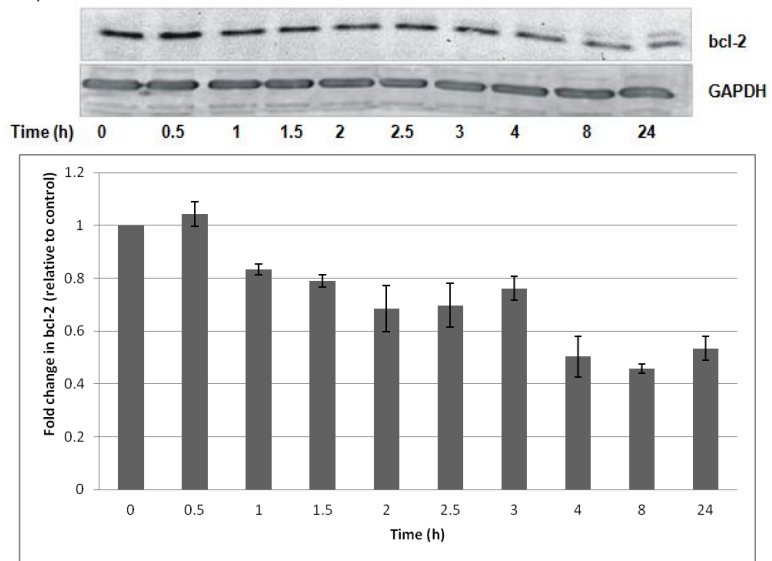


**Figure 41.** Coumarin polysulfides induce PARP cleavage. HCT116 cells were treated for 24, 48 and 72 h with 0.05% DMSO as a control or 50  $\mu$ M SV25 or SV29 and cell extracts were treated for PARP cleavage using SDS polyacrylamide gel electrophoresis and Western blotting. Total protein extract (75  $\mu$ g) was separated on a 7.5% SDS–polyacrylamide gel and blotted on a PVDF membrane. PARP was detected using the corresponding antibody. Nucleolin was used as a loading control.

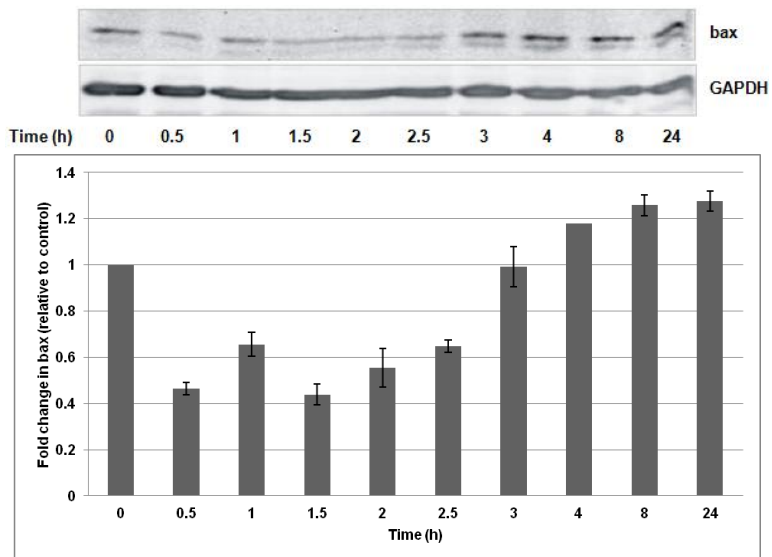
HCT116 cells were again either untreated (0 h) or treated with SV29 for 0.5, 1, 1.5, 2, 2.5, 3, 4, 8 and 24 h, and protein expression was studied by Western blotting as described above. After protein transfer to a PVDF membrane, the membrane was analysed with antibodies against bcl-2 and bax. As shown in Figure 42, a decrease in the level of the anti-apoptotic bcl-2 protein (Fig. 42A) was found along with an increase in the level of the pro-apoptotic bax protein (Fig. 42B) in a time dependent manner. An antibody against GAPDH was used as a loading control. Since mitochondrial cytochrome c release is regulated by a decrease in the bcl-2 level, cytochrome c release into the cytosol after treatment of the cells with coumarin polysulfides was analysed. Accordingly, an increase in cytosolic cytochrome c was detected after treatment with SV29 (Fig. 42C). Finally, caspase 3 activation after treatment of HCT116 cells with coumarin polysulfides was also analysed. After 24 and 48 h treatment, activation of caspase 3 (Fig. 42D) was detected. Thus, from these results, it is quite credible that apoptosis is induced in HCT116 cells after treatment with coumarin polysulfides. Furthermore, the reduction in bcl-2, the increase in bax, cytochrome c release and caspase 3 activation all clearly argue for the induction of the intrinsic pathway of apoptosis.

# Results

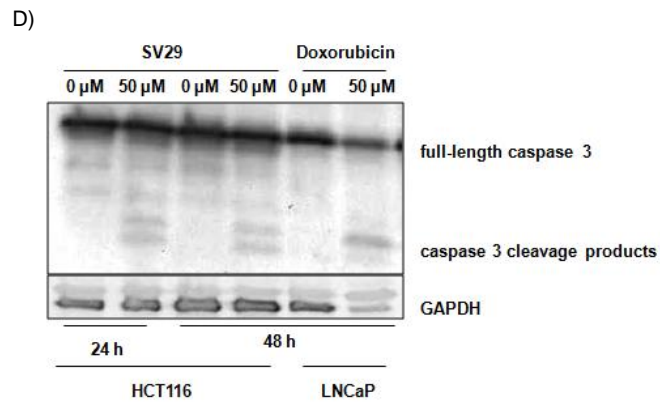
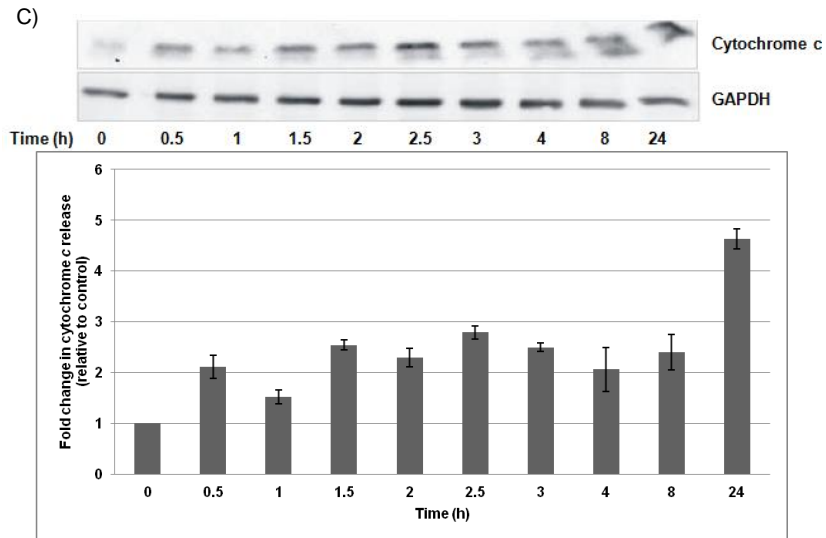
A)



B)



# Results



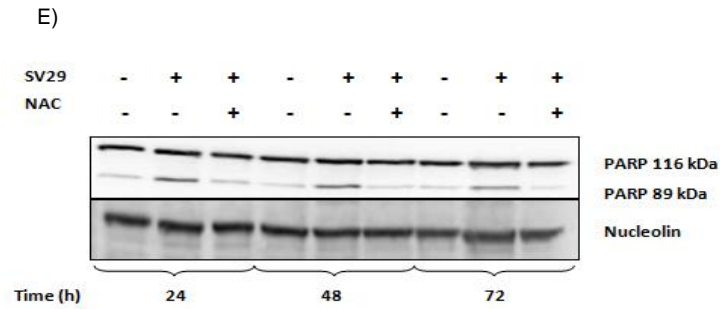


**Figure 42.** SV29 modulates bcl-2 and bax expression, induces cytochrome *c* release and activates caspase 3/7 in HCT116 cells. HCT116 cells were untreated (0 h) or treated with SV29 for 0.5, 1, 1.5, 2, 2.5, 3, 4, 8 and 24 h, and protein expression was studied by Western blotting. The proteins (50  $\mu$ g) were separated on a 12.5% SDS–polyacrylamide gel, blotted on a PVDF membrane and bcl-2 (A), bax (B) or cytochrome *c* (C) was visualized with the appropriate antibody. For (D), HCT116 cells were treated with 0 or 50  $\mu$ M SV29 for 24 and 48 h. As a positive control, LNCaP cells were treated with 20  $\mu$ g/ml doxorubicin for 24 h or left untreated. Caspase activation was analysed by Western blot. Cell lysates were separated by electrophoresis as in (A). Full-length caspase 3 and its cleavage products were detected with a caspase 3-specific antibody. One representative of at least 3 Western blots is shown here. NAC pretreatment reduces coumarin polysulfide-mediated apoptosis in HCT116 cells. (E) pretreatment of HCT116 colon cancer cells with NAC at a concentration of 5 mM for 0.5 h before treatment with 50  $\mu$ M SV29 prevented PARP cleavage (E). HCT116p53wt cells were treated for 24, 48 and 72 h with 0.05% DMSO, or 50  $\mu$ M SV29 following NAC treatment and cell extracts were treated for PARP cleavage using SDS–polyacrylamide gel electrophoresis and Western blotting. Total protein extract (75  $\mu$ g) was separated on a 7.5% SDS–polyacrylamide gel, blotted on a PVDF membrane and PARP was detected using the corresponding antibody. Nucleolin or GAPDH were used as a loading control.

Coumarin polysulfides like other polysulfides might induce reactive oxygen species (ROS). In order to evaluate the contribution of ROS to the coumarin polysulfide-induced apoptosis, HCT116 cells were with SV29 either in the absence or presence of N-acetyl cysteine (NAC). Cells were lysed and then the cell extract analysed by SDS polyacrylamide gel electrophoresis followed by Western blot with a PARP specific antibody. As shown in Figure 42 (E), SV29 induced PARP cleavage already after 24 h and also after 48 h and 72 h. In the presence of NAC, however, there was no cleavage of PARP, indicating that NAC prevented apoptosis. Thus, these results strongly indicated that ROS contribute to the coumarin polysulfides induced apoptosis.

In order to evaluate the potential of the coumarin polysulfides, their activities were compared to those of the well characterised diallyl polysulfides (Fig. 43A). HCT116 cells were therefore treated with the coumarin disulfide (SV25), or with the diallyl disulfide (DADS), and in a second set of experiments with coumarin tetrasulfide (SV28) or with diallyl tetrasulfide (DATTS). After 24 h or 48 h, cell viability was measured with an MTT assay. As shown in Figure 43 (B) and (C), SV25 reduced cell viability more efficiently than the corresponding diallyl disulfide, whereas the corresponding tetrasulfides exhibited nearly the same activity. Thus, this result indicated that the activity of the coumarin derivatives is not dependent on the length of the sulfur chain as it is the case for the diallyl polysulfides. This result also supports the observation shown in Figure 43 (B). To analyse whether this behaviour might also lead to a more efficient apoptosis induction, we treated HCT116 cells with SV25 or with DADS. After 24 or 48 h of treatment, cells were extracted and the cell extract analysed on a SDS polyacrylamide gel followed by Western blot analysis for PARP cleavage. As shown in Figure 43 (D), the PARP cleavage product was clearly detectable for SV25 after 24 h and even more after 48 h. In contrast only a very faint protein band for the cleavage product was found for DADS. This result supported the observation that the coumarin disulfide was more active inducing apoptosis than the corresponding diallyl disulfide.

## Results

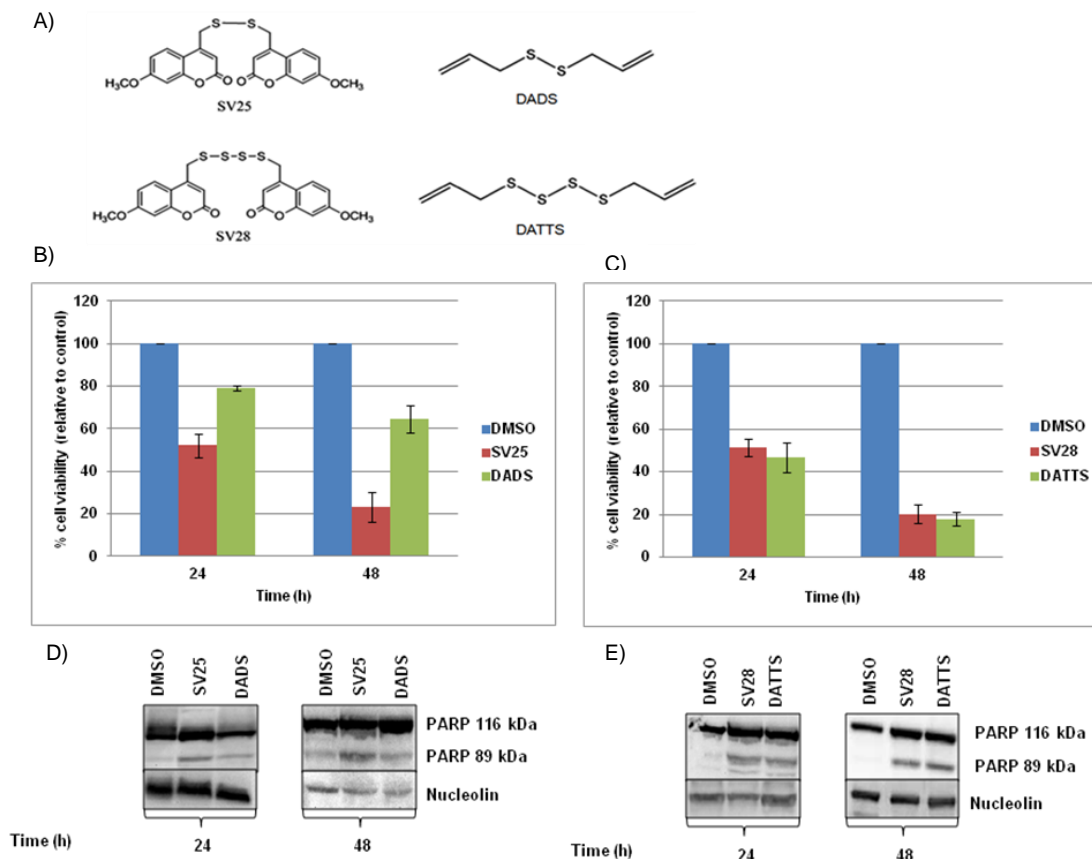


**Figure 43.** Coumarin polysulfides compared with diallyl polysulfides. (A) structures of two of the newly synthesised compounds 4,4'-disulfanediyldis(methylene)bis(2H-chromen-2-one) (SV25), and 4,4'-tetrasulfanediyldis(methylene)bis(2H-chromen-2-one) (SV28) with their corresponding well characterised diallyl polysulfides - diallyldisulfide (DADS) and diallyl tetrasulfide (DATTS). (B) Cells were seeded in 24-well plates and treated with 0.05% DMSO as a control, 50  $\mu$ M SV25 or 50  $\mu$ M DADS for 24 h or 48 h. In a second set of experiments, cells were treated with 0.05% DMSO as a control, 50  $\mu$ M SV28 or DATTS for 24 h or 48 h. Afterwards, MTT assay was carried out to determine the number of viable cells in both set of experiments as in Figure 41 (B) and (C). Data are depicted as means  $\pm$  SD, (n = 3). (D) HCT116 cells were treated for 24 or 48 h with 0.05% DMSO as a control or 50  $\mu$ M SV25 or DADS. In a second set of experiments, cells were treated with 0.05% DMSO as a control, 50  $\mu$ M SV28 or DATTS for the same time periods (E). Cell extracts were treated for PARP cleavage (D) and (E) as in Figure 41. Nucleolin was used as a loading control.

p53 is known to be a key player in the regulation of life and death of a cell. Therefore, the question was asked whether an increase in p53 protein expression could be detected after incubation of the cells with SV25 and SV29. After incubating the cells for different time periods, ranging from 8 to 48 h with SV25 and SV29, cells were lysed and p53 analysed by SDS–polyacrylamide gel electrophoresis followed by Western blot with a p53-specific antibody (DO1). GAPDH was used as a loading

control. Figure 44 shows an increase in the level of p53 over the indicated time periods following treatment.

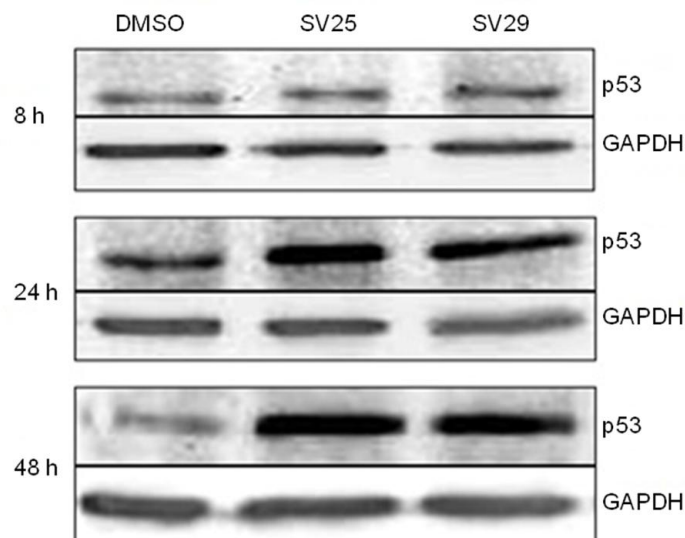


**Figure 44.** Coumarin polysulfides induce p53 expression in HCT116 cells. HCT116 cells were treated for 8, 24 and 48 h with 0.05% DMSO as a control or 50  $\mu$ M SV25 or SV29, and p53 protein expression was studied by Western blotting. Total proteins (50  $\mu$ g) from the cell extract were separated on a 12.5% SDS–polyacrylamide gel, blotted on a PVDF membrane and p53 was visualized with the mouse monoclonal p53 (DO-1) antibody. One representative of at least 3 Western blots is shown here.

Since *cdc25C* is one of the key enzymes responsible for  $G_2/M$  phase transition [144], it was tested whether the coumarin polysulfides might influence the level of *cdc25C* and its activity. HCT116 cells were incubated for various time periods with SV29. Cells were extracted and the cell extract analysed on a 10% SDS polyacrylamide gel. Proteins were transferred to a membrane and blotted with the *cdc25C* specific antibody H6. As shown in Figure 45 (A), a time dependent decrease in the level of *cdc25C* was found. In the next step, the question of whether coumarin polysulfides might also influence the phosphatase activity was addressed. For this type of analysis, the human glutathione-S-transferase (GST)-*cdc25* recombinant enzyme which was prepared as previously described [146] was used. This experiment was actually carried out by one of my colleagues (Emilie Bana, University of Metz, France). The inhibitory potential of the coumarin polysulfides, SV25, SV28, SV29,



was tested and compared to BN82002 (Sigma–Aldrich), used as reference inhibitor drug. The inhibitory activity was also compared to that of DMSO (i.e., expressed as a percentage relative to DMSO control). As shown in Figure 45 (B), these compounds were able to inhibit cdc25 phosphatase activity. Specifically, the disulfide (SV25) and the trisulfide (SV29) were able to inhibit cdc25A and cdc25C. However, the progressive introduction of sulfur atoms increased the inhibiting activity of such molecules, showing the tetrasulfide to be more potent than the trisulfide, and the trisulfide more potent than the disulfide. All three polysulfides were less active than the established cdc25 inhibitor BN82002 (Fig. 45B). Nevertheless, this study was able to show that the coumarin polysulfides down-regulated the level cdc25C and also the phosphatase activity of cdc25C and cdc25A, both of which might be responsible for the G<sub>2</sub>-arrest of the cells.

## Results

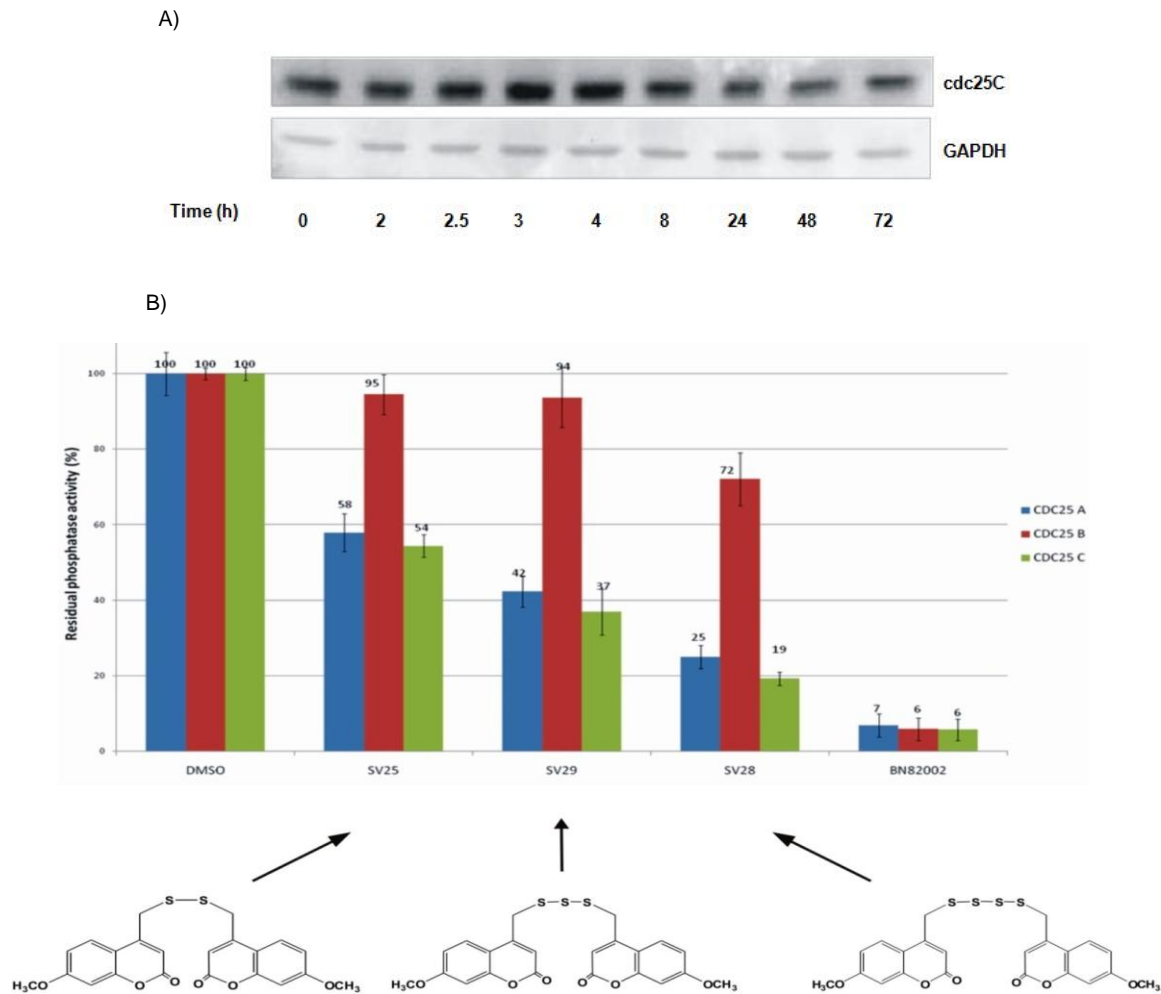


**Figure 45.** Coumarin polysulfides down-regulate *cdc25C* expression in HCT116 cells and inhibit the phosphatase activity of recombinant *cdc25C* phosphatase. (A) HCT116 cells were treated with 50  $\mu\text{M}$  SV29 and *cdc25C* protein expression was determined by Western blotting. Total protein extract (50  $\mu\text{g}$ ) was separated on a 12.5% SDS polyacrylamide gel, blotted on a PVDF membrane and *cdc25C* was detected using anti-*cdc25C* (H6) antibody. GAPDH was used as a loading control. (B) Residual activity of *cdc25* phosphatases was measured by a dephosphorylation assay with 3-O-methyl fluorescein phosphate following incubation with 100  $\mu\text{M}$  SV25, SV29 and SV28. DMSO treated cells were set at 100%.

## 6 Discussion

Organosulfur compounds (OSCs) including diallyl polysulfides are well known for various possible beneficial properties regarding human health. Recent studies even point to a potential role of these compounds as chemopreventive and therapeutic agents in the treatment of cancer due to their selective anti-proliferative effects [69, 70, 79, 146, 147]. Most of the experiments published up to now are performed with diallyl sulfide (DAS), diallyl disulfide (DADS) and diallyl trisulfide (DATS) (all of which occurs naturally in garlic), whereas, the corresponding tetrasulfide (DATTS), which also occurs in garlic, is more difficult to obtain and use, and therefore has rarely been studied in more detail. Furthermore, most studies have focused on either antioxidant or pro-apoptotic pathways, which leads to partially conflicting results regarding polysulfide activity and toxicity. In fact, the vast majority of the molecular mechanisms underlining the biological activities of these compounds remain elusive. There is increasing evidence, however, that parallel induction of multiple signal transduction pathways regulating cell cycle progression and induction of apoptosis by diallyl polysulfides occurs, which is, in fact, linked to their ability to oxidize essential thiols either directly or by generating ROS [59, 61, 69, 116]. Despite their rather simple chemical structure, such compounds are able to participate in a network of different redox reactions as described by Jacob [148]. These reactions include: participating in thiol/polysulfide exchange; reactive radical generation; one- or two-electron transfers; radical reactions; and coordination of metal ions. Available evidence indicates that oxidative mechanisms in particular are involved in most cell deaths [70, 79]. ROS are unstable, partially reduced forms of oxygen, and are generated in respiring cells. ROS damage the cell, including membrane lipid peroxidation, oxidative modification of proteins, and DNA strand breaks, resulting in the impairment of cellular integrity and function [87].

The aim of the present study was to identify the most active biological polysulfide from the various coumarin and dially polysulfides we had in the lab, and to

demonstrate its efficiency in both normal and cancer cells. I wanted to test the ability of the most active polysulfide (in terms of cell viability and apoptosis) to generate ROS and to cause polysulfide stress, and I also wanted to further elucidate downstream events of polysulfide-induced ROS or disulfide stress. Special reference was given to certain transcription factors and detoxifying enzymes that are associated with oxidative stress.

In the present study, dealing with the anticancer activities of polysulfides with a chain length from one to four sulfur atoms, toxicity against HCT116 colorectal cancer cells, which was determined by an MTT assay and Western blot analysis (Fig. 17), is particularly pronounced for the tri- and tetrasulfide. Using a concentration of 50  $\mu\text{M}$  for all four diallyl sulfides, only the di-, tri- and tetrasulfides showed a significant influence on HCT116 cell viability, with diallyl tetrasulfide been the most potent (Fig. 17). The mono sulfide in particular, had only a slight if any effect at all on HCT116 cancer cells. Münchberg *et al.*, (2007) [58] however, have reported that the redox- and metal-binding chemistries of the thiol–disulfide pair may provide the basis for many different biological events from which the monosulfide is excluded. This is because monosulfides do not act as oxidants, and therefore cannot be reduced to thiols. There is no obvious sulphur-sulphur-bond chemistry associated with the monosulfides and the redox conditions provided by the sulphur chain appears crucial for activity of the compound. On the other hand, disulfides, along with other higher polysulfides, are oxidants and can form thiols. A contribution of such redox processes was supported by cell culture studies employing the antioxidants glutathione (GSH), *N*-acetyl-cysteine (NAC) and ascorbic acid (ASC) (Fig. 10). Whilst morphological indications for apoptosis were inconclusive in cells that were pretreated with NAC and GSH (Fig. 23A),  $\gamma\text{H2AX}$  protein expression was significantly reduced in cells that were pretreated with NAC (Fig. 23C). Also, in agreement with studies reported by Busch *et al.*, (2010) [82], pretreatment of cells with either NAC or ascorbic acid (ASC), prevented PARP cleavage (a late event of apoptosis) (Fig. 23B).

Apoptosis - or programmed cell death - is an evolutionarily highly conserved physiological process for the regulation of cellular homeostasis and cell differentiation and defense [149]. Apoptosis can be initiated by the activation of the extracellular pathway, which involves Fas and TRAIL receptors that can then form a death-inducing signaling complex called DISC (death inducing signaling complex). DISC contains Fas and FADD (Fas-associated via death domain), which recruit procaspase 8 to the complex. Procaspase 8 is activated by proteolysis to generate caspase 8, which then activates the down-stream caspases 3 and 7. Caspase 3 cleaves the DNA fragmentation factor ICAD (inhibitor of caspase-activated DNase) in complex with CAD. CAD dissociates from ICAD, which leads to the activation of the DNase activity of CAD. Alternatively, caspase 3 can activate procaspase 9 to induce apoptosis. Apoptosis can also occur via an intrinsic pathway, which can be induced by oncogenes, DNA damage, growth factor deprivation or hypoxia. One important player for the induction of the intrinsic pathway of apoptosis is the growth suppressor protein p53 [150]. DNA quality control proteins such as the ataxia telangiectasia mutated protein ATM and the checkpoint regulator 2, chk2, can directly phosphorylate and stabilize p53. p53 induces apoptosis by transcriptionally activating the pro-apoptotic bcl-2 family members and by repressing the anti-apoptotic bcl-2 family members. Other p53 targets are bax, bid, Noxa, Puma, PTEN, p53AIP1 and other genes that lead to an increase in reactive oxygen species (ROS). ROS induce a generalised oxidative damage of the mitochondria. Following this mitochondrial damage, pro-apoptotic bcl-2 family proteins are activated, allowing them to interact with and inactivate anti-apoptotic bcl-2 family members. Furthermore, mitochondrial damage leads to a release of cytochrome c from the mitochondria, which then activates caspase 9, followed by apoptosis.

Studies have shown that diallyl disulfide and diallyl trisulfide cause a decrease in the protein expression levels of the anti-apoptotic bcl-2, an increase in the pro-apoptotic bax, p53 and activation of the caspases [9, 82, 104]. These seem to be in strong agreement with the findings of the present study with diallyl tetrasulfide (DATTS). DATTS was solely used in all subsequent experiments as it was deemed the most biologically active (based on cell viability and apoptosis studies) out of all four diallyl polysulfides (Fig. 17). DATTS treatment of HCT116 cells resulted in a decreased

level of bcl-2, an elevated level of p53, bax, cytochrome *c* release into the cytoplasm and activation of caspases 3/7 (Fig. 22A - F), all of which are events in the apoptotic pathway as shown in Figure 46. Moreover, there were clear morphological indications for apoptosis when DATTS was employed, such as blebbing of the cells, formation of apoptotic bodies, nuclear disintegration and DNA degradation.

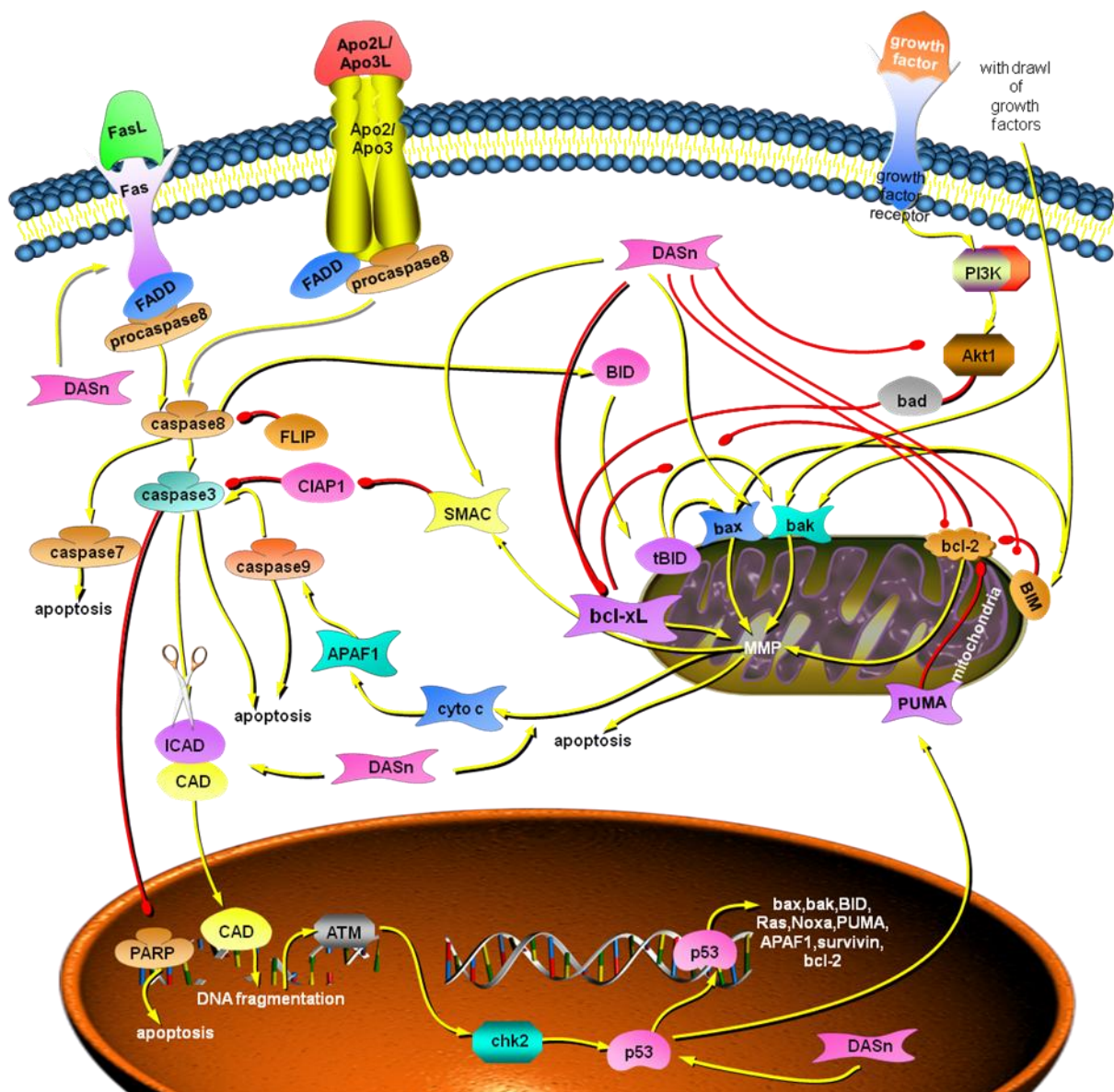


**Figure 46.** Scheme of a generalised DATTS-induced signalling cascade leading to apoptosis. Figure adopted from Montenarh and Saidu [151].

In the study presented, apoptosis and cell cycle arrest appear to be closely related. Eight and even more so, 24 h after DATTS treatment, an increase in both subG<sub>1</sub> and G<sub>2</sub> phase population of cells were observed; pointing towards a G<sub>2</sub>-cell cycle arrest and subsequent apoptosis (Fig. 20). It is known that p53 can act as a transcriptional suppressor of cdc25C, and therefore p53 induction might be responsible for the down-regulation of cdc25C [152]. cdc25C is a member of the cdc25 family of phosphatases, which are implicated in cell cycle check point control [144]. In particular, cdc25C is responsible for G<sub>2</sub>/M transition by dephosphorylation of CDK1. In agreement with a G<sub>2</sub>-arrest of cells after DATTS treatment, a marked decrease in the amount of both CDK1 (a p53 target) and cdc25C were also observed (Fig. 20A and B). Furthermore, a G<sub>2</sub>/M cell cycle arrest and timely associated bcl-2 down-regulation are reported to occur in apoptosis induced by microtubule-interfering agents [136]. Diallyl polysulfides such as DATTS may alter the redox system in cancer cells by directly targeting tubulin thiols, which may result in cell cycle arrest and or apoptosis. In the present study, DATTS caused a dose-dependent loss of microtubule network, with only a diffuse stain visible throughout the cytoplasm (Fig. 32). It inhibited tubulin assembly and destabilised spindles within 24 h of cell treatment, which probably is responsible for the mitotic block and cell death observed in this study. In stark contrast, DMSO-controlled cells exhibited normal arrangement, with microtubules seen to traverse intricately throughout the cell, and these cells displayed a normal compact rounded nucleus (Fig. 32). A hypothetical scheme of the apoptotic signal transduction pathway activated by DATTS, involving inhibition of microtubule dynamics is given in Figure 47.

In the present study, it is demonstrated that treatment of the colon carcinoma cell line HCT116 with DATTS, resulted in a very rapid induction of ROS production in a transient and dose-dependent manner. DATTS-induced superoxide anion (O<sub>2</sub><sup>•-</sup>) production in HCT116 cells was observed as early as 5 min following treatment and it increases with time (Fig. 23C and D). DATTS also induced hydrogen peroxide (H<sub>2</sub>O<sub>2</sub>) production in a similar manner, but at a lower level compared to the O<sub>2</sub><sup>•-</sup> induction (Fig. 23E and F).

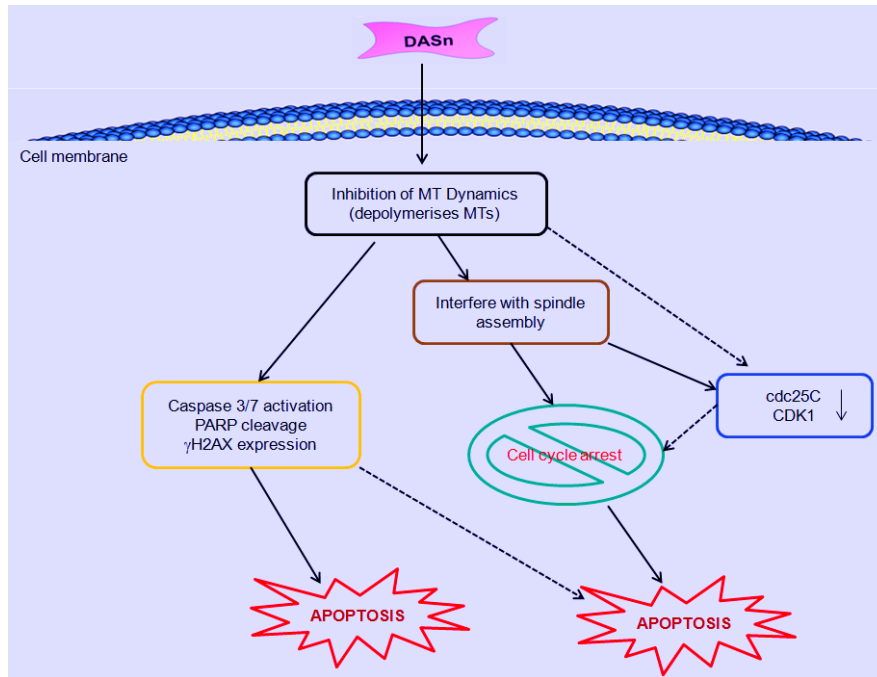


**Figure 47.** Proposed mechanism of other apoptotic signal transduction pathways activated by DATTS, involving inhibition of microtubule dynamics.

In contrast, intracellular thiol levels are depleted rapidly in response to DATTS treatment. Following treatment of the colon carcinoma cell line HCT116 with increasing concentrations of DATTS or with the same concentration of DATTS for various time intervals a significant time and dose-dependent depletion of total thiols could be observed (Fig 25A and B). Intracellular thiol depletion has been reported as an early hallmark in the progression of cell death in response to different apoptotic stimuli [119, 120, 153]. Several studies have shown a correlation between cellular thiol depletion and the progression of apoptosis [119, 120]. Evaluating the relationship between thiol depletion, the generation of ROS, and the progression of apoptosis, Rodriguez-Ramiro and colleagues [154] have recently demonstrated that loss of intracellular thiol was paralleled with the generation of different ROS including hydrogen peroxide, superoxide anion, hydroxyl radical, and lipid peroxides. They found that thiol depletion was necessary for ROS levels to increase and also for the progression of apoptosis activated by both the extrinsic and intrinsic signalling pathways [154]. In the present study, it is demonstrated that DATTS-induced thiol depletion and ROS production occurs at almost similar times (Figs. 24C and 25A),



suggesting a possible relationship between the two processes as proposed by Rodriguez-Ramiro and colleagues [154].

Oxidative stress can disrupt protein folding in the endoplasmic reticulum (ER), and this protein misfolding contributes to the pathogenesis of many diseases [73, 155]. Studies have shown that ROS can exacerbate protein misfolding in the ER lumen by oxidising amino acids in folding proteins or modifying chaperone and/or ERAD functions, thereby amplifying the unfolded protein response (UPR) signalling [156, 157]. In addition, accumulation of unfolded protein in the ER lumen may signal ROS production as a second messenger to activate the unfolded protein response [154]. This response is an adaptive signalling pathway designed to prevent the accumulation of unfolded protein in the ER lumen [158, 159]. In most cells, the antioxidative stress response is put in place in order to limit ROS accumulation and protein misfolding, and this is particularly important for the function and survival of the cell. Recent studies suggest that during oxidative or ER stress, both the eIF2 $\alpha$  and Nrf2 signalling pathways become activated by a coordinated process which involves upstream kinases such as PERK. PERK phosphorylates eIF2 $\alpha$  at serine 51 which then allows the activation of ATF4 and its downstream targets [160]. Nrf2 also becomes activated by PERK or other kinases and is released from its repressor – Keap-1 residing in the cytoplasm. Nrf2 is then translocated into the nucleus where it binds to ARE/StRE in the promoter region of the Phase 2 genes such as *HO-1*, thereby stimulating transcription [161] as depicted in Figure 48. In 2004, it was reported that diallyl di- and trisulfide dramatically increase both the Nrf2 and HO-1 protein levels [71]. Here, it is shown for the first time that DATTS also induces the up-regulation of phosphorylated PERK, eIF2 $\alpha$ , Nrf2 and HO-1 proteins in both a time- and dose-dependent manner (Fig. 26, 27 and 28). More importantly, pre-treatment of HCT116 cells with the ROS scavengers GSH, NAC or ASC partly or in some instances completely blocked the DATTS induced up-regulation of all the proteins. This strongly suggests that a pathway involving p-eIF2 $\alpha$  and Nrf2 signalling is dependent on ROS and that DATTS does indeed cause oxidative and/or ER stress by increasing the production of ROS in HCT116 cells. It is also possible that DATTS simply oxidises cellular thiols and the resulting increase of ROS is a secondary event as suggested [154].

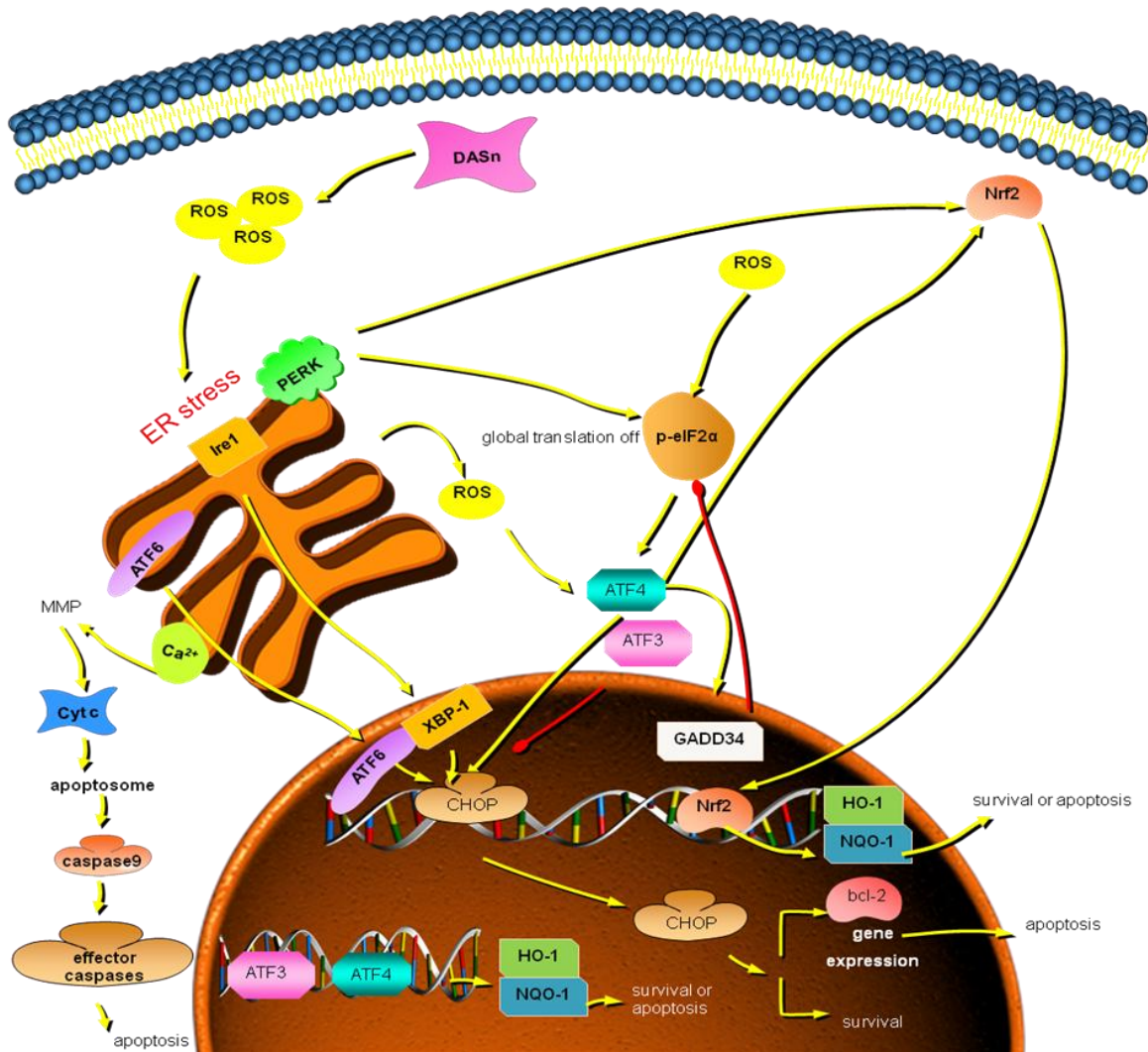


**Figure 48.** Proposed mechanism of the endoplasmic reticulum signal transduction pathway activated by DATTS. Figure adopted from Montenarh and Saidu [151].

What is even more interesting, is that glutathione may be consumed during reduction of unstable and/or improper disulfide bonds in misfolded proteins [119, 120, 153]. Consistent with this hypothesis, GSH levels were depleted in response to DATTS treatment (Fig. 26E and 27C). It is further shown here that DATTS promotes the nuclear translocation of Nrf2 in HCT116 cells leading to the up-regulation of HO-1 expression (Fig. 28A). Furthermore, it is demonstrated that DATTS increases ARE/StRE promoter activity, which corresponds with an increase in HO-1 protein levels (Fig. 28D and E). By using a wild-type and a dominant negative form of Nrf2, the observation is further supported that Nrf2 is indeed responsible for the HO-1 induction (Fig. 28F and G). It is shown in this study that diallyl tetrasulfide induces

ROS in HCT116 tumour cells, which leads to or parallels a significant depletion of cellular thiols, and furthermore, that DATTS induces the eIF2 $\alpha$ , Nrf2 pathway leading to an upregulation of the oxidative protection factor HO-1 and NQO1 (Fig. 28H and I). Time course experiments showed, however, that the signalling leading to antioxidant defense is a rapid but transient event. Obviously, this antioxidant defense is not sufficient to protect cells from cell death over a longer period of time. A reduction in cell viability which is accompanied by morphological changes of cells treated with DATTS was observed (Fig. 31A - C). An increase in the level of the pro-apoptotic bax protein and a decrease in the level of anti-apoptotic bcl-2 protein, as well as an elevated level of cytochrome c in cytoplasm support the idea that DATTS treated cells do eventually go into apoptosis (Fig. 31D and E). Poly (ADP-ribose) polymerase (PARP) was originally identified as a repair enzyme, which acts when DNA is damaged by oxidative stress and which can cleave or modify DNA [82, 104, 105, 106]. PARP activation or PARP cleavage also occurs at late stages of apoptosis. In the present study, the timing of DATTS-induced PARP cleavage did not correspond with that of ROS production. PARP cleavage was rather late, occurring after 24 h of DATTS treatment of the cells (Fig. 31F). This observation, together with previously published data [82, 104], indicates that cells treated with DATTS finally do go into apoptosis. Thus, the induction of the oxidative stress response is not sufficient to prevent apoptosis in these tumour cells over a longer period of time. Figure 49 is a hypothetical scheme that demonstrates this kind of DATTS effect in HCT116 cancer cells.

Polysulfides, like many other stress inducers, may trigger a host of other signalling pathways leading to cell cycle arrest and subsequently apoptosis. The Mitogen-activated protein kinase (MAPK) signalling pathway for example may be activated by some polysulfides leading to the phosphorylation to certain transcription factors, which may play vital roles in adaptive response mechanisms.

Mitogen-activated protein kinases are a family of serine/threonine kinases that comprise three major subgroups, namely extracellular signal-regulated kinase (ERK), p38 MAPK and c-Jun N-terminal kinases (JNKs). Despite the diversity in

function and upstream signaling events, all MAP kinases are activated by phosphorylation of either a threonine or a tyrosine residue.

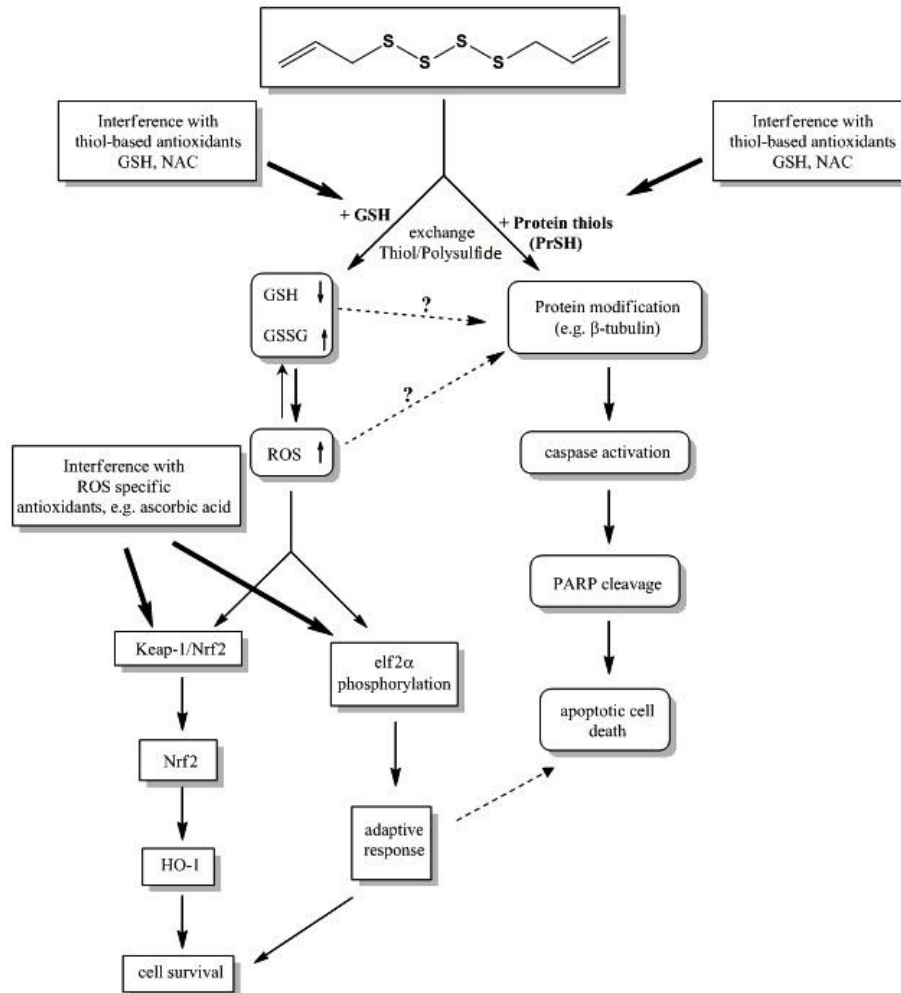


**Figure 49.** Proposed mechanism for DATTS-induced ROS generation, elf2 $\alpha$  phosphorylation, Nrf2 and HO-1 inductions. DATTS can induce ROS generation, which then induces elf2 $\alpha$  phosphorylation, Nrf2 and HO-1 inductions. It may also bind to and modify Keap-1 cysteine residues thereby allowing Keap-1/Nrf2 dissociation. Nrf2 is then translocated into the nucleus where it binds to stress-response elements leading to HO-1 expression. Sufficient HO-1 expression may allow cell survival. An insufficient adaptive response, however, may facilitate cell death.

Members of the p38 MAP kinase subgroup play important roles in cytokine production, stress response, cell cycle regulation, developmental processes and

differentiation. These family members are activated by cellular stress such as UV irradiation, heat shock, osmotic stress and certain cytokines and growth factors.

The JNK cascade is activated by UV irradiation, heat shock or inflammatory cytokines. The various signalling cascades converge on MAP kinase/ERK kinase kinases (MEKK1, MEKK 4/7) which directly phosphorylate JNKs. The phosphorylated and activated JNKs translocate to the nucleus where they phosphorylate transcription factors such as c-Jun or c-Fos. Activation of the JNK signaling cascade generally results in apoptosis although under certain conditions other outcomes are possible.

The ERK pathway is mainly implicated in the regulation of cell growth and differentiation. The signalling cascade leading to ERK activation is induced by a wide variety of growth factors, hormones, cytokines, integrins and ion channels and their corresponding receptors. The signalling cascades finally converge on ERK which is phosphorylated by MAPK/ERK kinases 1/2 (MEK 1/2). An activated ERK dimer can regulate targets in the cytosol but it can also translocate to the nucleus where it phosphorylates a variety of different transcription factors, which regulate gene expression (Fig. 50) [162, 163, 164, 165, 166, 167].

In the present study, it has also been shown that DATTS treatment triggers the biosynthesis of the transcription factors ATF3 and ATF4 (Fig. 29A and B). ATF3 is a downstream target for ATF4. During the course of this study, ATF3 was considered for further investigation because lots of studies have suggested that the *ATF3* gene is involved in a host of cellular activities such as cell proliferation, apoptosis (pro- and anti-apoptotic), and invasion, and its expression is down-regulated in colorectal tumours [134]. The expression of ATF3 is modulated by a variety of compounds including diallyl disulfides [72], and its induction is believed to occur at the promoter level as well for most of these compounds. Furthermore, numerous gene regulatory pathways are known to regulate ATF3 which includes p53, p38, mitogen-activated protein kinase 1, c-jun-N-terminal kinase, and of course its own promoter [168, 169, 170, 171, 172]. In 2010, Spohn and colleagues also reported that thapsigargin which is known to empty intracellular  $\text{Ca}^{2+}$  stores and

increase cytoplasmic  $\text{Ca}^{2+}$  concentrations, can induce the expression of ATF3 in human keratinocytes involving  $\text{Ca}^{2+}$  and c-jun-N-terminal kinase [135]. Now it is shown that DATTS induces ATF3 protein expression, raising the question of whether DATTS does indeed increase ATF3 promoter activity as well as it was reported for DADS, and if the DATTS-induced ATF3 process involve specific MAPK kinases and  $\text{Ca}^{2+}$  ions. Interestingly, it was found that not only does DATTS induce ATF3 in a number of cell lines, but also that it increases its promoter activity, which correlates with its DATTS-induced protein expression (Fig. 29D and E). This indicates that DATTS enhances transcription of the *ATF3* gene, which might be responsible for the higher protein levels of ATF3 observed. This result agrees well with the DADS effect on ATF3, which was reported by Bottone *et al.*, [72]. This study has also shown that the signalling cascade leading to ATF3 expression in HCT116 colorectal cells involves not only  $\text{Ca}^{2+}$  ions, but also p38 and phospho-c-jun. Preincubation with the ERK-specific inhibitor compound PD98059, however, did not block the biosynthesis of ATF3 in DATTS-stimulated HCT116 cells, indicating that unlike p38 and c-jun, activation of ERK may not be required for the induction of ATF3 gene transcription. In summary, these data suggest that stimulation of HCT116 colorectal cells with diallyl tetrasulfide induces a signalling cascade involving calcium ions, activation of p38 protein kinase, activation of c-jun, and up-regulation of ATF3 expression.

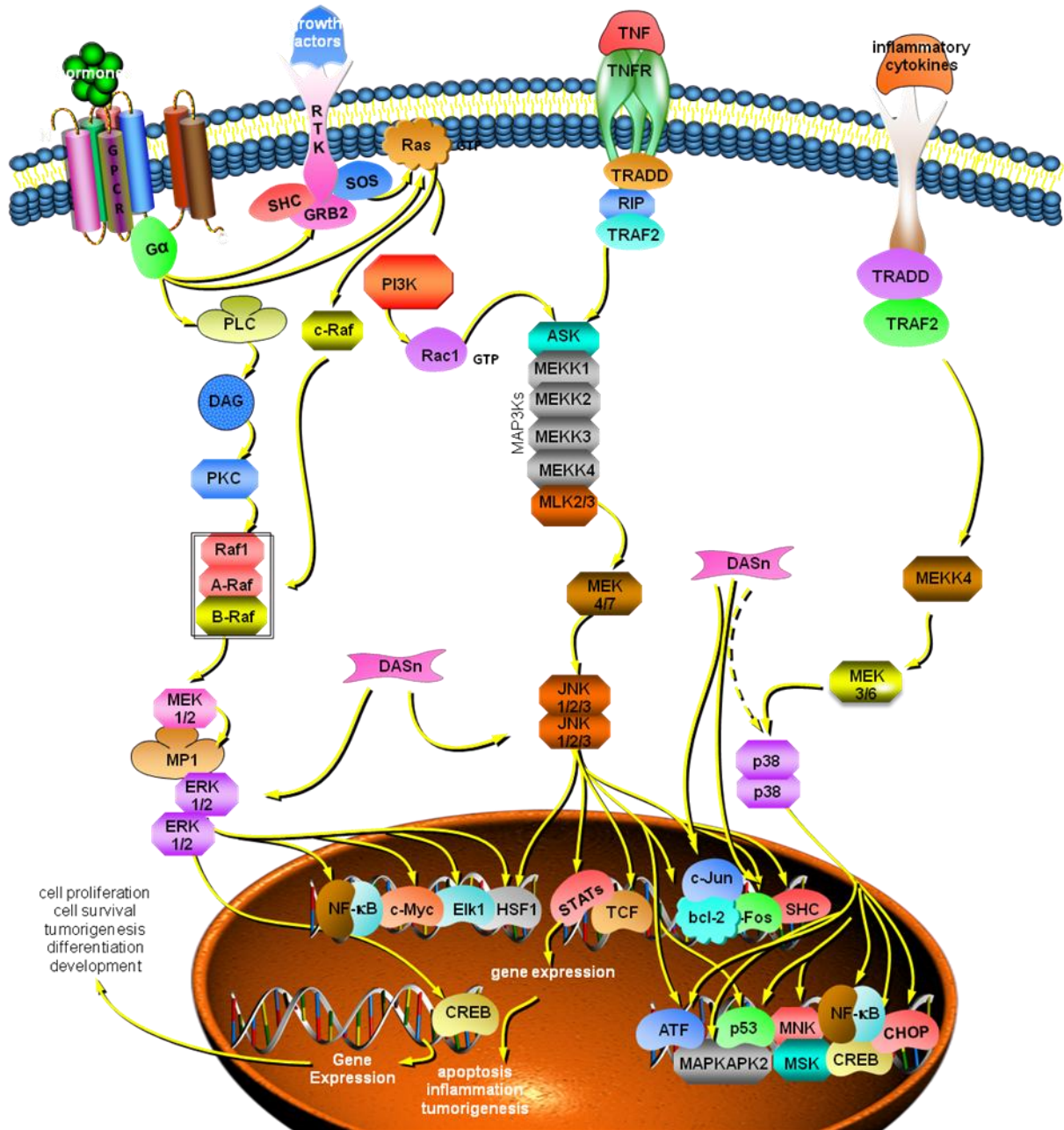


**Figure 50.** Scheme of the MAP kinase signalling pathway activated by DATTs. Figure adopted from Montenarh and Saidu [151].

Protein kinase CK2 is another enzyme besides the MAPKs that is involved in numerous cellular processes. CK2 is an ubiquitously expressed serine/threonine kinase consisting of two catalytic  $\alpha/\alpha'$  and two regulatory  $\beta$  subunits. Expression of CK2 is highly elevated in tumour cells where it protects cells from apoptosis. Hessenauer and colleagues reported in 2011 that inhibiting CK2 with 4,5,6,7-

tetrabromobenzotriazole (TBB), induces apoptosis via ER stress response in prostate tumour cells [173]. There have also been further suggestions that CK2 might inhibit PERK-mediated eIF2 $\alpha$  phosphorylation at basal conditions [174]. Besides ER stress and apoptosis, protein kinase CK2 is also implicated in diverse processes such as transcriptional/translational control, splicing, DNA replication and repair, proliferation and cell cycle regulation [175]. However, several reports point to a specific role for protein kinase CK2, especially in the control of G<sub>2</sub>/M transition, where it plays a crucial role in mitotic progression. It has been shown in our lab that inhibiting CK2 activity leads to a down-regulation of the level of cdc25C in prostate cancer cells [176]. Inhibition of CK2 activity by transfecting the dominant-negative CK2 $\alpha$  subunit also resulted in a down-regulation of the level of cdc25C.

Since it was shown in the present study that not only does DATTS inhibit cdc25C in HCT116 colorectal cancer cells, but also induces the phosphorylation of both PERK and eIF2 $\alpha$  leading to an antioxidant response, it became imperative to investigate whether DATTS have any influence on CK2 activity. Interestingly, it is shown here for the first time that DATTS induces both CK2 activity and protein expression (Fig. 33A and B) in a timely manner that coincides with DATTS-induced PERK phosphorylation (Fig. 26A). DATTS treatment seems to have little or no effect on both CK2 protein expression and kinase activity beyond 1.5 h. Whether the observed early increase in CK2 activity has an influence on PERK phosphorylation and its downstream targets, and/or cdc25C, opens more avenues for investigation. It could also be that the increase in CK2 activity and protein expression along with that of phospho-PERK and eIF2 $\alpha$  protein levels, observed upon DATTS treatment, signifies an early attempt of the cells to cope with ER stress. This study has shown that the DATTS-induced apoptosis was time-dependent, and also stronger at later time points between 8 h to 72 h. One could therefore argue that at these late times, it is likely that the pro-death pathways prevail over the compensatory mechanisms seen in CK2 and phospho-PERK.

One of the major goals of this study was to evaluate the effect of DATTS on both cancer and normal cells. To do this, HCT116 and ARPE-19 cell lines were used.



Both of these cells are epithelial and of human origin, which makes them good choices for comparison. One of the most important feature of the ARPE-19 cell line is its apparent normal karyology. This cell line retains many of the characteristics of RPE cells, including cell morphology, functional tight junctions and expression of CRALAB and RPE65, both of which are synthesised by differentiated RPE in vivo [177, 178]. Furthermore, like HCT116 cells, it has an increased growth potential relative to other primary RPE cell cultures [179].

Here, it was shown that DATTS inhibited cell viability (Fig. 34A - F) and induced apoptotic cell death in HCT116 cells, and that the apoptotic cell death is caspase-dependent (Fig. 37C). This, however, is not the case with ARPE-19 cells, where DATTS seems to have very little effect (Fig. 37A - D). In ARPE-19 cells, DATTS failed to induce cytochrome *c* release into the cytosol (Fig. 37C) and also failed to cleave and activate caspase 3 (Fig. 37C) and its substrate PARP (Fig. 37B), which is involved in DNA damage and repair. DATTS also failed to up-regulate H2AX phosphorylation in ARPE-19 cells (Fig. 37D). This is particularly important as phosphorylation of H2AX plays a key role in DNA damage response, and is required for the assembly of DNA repair proteins at the sites containing damaged chromatin, as well as for activation of checkpoint proteins which arrest the cell cycle progression [180]. The result does suggest that in ARPE-19 cells during the DATTS-induced cell cycle arrest, the cell cycle checkpoint proteins put in place to check DNA damage and repair are sufficient and able to reverse the cell damage inflicted by DATTS, whereas in HCT116 cells this is not the case.

Of course, this is only one explanation for the difference in DATTS-induced cell death in these two cell lines. Another explanation for the difference will probably point towards caspase mediated cell death reported by Yang and colleagues in 2007 [181]. In their study, they measured and compared human RPE cell caspase-8 mRNA and protein levels to that in cancer cells. They found out that RPE cell caspase-8 mRNA and protein levels were much lower than those in HCT116 cancer cells, which they suggest may be regulated postranscriptionally [181]. They were able to use tumour necrosis factor (TNF)- $\alpha$  (which is known to activate the extrinsic apoptotic pathway) to induce apoptosis in HCT116 cancer cells but not in RPE normal cells. However, when they overexpressed caspase 8 in RPE cells, they

noticed a significant decrease in cell number followed by activation of caspase-8 and caspase-3, decreased full-length bid, caspase-9, and caspase-7, and significantly increased DNA fragmentation similar to those observed in nonneoplastic ocular cells and cancer cells, including HCT116 cells. One could therefore assume that caspases may in part be responsible for the DATTS-induced apoptosis observed in HCT116 cell but not in ARPE-19 cells.

Redox modulations may also count for the differential DATTS effect in the two cell lines. Cancers in general are rich in ROS and are associated with a disturbed intracellular redox balance and oxidative stress [59, 182]. Therefore, using a ROS inducing agent such as DATTS on these cancer cells will turn the oxidising redox environment present in cells into a lethal cocktail of reactive species that pushes these cells over a critical redox threshold and ultimately kills them through apoptosis. Whereas normal cells naturally have low levels of oxidising species, applying a ROS inducing agent such as DATTS on these cells will produce little effect as shown in Figure 51.

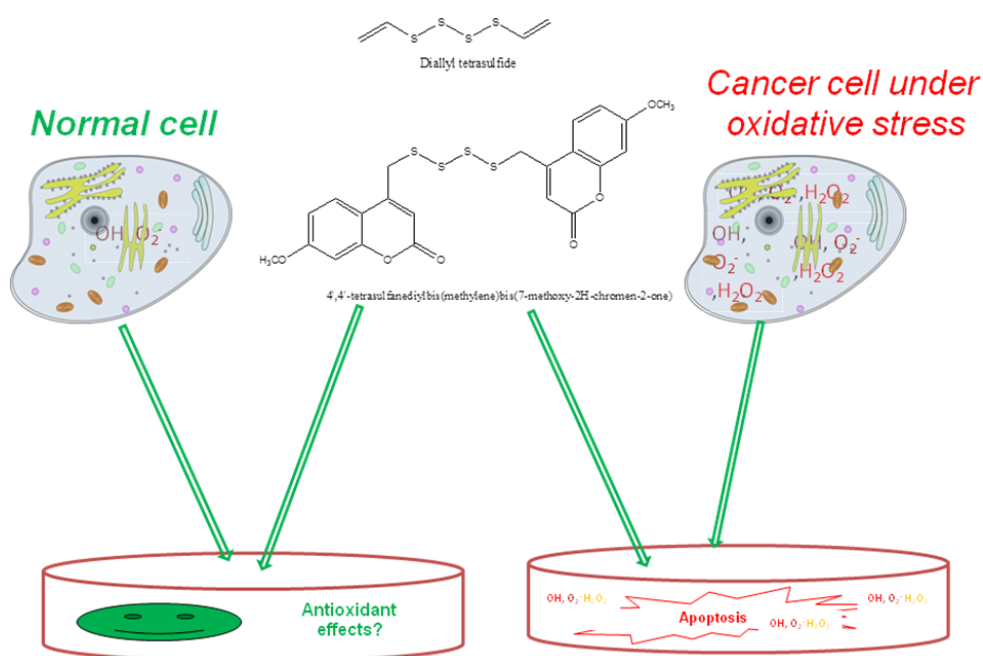


**Fig. 51.** Influence of polysulfides on cancer cell and norman cells.

We do know that most diallyl polysulfides can act both as pro-oxidants, where they stimulate intracellular ROS production leading to apoptosis induction, and as an anti-oxidant, where they can directly or indirectly scavenge ROS. In the present study, this phenomena is presented in the two cell lines. Here, it is shown that DATTS up-regulated the oxidative stress defence enzyme HO-1 in a time-dependent manner in both human epithelial HCT116 cancer cells and ARPE-19 noncancer cells (Fig. 38D). DATTS-induced ATF3 expression may serve different purposes in these two cell lines. The DATTS-induced up-regulation of this oxidative stress defence enzyme was, however, slightly higher in ARPE-19 cells than in HCT116 cells. These results indicate that DATTS may in fact cause oxidative stress in both of these cell lines leading to an antioxidant response. That is, DATTS influences the stimulation of signal transduction pathways influencing genes controlled by the antioxidant response elements in these cells. In HCT116 cancer cells, though, the pro-death pathways seem to prevail over the compensatory antioxidant response, whilst in ARPE-19 cells, rather than a harmful role, DATTS seems to protect ARPE-19 cells from oxidative stress through induction of sustained cellular antioxidant genes. These are just few of the possible reasons for the differences in DATTS-induced cell cycle arrest and apoptosis in these two different cell lines, and there may well be other contributing factors.

Most of the discussion so far has been focused on diallyl polysulfides. However, another key area which mustn't be left out is the effect of the newly synthesised coumarin derivatives on HCT116 cells.

Coumarins have a long history as anticancer agents (for review see: [37]). On the other hand, diallyl polysulfides are among the most studied organosulfur compounds from garlic, which are known to be highly effective in affording protection against various cancers in animal models [183]. As mentioned earlier, most of the experiments published up to now are performed with diallyl sulfide, diallyl disulfide and diallyl trisulfide, whereas the corresponding tetrasulfide was almost recently used. Beside allyl groups, propyl groups were also attached to the sulfur chain [184]. Now, Dr. Sargio Valente has combined the power of coumarins with those of

polysulfides and has come up with novel coumarin polysulfides. Treatment of the colon carcinoma cell line HCT116 with coumarin polysulfide resulted in reduced cell viability as shown in Figure 39, (B) and (C). The coumarin disulfide (SV25), trisulfide (SV29) and the tetrasulfide (SV28) were nearly equally active, whereas in the case of the diallyl polysulfides, the trisulfide (DATS) is more active than the disulfide (DADS) and the tetrasulfide (DATTS) is more active than the trisulfide (DATS). These differences in the activities were shown in a direct comparison of the corresponding disulfides and tetrasulfides. The coumarin disulfide was considerably more active than the corresponding diallyl disulfide, whereas the activities of the coumarin tetrasulfide and that of the diallyl tetrasulfide are comparable (Fig. 43B - E). All three coumarin derivatives acted in a time and concentration dependent manner (Fig. 39B and C).

A decrease in cell viability may be caused by apoptosis which may be induced via an extrinsic or an intrinsic or mitochondria-mediated pathway. As discussed before, the intrinsic pathway is regulated by the anti-apoptotic bcl-2 family of proteins and by the pro-apoptotic bax protein. Here, we show a decrease of the level of bcl-2 (Fig. 42A) and an increase in the level of bax (Fig. 42B) after incubation of HCT116 cells with coumarin-polysulfides, indicating that the coumarin polysulfides act via the intrinsic pathway of apoptosis. Moreover, we observed a cytochrome c release (Fig. 42C) from the mitochondria after treatment of HCT116 cells with coumarin polysulfides, further supporting the idea of the induction of the intrinsic pathway of apoptosis. Apoptosis was further documented by PARP cleavage (Fig. 41) as well as by the upregulation of the level of  $\gamma$ H<sub>2</sub>AX. Furthermore, as in the case of diallyl polysulfides discussed earlier, pretreatment of cells with NAC prevented coumarin polysulfide-induced apoptosis (Fig. 42E). These observations are in agreement with the results showing that bcl-2 overexpression confers protection against diallyl polysulfide-induced apoptosis [185] at least in prostate cancer cells.

There are contradictory results concerning the role of p53 in diallyl polysulfide-induced apoptosis in human colon cancer cells. Song *et al.*, (2009) reported no

change in the expression level of p53 by less than 12 h post-exposure [186], whereas Busch *et al.*, (2010) found an increase in the p53 level [82]. Furthermore, down-regulation of p53 siRNA prevented apoptosis after diallyl polysulfide treatment. Here, it is shown that coumarin polysulfides induced a rapid increase in the p53 level within 24 h after treatment (Fig. 44). On the other hand HCT116 cells lacking p53 were also stimulated to apoptosis by diallyl polysulfides, indicating that p53 might be implicated in apoptosis induction but it also seems to be dispensable [82].

Knowles and Milner were the first to show that diallyl disulfide caused an accumulation in the G<sub>2</sub>/M phase of the cell cycle [187, 188]. Here, it is shown that the coumarin polysulfides also caused a growth arrest in the G<sub>2</sub>-phase of HCT116 cells (Fig. 40). The results further show that the growth arrest was accompanied by a decrease in the level of the cdc25C phosphatase (Fig. 45A), which is in agreement with data published for diallyl disulfide [82, 188]. In addition to the down-regulation of the level of cdc25C, it is also shown here that coumarin polysulfides directly inhibited the phosphatase activity of purified cdc25C and also the other family members, namely cdc25A and cdc25B (Fig. 45B). This inhibitory activity increased with the length of the sulfur chain [189]. cdc25C phosphatases contain an active-site cysteine. It has been shown that redox reactions of active-site cysteines serve as a form of reversible regulation of cdc25s. Furthermore, it has been shown that the active-site cysteines of cdc25s are highly susceptible to oxidation [190]. Thus, it might well be that coumarin polysulfides directly target the active centres of the cdc25 family of phosphatases. Down-regulation of the cdc25s as well as inhibition of the phosphatase activities are probably both responsible for the observed growth arrest of the cells in G<sub>2</sub>-phase of the cell cycle. A hypothetical scheme of the signalling pathway activated by coumarin polysulfides is shown in Figure 52.

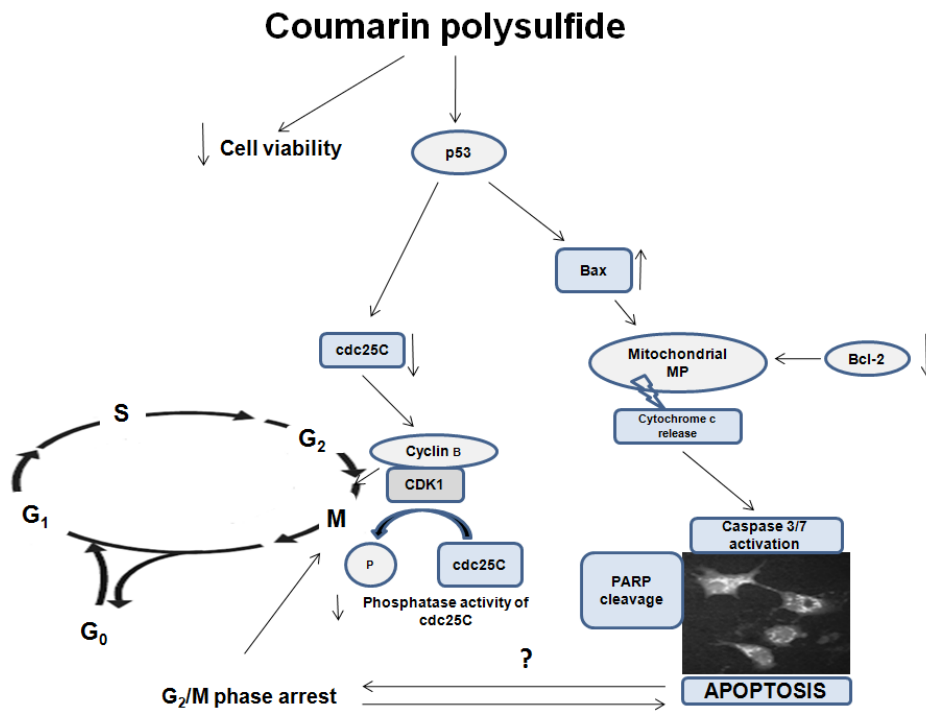


**Figure 52.** Proposed mechanism of cell growth inhibition and apoptotic signal transduction pathway activated by coumarin polysulfides in HCT116 colon cancer cell. Figure adopted from Saidu *et al.*, [9].

In conclusion, the findings from the present study suggest that both coumarin and diallyl polysulfides reduced HCT116 cell viability in a time- and concentration-dependent manner. Cells tested with these sulfur compounds accumulate in the G<sub>2</sub>/M phase of the cell cycle before finally going into apoptosis. A decrease in bcl-2 level and increase in the level of bax, cytochrome c release into the cytosol, activation of caspase 3/7 and PARP cleavage and an increase in the level of  $\gamma$ H<sub>2</sub>AX suggested that these compounds induced the intrinsic pathway of apoptosis. These compounds regulated the phosphatase activity of the cell cycle regulating cdc25 family members, indicating that these phosphatases are implicated in the induction of cell cycle arrest and possibly in apoptosis induction as well. In addition, these polysulfides also down-regulated the level of cdc25C, which also contributed to the arrest in the G<sub>2</sub>-phase of the cell cycle. These findings also suggest that DATTS in particular is a potent agent that augments cellular antioxidant defence capacity through activation of the PERK, eIF2 $\alpha$  and Nrf2 signalling pathways, that subsequently leads to the induction of HO-1, thereby protecting HCT116 cells from

ROS-induced oxidative stress. This DATTS-induced HO-1 expression, however, runs in parallel to pro-apoptotic events, and the ultimate fate of the cell seems to depend on the outcome of the competition between these two activated signalling pathways. A hypothetical scheme for this signalling pathway triggered by DATTS is shown in Figure 50. As this outcome may differ from cell type to cell type, one may speculate that this competition adds some selectivity as observed for polysulfides on the context of antioxidant activity and cancer cell selectivity. Finally, findings from this study suggest that the cell inhibitory and apoptotic effects of DATTS are more pronounced in the human epithelial HCT116 colorectal cancer than the ARPE-19 noncancer cells.

Despite the advances made in understanding the effect of coumarin and diallyl polysulfides on HCT116 cancer cells in this thesis, a number of questions still remain to be answered.

To begin with, findings from this study suggest that DATTS induces protein misfolding in the ER lumen, which may cause  $\text{Ca}^{2+}$  leak from the ER. The major question, therefore, is what effect does this  $\text{Ca}^{2+}$  leak have on cell cycle arrest and apoptosis? Studies have already shown that protein misfolding in the ER lumen can cause  $\text{Ca}^{2+}$  leak from the ER and uptake into the mitochondria to disrupt the electron transport chain [191]. This, in turn, may cause disturbances to the mitochondria membrane potential, which subsequently leads to cytochrome *c* release, activation of the caspases and finally apoptosis. It is not yet quite clear whether this is in fact the turn of events leading to the observed apoptosis in this study. Further studies are therefore required to elucidate the impact of DATTS on not only protein misfolding and how this protein misfolding in the ER lumen produces ROS, but also  $\text{Ca}^{2+}$  leak from the ER and how this may contribute to apoptotic cell death.

Following the point mentioned above, it has also been shown in this study that diallyl tetrasulfide may target tubulin directly, and the outcome of this may be a contributing factor to the observed inhibitory, cell cycle arrest and apoptotic effects. Microtubules

are vastly dynamic cytoskeletal fibers that are made of  $\alpha$  and  $\beta$  tubulin and play a vital role in many physiological processes, especially mitosis and cell division. Their importance in mitosis and cell division makes microtubules a key target for anticancer therapy [192]. This makes the findings of this study particularly important, as cancer cells are developing resistance against most of the antispindle drugs known to date. There is, therefore, an urgent need for compounds targeting alternative mitotic targets. What is still, however, not clear from this study is whether polysulfides in general cause microtubule polymerisation or depolymerisation in both cancer and normal cells. A better understanding of the molecular mechanisms underlying the apoptotic effects of these polysulfides is therefore absolutely essential for them to fulfil this role. It would be interesting to see whether DATTS actually binds tubulin *in vitro*, and whether the binding causes microtubule polymerisation or depolymerisation in both cancer and normal cells. This is essential, as it will either confirm or cross out coumarin and diallyl polysulfides as novel candidates for antineoplastic therapy.

It was shown in this study that DATTS induces an antioxidant response by up-regulating both Nrf2 and HO-1 expressions in HCT116 cancer cells. This antioxidant response is however not sufficient to prevent cells from going into apoptosis. It will therefore be interesting to use stable Nrf2 or HO-1 positive cell lines to check for DATTS-induced apoptosis. This will not only throw more weight on the findings of the present study, but will also help in designing drugs that will specifically target either the transcription factor Nrf2, or its downstream target, the HO-1 enzyme, all of which will aid in our fight against cancer.

The question - "are there other targets for polysulfides in HCT116 cancer cells?" will be another fascinating area to explore. The antitumor effect of coumarin and diallyl polysulfides has been established in the present study. However, only a handful of targets for these compounds have been identified in this study. Therefore, a gene expression profiling study to identify more novel targets will be a fundamental step forward. One way of doing this will involve the construction of a cDNA array



comprising of numerous probes. These can then be compared to RNA extracted from polysulfide-treated and untreated cells for differential gene expression. The identification of some of these putative, novel molecular targets of polysulfides may help in understanding how these compounds induce cell cycle arrest, ER and/or oxidative stress and apoptosis. Other proteomic methods may involve using quantitative real time RT-PCR along with 2D electrophoresis and Mass Spectrometry, all of which will help in studying the responses of protein expressions in either HCT116 cancer cells or in ARPE-19 cells induced by polysulfides. Western blot analysis can then be employed to confirm the polysulfide-induced expression of some of these proteins.

Other areas that can be exploited include overexpression or downregulation of CK2, cdc25C, and caspases in these HCT116 colorectal cancer cells, and studying the effects of polysulfides on them. Measurement of both intracellular and extracellular  $\text{Ca}^{2+}$  ions in polysulfide treated cells may help in shedding more light of their role(s) (if any) in polysulfide-induced apoptosis.

Furthermore, it may well be that the longer penta and hexasulfides are more potent than the shorter diallyl polysulfides in HCT116 cells, which will be another area of exploration. In addition, the use of nano-particle technology might help in optimising the uptake of these diallyl polysulfides, which will subsequently help to reduce the optimal dosage use in treatment.

Lastly, although a few studies have been conducted to evaluate the effect of diallyl sulfide, diallyl disulfide and diallyl trisulfide in animals [193, 194], not a lot has been done for the corresponding diallyl tetrasulfide or the coumarin derivatives. It would be interesting to conduct animal experiments with some of these compounds, as it would give us an idea on how their effects observed in cell culture differs from that in animals. This will not only shed more light on the various signalling pathways that are triggered by these polysulfides, but also aid in planning and implementing future clinical trials involving humans.

## 7 References

- [1] Kristina I, Heitz A, Joll C and Sathasivan A. (2010) Analysis of polysulfides in drinking water distribution systems using headspace solid-phase microextraction and gas chromatography-mass spectrometry. *J Chromatogr A.*, **217**, 5995-6001.
- [2] Kuhlmann M, Singh S and Groll J. (2012) Controlled ring-opening polymerization of substituted episulfides for side-chain functional polysulfide-based amphiphiles. *Macromol Rapid Commun.*, **33**, 1482-6.
- [3] Kuo MC and Ho CT. (1992) Volatile polysulfides identified from thermal interaction of onion components propyl-1-propenyl disulfide dipropyl disulfide and dimethyl disulfide, *Abstracts of Papers American Chemical Society.*, **204**, AGFD 144.
- [4] Jacob C and Anwar A. (2009) Sulfides in Allium vegetables, in *Chemoprevention of Cancer and DNA Damage by Dietary Factors*. Knasmueller S, DeMarini D, Johnson I and Gerhaeuser C. *Editors. Wiley-VCH Verlag GmbH & Co., Weinheim, Germany.*
- [5] Corzo-Martinez M, Corzo N and Villamiel M. (2007) Biological properties of onions and garlic. *Trends Food Sci. Technol.*, **18**, 609- 625.
- [6] Prasad S, Sung B and Aggarwal BB. (2012) Age-associated chronic diseases require age-old medicine: role of chronic inflammation. *Prev Med.*, **54**, 29-37
- [7] Keating G and O’Kennedy R. (1997) The Chemistry and Occurrence of Coumarins. *Coumarins: Biology, Applications and Mode of Action. Chichester, John Wiley & Sons.*, 23-66.
- [8] Valente S, Bana E, Viry E, Bagrel D and Kirsch G. (2010) Synthesis and biological evaluation of novel coumarin-based inhibitors of Cdc25 phosphatases. *Bioorg Med Chem Lett.*, **19**, 5827-30.

- [9] Saidu NEB, Valente S, Bana E, Kirsch G, Bagrel D and Montenarh M. (2012) Coumarin polysulfides inhibit cell growth and induce apoptosis in HCT116 colon cancer cells. *Bioorganic & Medicinal Chemistry.*, **20**, 1584-1593.
- [10] Morita K and Kobayash S. (1966) Isolation and Synthesis of Lenthionine an Odorous Substance of Shiitake an Edible Mushroom. *Tetrahedron Letters.*, **6**, 573-576.
- [11] Chen CC and Ho CT. (1986) Identification of Sulfurous Compounds of Shiitake Mushroom (*Lentinus-Edodes* Sing). *J. Agric. Food Chem.*, **34**, 830-833.
- [12] Hausen BM and Wolf C (1996) 1,2,3-Trithiane-5-carboxylic acid, a first contact allergen from *Asparagus officinalis* (Liliaceae). *Am. J. Contact Dermat.*, 41-46.
- [13] Gmelin R, Susilo R and Fenwick GR. (1981) Cyclic Polysulphides from *Parkia Speciosa*. *Phytochemistry.*, **20**, 2521-2523.
- [14] Copp BR, Blunt JW, Munro MHG and Pannell LK. (1989) A Biologically-Active 1,2,3-Trithiane Derivative from the New- Zealand Ascidian *Aplidium* Sp-D. *Tetrahedron Lett.*, **30**, 3703-3706.
- [15] Pearce AN, Babcock RC, Battershill CN, Lambert G and Copp BR (2001) Enantiomeric 1,2,3-trithiane-containing alkaloids and two new 1,3-dithiane alkaloids from New Zealand ascidians. *J. Org. Chem.*, **66**, 8257-8259.
- [16] Anthoni U, Christophersen C, Madsen JO, Wiemandersen S and Jacobsen N (1980) Biologically-Active Sulfur-Compounds from the Green-Alga *Chara-Globularis*. *Phytochemistry.*, **19**, 1228-1229.
- [17] Ichimaru M, Kato A and Hashimoto Y. (2000) Cassipoureamide-A and -B: new sulfur-containing amides from stem wood of *Cassipourea guianensis*. *J. Nat. Prod.*, **63**, 1675-6.
- [18] Derbesy G and Harpp DN. (1994) A simple method to prepare unsymmetrical disulfide, trisulfide and tetrasulfide. *Tetrahedron Lett.*, **35**, 5381-5384.

- [19] Bruneton J. (1999) *Pharmacognosy, Phytochemistry, Medicinal Plants. Second Edition, Hampshire UK, Intercept Ltd., 263-277.*
- [20] Floc'h F. (2002) "Coumarin in plants and fruits: implications in perfumery." *Perf. & Flav.* **27**, 32-36.
- [21] Heddle JG, Barnard FM, Wentzell LM and Maxwell A. (2000) The interaction of drugs with DNA gyrase: a model for the molecular basis of quinolone action. *Nucleosides, Nucleotides and Nucleic Acids.*, **8**, 1249-64.
- [22] Kostova I. (2005) Synthetic and natural coumarins as cytotoxic agents. *Curr. Med. Chem. Anticancer Agents.*, **5**, 29- 46.
- [23] Kostova I. (2006) Synthetic and natural coumarins as antioxidants. *Mini. Rev. Med. Chem.*, **6**, 365- 374.
- [24] Wu L, Wang X, Xu W, Farzaneh F and Xu R. (2009) The structure and pharmacological functions of coumarins and their derivatives. *Curr. Med. Chem.*, **16**, 4236- 4260.
- [25] Curir P, Galeotti F, Dolci M, Barile E and Lanzotti V. (2007) Pavietin, a coumarin from *Aesculus pavia* with antifungal activity. *J. Nat. Prod.*, **70**, 1668-1671.
- [26] Pisani L, Muncipinto G, Miscioscia TF, Nicolotti O, Leonetti F, Catto M, Caccia C, Salvati P, Soto-Otero R, Mendez-Alvarez E, Passeleu C and Carotti A. (2009) Discovery of a novel class of potent coumarin monoamine oxidase B inhibitors: development and biopharmacological profiling of 7-[(3-chlorobenzyl)oxy]-4-[(methylamino)methyl]-2H-chromen-2-one methanesulfonate (NW-1772) as a highly potent, selective, reversible, and orally active monoamine oxidase B inhibitor. *J. Med. Chem.*, **52**, 6685- 6706.
- [27] Matos MJ, Vina D, Picciau C, Orallo F, Santana L and Uriarte E. (2009) Synthesis and evaluation of 6-methyl-3-phenylcoumarins as potent and selective MAO-B inhibitors. *Bioorg. Med. Chem. Lett.*, **19**, 5053- 5055.

- [28] Piazzzi L, Cavalli A, Colizzi F, Belluti F, Bartolini M, Mancini F, Recanatini M, Andrisano V and Rampa A. (2008) Multi-target-directed coumarin derivatives: hAChE and BACE1 inhibitors as potential anti-Alzheimer compounds. *Bioorg. Med. Chem. Lett.*, **18**, 423- 426.
- [29] Appendino G, Maxia L, BascopeM, Houghton PJ, Sanchez-Duffhues G, Munoz E and Sterner O. (2006) A meroterpenoid NF-kappaB inhibitor and drimane sesquiterpenoids from *Asafetida*. *J. Nat. Prod.*, **69**, 1101- 1104.
- [30] Donnelly A and Blagg BS. (2008) Novobiocin and additional inhibitors of the Hsp90 C-terminal nucleotide-binding pocket. *Curr. Med. Chem.*, **15**, 2702-2717.
- [31] Reddy MV, Rao MR, Rhodes D, Hansen MS, Rubins K, Bushman FD, Venkateswarlu Y and Faulkner DJ. (1999) Lamellarin alpha 20-sulfate, an inhibitor of HIV-1 integrase active against HIV-1 virus in cell culture. *J. Med. Chem.*, **42**, 1901- 1907.
- [32] Ong EB, Watanabe N, Saito A, Futamura Y, Abd El Galil KH, Koito A, Najimudin N and Osada H. (2011) Vipirinin, a Coumarin-based HIV-1 Vpr Inhibitor, Interacts with a Hydrophobic Region of VPR. *J. Biol. Chem.*, **286**, 14049- 14056.
- [33] Yamazaki T and Tokiwa T. (2010) Isofraxidin, a coumarin component from *Acanthopanax senticosus*, inhibits matrix metalloproteinase-7 expression and cell invasion of human hepatoma cells. *Biol. Pharm. Bull.*, **33**, 1716- 1722.
- [34] Starcevic S, Brozic P, Turk S, Cesar J, Lanisnik RT and Gobec S. (2010) Synthesis and Biological Evaluation of (6- and 7-Phenyl) Coumarin Derivatives as Selective Nonsteroidal Inhibitors of 17beta-Hydroxysteroid Dehydrogenase Type 1. *J. Med. Chem.*, **54**, 248-61
- [35] Starcevic S, Kocbek P, Hribar G, Lanisnik RT and Gobec S. (2011) Biochemical and biological evaluation of novel potent coumarin inhibitor of 17beta-HSD type 1. *Chem. Biol. Interact.*, **191**, 60-65.

- [36] Behrenswerth A, Volz N, Torang J, Hinz S, Brase S and Muller EC. (2009) Synthesis and pharmacological evaluation of coumarin derivatives as cannabinoid receptor antagonists and inverse agonists. *Bioorg. Med. Chem.*, **17**, 2842- 2851.
- [37] Riveiro ME, De KN, Moglioni A, Vazquez R, Monczor F, Shayo C and Davio C. (2010) Coumarins: old compounds with novel promising therapeutic perspectives. *Curr. Med. Chem.*, **17**, 1325- 1338.
- [38] Sun JG, Chen CY, Luo KW, Yeung CL, Tsang TY, Huang ZZ, Wu P, Fung KP, Kwok TT and Liu FY. (2011) 3,5-Dimethyl-H-Furo[3,2-g]Chromen-7-One as a Potential Anticancer Drug by Inducing p53-Dependent Apoptosis in Human Hepatoma HepG2 Cells. *Chemotherapy.*, **57**, 162- 172.
- [39] Miri R, Motamedi R, Rezaei RM, Firuzi O, Javidnia A and Shafiee A. (2011) Design, synthesis and evaluation of cytotoxicity of novel chromeno[4,3-b]quinoline derivatives. *Arch. Pharm. (Weinheim)* **344**, 111- 118.
- [40] Musa MA, Zhou A and Sadik OA. (2011) Synthesis and antiproliferative activity of new coumarin-based benzopyranone derivatives against human tumor cell lines. *Med. Chem.*, **7**, 112- 120.
- [41] Weber US, Steffen B and Siegers CP. (1998) Antitumor-activities of coumarin, 7-hydroxy-coumarin and its glucuronide in several human tumor cell lines. *Res Commun Mol Pathol Pharmacol.*, **99**, 193-206.
- [42] Chuang JY, Haung YF, Lu HF, Ho HC, Yang JS, Li TM, Chang NW and Chung JG. (2007) Coumarin induces cell cycle arrest and apoptosis in human cervical cancer HeLa cells through a mitochondria- and caspase-3 dependent mechanism and NF-kappaB down-regulation. *In Vivo.*, **21**, 1003-1009.
- [43] Velasco-Velazquez MA, Agramonte-Hevia J, Barrera D, Jimenez-Orozco A, Garcia-Mondragon MJ, Mendoza-Patino, Landa A and Mandoki J. (2003) 4-Hydroxycoumarin Disorganizes the Actin Cytoskeleton in B16-F10 Melanoma Cells but not in B82 Fibroblasts, Decreasing their Adhesion to Extracellular Matrix Proteins and Motility. *Cancer Letts.*, **198**, 179-186.

- [44] Thornes RD, Edlow DW and Wood S Jr. (1968) Inhibition of Locomotion in Cancer Cells *In Vivo* By Anticoagulant Therapy. 1. Effect of Sodium Warfarin on V2 Cancer Cells, Granulocytes, Lymphocytes and Macrophages in Rabbits. *Johns Hopkins Med J.*, **123**, 305-316.
- [45] Feuer G. (1974) The metabolism and biological actions of coumarins. *Prog Med Chem.*, **10**, 85-158.
- [46] Zhang L, Jiang G, Yao F, He Y, Liang G, Zhang Y, Hu B, Wu Y, Li Y and Liu H. (2012) Growth inhibition and apoptosis induced by osthole, a natural coumarin, in hepatocellular carcinoma. *PLoS One.*, **5**, 37865.
- [47] Ahmad R, Asad M, Siddiqui ZN and Kumar A. (2009) Screening of synthetic new heterocyclic derivatives of 3-formyl-4-hydroxycoumarin for anti-inflammatory activity in albino rats. *JPRHC.*, **1**, 46-62.
- [48] Manojkumar P, Kochupappy T and Subbuchettiar RG. (2009) Synthesis of coumarin heterocyclic derivatives with antioxidant activity and *in vitro* cytotoxic activity against tumour cells. *Acta Pharm.*, **59**, 159–170.
- [49] Sandeep G, Ranganath YS, Bhasker S and Rajkumar N. (2009) Synthesis and Biological Screening of Some Novel Coumarin Derivatives. *Asian J. Research Chem.*, **2**, 155-160.
- [50] Mohareb RM, EL-Arab EE and El-Sharkawy KA. (2009) The reaction of cyanoacetic acid hydrazide with 2-acetylfuran: Synthesis of coumarin, pyridine, thiophene and thiazole derivatives with potential antimicrobial activities. *Sci Pharm.*, **77**, 355–366.
- [51] Kolancilar H and Mozioglu E. (2008) Antimicrobial Activities of some Benzocoumarines and benzochromone. *Trakya Univ J Sci.*, **9**, 59-62.
- [52] Kotali A, Lafazanis IS, Papageorgiou A, Eleni Chrysogelou E, Lialiaris T and Sinakos Z. (2008) Synthesis, Characterization and Antileucemic Activity of 7-Hydroxy-8-acetylcoumarin Benzoylhydrazone. *Molecules.*, **M574**.

- [53] Finn GJ, Kenealy E, Creaven BS, and Egan DA. (2002) In vitro cytotoxic potential and mechanism of action of selected coumarins, using human renal cell lines. *Cancer Lett.*, **183**, 61-68.
- [54] Finn GJ, Creaven B and Egan DA. (2001) Study of the *in vitro* cytotoxic potential of natural and synthetic coumarin derivatives using human normal and neoplastic skin cell lines. *Melanoma Res.*, **11**, 461-467.
- [55] Lopez-Gonzalez JS, Prado-Garcia H, Aguilar-Cazares D, Molina-Guarneros JA, Morales-Fuentes J, and Mandok JJ. (2004). Apoptosis and cell cycle disturbances induced by coumarin and 7-hydroxycoumarin on human lung carcinoma cell lines. *Lung Cancer.*, **43**, 275-283.
- [56] Seliger B and Pettersson H. (1994) 7-Hydroxycoumarin inhibits oncogene-induced transformation of murine fibroblasts. *J Cancer Res Clin Oncol.*, **120**, 23-27.
- [57] Rivlin RS. (2001) Historical perspective on the use of garlic. *J Nutr.*, **131**, 951-954.
- [58] Münchberg U, Anwar A, Mecklenburg S and Jacob C. (2007) Polysulfides as biologically active ingredients of garlic. *Org.Biomol.Chem.*, **5**, 1505- 1518.
- [59] Jacob C, Jamier V and Ba LA. (2011) Redox active secondary metabolites. *Curr Opin Chem Biol.*, **1**, 149-55.
- [60] Block E, Naganathan S, Putman D and Zhao S-H. (1993) Organosulfur chemistry of garlic and onion: Recent results. *Pure & Appl. Chem.*, **65**, 625-632.
- [61] Jacob C, Anwar A and Burkholz T. (2008) Perspective on recent developments on sulfur-containing agents and hydrogen sulfide signaling. *Planta Med.*, **74**, 1580- 1592.
- [62] Munday R, Munday JS and Munday CM. (2003) Comparative effects of mono-, di-, tri-, and tetrasulfides derived from plants of the Allium family:



- redox cycling in vitro and hemolytic activity and Phase 2 enzyme induction in vivo. *Free Radical Biology and Medicine*, **34**, 1200- 1211.
- [63] Iciek M, Kwiecien I and Wlodek L. (2009) Biological properties of garlic and garlic-derived organosulfur compounds. *Environmental and Molecular Mutagenesis*, **50**, 247- 265.
- [64] Haber JE. (1999) DNA recombination: the replication connection. *Trends in Biochemical Sciences*, **24**, 271- 275.
- [65] Steudel R. (2002) The chemistry of organic polysulfanes R-S(n)-R (n > 2). *Chem. Rev*, **102**, 3905–3945.
- [66] Filomeni G, Aquilano K, Rotilio G and Ciriolo MR. (2003) Reactive oxygen species-dependent c-Jun NH2-terminal kinase/c-Jun signaling cascade mediates neuroblastoma cell death induced by diallyl disulfide. *Cancer Research*, **63**, 5940- 5949.
- [67] Filomeni G, Aquilano K, Rotilio G and Ciriolo MR. (2005) Glutathione-related systems and modulation of extracellular signal-regulated kinases are involved in the resistance of AGS adenocarcinoma gastric cells to diallyl disulfide-induced apoptosis. *Cancer Research*, **65**, 11735- 11742.
- [68] Schneider T, Ba LA, Khairan K, Zwergel C, Bach ND, Bernhardt I, Brandt W, Wessjohann L, Diederich M and Jacob C. (2011) Interactions of polysulfanes with components of red blood cells. *MedChemCommun*, **2**, 196.
- [69] Das A, Banik NL and Ray SK. (2007) Garlic compounds generate reactive oxygen species leading to activation of stress kinases and cysteine proteases for apoptosis in human glioblastoma T98G and U87MG cells. *Cancer*, **110**, 1083- 1095.
- [70] Yang JS, Chen GW, Hsia TC, Ho HC, Ho CC, Lin MW, Lin SS, Yeh RD, Ip SW, Lu HF and Chung JG. (2009) Diallyl disulfide induces apoptosis in human colon cancer cell line (COLO 205) through the induction of reactive oxygen species, endoplasmic reticulum stress, caspases cascade and

- mitochondrial-dependent pathways. *Food and Chemical Toxicology*, **47**, 171-179.
- [71] Chen C, Pung D, Leong V, Hebbar V, Shen G, Nair S, Li W and Kong AN. (2004) Induction of detoxifying enzymes by garlic organosulfur compounds through transcription factor Nrf2: effect of chemical structure and stress signals. *Free Radical Biology and Medicine*, **37**, 1578- 1590.
- [72] Bottone FG, Jr., Moon Y, Kim JS, Alston-Mills B, Ishibashi M and Eling TE. (2005) The anti-invasive activity of cyclooxygenase inhibitors is regulated by the transcription factor ATF3 (activating transcription factor 3). *Mol.Cancer Ther.*, **4**, 693- 703.
- [73] Knight JA. (1995) Diseases related to oxygen-derived free radicals. *Ann.Clin.Lab Sci.*, **25**, 111- 121.
- [74] Xiao D, Pinto JT, Soh JW, Deguchi A, Gundersen GG, Palazzo AF, Yoon JT, Shirin H and Weinstein IB. (2003) Induction of apoptosis by the garlic-derived compound S-allylmercaptocysteine (SAMC) is associated with microtubule depolymerization and c-Jun NH(2)-terminal kinase 1 activation. *Cancer Research*, **63**, 6825- 6837.
- [75] Aquilano K, Vigilanza P, Filomeni G, Rotilio G and Ciriolo MR. (2010) Tau dephosphorylation and microfilaments disruption are upstream events of the anti-proliferative effects of DADS in SH-SY5Y cells. *J.Cell Mol.Med.*, **14**, 564-577.
- [76] Giles GI and Jacob C. (2002) Reactive sulfur species: an emerging concept in oxidative stress. *Biol Chem*, **383**, 375-388.
- [77] Bordia A and Bansal HC. (1973) Essential oil of garlic in prevention of atherosclerosis. *Lancet*, **2**, 1491-1492.
- [78] Lin HL, Yang JS, Yang JH, Fan SS, Chang WC, Li YC and Chung JG. (2006) The role of Ca<sup>2+</sup> on the DADS-induced apoptosis in mouse-rat hybrid retina ganglion cells (N18). *Neurochemical Research*, **31**, 383- 393.

- [79] Xiao D, Herman-Antosiewicz A, Antosiewicz J, Xiao H, Brisson M, Lazo JS and Singh SV. (2005) Diallyl trisulfide-induced G(2)-M phase cell cycle arrest in human prostate cancer cells is caused by reactive oxygen species-dependent destruction and hyperphosphorylation of Cdc25C. *Oncogene*, **24**, 6256- 6268.
- [80] Antosiewicz J, Herman-Antosiewicz A, Marynowski SW and Singh SV. (2006) c-Jun NH(2)-terminal kinase signaling axis regulates diallyl trisulfide-induced generation of reactive oxygen species and cell cycle arrest in human prostate cancer cells. *Cancer Research*, **66**, 5379- 5386.
- [81] Fleischauer AT and Arab L. (2001) Garlic and cancer: a critical review of the epidemiologic literature. *J Nutr*, **131**, 1032-40.
- [82] Busch C, Jacob C, Anwar A, Burkholz T, Ba LA, Cerella C, Diederich M, Brandt W, Wessjohann L and Montenarh M. (2010) Diallylpolsulfides induce growth arrest and apoptosis. *Int.J.Oncol.*, **36**, 743- 749.
- [83] Tsimbouri P, O'Donnell M A and Wilson JB. (2001) Selection and Enrichment of B Cells from Lymphoid Tissues. *Methods in molecular biology - Epstein-Barr Virus Protocols.*, **172**, 411–421.
- [84] Roche molecular biochemicals: Apoptosis and cell proliferation. 2nd edition: 72–74.
- [85] Ho YS, Wu CH, Chou HM, Wang YJ, Tseng H, Chen CH, Chen LC, Lee CH and Lin SY. (2005) Molecular mechanisms of econazole-induced toxicity on human colon cancer cells: G0/G1 cell cycle arrest and caspase-8 independent apoptotic signaling pathways. *Food Chem Toxicol*, **43**, 1483–1495.
- [86] Kuo YC, Huang KY, Yang CH, Yang YS, Lee WY, and Chiang CW. (2008) Regulation of phosphorylation of Thr-308 of Akt, cell proliferation, and survival by the B55alpha regulatory subunit targeting of the protein phosphatase 2A holoenzyme to Akt. *J Biol Chem* **283**,1882–1892.

- [87] Dikalov S, Griendling KK and Harrison DG. (2007) Measurement of Reactive Oxygen Species in Cardiovascular Studies. *Hypertension*, **49**, 717–727.
- [88] Pappa G, Bartsch H and Gerhauser C. (2007) Biphasic modulation of cell proliferation by sulforaphane at physiologically relevant exposure times in a human colon cancer cell line. *Mol. Nutr. Food Res*, **51**, 977–984.
- [89] Hanahan D. (1983) Studies on transformation of *Escherichia coli* with plasmids. *J. Mol. Biol*, **166**, 557-80.
- [90] Gong P, Hu B, Stewart D, Ellerbe M, Figueroa YG, Blank V, Beckman BS and Alam J. (2001) Cobalt induces heme oxygenase-1 expression by a hypoxia-inducible factor-independent mechanism in Chinese hamster ovary cells: regulation by Nrf2 and MafG transcription factors. *J. Biol. Chem*, **276**, 27018–27025.
- [91] Choi AM and Alam J. (1996) Heme oxygenase-1: function, regulation, and implication of a novel stress-inducible protein in oxidant-induced lung injury. *Am. J. Respir. Cell Mol. Biol*, **15**, 9–19.
- [92] Alam J, Stewart D, Touchard C, Boinapally S, Choi AM and Cook JL. (1999) Nrf2, a Cap'n'Collar transcription factor, regulates induction of the heme oxygenase-1 gene. *J. Biol. Chem*, **274**, 26071–26078.
- [93] Caspase-Glo<sup>®</sup> 3/7 Assay Technical Bulletin - Promega - Part# TB323
- [94] Harrington HA, Ho KL, Ghosh S and Tung KC. (2008) Construction and analysis of a modular model of caspase activation in apoptosis. *Theor Biol Med Model*, **5**, 26.
- [95] Volkman X, Fischer U, Bahr MJ, Ott M, Lehner F, MacFarlane M, Cohen GM, Manns MP, Schulze-Osthoff K and Bante H. (2007) Increased hepatotoxicity of tumor necrosis factor-related apoptosis-inducing ligand in diseased human liver. *Hepatology*, **46**, 1498.

- [96] Bradford MA. (1976) A rapid and sensitive method for the quantification of microgram quantities of protein utilising the principle of protein-dye binding. *Anal. Biochem*, **72**, 248–254.
- [97] Laemmli UK. (1970) Cleavage of structural proteins during the assembly of the head of bacteriophage T4. *Nature*, **227**, 680-685.
- [98] Weber K and Osborn M. (1969) The reliability of molecular weight determinations by sodium dodecyl sulfate polyacrylamide gel electrophoresis. *J. Biol. Chem*, **244**, 4406-4412.
- [99] Shirasawa S. (1993) Analysis of molecular mechanism in colorectal tumorigenesis. *Fukuoka Igaku Zasshi.*, **84**, 25-35.
- [100] Awwad RA, Sergina N, Yang H, Ziober B, Willson JK, Zborowska E, Humphrey LE, Fan R, Ko TC, Brattain MG and Howell GM. (2003) The role of transforming growth factor alpha in determining growth factor independence. *Cancer Res.*, **63**, 4731-8.
- [101] Ishizuka J, Townsend CM Jr, Bold RJ, Martinez J, Rodriguez M and Thompson JC. (1994) Effects of gastrin on 3',5'-cyclic adenosine monophosphate, intracellular calcium, and phosphatidylinositol hydrolysis in human colon cancer cells. *Cancer Res.*, **54**, 2129-35.
- [102] Howell GM, Humphrey LE, Ziober BL, Awwad R, Periyasamy B, Koterba A, Li W, Willson JK, Coleman K, Carboni J, Lynch M and Brattain MG. (1998) Regulation of transforming growth factor alpha expression in a growth factor-independent cell line. *Mol Cell Biol.*, **18**, 303-13.
- [103] Suzuki K, Dashzeveg N, Lu ZG, Taira N, Miki Y and Yoshida K. (2012) Programmed cell death 6, a novel p53-responsive gene, targets to the nucleus in the apoptotic response to DNA damage. *Cancer Sci.*, **103**, 1788-94.
- [104] Cerella C, Scherer C, Cristofanon S, Henry E, Anwar A, Busch C, Montenarh M, Dicato M, Jacob C and Diederich M. (2009) Cell cycle arrest in early

- mitosis and induction of caspase-dependent apoptosis in U937 cells by diallyltetrasulfide (Al<sub>2</sub>S<sub>4</sub>). *Apoptosis*, **14**, 641- 6.
- [105] Gobeil S, Boucher CC, Nadeau D and Poirier GG. (2001) Characterization of the necrotic cleavage of poly(ADP-ribose) polymerase (PARP-1): implication of lysosomal proteases. *Cell Death Differ*, **8**, 588-94.
- [106] Strathmann J, Klimo K, Sauer SW, Okun JG, Prehn JH and Gerhäuser C. (2010) Xanthohumol-induced transient superoxide anion radical formation triggers cancer cells into apoptosis via a mitochondria-mediated mechanism. *FASEB J*, **24**, 2938-50.
- [107] Arellano M and Moreno S. (1997) Regulation of CDK/cyclin complexes during the cell cycle. *International Journal of Biochemistry and Cell Biology*, **29**, 559-573.
- [108] Bernander R. (1994) Universal cell cycle regulation. *Trends in Cell Biology*, **4**, 76- 79.
- [109] Boutros R, Dozier C and Ducommun B. (2006) The when and wheres of CDC25 phosphatases. *Current Opinion in Cell Biology*, **18**, 185- 191.
- [110] Evan GI and Vousden KH. (2001) Proliferation, cell cycle and apoptosis in cancer. *Nature*, **411**, 342- 348.
- [111] Karlsson-Rosenthal C and Millar JB. (2006) Cdc25: mechanisms of checkpoint inhibition and recovery. *Trends in Cell Biology*, **16**, 285- 292.
- [112] Malumbres M. (2011) Physiological relevance of cell cycle kinases. *Physiol Rev.*, **91**, 973- 1007.
- [113] Ferrell JE, Jr., Tsai TY and Yang Q. (2011) Modeling the cell cycle: why do certain circuits oscillate? *Cell*, **144**, 874- 885.
- [114] Johnson DG and Walker CL. (1999) Cyclins and cell cycle checkpoints. *Annual Review of Pharmacology and Toxicology*, **39**, 295- 312.

- [115] Mils V, Baldin V, Goubin F, Pinta I, Papin C, Waye M, Eychene A and Ducommun B. (2000). Specific interaction between 14-3-3 isoforms and the human CDC25B phosphatase. *Oncogene*, **19**, 1257- 1265.
- [116] Lin YT, Yang JS, Lin SY, Tan TW, Ho CC, Hsia TC, Chiu TH, Yu CS, Lu HF, Weng YS and Chung JG. (2008) Diallyl disulfide (DADS) induces apoptosis in human cervical cancer Ca Ski cells via reactive oxygen species and Ca<sup>2+</sup>-dependent mitochondria-dependent pathway. *Anticancer Res.*, **28**, 2791-2799.
- [117] Campana F, Zervoudis S, Perdereau B, Gez E, Fourquet A, Badiu C, Tsakiris G and Koulaloglou, S. (2004) Topical superoxide dismutase reduces post-irradiation breast cancer fibrosis. *J Cell Mol Med*, **8**, 109-116.
- [118] Guaiquil VH, Vera JC and Golde DW. (2001) Mechanism of Vitamin C Inhibition of Cell Death Induced by Oxidative Stress in Glutathione-depleted HL-60 Cells. *J Biol Chem*, **276**, 40955-61.
- [119] Franco R and Cidlowski JA. (2006) SLCO/OATP-like transport of glutathione in FasL-induced apoptosis: glutathione efflux is coupled to an organic anion exchange and is necessary for the progression of the execution phase of apoptosis. *J. Biol. Chem.*, **281**, 29542-29557.
- [120] Ghibelli L, Fanelli C, Rotilio G, Lafavia E, Coppola S, Colussi C, Civitareale P and Ciriolo MR. (1998) Rescue of cells from apoptosis by inhibition of active GSH extrusion. *FASEB J.*, **12**, 479-486.
- [121] Harding HP, Zhang Y, Zeng H, Novoa I, Lu PD, Calton M, Sadri N, Yun C, Popko B, Paules R, Stojdl DF, Bell JC, Hettmann T, Leiden JM, Ron D. (2003) An integrated stress response regulates amino acid metabolism and resistance to oxidative stress. *Molecular Cell*, **11**, 619- 633.
- [122] Zhao P, Xiao X, Kim AS, Leite MF, Xu J, Zhu X, Ren J and Li J. (2008) c-Jun inhibits thapsigargin-induced ER stress through up-regulation of DSCR1/Adapt78. *Exp Biol Med*, **233**, 1289-300.

- [123] Li H, Wu S, Shi N, Lian S and Lin W. (2011) Nrf2/HO-1 pathway activation by manganese is associated with reactive oxygen species and ubiquitin-proteasome pathway, not MAPKs signaling. *J. Appl. Toxicol.*, **31**, 690-697.
- [124] Cullinan SB, Diehl JA. (2006) Coordination of ER and oxidative stress signaling: the PERK/Nrf2 signaling pathway. *International Journal of Biochemistry and Cell Biology*, **38**, 317- 332.
- [125] Venugopal R, Jaiswal AK. (1998) Nrf2 and Nrf1 in association with Jun proteins regulate antioxidant response element-mediated expression and coordinated induction of genes encoding detoxifying enzymes. *Oncogene*, **17**, 3145- 3156.
- [126] Alam J and Cook JL. (2003) Transcriptional regulation of the heme oxygenase-1 gene via the stress response element pathway. *Curr. Pharm.*, **9**, 2499-2511.
- [127] Alam J, Wicks C, Stewart D, Gong P, Touchard C, Otterbein S, Choi AM, Burow ME and Tou J. (2000) Mechanism of heme oxygenase-1 gene activation by cadmium in MCF-7 mammary epithelial cells. Role of p38 kinase and Nrf2 transcription factor, *J. Biol. Chem.*, **275**, 27694-27702.
- [128] Itoh K, Chiba T, Takahashi S, Ishii T, Igarashi K, Katoh Y, Oyake T, Hayashi N, Satoh K, Hatayama I, Yamamoto M and Nabeshima Y. (1997) An Nrf2/small Maf heterodimer mediates the induction of phase II detoxifying enzyme genes through antioxidant response elements. *Biochem. Biophys. Res. Commun.*, **236**, 313-322.
- [129] Siegel D, Bolton EM, Burr JA, Liebler DC, Ross D. (1997) The reduction of alpha-tocopherolquinone by human NAD(P)H: quinone oxidoreductase: the role of alpha-tocopherolhydroquinone as a cellular antioxidant. *Mol. Pharmacol*, **52**, 300–305.
- [130] Siegel D, Gustafson DL, Dehn DL, Han JY, Boonchoong P, Berliner LJ and Ross D. (2004) NAD(P)H:quinone oxidoreductase 1: role as a superoxide scavenger. *Mol. Pharmacol*, **65**, 1238–1247.



- [131] Jiang HY, Wek SA, McGrath BC, Lu D, Hai T, Harding HP, Wang X, Ron D, Cavener DR and Wek RC. (2004) Activating transcription factor 3 is integral to the eukaryotic initiation factor 2 kinase stress response. *Mol. Cell Biol.*, **24**, 1365-1377.
- [132] Vallejo M, Ron D, Miller CP and Habener JF. (1993) C/ATF, a member of the activating transcription factor family of DNA-binding proteins, dimerizes with CAAT/enhancer-binding proteins and directs their binding to cAMP response elements. *Proc Natl Acad Sci U S A*, **90**, 4679-83.
- [133] Bruhat A, Jousse C, Carraro V, Reimold AM, Ferrara M and Fafournoux P. (2000) Amino acids control mammalian gene transcription: activating transcription factor 2 is essential for the amino acid responsiveness of the CHOP promoter. *Mol. Cell Biol.*, **20**, 7192-7204.
- [134] Hai T, Wolfgang CD, Marsee DK, Allen AE and Sivaprasad U. (1999) ATF3 and stress responses. *Gene Expr*, **7**, 321-35.
- [135] Spohn D, Rössler OG, Philipp SE, Raubuch M, Kitajima S, Griesemer D, Hoth M and Thiel G. (2010) Thapsigargin induces expression of activating transcription factor 3 in human keratinocytes involving Ca<sup>2+</sup> ions and c-Jun N-terminal protein kinase. *Mol Pharmacol*, **78**, 865-76.
- [136] Wassmann K and Benezra R (2001) Mitotic checkpoints: from yeast to cancer. *Curr Opin Genet Dev*, **11**, 83–90.
- [137] Litchfield DW. (2003) Protein kinase CK2: structure, regulation and role in cellular decisions of life and death. *Biochem J*. **369**, 1-15.
- [138] Slaton JW, Unger GM, Sloper DT, Davis AT, and Ahmed K. (2004) Induction of apoptosis by antisense CK2 in human prostate cancer xenograft model. *Mol Cancer Res*, **2**, 712-21.
- [139] Perea SE, Reyes O, Puchades Y, Mendoza O, Vispo NS, Torrens I, Santos A, Silva R, Acevedo B, Lopez E, Falcon V, and Alonso DF. (2004) Antitumor

- effect of a novel proapoptotic peptide that impairs the phosphorylation by the protein kinase 2 (casein kinase 2). *Cancer Res*, **64**, 7127-9
- [140] Apopa PL, He X and Ma Q (2008) Phosphorylation of Nrf2 in the transcription activation domain by casein kinase 2 (CK2) is critical for the nuclear translocation and transcription activation function of Nrf2 in IMR-32 neuroblastoma cells. *J Biochem Mol Toxicol*, **22**, 63-76.
- [141] Wang X and Johnsson N (2005) Protein kinase CK2 phosphorylates Sec63p to stimulate the assembly of the endoplasmic reticulum protein translocation apparatus. *J Cell Sci*, **118**, 723-32.
- [142] Ahmed SU and Milner J. (2009) Basal Cancer Cell Survival Involves JNK2 Suppression of a Novel JNK1/c-Jun/Bcl-3 Apoptotic Network. *PLoS One*, **4**, e7305.
- [143] Shukla Y and Kalra N. (2007) Cancer chemoprevention with garlic and its constituents. *Cancer Lett*, **247**, 167- 181.
- [144] Hoffmann I. (2000) The role of Cdc25 phosphatases in cell cycle checkpoints. *Protoplasma*, **211**, 8- 11.
- [145] Brault L, Denance M, Banaszak E, El MS, Battaglia E, Bagrel D and Samadi M. (2007) Synthesis and biological evaluation of dialkylsubstituted maleic anhydrides as novel inhibitors of Cdc25 dual specificity phosphatases. *Eur J Med Chem*, **42**, 243- 247.
- [146] Milner JA. (1996) Garlic: its anticarcinogenic and antitumorigenic properties. *Nutr.Rev.*, **54**, S82- S86.
- [147] Milner JA. (2001) Mechanisms by which garlic and allyl sulfur compounds suppress carcinogen bioactivation. Garlic and carcinogenesis. *Advances in Experimental Medicine and Biology*, **492**, 69- 81.
- [148] Jacob C. (2006) A scent of therapy: pharmacological implications of natural products containing redox-active sulfur atoms. *Nat Prod Rep*, **23**, 851–863.

- [149] Indran IR, Tufo G, Pervaiz S and Brenner C. (2011) Recent advances in apoptosis, mitochondria and drug resistance in cancer cells. *Biochim Biophys Acta*, **1807**, 735- 745.
- [150] Haupt S, Berger M, Goldberg Z and Haupt Y. (2003) Apoptosis - the p53 network. *Journal of Cell Science*, **116**, 4077- 4085.
- [151] Montenarh M and Saidu NEB. (2012) The effect of diallyl polysulfanes on cellular signalling cascades. *Nat. Prod. Commun*, **7**, 401-408.
- [152] Thanasoula M, Escandell JM, Suwaki N and Tarsounas M. (2012) ATM/ATR checkpoint activation downregulates CDC25C to prevent mitotic entry with uncapped telomeres. *EMBO J*, **31**, 3398-3410.
- [153] Hammond CL, Madejczyk MS and Ballatori N. (2004) Activation of plasma membrane reduced glutathione transport in death receptor apoptosis of HepG2 cells. *Toxicol. Appl. Pharmacol*, **195**, 12-22.
- [154] Rodriguez-Ramiro I, Ramos S, Bravo L, Goya L and Martin MA. (2011) Procyanidin B2 and a cocoa polyphenolic extract inhibit acrylamide-induced apoptosis in human Caco-2 cells by preventing oxidative stress and activation of JNK pathway. *J Nutr Biochem*, **22**, 1186–1194.
- [155] Gregersen N, Bross P, Vang S and Christensen JH. (2006) Protein Misfolding and Human Disease. *Annu Rev Genomics Hum Genet*, **7**, 103-124.
- [156] Ron D and Walter P. (2007) Signal integration in the endoplasmic reticulum unfolded protein response. *Nat Rev Mol Cell Biol*, **8**, 519- 529.
- [157] Harding HP, Zhang Y and Ron D. (1999) Protein translation and folding are coupled by an endoplasmic-reticulum-resident kinase. *Nat*, **397**, 271- 274.
- [158] Malhotra JD and Kaufman RJ. (2007) Endoplasmic reticulum stress and oxidative stress: a vicious cycle or a double-edged sword? *Antioxid Redox Signal*, **9**, 2277-93.

- [159] Malhotra JD, Miao H, Zhang K, Wolfson A, Pennathur S, Pipe SW and Kaufman RJ. (2008) Antioxidants reduce endoplasmic reticulum stress and improve protein secretion. *Proc Natl Acad Sci U S A*, **105**, 18525-30.
- [160] Malhotra JD and Kaufman RJ. (2007) The endoplasmic reticulum and the unfolded protein response. *Semin Cell Dev Biol*, **18**, 716-31.
- [161] Tu BP and Weissman JS. (2004) Oxidative protein folding in eukaryotes: mechanisms and consequences. *J Cell Biol*, **164**, 341-346.
- [162] Kostenko S, Dumitriu G, Laegreid KJ, Moens U. (2011) Physiological roles of mitogen-activated-protein-kinase-activated p38-regulated/activated protein kinase. *World J.Biol.Chem.*, **2**, 73- 89.
- [163] Cargnello M, Roux PP. (2011) Activation and function of the MAPKs and their substrates, the MAPK-activated protein kinases. *Microbiology and Molecular Biology Reviews*, **75**, 50- 83.
- [164] Plotnikov A, Zehorai E, Procaccia S, Seger R. (2011) The MAPK cascades: Signaling components, nuclear roles and mechanisms of nuclear translocation. *Biochim.Biophys.Acta*, **1813**, 1619- 1633.
- [165] Wortzel I, Seger R. (2011) The ERK Cascade: Distinct Functions within Various Subcellular Organelles. *Genes Cancer*, **2**, 195- 209.
- [166] Whelan JT, Hollis SE, Cha DS, Asch AS, Lee MH. (2011) Post-transcriptional regulation of the Ras-ERK/MAPK signaling pathway. *J.Cell Physiol*, **227**, 1235-41.
- [167] Bogoyevitch MA, Ngoei KR, Zhao TT, Yeap YY, Ng DC. (2010) c-Jun N-terminal kinase (JNK) signaling: recent advances and challenges. *Biochim.Biophys.Acta*, **1804**, 463- 475.
- [168] Fawcett TW, Martindale JL, Guyton KZ, Hai T and Holbrook NJ. (1999) Complexes containing activating transcription factor (ATF)/cAMP-responsive-element-binding protein (CREB) interact with the CCAAT/enhancer-binding

- protein (C/EBP)-ATF composite site to regulate Gadd153 expression during the stress response. *Biochem. J*, ( Pt 1) **339**, 135-141.
- [169] Stearns ME, Kim G, Garcia F and Wang M. (2004) Interleukin-10 induced activating transcription factor 3 transcriptional suppression of matrix metalloproteinase-2 gene expression in human prostate CPTX-1532 cells. *Mol Cancer Res*, **2**, 403–416.
- [170] Bottone FG Jr, Martinez JM, Alston-Mills B and Eling TE. (2004) Gene modulation by Cox-1 and Cox-2 specific inhibitors in human colorectal carcinoma cancer cells. *Carcinogenesis*, **25**, 349–357.
- [171] Corpet DE and Pierre F. (2003) Point: From animal models to prevention of colon cancer. Systematic review of chemoprevention in min mice and choice of the model system. *Cancer Epidemiol Biomarkers Prev*, **12**, 391–400.
- [172] Baek SJ, Horowitz JM and Eling TE. (2001) Molecular cloning and characterization of human nonsteroidal anti-inflammatory drug-activated gene promoter. Basal transcription is mediated by Sp1 and Sp3. *J Biol Chem*, **276**, 33384–92.
- [173] Hessenauer A, Schneider CC, Götz C and Montenarh M (2011) CK2 inhibition induces apoptosis via the ER stress response. *Cell Signal*, **23**, 145-151.
- [174] Manni S, Brancalion A, Tubi LQ, Colpo A, Pavan L, Cabrelle A, Ave E, Zaffino F, Di Maira G, Ruzzene M, Adami F, Zambello R, Pitari MR, Tassone P, Pinna LA, Gurrieri C, Semenzato G and Piazza F. (2012) Protein kinase CK2 protects multiple myeloma cells from ER stress-induced apoptosis and from the cytotoxic effect of HSP90 inhibition through regulation of the unfolded protein response. *Clin Cancer Res*, **18**, 1888-900.
- [175] Götz C, Bachmann C and Montenarh M. (2007) Inhibition of protein kinase CK2 leads to a modulation of androgen receptor dependent transcription in prostate cancer cells. *Prostate*, **67**, 125-134.

- [176] Schneider CC, Götz C, Hessenauer A, Günther J, Kartarius S and Montenarh M. (2011) Down-regulation of CK2 activity results in a decrease in the level of cdc25C phosphatase in different prostate cancer cell lines. *Mol Cell Biochem*, **356**, 177-184.
- [177] Bunt-Milam AH and Saari JC. (1983) Immunocytochemical localization of two retinoid-binding proteins in vertebrate retina. *J Cell Biol*, **97**, 703-712.
- [178] Hamel CP, Tsilou E, Pfeffer BA, Hooks JJ, Detrick B and Redmond TM. (1993) Molecular cloning and expression of RPE65, a novel retinal pigment epithelium-specific microsomal protein that is post-transcriptionally regulated in vitro. *J Biol Chem*, **268**, 15751-7.
- [179] Dunn KC, Aotaki-Keen AE, Putkey FR and Hjelmeland LM. (1996) ARPE-19, A Human Retinal Pigment Epithelial Cell Line with Differentiated Properties. *Exp. Eye Res*, **62**, 155-169.
- [180] Podhorecka M, Skladanowski A, Bozko P. (2010) H2AX Phosphorylation: Its Role in DNA Damage Response and Cancer Therapy. *J Nucleic Acids*, **2010**, 1-9.
- [181] Yang P, Peairs JJ, Tano R, Zhang N, Tyrell J and Jaffe GJ. (2007) Caspase-8-Mediated Apoptosis in Human RPE Cells. *Invest Ophthalmol Vis Sci*, **48**, 3341-9.
- [182] Jamier V, Ba LA and Jacob C. (2010) Selenium- and tellurium-containing multifunctional redox agents as biochemical redox modulators with selective cytotoxicity. *Chemistry*, **36**, 10920-8.
- [183] Stan SD, Kar S, Stoner GD, and Singh SV. (2008) Bioactive food components and cancer risk reduction. *J. Cell Biochem*, **104**, 339-356.
- [184] Hu X, Benson PJ, Srivastava SK, Xia H, Bleicher RJ, Zaren HA, Awasthi S, Awasthi YC, and Singh SV. (1997) Induction of glutathione S-transferase pi as

- a bioassay for the evaluation of potency of inhibitors of benzo(a)pyrene-induced cancer in a murine model. *Int. J. Cancer*, **73**, 897-902.
- [185] Xiao D, Choi S, Johnson DE, Vogel VG, Johnson CS, Trump DL, Lee YJ and Singh SV. (2004) Diallyl trisulfide-induced apoptosis in human prostate cancer cells involves c-Jun N-terminal kinase and extracellular-signal regulated kinase-mediated phosphorylation of Bcl-2. *Oncogene.*, **23**, 5594-5606.
- [186] Song JD, Lee SK, Kim KM, Park SE, Park SJ, Kim KH, Ahn SC and Park YC. (2009) Molecular mechanism of diallyl disulfide in cell cycle arrest and apoptosis in HCT-116 colon cancer cells. *J. Biochem. Mol. Toxicol.*, **23**, 71-79.
- [187] Knowles LM and Milner JA. (1998) Depressed p34cdc2 kinase activity and G2/M phase arrest induced by diallyl disulfide in HCT-15 cells. *Nutr. Cancer*, **30**, 169-174.
- [188] Knowles LM and Milner JA. (2000) Diallyl disulfide inhibits p34(cdc2) kinase activity through changes in complex formation and phosphorylation. *Carcinogenesis*, **21**, 1129-1134.
- [189] Viry E, Anwar A, Kirsch G, Jacob C, Diederich M and Bagrel D. (2011) Antiproliferative effect of natural tetrasulfides in human breast cancer cells is mediated through the inhibition of the cell division cycle 25 phosphatases. *Int. J. Oncol*, **38**, 1103-1111.
- [190] Sohn J and Rudolph J. (2003) Catalytic and chemical competence of regulation of cdc25 phosphatase by oxidation/reduction. *Biochemistry*, **42**, 10060-10070.
- [191] Schroder M, and Kaufman RJ. (2005) The mammalian unfolded protein response. *Annu Rev Biochem*, **74**, 739–789.
- [192] Jordan MA and Wilson L. (2004) Microtubules as a target for anticancer drugs. *Nat Rev Cancer*, **4**, 253–265.

- [193] Wu CC, Sheen LY, Chen HW, Kuo WW, Tsai SJ and Lii CK. (2002) Differential Effects of Garlic Oil and Its Three Major Organosulfur Components on the Hepatic Detoxification System in Rats. *J. Agric. Food Chem*, **50**, 378–383.
- [194] Yu FS, Wu CC, Chen CT, Huang SP, Yang JS, Hsu YM, Wu PP, Ip SW, Lin JP, Lin JG and Chung JG. (2009) Diallyl sulfide inhibits murine WEHI-3 leukemia cells in BALB/c mice in vitro and in vivo. *Hum Exp Toxicol*, **28**, 785-90.





## Publications

**Saidu NEB**, Touma R, Asali IA, Jacob C, Montenarh M. Diallyl tetrasulfane activates both the eIF2 $\alpha$  and Nrf2/HO-1 pathways. *Biochim Biophys Acta*. 2012 Oct 6;1830(1):2214-2225.

**Saidu NEB**, Valente S, Bana E, Kirsch G, Bagrel D, Montenarh M. Coumarin polysulfides inhibit cell growth and induce apoptosis in HCT116 colon cancer cells. *Bioorg Med Chem*. 2012 Feb 15;20(4):1584-93.

Montenarh M, **Saidu NEB**. The effect of diallyl polysulfanes on cellular signaling cascades. *Nat Prod Commun*. 2012 Mar;7(3):401-8. Review.

## Curriculum Vitae

### Personal Information

Name: **Nathaniel Edward Bennet Saidu**  
Date of Birth: 23/03/1984  
Gender: Male  
Nationality: British  
Tel: +49 6841 1626501  
Fax: +49 6841 1626027  
Email: s9nasaid@stu.uni-saarland.de

### Education

- 12.2009 - **Ph.D Candidate and Early Stage Researcher, RedCat Project**  
present Department of Medical Biochemistry and Molecular Biology  
University of the Saarland, Homburg, Germany.  
Supervisor: Prof. Dr. Mathias Montenarh
- 2008 - 2009 **Master of Science (Merit) - Biocatalysis.**  
University of Exeter, Department of Biocatalysis, Exeter, UK.  
Supervisor: Prof. Jennifer Littlechild
- 2004 - 2008 **Bachelor of Science (Hons) - Medical Biochemistry**  
University of Surrey, Department of Biomedical Sciences, Guildford,  
UK.  
Supervisors: Dr. Nick Plant and Dr. Malcolm von Schantz